

Facing the Future of Craniofacial Genetics

Jacqueline Antonia Christiana Goos

ISBN: 978-94-6299-805-6

Financial support was provided by: Afdeling Bioinformatica, Chipsoft, Maatschap Plastische Chirurgie EMC, NVPC, Stichting Hoofdzaak, Van Wijngaarden Medical.

Cover: the image on the cover is based on Sleeping Muse, a sculpture created by Constantin Brancusi. Searching his whole life for the essence of things, to date Brancusi is seen as one of the founding fathers of abstract art. Might the essence of life be hidden in the abstraction of DNA?

Cover design & layout: Design Your Thesis | www.designyourthesis.com

Printing: Ridderprint | www.ridderprint.nl

© 2017 JAC Goos: All rights reserved. No part of this thesis may be reproduced, stored in a retrieval system of any nature, or transmitted in any form or mean, without written permission of the author or, when appropriate, of the publishers of the publications.

This thesis is based on articles published in various scientific journals. Differences may exist between the text in this thesis and the published version due to editorial changes and linguistic differences. Permission to reproduce the articles in this thesis was obtained from the publishers of the various scientific journals.

Facing the Future of Craniofacial Genetics

De toekomst van de craniofaciale genetica

Proefschrift

ter verkrijging van de graad doctor aan de
Erasmus Universiteit Rotterdam

op gezag van de rector magnificus
Prof.dr. H.A.P. Pols

en volgens besluit van het College voor Promoties.

De openbare verdediging zal plaatsvinden op
woensdag 20 december 2017 om 11.30 uur

door

Jacqueline Antonia Christiana Goos
geboren te Rotterdam

Erasmus University Rotterdam



Promotiecommissie

Promotor	Prof.dr. I.M.J. Mathijssen Prof.dr. P.J. van der Spek
Overige leden	Prof.dr. H.G. Brunner Prof.dr. R.M.W. Hofstra Prof.dr. A.O.M. Wilkie
Copromotor	Dr. A.M.W. van den Ouweland

Voor mijn lieve moeder en mijn lieve broer

Table of contents

Chapter 1	General introduction	11
Part 1	Genes previously associated with craniofacial malformations	
Chapter 2	A novel mutation in <i>FGFR2</i>	45
Chapter 3	Apparently synonymous substitutions in <i>FGFR2</i> affect splicing and result in mild Crouzon syndrome	55
Chapter 4	Phenotypes of craniofrontonasal syndrome in patients with a pathogenic mutation in <i>EFNB1</i>	65
Part 2	Novel genetic causes of craniofacial malformations identified with next generation sequencing	
Chapter 5	Mutations in <i>TCF12</i> , encoding a basic helix-loop-helix partner of TWIST1, are a frequent cause of coronal craniosynostosis	81
Chapter 6	Identification of intragenic exon deletions and duplication of <i>TCF12</i> by whole genome or targeted sequencing as a cause of <i>TCF12</i> -related craniosynostosis	93
Chapter 7	Gain-of-function mutations in <i>ZIC1</i> are associated with coronal craniosynostosis and learning disability	107
Chapter 8	Identification of causative variants in <i>TXNL4A</i> in Burn-McKeown syndrome and isolated choanal atresia	135
Part 3	Assess next generation sequencing as a diagnostic tool in craniofacial malformations	
Chapter 9	Diagnostic value of exome and whole genome sequencing in craniosynostosis	155
Chapter 10	General discussion	179
Chapter 11	Summary	233
Chapter 12	Dutch summary	241
Appendices	Supplementary Figures	251
	Supplementary Tables	263
	References	299
	List of publications	319
	Affiliations	323
	PhD portfolio	329
	Curriculum Vitae	335
	Acknowledgements	337

What is real is not the appearance, but the idea, the essence of things

Constantin Brancusi



Chapter 1

General Introduction

General introduction

"It is the common wonder of all men, how among so many millions of faces, there should be none alike," wrote Sir Thomas Browne in *Religio Medici* published in 1643. Ever since, people have been intrigued by the development of the human head and face and its biodiversity. Nowadays, we know that both nurture and nature, like cellular and molecular pathways, play a key role in this craniofacial development. If the cellular and/or molecular pathways are disturbed by gene mutations and/or teratogens during the embryonic period, a malformation can occur.¹ The term malformation is derived from the Latin words *malus* meaning "bad" or "wretched," and *formare* meaning "to form, to shape."¹



The aim of this thesis is to explore the genetic alterations that cause craniofacial malformations.

Craniofacial malformations

Craniofacial malformations can be subdivided in craniosynostosis, craniofacial clefts and facial dysostosis.

Craniosynostosis occurs in 1:2,100-2,500 live births,²⁻⁴ and the prevalence is reported to be rising.⁵ It is characterized by the premature fusion of calvarial sutures. This fusion restricts the normal growth of the skull, brain and face (Figure 1.1). Therefore, surgical correction is often needed within the first year of life.⁶ Craniosynostosis can occur isolated, without any additional anomalies, or as part of a syndrome often caused by a genetic alteration. A genetic cause is implied if coronal or multiple suture synostosis is observed, if a patient shows symptoms of growth or developmental retardation, and/or if a patient shows other congenital anomalies.

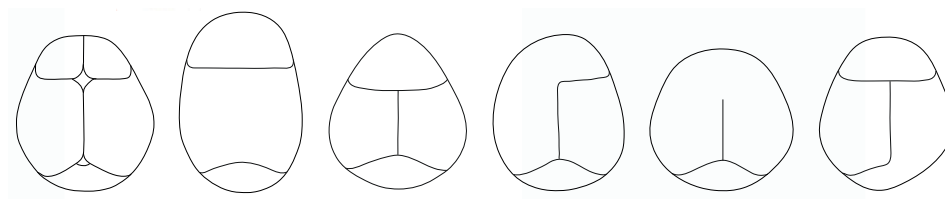


Figure 1.1. Craniosynostosis. From left to right: normal calvarial sutures; sagittal suture synostosis leading to a scaphocephalic head shape; metopic suture synostosis leading to a trigonocephaly; left coronal suture synostosis leading to left-sided plagiocephaly; bicoronal suture synostosis leading to a brachycephalic head shape and right lambdoid suture synostosis leading to left-sided occipital plagiocephaly.

Craniofacial clefts are very rare, they occur in approximately 1 per 400,000 births.⁷ Just like in clefts of the lip and palate (CLP), a fusion defect occurs of various embryologic facial prominences that frequently manifests as an epithelially lined fissure. Also, these craniofacial clefts can occur due to failure of mesodermal penetration or due to disturbances of outgrowth of bone centres (for example in the mandible).⁸ However, in contrast to CLP, all facial parts and all tissues of the face can be affected in craniofacial clefts. The severity of the malformation differs, depending on the involved facial structures and the extend of the cleft. Often, the classifications of Tessier⁹ and Van der Meulen¹⁰ are used to describe the cleft (Figure 1.2). A genetic cause is implied if the cleft occurs in the midline and -just like in craniosynostosis- if a patient shows symptoms of growth or developmental retardation, and/or if a patient shows other congenital anomalies.

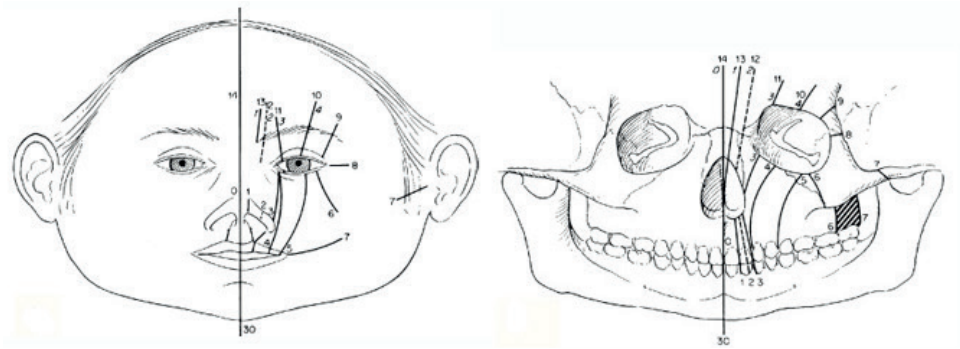


Figure 1.2. Tessier classification. Every line indicates one of the possible craniofacial clefts (Journal of Maxillofacial Surgery 1976).

The incidence of facial dysostosis ranges from 1 per 50,000 live births for Treacher Collins syndrome¹¹ to for example 3 per 1,000,000 for Nager syndrome in Finland.¹² Facial dysostoses are caused by underdevelopment of the structures derived from the first and second pharyngeal arches leading to malar and mandibular hypoplasia, dysplastic ears and eyelids, hearing loss and cleft palate.¹¹ A subdivision can be made into mandibulofacial dysostosis (without limb anomalies), and acrofacial dysostosis (with limb anomalies).¹¹ These disorders can be further subdivided in many subtypes. A genetic cause is identified in many of these subtypes.

The anatomy of the human head

As discussed previously, in case of a craniofacial malformation, the normal anatomy of the head is disrupted. As one might say that the head is the most complex structure of the body,¹³ the normal anatomy will be described first.

The human skull can be subdivided in two major parts:

1. the viscerocranium (or splanchnocranium). This is phylogenetically the oldest part of the head, representing the skeleton of the face, surrounding the oral cavity, the pharynx and the upper respiratory system. And 2. the neurocranium, surrounding the brain. The neurocranium, can be divided in two as well: a. the chondrocranium (or cranial base) and b. the dermatocranium (or cranial vault).¹⁴

The cranial vault consists of five principal bones (the paired frontals, paired parietals and the unpaired occipital).¹⁴ Between the cranial bones, fibrous joints are found consisting of mesenchymal cells, that are called sutures.¹⁴ Hence, there are six primary sutures: the paired coronal and paired lambdoid sutures, and a single metopic

and sagittal suture.^{14,15} The sutures allow temporary deformation and compression during partition, and serve as growth sites during development.¹⁶ If one of these sutures is fused prematurely, it is regarded as craniosynostosis.

The cranial base consists of eight paired cartilages on the ventral surface of the brain forming three fossa in which the brain rests. Cartilaginous joints are located between some of the bones, called synchondroses. These synchondroses are important growth centres of the craniofacial skeleton.¹⁴

The viscerocranium consists of several bones: two inferior nasal conchae, two lacrimal bones, one mandible, two maxillae, two nasal bones, two palatine bones, one vomer and two zygomatic bones.¹⁴ Sometimes, the hyoid bone, the ethmoid bone and the sphenoid bone are also considered as part of the viscerocranium. As in the cranial vault, sutures are located between the bones of the face.¹⁴ Disrupted fusion and outgrowth of progenitors of the facial bones play a key role in the development of facial clefts.

Embryology of the head and face

To understand the development of craniofacial malformations, it is essential to understand the development of the face and skull. This development begins early in embryonic life and continues until adolescence.¹⁷

Development of the embryo

It all starts with fertilization; a sperm and egg cell fuse and their pronuclei subsequently fuse to form a zygote.^{17,18} The zygote divides with a cleavage division of one per day. Reaching the morula stage (16 cells) at day three and a stage of compaction at day 4.¹⁷ During this process, the embryonic genome becomes activated.^{17,18} Then cavitation occurs; a blastocoel forms within the embryo. The embryo becomes a blastocyst with an inner cell mass, which will form the body of the embryo, and a trophoblast, the outer epithelial layer.¹⁷ Just before implantation in the endometrium of the uterus (day 6/7), the cells of the inner cell mass become arranged in an epithelial configuration.¹⁷ The main upper (dorsal) layer of cells is known as the epiblast and the lower (ventral) layer is called the hypoblast or primitive endoderm, leading to a bilaminar disk.¹⁷ Gastrulation starts at the beginning of the third week. During gastrulation a primitive streak is formed in the epiblast at the caudal end of the bilaminar embryo.¹⁷ Cells migrating through the primitive streak form the mesoderm and endoderm, and the remaining epiblast becomes ectoderm.¹⁷ At the anterior end of the primitive streak, the primitive node is formed, that eventually will give rise to the notochord.¹⁷ Cranial to the notochord the oropharyngeal membrane comes into existence.¹⁷ The primitive streak and notochord act as the primary inductors of the nervous system. The neural plate is formed and, after

further shaping, neurulation occurs;¹⁷ the neural plate is folded laterally to form a neural groove.¹⁷ Opposing sides of the thickened epithelium of the neural groove fuse to form the neural tube that will give rise to the brain.¹⁷



Development of the face

The development of the face occurs predominantly during the 5th and 8th week of development.¹⁴

Very early, the brain is the dominant component of the craniofacial region.¹⁷ Beneath the brain, the face is represented by the stomodeum, the primitive mouth.^{14,17} The stomodeum is sealed off from the primitive gut by the oropharyngeal membrane, which breaks down by the end of the first embryonic month.¹⁷ At week four of gestation, the facial development is centred around the stomodeum.^{14,17,19} Surrounding the stomodeum, several prominences constitute the building blocks of the face: the unpaired frontonasal prominence in the rostral midline, the paired maxillary (more rostrally) and the paired mandibular processes (more caudally) originating from the first pharyngeal arch.^{14,17,19}

On either side of the frontonasal prominence, nasal placodes develop into horseshoe-shaped structures, each consisting of a nasomedial process and a nasolateral process.¹⁷ Subsequently, nasal pits begin to form that deepen until they break through into the oral cavity.¹⁴

The mandibular and maxillary processes fuse. Subsequently, the maxillary processes fuse to the nasomedial processes to form the upper lip and jaw.^{14,17} The region of fusion of the nasomedial and maxillary processes is marked by an epithelial seam, the nasal fin that will form the nasolacrimal duct and lacrimal sac.^{14,17} The maxillary processes contribute to the maxilla (upper jaw), sides of the face and lips and the secondary palate.^{14,20}

The frontonasal prominence is displaced cranially, contributing to the forehead, bridge of the nose, primary palate, philtrum and upper lip.^{14,17,20} The nasomedial processes merge in the midline forming the intermaxillary segment, which gives rise to the philtrum of the lip, the premaxillary component of the upper jaw and the primary palate, the tip and crest of the nose, and a part of the nasal septum.^{14,17} The nasolateral processes form the alae of the nose.^{14,20}

The mandibular prominences form the mandible (lower jaw), including the caudal parts of the cheeks, the lower lip and chin.^{17,20}

When the basic facial structures take shape, they are invaded by cells associated with the first and second pharyngeal arches, that form several facial muscles.¹⁴ The remaining three pharyngeal arches produce small bones and cartilages of the ear and pharyngeal apparatus.^{11,14}

Development of the skull

The development of the skull starts between day 23 and 26 of human embryological development, when ossification centres destined to become bones of the cranial vault begin to form.²¹

Bones can develop either via endochondral ossification or intramembranous ossification. In endochondral ossification, chondroblasts form a cartilaginous model that is converted into bone by osteoblasts.^{14,15,22} Intramembranous ossification, on the other hand, occurs when bone is formed directly without passing through a cartilaginous stage.^{14,15,23}

The bones of the cranial base, that underlie the brain, are formed via endochondral ossification.¹⁴ The synchondroses serve as important growth sites.¹⁴

The majority of the bones of the facial skeleton (e.g. nasals, maxillae, premaxillae, zygomatic, mandible) and all cranial vault bones (e.g. frontal, parietal, and squamous temporal) are primarily formed by intramembranous ossification.¹⁴ The bones begin as ossification centres (a single ossification centre in, for example, the zygoma, and two or more ossification centres in the cranial vault bones). The ossification centres of the cranial vault fuse and growth occurs at the sutures from the edges of two opposing bones.^{16,24,25} Studies have shown that the expanding brain and dura mater play an important role in this growth.^{15,26-28} In humans, the biggest growth occurs in the first two years of life. At the age of seven, the growth of the neurocranium stops almost completely while the bones of the facial skeleton grow throughout puberty.¹⁴

Origin of cells

The tissues of the vertebrate head and face are derived from endoderm, mesoderm, ectoderm and cranial neural crest cells.¹⁹ The mesoderm and neural crest contribute to the facial mesenchyme.¹⁹ The mesodermal component gives rise to the voluntary muscles and endothelial cells while the neural crest-derived mesenchyme forms the majority of the facial skeleton.^{19,29,30} The pharyngeal arches are consisting of an outer ectodermal layer and an inner endodermal layer. In between these two layers are mesodermal cores which are initially surrounded by neural crest-derived mesenchyme.^{19,31-35} The cranial vault has a mixed origin. In mice and presumably in humans as well, the frontal bone is formed from neural crest, the parietal bones are formed by mesoderm.^{19,29,30} The sutures contain mesenchymal stem cells³⁶ and in the coronal sutures these stem cells originate from cephalic paraxial mesoderm.³⁷ The cranial base is also mixed; the anterior cranial base is largely derived from neural crest, while the posterior cranial base is formed by paraxial mesoderm.^{19,38-40}



It was the best of times, it was the worst of times, it was the age of foolishness, it was the epoch of belief: deoxyribonucleic acid⁴¹

Deoxyribonucleic acid (or DNA) codes for the information that is needed to synthesize proteins. The way the information is coded in DNA is extremely clever; 1. it is very densely stored, 2. it is three-dimensionally stored, and 3. it often remains readable over millennia.⁴²⁻⁴⁴ These remarkable characteristics of DNA have led to more and more research concerning data storage in DNA. Now, one can store the opening sentence of "A Tale of Two Cities"⁴¹ (and the header of this chapter) and even an entire book in DNA.⁴⁴

DNA exists of two polymers of nucleotides.⁴⁵ Nucleotides exist from deoxyribose (a sugar with five C-atoms), a nitrogenous base (attached to C1' of the sugar) and a phosphate group (attached to C5').⁴⁵ The nucleotides bind via phosphodiester bonds, forming a polynucleotide.⁴⁵ The nitrogenous bases of two polynucleotide strands bind by hydrogen bonds and Van der Waals forces.⁴⁵ Adenine binds to Thymine (two hydrogen bonds) and Guanine binds to Cytosine (three hydrogen bonds). This phenomenon is called base pairing.^{18,45} The two connected polynucleotide strands are coiled around a common axis and form a double helix.⁴⁵ These double helices are wind around histones and non-histone proteins, forming the nucleosome.⁴⁵ Without the nucleosome the DNA would be too long to fit in the nucleus.⁴⁵

In the nucleus the DNA is organized into chromosomes. Humans have 22 pairs of autosomal chromosomes and one pair of sex chromosomes (XX for females or XY for males).¹⁸ From each pair of chromosomes, in principle, one chromosome is inherited from the mother and one from the father.⁴⁵

Mitochondria

Besides the DNA in the nucleus (called genomic DNA), there is also DNA present in the mitochondria (called mitochondrial DNA). These organelles are located in the cytoplasm of the cell. The mitochondrial DNA codes for only 37 genes and is usually inherited completely from the mother.⁴⁶

Coding DNA

The genomic DNA of humans comprises of approximately 3.2 billion base pairs.⁴⁵ Specific segments of the genome, called genes, contain the information for proteins.^{18,45} Less than 5% of the 3.2 billion base pairs give rise to genes. People used to consider the remaining base pairs as "junk DNA".¹⁸ However, more and more we start to learn that this so-called junk DNA encodes regulatory elements.^{47,48}

Most genes contain regions coding for proteins, called exons. In most genes, these exons are interrupted by noncoding regions, called introns.¹⁸ Two consecutive processes are used to convert the coding information of the exons into proteins. First, the protein RNA polymerase starts at the transcription start site (5' of the gene) to transcribe the gene resulting in an unstable heteronuclear RNA.^{18,45} RNA processing takes place and the introns are removed by splicing.⁴⁵ Single-stranded messenger RNA (mRNA) moves out of the nucleus to the ribosomes. The ribosomes translate the mRNA into proteins, linking various amino acids via multiple steps.^{18,45} Three nucleotides (=one triplet) encode one amino acid. In human proteins, 20 different amino acids are used to build the proteins from the messenger RNA molecules.^{18,45}

Splice sites

Within the intron, a donor site (5'end of the intron) and an acceptor site (3'end of the intron) are required for splicing. Comparison of many genes resulted in the observation that there is a consensus sequence around the splice donor (-gt) and splice acceptor site (ag-).^{49,50} Mutations in the consensus sequence can lead to extension of the exon, exon skipping, or retaining of (part of) the intron when the splice site becomes useless or a cryptic splice site is being preferred. Cryptic splice sites are sites in the genome that contain the consensus sequence, but are normally not used as a splice site or are used only at a low frequency.⁵¹ Also, alternative splicing is seen, which means that the same gene can be spliced in several ways resulting in different proteins.

Expression

In principle, all cells from an organism contain the same DNA coding information. However, each cell type shows its own protein expression pattern which can also vary in time of development (an osteoblast expresses different proteins than a cell of the skin, and the osteoblast expresses different proteins in early embryological stages than later in life). Several factors, like transcription factors or external signals, play a key-role in this expression pattern.^{18,45}

Mitosis

Most eukaryotic cells are diploid.¹⁸ Which means that a nucleus contains two copies of each chromosome.¹⁸ Before a cell can divide into two new cells, the DNA must be replicated resulting in two identical replicas of the original DNA.^{18,45} Several control mechanisms, like proofreading and mismatch repair, prevent and/or correct mistakes. This all happens in the Synthesis phase (S) of the cell cycle, consisting of a prophase, metaphase, anaphase and telophase.¹⁸ In the Mitotic phase (M), the nucleus divides and the cell splits in two.⁴⁵ Hence, the replicated chromosomes separate, with each daughter

cell getting a copy of each chromosome during cell division.¹⁸ The S and M phase are separated by a G1 and G2 phase, in which mRNA and proteins are synthesized and the cell grows.^{18,45}



Meiosis

Meiosis is a special type of cell division forming germ cells (sperm or egg cells).⁴⁵ It comprises of two rounds, each round containing a prophase, a metaphase, an anaphase and a telophase.¹⁸ Meiosis I separates homologous chromosomes.^{18,45} Meiosis II separates sister chromatids. Leading to the formation of 4 haploid germ cells.^{18,45} The four germ cells are genetically different from each other and from the parental cell, due to recombination. Fusion with a germ cell of another individual generates a diploid zygote.^{18,45}

What if it goes wrong: heritable diseases

During meiosis, chromosome pairs are divided over daughter cells. Although the chromosomes appear alike under the microscope, they may be slightly different at specific base pairs (alleles).¹⁸ This variation can cause heritable traits leading to a specific phenotype. Hence, the genotype is the genetic information that an individual carries, the phenotype is any characteristic of an organism caused by the genotype and environmental factors.^{45,52,53}

Variation

Approximately 3,000,000 nucleotides per genome differ from the reference genome, at least 20,000 of these differences are located within the coding regions.^{53,54} These variants can be common, present in more than 1% of the population, or rare, occurring in less than 1% of the population.

Variants can exist of substitutions meaning that a certain nucleotide is changed into one of the other nucleotides.¹⁸ If this change is common it is also called a Single Nucleotide Polymorphism (SNP), and if it is a rare change, theoretically, it's called a Single Nucleotide Variant (SNV).⁵³ However, this terminology is often used interchangeably. SNPs are the most common cause of genetic variation.^{53,55} If the variant leads to a substitution of the encoded amino acid into another amino acid, it is called a missense mutation. If it leads to a premature stop-codon, it is called a nonsense mutation.¹⁸

A nucleotide can also be deleted or inserted.¹⁸ These small "indels" are the second most common cause of genetic variation.^{53,56} If an indel is not a multiple of 3 bp in length it can cause a shift of the reading frame (frameshift)⁵⁷ leading to the possible introduction of a stop codon or nonsense mediated decay.¹⁸ Nonsense mutations and indels combined are called truncating mutations.

Variants that do not alter the encoded amino acid are called synonymous variants.⁵³ Occasionally, these synonymous changes alter transcription because a cryptic splice site is created and this phenomenon can result in a non-functional protein. A good example of this phenomenon has been described for a synonymous sequence change in *FGFR2*. Using RNA analysis it was shown that the synonymous sequence change was a pathogenic mutation, confirming the diagnosis.⁵⁸

Besides of the small indels, deletions and insertions can also occur on a much larger scale.⁵⁷ These large variants are called Copy Number Variation (CNV).⁵³ Also, structural variants can occur, like inversions and translocations.⁵³

Inheritance

The current theory concerning the classical division of heritable traits was initially postulated by George Mendel. However, more and more traits are identified that are not inherited in accordance to these so-called Mendelian inheritance patterns. The following inheritance patterns are known:

Autosomal dominant

Inheritance of one affected allele can cause a certain trait. Usually one of the parents is affected. An autosomal dominant disorder can affect and be transmitted by both males and females. There's a 50% chance to transmit the trait to the next generation. Many of the craniosynostosis-syndromes show an autosomal dominant inheritance pattern.⁴⁶ Non-penetrance and clinical variability can play a key role in the presentation of these diseases. Reduced penetrance means that a person carries a mutation without showing any signs of the disease⁴⁶ (this is the case in for example *TCF12*-related craniosynostosis; many of the parents do not suffer from craniosynostosis although they do carry the mutation).⁵⁹ Variability means that people with the same mutation have a varying severity of the disease⁴⁶ (in for example families with Crouzon syndrome the expression of the disease can vary from exorbitism in one member, to severe pansynostosis with increased intracranial pressure in the other).

Autosomal recessive

Both alleles, so both the paternal and the maternal allele, need to carry a pathogenic mutation to cause the disease.⁴⁶ This can be a. homozygous recessive: the alleles are exactly the same, as is seen in *IL11RA*-related craniosynostosis⁶⁰ or b. compound heterozygous: the alleles are different, like in Burn-McKeown syndrome⁶¹ or Carpenter Syndrome.⁶² Usually parents are asymptomatic carriers. It can affect and be transmitted by all sex. There is a 25% risk that a subsequent child is affected.⁴⁶

***X-linked dominant***

The inherited trait is located on the X-chromosome and causes a disease in males and in females. Females are usually more mildly affected compared to males due to X inactivation. A female carrier of the pathogenic mutation has a 50% chance to transmit the trait. In case of an affected male, all his daughters but none of his sons will be carrier of the pathogenic mutation.⁴⁶ A remarkable example of an X-linked dominant disorder is craniofrontonasal syndrome. This syndrome is caused by pathogenic mutations in *EFNB1*, located on the X-chromosome. In contrast with the expected, females are more severely affected than males, due to cellular interference.⁶³

X-linked recessive

The inherited trait is located on the X-chromosome and pathogenic mutations in these X-linked genes will result in a phenotype in carrier males (who are hemizygous, meaning that they have only one X chromosome with the pathogenic mutation) and in a female who is homozygous for the pathogenic mutation, or in case of skewed X-inactivation. The mother is usually an asymptomatic carrier.⁴⁶

Y-linked

The trait is located on the Y-chromosome. So, only males can be affected. All sons of an affected father are affected.⁴⁶

Mitochondrial

Mitochondrial DNA is transmitted solely by the ovum. Therefore, mutations in this DNA are only transmitted from mother to child. All sexes can be affected.⁴⁶

Parental imprinting

One of the copies of a gene is silenced or “switched off”. This is a normal phenomenon. But if a variant is located on the other allele (which is “on”), a trait can occur.⁴⁶ This is seen in Prader-Willi and Angelman syndrome.⁶⁴

Mosaicism

The mutation is not present in all cell types. For example, a mutation can be present in buccal cells, but not in blood cells. Therefore, a mutation can be easily missed, since DNA diagnostic testing is often performed on DNA derived from blood.⁴⁶ An example of mosaicism is described in *ZIC1*-related craniosynostosis.⁶⁵

Chromosomal abnormalities:

- Numerical: an abnormal number of chromosomes can occur. Well-known is trisomy 21 causing Down syndrome. Trisomy 18 (Edwards syndrome) and trisomy 13 (Patau syndrome) occur less frequently.
- Structural abnormalities vary from deletions (part of the chromosome is missing), duplications (part of the chromosome is duplicated), inversions (part of the chromosome is inverted), insertions (part of the chromosome is inserted in another chromosome), rings (part of the chromosome is forming a ring structure) and translocations (parts of two chromosomes are rearranged; exchanging material from one chromosome to another). Structural abnormalities can be balanced, which means that the normal amount of chromosomal material is present in a germ cell, or unbalanced, resulting in one germ cell having extra chromosomal material, while the other one is missing chromosomal material.^{18,46}

Complex

A certain trait is caused by a combination of multiple different variants at different locations.

De novo mutations

Mutations can be inherited, but can also occur *de novo*, which means that the mutation is not present in one of the parents, but has arisen in the proband during meiosis. Note that germline mosaicism cannot be excluded. The *de novo* mutation rate is estimated between 1×10^{-8} and 3×10^{-8} per base per generation,⁶⁶⁻⁷¹ corresponding to approximately 74 novel SNVs per genome per generation,⁷² the indel mutation rate has been estimated to be approximately 4×10^{-10} per position (3 novel indels per genome per generation),⁷³ CNVs larger than 100kb are estimated to occur *de novo* in approximately one out of every 50 individuals.^{72,74} The mutation rates have been shown to vary throughout the genome,^{68,75} across families,^{67,68,70} and to depend on paternal age.^{67,76} If a *de novo* mutation occurs, the risk of a second child with the same mutation is very low, in the affected child, however, it will act exactly the same as an inherited mutation.

Examining the DNA

There are more than 2,500 human genes described that cause a disease if a mutation is present.⁷⁷ Over the years, different molecular techniques have been developed to study the genetic causes of heritable diseases.



Karyotyping

Karyotyping is one of the oldest tools to identify chromosomal aberrations. The technique stains chromosomes in metaphase which are then analysed using light microscopy. So cells have to be cultured to obtain an adequate number of dividing cells in metaphase. With the development of chromosome banding techniques, a resolution of 5-10 Mb can be achieved.⁴⁶

Traditional sequencing

In 1977, two papers have been published that changed the world of genetic research.⁷⁸ Maxam and Gilbert and Sanger, Nicklen and Coulson described methods for DNA sequencing.⁷⁸⁻⁸⁰ Since the publication of these papers, the latter has been used extensively for research and diagnostic purposes.⁷⁸ This dideoxy-sequencing or Sanger sequencing technique has also been used to generate the first data of the human genome in 2001.^{81,82}

The technique starts by annealing a primer to single stranded template DNA which is then amplified by Polymerase Chain Reaction (PCR).⁷⁸ The 3'-OH end of the primer serves as the starting point for synthesis of a new DNA strand.⁷⁸ A DNA polymerase catalyses the incorporation of dNTPs (dATP, dCTP, dGTP and dTTP) and ddNTPs (ddATP, ddCTP, ddGTP and ddTTP).⁷⁸ If a ddNTP is incorporated, synthesis terminates.⁷⁸ The reaction products are separated by size by subjecting them to polyacrylamide gel electrophoresis.⁷⁸ The traditional dideoxy-sequencing method uses radioactive labelled dNTPs to visualize them (hence referred to as radioactive Sanger sequencing).⁷⁸ The radioactive labels have been replaced by fluorophores, paving the way for automated DNA sequencing.^{78,83} Other developments that have contributed to the increased throughput of dideoxy sequencing are the use of a set of four chain-terminating ddNTPs carrying different fluorophore groups,⁸⁴ thermal cycle sequencing⁸⁵ and capillary sequencing, using capillary electrophoresis instead of polyacrylamide gel electrophoresis.^{78,86-88}

This method has become the gold standard for examining the DNA at the resolution of single nucleotides.⁵³ It has the potential to detect all kinds of genomic variation in a single experiment. However, disadvantages are the low throughput,⁵³ the use of synthetic primers and the possibility of false negative results due to SNPs underneath the primer.⁷⁸

Fluorescent *in situ* hybridisation (FISH)

In 1982 a molecular cytogenetic technique has been developed in which fluorescently labelled DNA probes are hybridized to metaphase spreads or interphase nuclei enabling the detection of aneuploidy and chromosomal rearrangements using light

microscopy.^{78,89} Locus-specific probes can be applied to detect specific micro-deletion syndromes and sub-telomere region-specific probes have been developed to detect chromosomal imbalances at the telomeres. One of the limitations of FISH is the inability to detect small deletions.⁷⁸

Microarray

In 1983 the first concepts of the microarray technique have been described.⁹⁰ This technique can assay large amounts of biological material (DNA for example). It is based on measuring differences between fluorescent signals of patient DNA compared to control DNA.⁷⁸ Patient and control DNA are labelled using fluorescent dyes and hybridized onto a microarray chip that contains a collection of microscopic spots of DNA sequences (Bacterial Artificial Chromosome clones or oligonucleotides).^{53,78} For each spot, the ratio of the fluorescent signals of patient and control DNA is measured.^{53,78} So, relative gains and/or losses of DNA can be detected.^{53,78,91,92} The oligonucleotide-based arrays have a resolution of 1 kb.⁹³ Therefore, the microarray technique has replaced karyotyping for most implications. However, because a ratio is used, balanced genomic rearrangements such as inversions remain undetected⁹⁴ and the location of additional copies on the genome remains unknown.^{53,78,95}

Multiplex ligation-dependent probe amplification (MLPA)

MLPA is a method by which up to 60 different sequences can be targeted in a single semi quantitative polymerase chain reaction-based assay.^{96,97} Each MLPA probe consists of two parts that can be ligated to each other when hybridized to a target sequence.⁹⁸ The two parts of the probe differ in length.⁹⁸ The short part contains a target-specific sequence (21–30 nucleotides) at the 3' end and a common 19 nucleotide sequence, identical to the labelled PCR primer, at the 5' end.⁹⁸ The long part contains a 25–43 nucleotide target-specific sequence at the 5' phosphorylated end, a 36 nucleotide sequence that contains the complement of the unlabelled PCR primer and is common to all probes at the 3' end, and a stuffer sequence of variable length in between.⁹⁸ It is only when the two parts of the probe are both hybridised to their target that they can be ligated into a single probe, containing both the forward and reverse primer sequence.⁹⁷ PCR amplification of the ligation products follows. Following the PCR, the resulting amplification products are separated by sequencing electrophoresis.⁹⁷ An MLPA probe set is designed so that the length of each of its amplification products is unique.⁹⁷

Applications include the detection of exon deletions/duplications, detection of trisomies, characterisation of chromosomal aberrations, SNP and mutation detection; DNA methylation analysis and relative quantification of mRNA.⁹⁷ The MLPA reaction is fast, relatively inexpensive, and easy to perform, and the equipment needed for

MLPA analysis is present in most molecular biology laboratories.⁹⁶ Limitations are the sensitivity to contaminants, the complicated development of the probes, and the inability to investigate single cells or detect unknown point mutations.⁹⁷



Next generation sequencing

With the increasing need of sequencing complete genomes instead of single genes, new massive parallel sequencing techniques have been developed.⁷⁸ This so-called next generation sequencing has the ability to sequence millions of DNA fragments in a highly parallel fashion, and the potential to detect all kinds of genomic variation in a single analysis.^{53,78} Different techniques have been developed. Well-known platforms are those of Roche (the “traditional” 454 pyrosequencing),^{99,100} Illumina HiSeq^{101,102} and Life Technologies (SOLiD and Ion Torrent semiconductor sequencing).^{78,103} Nowadays, these companies offer benchtop sequencers and revolutionary developments resulted in faster and cheaper equipment and chemistry.

Currently, whole exome sequencing is mostly applied. This means that the complete coding region of the human genome is sequenced. But, with the improving throughput, whole genome sequencing is more and more applied, which means that both the coding regions and non-coding regions are sequenced. One of the leading companies that offers whole genome sequencing is Complete Genomics, a BGI Company.

Whole genome sequencing

Since whole genome sequencing by Complete Genomics Inc., a BGI company (CGI) has been used in many of the studies described in this thesis, this technique will be explained in more detail. CGI uses a technique called sequencing by ligation to sequence the whole genome and the mitochondrial DNA at high coverage ($\geq 80\times$) as described by Drmanac *et al.*¹⁰⁴

Genomic DNA (gDNA) is fragmented by type IIS restriction enzymes and directional adapters are inserted, resulting in circles of DNA.¹⁰⁴ The circles are replicated with Phi529 polymerase,¹⁰⁵ leading to hundreds of tandem copies of single-stranded DNA.¹⁰⁴ These long copies consolidate; they ball up to small particles of DNA that are referred to as DNA nanoballs.¹⁰⁴ These DNA nanoballs are approximately 200 nanometres in diameter. They contain both genomic DNA sequence and adapter sequence. A genomic library (the collection of total genomic DNA from a single organism) contains millions of DNA nanoballs that together represent the complete genome.

The DNA nanoballs are adsorbed to a silicon chip of 25 by 75 mm.¹⁰⁴ The silicon is photolithographically etched (the same technique that is used in the semiconductor industry) to create a grid pattern of small spots of ~ 300 nm.¹⁰⁴ One DNA nanoball sticks to one spot. When the silicon chip is filled with DNA nanoballs it is called a DNA nanoball

array. One array contains up to 180 billion bases of genomic DNA. The DNA array will now be sequenced. An anchor probe binds to the adapter sequence (still present in the DNA nanoball). A ligase enzyme then attaches one of four possible fluorescent-labelled probes to the anchor (corresponding to an A, T, C or a G), depending on the sequence being read in the fragment. By imaging the fluorescence during each ligation step, the sequence of nucleotides in each DNA nanoball can be determined. This technique is called combinatorial probe anchor ligation sequencing (cPAL).¹⁰⁴

cPAL is based on unchained hybridisation and ligation technology.^{103,106,107} Via this technique, up to 10 bases adjacent to each of eight anchor sites can be read, resulting in a total of 31- to 35-base mate-paired reads (62 to 70 bases per DNA nanoball).¹⁰⁴ After sequencing, the reads are mapped to a human genome reference and assembled as described by Carnevali *et al.*¹⁰⁸ A custom software suite (SOM) employing both Bayesian and de Bruijn graph techniques is used for this purpose.¹⁰⁴ For every genomic location it's determined if there is a diploid reference, a variant or a no-call present.¹⁰⁴ Detected variants include single nucleotide polymorphism (SNPs), indels, substitutions, copy number variants (CNVs, up to 50 bps), structural variants (SVs), and mobile element insertions (MEIs)(see also <http://www.completegenomics.com/customer-support/>).

Getting rid of the noise: filtering

By whole genome sequencing, a huge amount of data is generated; per patient sample 1.9 Tb. Hence, storage and data management ask more and more attention, especially since the costs of data storage grow out of proportion. To identify the genetic cause of a certain trait (i.e. craniofacial malformations) in this "Big Data" also clever data analysis methods are needed. The variants need to be filtered in a structured approach. The approach used in many of the studies described in this thesis is described below.

Inheritance pattern

First of all, the variants need to be present according to the correct inheritance pattern based on the family pedigree.

If a proband is affected, but the parents of the proband are not affected, the following inheritance patterns are tested: *de novo*, dominant with reduced penetrance, recessive (both homozygous and compound heterozygous) or, in case of a male proband, X-linked. If a proband is affected, and one of the parents as well, the tested inheritance pattern is: dominant, and, if applicable, X-linked. If a proband is affected and the parents are consanguineous: homozygous recessive.



Minor allele frequency

The patients in our cohort show craniofacial malformations, which are very rare. Therefore, one might expect that the genetic cause should be very rare as well. This assumption implies that variants should be discarded that occur in a public database and have a minor allele frequency of >1%. Databases that are used for filtering are dbSNPv37, the Welllderly cohort,¹⁰⁹ Public60,¹¹⁰ ExAC,¹¹¹ Exome Variant Server,¹¹² Genome of the Netherlands (GoNL)^{70,76} and 1000 Genomes.¹¹³

Predicted effect of the variant

Looking at the remaining variants, the pathogenicity can be scored based on *in silico* prediction programs and conservation of the affected nucleotide and amino acid.

In silico prediction programs

In silico prediction programs try to discriminate between pathogenic and benign variants by predicting the deleteriousness of a nonsynonymous variant. This deleteriousness is based on the predicted effect of the variant on the sequence homology, the damage it may cause to the protein structure and function and on the evolutionary conservation. RNA *in silico* prediction programs are used to predict the effect on splicing (of both non-synonymous and synonymous variants). Used programs are SIFT,¹¹⁴ Polyphen,¹¹⁵ LRT,¹¹⁶ Mutation Taster,¹¹⁷ FATHMM,¹¹⁸ Radial SVM LR,¹¹⁹ VEST3¹²⁰ and CADD raw/phred.¹²¹

Conservation

DNA sequences between different species are highly similar. For example, chimpanzees and humans share more than 98% of their DNA sequence.^{45,122,123} By comparing different species, many evolutionary conserved regions are identified both at DNA and protein level. That is, regions that are highly similar in a large amount of species. If a variant occurs in such a region, theoretically, one might expect it to be more harmful. Programs that can be used are GERP++¹⁰⁹ and PhyloP.¹²⁴

Evaluation of the gene

Occasionally, a mutation is identified that has been described previously as a cause of a craniofacial malformation. However, often other variants occur in genes associated with craniofacial malformations. To identify known craniofacial malformation genes more easily, manually curated lists with “known cranio genes” are generated based on literature and the POSSUMweb database (Pictures of Standard Syndromes and Undiagnosed Malformations, Murdoch Children’s Research Institute, Royal Children’s Hospital, Melbourne, Australia). Also, a list containing all genes that are associated with a “craniofacial” phenotype in the Mouse Genome Database (at the Mouse Genome

Informatics website, The Jackson Laboratory, Bar Harbor, Maine, USA) and a list with all the genes that do not have a loss-of-function variant in Exome Variant Server¹¹² are used to evaluate the mutated gene.

If a pathogenic variant is identified in a gene that is not in one of these lists, a thorough literature search is performed to evaluate the function of the gene, its pathway and, if available, functional data.

Validation cohorts

If a new candidate gene is identified, repeated occurrence of variants in that specific candidate gene across multiple families indicates a stronger association. Hence, re-sequencing the gene in other clinically similar patient samples might result in the identification of multiple families with variants in the gene.

Why tell me, why

Identification of the genetic cause is critical for genetic counselling. But it can also have implications for clinical management.

A precise molecular diagnosis is essential for genetic counselling

Based on the molecular diagnosis, a legitimate recurrence risk for a following pregnancy can be given. Also, more clarity about heredity can be given to the proband when he or she enters the reproductive phase.

If a child is born with craniosynostosis, for example, and tested negative with appropriate gene-specific tests and the parents are clinically not-affected, an empiric recurrence risk of 5-7% is given to the parents (2% for sagittal and metopic synostosis, 5% for unicoronal synostosis and 10% for bicoronal and multisuture synostosis).^{125,126} It is estimated that a proband with non-syndromic sagittal, metopic or unicoronal synostosis has a risk of ~5% of passing the disease on while probands with bicoronal or multisuture synostosis have a ~30-50% risk.¹²⁵ Since the most common genetic causes of other craniofacial malformations like Treacher Collins syndrome are dominant, the proband is often told that he/she has a risk of 50% of passing the disease further on. These numbers affect reproductive decision-making significantly, and can lead to the wish of preimplantation genetic diagnosis or not having children.



The molecular diagnosis has implications for clinical management

By increased knowledge of the association between the genotype and the phenotype, clinical management can be ameliorated. When a genetic cause is known, patients can be screened for associated symptoms earlier. Muenke syndrome, for example, is associated with sensory hearing deficits that can lead to speech- and language delay. Patients with a p.Pro250Arg mutation in *FGFR3*, the genetic cause of Muenke syndrome, should be monitored for hearing deficits so therapy can be offered early and speech- and language delay will be prevented.

What we know now

Craniofacial malformations can be subdivided in craniosynostosis, craniofacial clefts and facial dysostosis. During embryological development, the normal anatomy of the craniofacial region is disturbed. This disruption of the normal development can be caused by alterations in the genetic code. Thanks to genetic research we now know:

Craniosynostosis

That monogenic and chromosomal factors play a role in the aetiology of craniosynostosis.^{125,127,128} Over 100 human syndromes are reported to be associated with craniosynostosis.¹²⁹ Since the identification of a mutation in *MSX2* as a cause of craniosynostosis-Boston type in 1993,¹³⁰ mutations in at least 57 genes are identified in syndromic craniosynostosis.¹²⁷ However, a genetic cause can be identified in only ~24% of the cases,⁵⁹ with mutations in *FGFR2*,¹³¹⁻¹³⁴ *FGFR3*,¹³⁵⁻¹³⁷ *TWIST1*,^{138,139} *TCF12*,⁵⁹ *ERF*¹⁴⁰ and *EFNB1*^{63,141} occurring most frequently. In clinical practice, patients with craniosynostosis are now tested for mutations in *FGFR2*, *FGFR3* and *TWIST1* and, if applicable, any of the 57 craniosynostosis genes as described by Twigg *et al.* To exclude chromosomal abnormalities, an array comparative genomic hybridisation analysis (aCGH) is undertaken (replacing karyotyping).

Craniofacial clefts

In contrast to craniosynostosis, only a small number of genetic causes have been identified in craniofacial clefts. This might be due to the very low incidence of these malformations. Until now, at least 11 genes and 2 genomic deletions are associated with craniofacial clefts. Remarkably, an overlap is seen with genes causing craniosynostosis. Mutations in for example *EFNB1*⁶³ cause a phenotype consisting of craniosynostosis and craniofacial clefting and mutations in *TWIST1* (personal communication) cause either craniosynostosis or craniofacial clefting.¹⁴² If a patient presents with craniofacial clefting and a genetic cause is suspected, *EFNB1*, *ALX3* and/or *SHH* can be tested and an aCGH analysis is undertaken.

Facial dysostosis

Patients with facial dysostosis can be affected symmetrically, which is the case in the Treacher-Collins like syndromes. But asymmetrical appearance also occurs, which is the case in hemifacial microsomia. Although hemifacial microsomia occurs much more often, familial occurrence is only rarely seen and genetic causes have not been described. On the other hand, in case of the Treacher-Collins like syndromes, at least eight genes have been identified to be mutated. If a patient presents with a Treacher-Collins like syndrome, these genes are tested and an aCGH analysis is undertaken.

Table 1.1. Overview of diagnostic tests.

Craniosynostosis	Craniofacial clefts	Facial dysostosis
<i>FGFR2</i>	<i>EFNB1</i>	<i>TCOF1</i>
<i>FGFR3</i>	<i>ALX3</i>	<i>POLR1A</i>
<i>TWIST1</i> + MLPA	<i>SHH</i>	<i>POLR1C</i>
aCGH	aCGH	<i>POLR1D</i>
Any of the 57 craniosynostosis genes as described by Twigg <i>et al.</i> ¹²⁷ can be added based on the phenotype		<i>EFTUD</i>
		<i>SF3B4</i>
		<i>DHODH</i>
		aCGH



What we want to know

Although many craniofacial malformations have been attributed to external factors like teratogens, foetal head constraint or bad luck, we now know that at least a part can be attributed to genetic alterations. In this era of rapidly developing genetic sequencing techniques, it seems a good time to study the genetic causes of craniofacial malformations further.

The aim of this thesis is to study genetic alterations that cause craniofacial malformations by addressing the following objectives:

1. Improve our knowledge on genes previously known to be causing craniofacial malformations.

Focusing predominantly on:

- *FGFR2*: a. identification of new mutations in *FGFR2* (**chapter 2**)
b. identification of synonymous mutations as a cause of Crouzon syndrome (**chapter 3**)
- *EFNB1*: expanding the general phenotype of patients with craniofrontonasal syndrome (**chapter 4**)

2. Identification of new craniofacial genes by next generation sequencing

Focusing predominantly on:

- *TCF12*: a. identification of mutations in *TCF12* as a frequent cause of coronal craniosynostosis (**chapter 5**)
b. identification of rearrangements in *TCF12* as a cause of *TCF12*-related craniosynostosis (**chapter 6**)
- *ZIC1*: identification of gain-of-function mutations in *ZIC1* as a cause of coronal craniosynostosis and learning disability (**chapter 7**)
- *TXNL4A*: identification of mutations in *TXNL4A* as a cause of Burn-McKeown syndrome and choanal atresia (**chapter 8**)

3. Assess next generation sequencing as a diagnostic tool in craniofacial malformations

Diagnostic value of exome and whole genome sequencing in craniosynostosis (**chapter 9**)

Methods

Patient selection

Based on clinical description, facial photographs and imaging (CT, MRI and/or invasive intracranial pressure measurements etc.), patients were selected that had coronal or multiple suture synostosis, or any other form of craniosynostosis in combination with an affected family member or in combination with growth or developmental retardation and/or other congenital anomalies. Also, patients with craniofacial clefts were selected if the cleft occurred in the midline and -just like in craniosynostosis- if family members were affected, and/or if a patient showed symptoms of growth or developmental retardation, and/or other congenital anomalies. Lastly, patients with facial dysostosis were selected.

The clinical phenotype of the probands was evaluated by a Plastic Surgeon and a Clinical Geneticist and appropriate genes were tested negative prior to whole genome sequencing. Overall, this accounted for dideoxy sequencing of *FGFR2*, *FGFR3*, *TWIST1*. MLPA of *TWIST1* and/or array comparative genomic hybridisation (aCGH) in case of craniosynostosis; *EFNB1*, *ALX3*, *SHH* and/or aCGH in case of craniofacial clefts; and *TCOF1*, *POLR1A*, *POLR1C*, *POLR1D*, *EFTUD*, *SF3B4*, *DHODH* and/or aCGH in case of facial dysostosis.

In general, whole genome sequencing was performed on trios (i.e. DNA of the proband and its parents). In case of other affected family members, this DNA was also included (see Table 10.3 for patient characteristics, tested genes and included family members).

Ethical approval was given by the board of the Medical Ethical Committee for whole genome sequencing (MEC-2012-140) and for retrospective data analyses (MEC-2013-547). Informed consent was received from the study participants or their legal representatives. A total of 317 samples was included.

Whole genome sequencing and data analysis

DNA was extracted from whole blood samples. Prior to shipment of the DNA, the quality of the DNA samples was measured by PicoGreen® (ThermoFisher Scientific, Waltham, MA, USA) and gel electrophoresis. At least 5 µg of DNA (50-200 µl of 75-300 ng/µl DNA) per patient was shipped to Complete Genomics, a BGI Company (Mountain View, CA, USA). There, internal quality control measurements and, to exclude sample swaps, a gender check and 96-SNP genotyping assay were performed.

Whole genome sequencing at high coverage ($\geq 80\times$) as described by Drmanac *et al.*¹⁰⁴ was performed subsequently. Mapping of the reads and calling of the variants was performed as described by Carnevali *et al.*¹⁰⁸ Reads were mapped using GRCh37/hg19 and dbSNP build 130. Data were analysed using cga tools version 1.6.0.43 and Spotfire 7.0.0 (TIBCO Software Inc., Boston, MA, USA).



Output files

The data were given per sample in a so-called 'Var-file'. A 'List variants-file' was extracted from the Var-files of the trio. Frequencies in the Welllderly cohort were added [Scripps Welllderly Genome Resource, The Scripps Welllderly Study, La Jolla, CA [December, 2015]], funding provided by Scripps Health and NIH/NCATS UL1 TR00114), genes were annotated and occurrence of the variant in the family was added ('Test variants'), contributing to the 'Small variants-table' (see Figure 1.3 for an overview of these output files and first filtering steps).

Identity by sequence (IBS)

To check the family relationship of the samples of a trio, a so-called IBS script (Complete Genomics) was run using the small variant table. Also, the samples were checked for regions of homozygosity using the Var-files. In that way, consanguinity of the samples and uniparental disomy could be visualized.

Identification of variants

De novo

Lists of *de novo* variants (SNVs and indels) were generated using the 'CallDiff script' (Python script kindly provided by Complete Genomics) as described by Gilissen *et al.*¹⁴³ Roughly, this script compared the variant file of the proband to the variant files of the father and the mother to identify if a variant was truly *de novo*. Two confidence scores were provided per variant (one for the comparison with the father and one for the comparison with the mother). Using these confidence scores, the authenticity of the *de novo* variants were ranked.

Dominant

The above mentioned analysis for *de novo* variants was performed using the CallDiff script. All the below mentioned analyses were performed using the 'Multiple genome analysis script', also provided by Complete Genomics. To analyse dominant inheritance, the mat_het (for variants inherited from the mother) and pat_het files (for variants inherited from the father) were used.

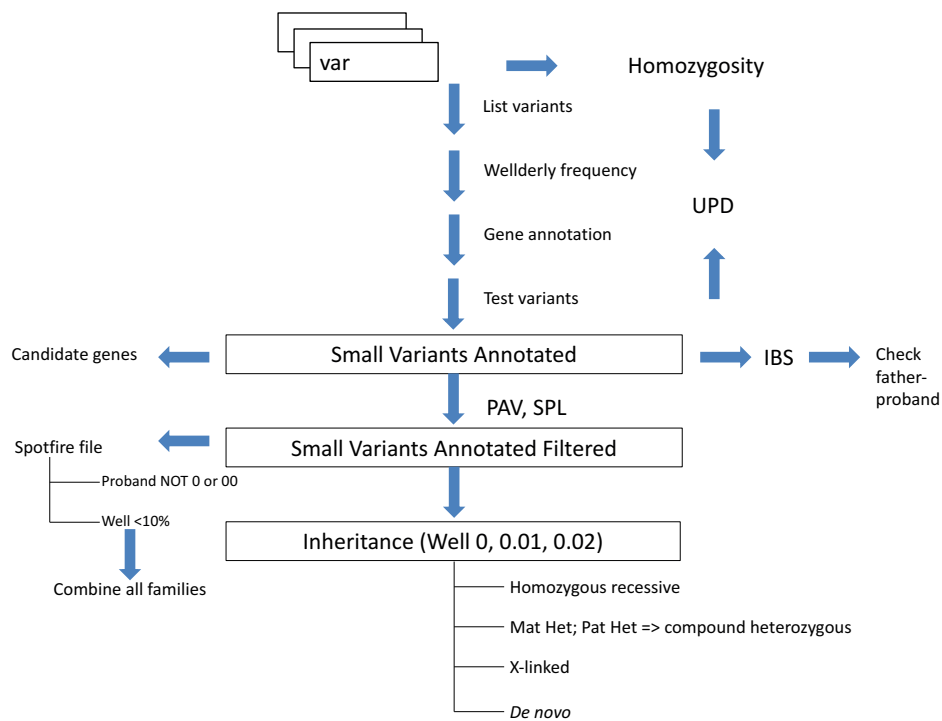


Figure 1.3. Overview of output files and first filtering steps of the Multiple genome analysis script. IBS = Identity by sequence, Mat Het = Inherited from the mother, Pat het = Inherited from the father, PAV = Protein affecting variant, SPL = Splice site variant, UPD = Uniparental Disomy, Var = Var-file, Well = Welllderly.

Recessive

The mat_het and pat_het files were also used to analyse recessive inheritance. Variants were selected that fit into the correct inheritance pattern (both homozygous variants as well as compound heterozygous variants).

X-linked

X-chromosomal variants in females and males were analysed using the Small Variants-table.

Copy number variation and structural variation

Detection of copy number and structural variants was done by discordant mate-pair analysis. Junctions were sequenced, e.g. adjacent regions in the sequenced genome that are not adjacent in the reference genome (due to tandem duplications, distal

duplications, deletions, inversions, translocations and complex events). Variants were filtered based on inheritance pattern and a Complete Genomics baseline frequency of 0. The called structural variants were ranked on mate pair count. The variants with a mate pair count >10 were manually curated.



Mode of inheritance

If a phenotype was seen only in the proband, a *de novo* inheritance pattern was tested. Based on the findings in *TCF12* and *ERF*,^{59,144} we know that reduced penetrance might also be possible, therefore a dominant inheritance pattern was also tested. Furthermore, an autosomal recessive inheritance pattern, a compound heterozygous inheritance pattern and in males an X-linked inheritance pattern was also tested for SNVs and CNVs/SVs. If one of the parents was also affected, a dominant inheritance pattern and (if applicable) an X-linked inheritance pattern was tested. Additionally, based on the phenotype, an overall comparison of the findings of the unrelated families was performed (cohort analysis).

Generation of gene lists involved in craniofacial malformations (cranio genes)

To classify genes as known cranio genes we used several gene lists.

1. Manually curated lists of genes that are described to be causative for the appropriate phenotype.
2. All genes associated with the appropriate phenotype in the POSSUMweb database (Pictures of Standard Syndromes and Undiagnosed Malformations, Murdoch Children's Research Institute, Royal Children's Hospital, Melbourne, Australia).
3. All genes that were associated with a "craniofacial" phenotype in the Mouse Genome Database (Mouse Genome Informatics website, The Jackson Laboratory, Bar Harbor, Maine, USA).
4. All genes without loss-of-function variants in Exome Variant Server.¹¹²
5. All genes with a *de novo* mutation in the Deciphering Developmental Disorders (DDD).¹⁴⁵

Annotation of variants

A custom in-house bioinformatics pipeline was created in Tibco Spotfire to annotate ANNOVAR data, Public60¹¹⁰ and 1000 Genomes¹¹³ data to the output of the Multiple Genome Analysis Script. The annotated information is shown in Table 1.3.

Table 1.2. Overview of different filtering steps.

	Father	Mother	Proband	Identification	Annotation	Scoring	Prioritization
Small variants							
<i>De novo</i>	00	00	01	CallDiff script	VarScores and VarFilter Gene components Impact Inheritance Frequency in variant databases Predicted effect Cratio genes	Minimal somatic score > 0	Within CDS and CSS ($\pm 2bp$) MAF $\leq 10^{-5}$ Welllderly Pathogenicity Gene
Dominant- inherited from the father	01	00	01	Multiple Genome Analysis script	See above	VarScore	Within CDS and CSS ($\pm 2bp$) MAF $\leq 10^{-5}$ Welllderly Pathogenicity Gene
Dominant- inherited from the mother	00	01	01	Multiple Genome Analysis script	See above	VarScore	Within CDS and CSS ($\pm 2bp$) MAF $\leq 10^{-5}$ Welllderly Pathogenicity Gene
Homozygous recessive	01	01	11	Multiple Genome Analysis script	See above	VarScore	Within CDS and CSS ($\pm 2bp$) MAF ≤ 0.03 Welllderly Pathogenicity Gene
Compound heterozygous	01 00	00 01	01 and 01	Multiple Genome Analysis script	See above	VarScore	Within CDS and CSS ($\pm 2bp$) MAF ≤ 0.1 Welllderly Pathogenicity Gene
X-linked	0 1 1	01 00 01	01 or 1 or 01 or 11	Multiple Genome Analysis script	See above	VarScore	Within CDS and CSS ($\pm 2bp$) VarScore MAF ≤ 0.03 Welllderly Pathogenicity Gene



Table 1.2. (continued)

	Father	Mother	Proband	Identification	Annotation	Scoring	Prioritization
Structural Variants							
De novo	See above			SV calling	Gene components	Mate pair count > 10	Inheritance pattern Complete Genomics baseline frequency of 0% Ranked on mate pair count
Autosomal dominant							
Autosomal recessive							
X-linked							
Multiple unrelated families analysis (cohort analysis)							
CS	NA			All above mentioned options	See above per item	See above per item	Inheritance pattern Within CDS and CSS (±2bp) MAF <= 0.1 Wellderly Pathogenicity Gene
S + FH							
Chiari							
IIICP							
Cleft and basal encephalocoele							
Rugose							

CDS = Coding Sequence, CNV = Copy number variants, CS = Coronal suture synostosis, CSS = Splice site, FH = Family history, IICP = Increased intracranial pressure, MAF = Minor Allele Frequency, NA = Not applicable, Rec = Recessive, S = Sagittal suture synostosis, SV = Structural variants.

Validation of candidates

All putatively causative variants were confirmed. SNVs were validated by dideoxy sequencing. PCR amplification was carried out in a total volume of 25 µl using Invitrogen (Life Technologies Ltd, Paisley, UK) or Takara master mix (Takara Bio Inc., Otsu, Shiga, Japan). PCR products were purified using Agencourt AMPure (Agencourt, Beckman Coulter Inc., Brea, CA, USA). Direct sequencing was performed using Big Dye terminator version 3.1 (Applied Biosystems, Foster City, CA, USA). Dye terminators were removed using Agencourt CleanSeQ (Agencourt) and loaded on an ABI 3130XL Genetic Analyzer (Applied Biosystems). The sequences were analysed using SeqPilot version 4.1.2 build 507 (JSI Medical Systems GmbH, Kippenheim, Germany).

Candidate pathogenic CNVs and SVs were validated using breakpoint spanning PCRs or deletion specific PCRs (as described by Goos *et al.*¹⁴⁶). For breakpoint spanning PCRs, primer sequences were chosen to be located ~100-200 base pairs from the predicted junction. For deletion specific PCRs, one forward and one reverse primer were designed outside the deletion. The third primer was designed in the deleted region in such a way that the PCR product resulting from the mutant allele was smaller than the PCR product produced from the wildtype allele. The amplification reactions were performed according to standard procedures. Products were electrophoresed on agarose gels. To confirm the exact position of the breakpoints, the PCR products were sequenced. PCR products were purified with ExoSAP-IT (USB, Affymetrix, Cleveland, OH, USA). Dideoxy sequencing of both strands was performed using Big Dye terminator version 3.1 (Applied Biosystems, Foster City, CA, USA) as recommended by the manufacturer. Dye terminators were removed using SephadexG50 (GE Healthcare, Pittsburgh, PA, USA) and loaded on an ABI 3130XL Genetic Analyzer or ABI 3730 (Applied Biosystems).

Classification system

A classification system based on five classes was used to classify the candidate variants.¹⁴⁷

Class 1: benign

Class 2: likely benign

Class 3: variant of unknown significance (VUS)

Class 4: likely pathogenic

Class 5: pathogenic

In figure 1.4 the classification flowchart is shown.

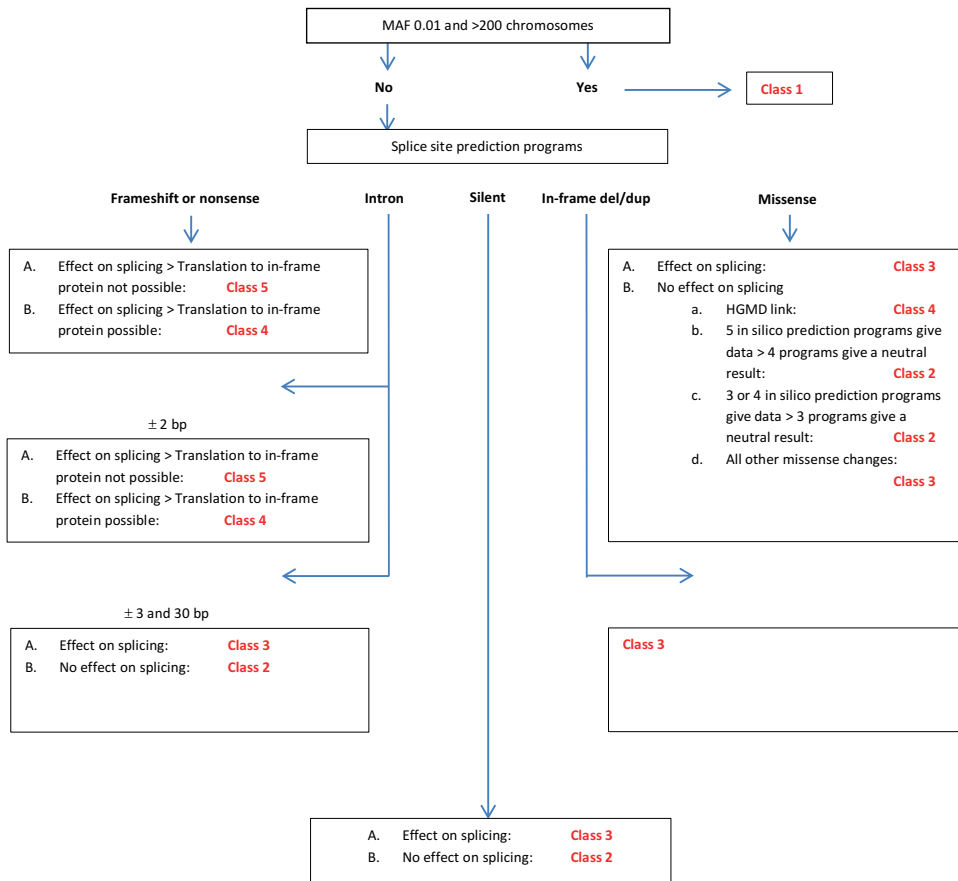


Figure 1.4. Classification flowchart. Del = Deletion, Dup = Duplication, MAF = Minor allele frequency.

Confirmation of pathogenicity

1. When a previously described pathogenic mutation was observed, the identified variant was assumed to be pathogenic.
2. If a mutation was observed in a previously described gene with a phenotype similar to our patient, the phenotype of the patient was re-evaluated for the syndrome (like the *ANKRD11* mutation) and if applicable assumed to be pathogenic.
3. If variants were identified in the same gene in more than one case with a similar phenotype, this observation was suggestive that the sequence change had a pathogenic effect. Especially if the sequence changes were present in a highly conserved domain. In these cases, repeated occurrence of candidate genes across multiple cases was checked in the 317 samples. To confirm pathogenicity, candidate genes were screened in our patient test cohort and a replication cohort in Oxford. Genes were inserted in GeneMatcher to identify similar cases in other cohorts (<https://genematcher.org/>). And, if possible, the biological consequence of a candidate was validated.

Pathogenic mutations

The pathogenic mutations were described according to HGVS nomenclature¹⁴⁸ and submitted to the Leiden Open Variation Database (<http://www.lovd.nl>).

**Table 1.3.** Annotated information.

Variant	Chromosome position	
	^a Variant type	Snp
		Sub
		Del
		Ins
	^a Reference and allele sequence	
	^a VarScore and VarFilter	
	^a Component	Coding sequence
		Splice site (acceptor/donor)
		Intron
		UTR
		Promoter region
	^a Impact	Missense
		Nonsense
Frameshift		
Delete		
Insert		
Disrupt		
Nonstop		
Nonstart		
^a Transcript		
^a Nucleotide position		
^a Protein position		
Inheritance		
Frequency in variant databases	^a dbSNPv37	
	^a Welllderly ¹⁰⁹	
	^b ExAC ¹¹¹	
	^b Exome Variant Server ¹¹²	
	^b GoNL ^{70,76}	
	^c Public60 ¹¹⁰	
	^c 1000 Genomes ¹¹³	
Predicted effect	^b <i>In silico</i> prediction	SIFT ¹¹⁴
		Polyphen ¹¹⁵
		LRT ¹¹⁶
		Mutation Taster ¹¹⁷
		FATHMM ¹¹⁸
		Radial SVM LR ¹¹⁹
		VEST3 ¹²⁰
	CADD raw/phred ¹²¹	
	^b Conservation	GERP++ ¹⁰⁹
		PhyloP ¹²⁴

Del = Deletion, Ins = Insertion, SNP = Single Nucleotide Polymorphism, Sub = Substitution, UTR = Untranslated region. ^aData from Complete Genomics, ^bdata from Annovar, ^cdata from sequencing projects.



Chapter 2

A novel mutation in *FGFR2*

Jacqueline A.C. Goos, Ans M.W. van den Ouweland, Sigrid M.A. Swagemakers, Annemieke J.M.H. Verkerk,
A. Jeannette M. Hoozeboom, Marie-Lise C. van Veelen, Irene M.J. Mathijssen, Peter J. van der Spek

American Journal of Medical Genetics Part A November 2014

Abstract

Craniosynostosis is a congenital anomaly that can occur as an isolated condition or as part of a syndrome. Although several genes are known to cause syndromic craniosynostosis, only 24% can be attributed to known genes. Therefore, it is likely that more mutations and other genes are involved. We present the identification of a novel point mutation in fibroblast growth factor receptor 2 (*FGFR2*), c.812G>T, p.(Gly271Val). Furthermore, we describe a mutation that has been identified just recently c.1851G>C, p.(Leu617Phe). In addition, we describe findings from a sequence analysis of all coding exons and exon/intron boundaries of *FGFR2* performed on 124 patients with syndromic craniosynostosis.

Introduction

Craniosynostosis, characterized by the premature fusion of calvarial sutures, can occur as an isolated condition or as part of a syndrome. Previously, a syndrome was diagnosed based on the patient's clinical appearance. For example, the distinct features in Apert syndrome, particularly, of the hands and feet, were easily recognizable, whereas differentiation between other syndromes, like Saethre-Chotzen and Muenke, was more difficult. In the last 20 years, genetic tests have been developed to confirm the genetic aetiology of many syndromes. Nowadays, the genetic causes of most common syndromes have been described and a causal mutation is identified in about 24% of patients with craniosynostosis.⁵⁹



Several craniosynostosis syndromes are caused by mutations in fibroblast growth factor receptor 2 (*FGFR2*). For example, the mutations first described cause a clinical appearance similar to Crouzon syndrome (CS);¹³³ however, mutations in *FGFR2* are also known to cause isolated craniosynostosis, Pfeiffer,¹⁴⁹ Apert,¹³¹ and Beare-Stevenson cutis gyrate syndrome.¹⁵⁰ In addition, cases are described in which phenotypically different craniosynostosis patients have exactly the same genotype.^{149,151,152} In particular, the distinction between Crouzon, Pfeiffer, and Jackson-Weiss syndrome appears to be irrelevant, although the diagnosis 'Pfeiffer syndrome' is most often used for the more severe presentation of the non-Apert *FGFR2* mutations. Consequently, the diagnosis of a syndrome is shifting from a solely clinical diagnosis towards a molecular one. In clinical practice, patients with craniosynostosis are now tested for mutations in *FGFR2*, *FGFR3*, and *TWIST1*. Usually, a limited number of exons of *FGFR2* are tested.

Here, we present the identification of a novel point mutation and a point mutation that has been described recently in *FGFR2* in these exons. In addition, we analysed all coding exons and exon/intron boundaries in 124 patients with syndromic craniosynostosis to gain more information on mutations in other *FGFR2* coding regions.

Patient 1

A Caucasian boy was born as the first child of non-consanguineous phenotypically normal parents; at birth the mother was 28 and the father 31 years old. The boy was born at 40 weeks of gestation and weighed 3,580 g. The pregnancy was uncomplicated. During neonatal examination, a severe scaphocephalic head shape was observed (Figure 2.1). Physical examination showed scaphocephaly with clear frontal bossing and exorbitism, and a head circumference of 43 cm (+2.24 SD). The upper and lower extremities showed broad first digits and partial syndactyly of the second and third toes. No symptoms of obstructive sleep apnoea (OSA) were diagnosed. A clinical suspicion of Crouzon/Pfeiffer syndrome was raised, due to the peri-orbital features. Bicoronal and

sagittal suture synostosis were seen on skull radiographs and confirmed by 3D-CT at age 3 months. No intracerebral anomalies were seen. At age 8 months, the boy underwent a supra-orbital advancement and fronto-parietal remodelling.

Over time, restricted growth of the maxilla became clear and resulted in dental crowding, with a narrow and retruded maxilla. At age 9 years, the skull growth stagnated and the boy developed papilledema. Intracranial pressure (ICP) measurements showed borderline elevated ICP with two plateaus higher than 25 mmHg and a mean value of 13 mmHg during sleep. The CT scan showed signs of elevated ICP, wide lateral ventricles and narrowed basal cisterns. An MRI scan showed widened third and lateral ventricles, scalloping of the skull, narrowed corpus callosum, deficient periventricular white matter, and a Chiari I malformation. Furthermore, a holocord syrinx, reaching to the caudal cone, and sacral arachnoid cysts were seen. Because of the borderline ICP, papilledema, and the Chiari I malformation a biparietal expansion with distraction was performed at age 10 years. The papilledema disappeared. The boy did not develop clinical signs of Chiari I malformation or holocord syrinx.

He had a normal development, with an IQ of 114. Since the clinical phenotype resembled Crouzon/Pfeiffer syndrome, genetic testing was performed for mutations in *FGFR2*. A heterozygous point mutation was found at c.812G>T, p.(Gly271Val) (see Supplementary Figure 2.1 for the sequence electropherogram). This mutation was not found in the parents, indicating that the mutation arose *de novo*. Paternity testing confirmed the family relationship. This mutation was not found in 378 control chromosomes. To determine whether this variant had been identified in other individuals, we checked our in-house Huvariome database¹⁵³ consisting of 290 genomes, and the Exome Variant Server (EVS). The variant was not present in either database. According to the 1000 Genomes (1000G) database,¹⁵⁴ another variant had been described in the COSMIC database^{155,156} at the same location [c.812G>A, p.(Gly271Glu) COSM29823] in a malignant melanoma sample (MAF = 0.001). This single-nucleotide polymorphism (SNP) was identified as probably damaging.

The p.Gly271Val variant was entered in Polyphen-2,¹¹⁵ SIFT,¹⁵⁷ MutationTaster¹¹⁷ and Align GVGD,¹⁵⁸ and results ranged from possibly damaging to disease causing (Table 2.1). Furthermore, the nucleotide and amino acid were highly conserved. Combining these results, this variant was very likely to be the mutation causing the phenotype of this patient.

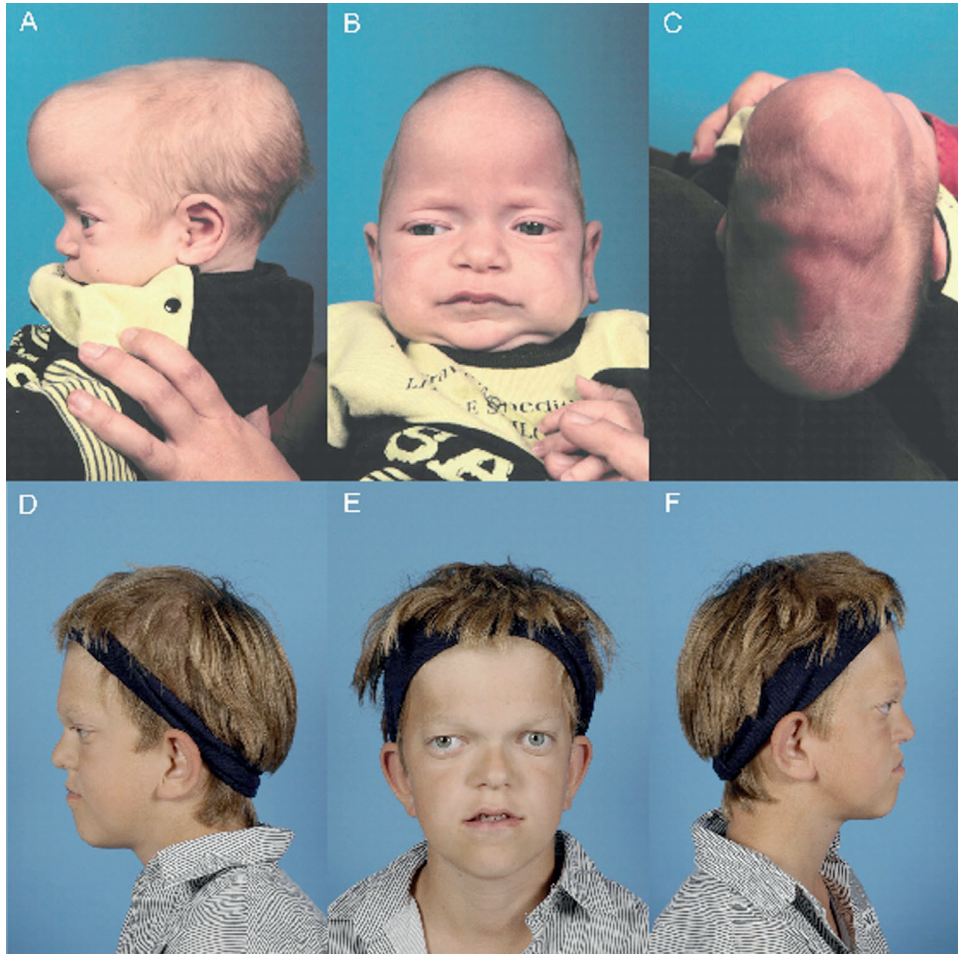


Figure 2.1. Facial photographs of Patient 1. A-C: pre-operatively at age 2 months. D-F: post-operatively at age 10 years.

Patient 2

A male patient aged 39 years with craniofacial features resembling Crouzon/Pfeiffer syndrome returned to our clinic. He wanted to know whether his condition was caused by a genetic alteration. At first referral (age 20 years) the patient had not received surgical treatment for his craniofacial disorder. He presented with mild retrusion of the forehead, low frontal hairline, exorbitism, mild orbital dystopia, a narrow maxilla, maxillary hypoplasia with mild malocclusion and small incisors, syndactyly of the third and fourth fingers, and camptodactyly of both fifth fingers. No information was

available regarding the presence of craniosynostosis, but the patient had no obvious abnormal head shape. On genetic testing, the same c.812G>T, p.(Gly271Val) mutation in *FGFR2* was identified.

Patient 3

A boy of African descent was born after an uncomplicated pregnancy at 40 weeks gestation with a birth weight of 3,580 g. An abnormal head shape was seen immediately after birth. Physical examination showed scaphocephaly with frontal bossing, a palpable ridge over the sagittal suture, and a head circumference of 52 cm (+5.68 SD). The eyes had some scleral show as a result of the hypoplastic infra-orbital rim. No hand or foot deformities were observed. Skull radiographs suggested synostosis of the sagittal suture. This was confirmed on 3D-CT. Besides slightly enlarged peripheral cerebrospinal fluid spaces, no intracranial abnormalities were seen. The boy underwent a fronto-biparietal remodelling of the skull at age 11 months with uneventful recovery. At age 3 years he underwent orchidopexy because of bilateral undescended testicles. When the boy was 8 years old, he presented clinical features of OSA and exorbitism. Moreover, he had maxillary hypoplasia. Therefore, at age 10 years he underwent Le Fort III osteotomy, combined with external distraction. He had delayed development with an IQ of 77.

Because of the mild exorbitism and maxillary hypoplasia the clinical diagnosis of CS was suggested. Therefore, genetic testing of *FGFR2* was performed. A heterozygous point mutation was found at c.1851G>C, p.(Leu617Phe) (Table 2.1). The DNA of both parents tested negative for the variant. Paternity tests confirmed the family relationship. The variant was not present in the Huvarome, 1000G, or the EVS database. The *in silico* programs predicted a probably damaging or even a disease-causing effect. The nucleotide was weakly conserved, but the amino acid was highly conserved. Combining these results, this SNP was very likely to cause the phenotype of our patient. During preparation of this case report, this mutation was also identified by Suh *et al.*¹⁵⁹

Sequencing coding exons and exon/intron junctions

Previously, patients were tested by Single Strand Conformation Polymorphism (SSCP) or sequence analysis for mutations in a limited number of exons of *FGFR2*. However, in several patients no mutation in *FGFR2* was found, even though such a mutation was suspected. Therefore, we decided to analyse all coding exons and the exon/intron junctions of *FGFR2* (NM_000141.4) of 124 patients with syndromic craniosynostosis (Supplementary Table 2.1 presents detailed information). Patients were selected if they had fusion of the coronal sutures or of more than one suture, if they had a positive family history, or if they had other congenital anomalies or psychomotor disability (Supplementary Table 2.2 presents the clinical features of the tested patients). By expanding the analysis, we found two previously described mutations, i.e. c.314A>G,

p.(Tyr105Cys) and c.755C>G, p.(Ser252Trp), and four unclassified variants (UVs). Table 2.1 presents a summary of these variants. An extensive overview of the clinical features of these patients is presented in Supplementary Table 2.3.

Discussion

It is established that all *FGFRs* originate from the same ancestral gene.¹⁶⁰ They code for a group of transmembrane-receptor proteins crucial for early embryonic development. Similar to *FGFR1* and *FGFR3*, *FGFR2* comprises three extracellular immunoglobulin-like domains (IgI, IgII, and IgIII), a single-pass transmembrane segment, and a split tyrosine kinase (TK1/TK2) domain.¹⁶⁰⁻¹⁶² The p.Gly271Val mutation is located in the IgIIIa domain, and the p.Leu617Phe mutation is located in the TK domain.

The clinical features of our three patients resemble Crouzon/Pfeiffer syndrome. The regions in which the mutations are located harbour other pathogenic missense mutations causing CS.¹⁶²⁻¹⁶⁴ Both mutations described here arose *de novo*. The mutations were not seen in the EVS, the Huvariome, or in the 1000G Database and the majority of the *in silico* data predicted a disease-causing effect (Table 2.1). Furthermore, because both amino acids were highly conserved, the mutations were considered disease-causing mutations.

On sequence analysis of *FGFR2*, two previously described mutations and four UVs were found. Three of the UVs (i.e. c.1084+8C>T, c.1531G>A and c.2190C>T) were also found in the DNA of the clinically unaffected fathers. Because most families with syndromic craniosynostosis showed an autosomal dominant mode of inheritance, the decision as to whether or not a variant present in a parent is pathogenic has often been based on the phenotype. However, the findings of Sharma *et al.*⁵⁹ of substantial non-penetrance in a dominant form of craniosynostosis argue against this approach.

Three UVs were not present in the EVS, or in the Huvariome, whereas the c.2190C>T, p.(=) variant was present in the 1000G database. The c.23T>G, p.(Ile8Ser) variant was present in the EVS, the Huvariome, and in the 1000G database. According to five prediction programs, no variant had an effect on RNA splicing. The predictions of the *in silico* programs, if applicable, varied from benign to tolerated. The nucleotides were weakly conserved. The amino acid was weakly conserved for the c.23T>G, p.(Ile8Ser) variant and moderately conserved for c.1531G>A, p.(Ala511Thr). Combining these data, the UVs were considered non-pathogenic.

It was estimated that 94% of *FGFR2* mutations occur in IgIIIa (exon 8; NM_000141.4) or IgIIIC (exon 10), or in the intron sequence flanking IgIIIC¹⁶⁵ (as cited in Kan *et al.*¹⁶²) The p.Tyr105Cys variant is one of the few pathogenic mutations outside these mutation hotspots.¹⁶⁶ Although we found few variants by expanding the analysis to all coding exons and the exon/intron junctions, we did find the p.Tyr105Cys variant in the IgI



domain. In contrast, an *FGFR2* mutation screen in 259 craniosynostosis patients by Kan *et al.* revealed mutations in seven additional exons.¹⁶² These authors claim that, since mutations are identified outside the hotspots, a more extensive search for mutations is justified; with the revolutionary developments in genetic research this will become cheaper and easier. However, the present study again demonstrates that pathogenic mutations predominantly occur in the well-conserved functional regions.

Web resources

EVS: NHLBI GO Exome Sequencing Project (ESP), Seattle, WA (URL: <http://evs.gs.washington.edu/EVS/>) [May, 2013]).

Table 2.1. Summary of variants in *FGFR2* (accession number reference sequence NM_000141.4).

c.DNA position and change	Protein position and change	In HGMD	In EVS	In Huvarome (290 samples)	In 1000Genomes	Present in parents	Phenotype parents	Polyphen	SIFT	Mutation Taster	Align GVD	Grantham [0-215]	Conservation nucleotide	PhyloP [14,16,4]	Conservation amino acid	Domain	Denominated pathogenic
c.23T>G	p.(Ile8Ser)	N	Y	Y	Y	Na	N	B	TS = 0.24, M = 3.34	DCP = 0.564	C0 GV:244.82- GD:0.00	142	Mo	3.11	W	Hydrophobic leader sequence	N
c.314A>G	p.(Tyr105Cys)	Y	N	N	N	N	Na	PrD	DS = 0.00, M = 3.33	DCP = 1.0	C0GV:353.86- GD:0.00	194	Mo	4.00	Mo	Igl	Y
c.755C>G	p.(Ser252Trp)	Y	N	N	N	N	Na	PrD	DS = 0.01, M = 3.33	DCP = 1.0	C0GV:134.86- GD:66.04	177	H	6.26	H up to Tetraodon	Igll-Iglll linker	Y
c.812G>T	p.(Gly271Val)	N	N	N	N	N	Na	PoD	DS = 0.01, M = 3.33	DCP = 1.0	C15GV:79.35- GD:77.22	109	H	6.26	H up to Tetraodon	Iglla	Y
c.1084+8C>T		N	Na	Na	Na	Y	N	Na	Na	Na	Na	Na	Na	Na	Na	Na	N
c.1531G>A	p.(Ala511Thr)	N	N	N	N	Y	N	B	TS = 0.27, M = 3.33	DCP = 1.0	C0 GV:130.02- GD:0.00	58	Mo	2.30	Mo	Tyrosine kinase domain I	N
c.1851G>C	p.(Leu617Phe)	N	N	N	N	N	Na	PrD	DS = 0.00, M = 3.33	DCP = 1.0	C15 GV:0.00- GD:21.82	22	W	0.29	H up to C. elegans	Tyrosine kinase domain I	Y
c.2190C>T	p.(=)	N	N	N	Y	Y	N	Na	Na	Na	Na	Na	Na	Na	Na	Tyrosine kinase domain II	N

B = Benign, D = Deleterious, DC = Disease causing, H = High, M = Median, Mo = Moderate, Na = Not applicable, N = No, PoD = Possibly damaging, PrD = Probably damaging, S = Score, T = tolerated, W = Weak, Y = Yes.





Apparently synonymous substitutions in *FGFR2* affect splicing and result in mild Crouzon syndrome

Jacqueline A.C. Goos,* Aimée L. Fenwick,* Julia Rankin, Helen Lord, Tracy Lester, A. Jeannette M. Hoozeboom, Ans M.W. van den Ouweland, Steven A. Wall, Irene M.J. Mathijssen, Andrew O.M. Wilkie

*Equal contributors

BMC Medical Genetics August 2014

Abstract

Mutations of *fibroblast growth factor receptor 2* (*FGFR2*) account for a higher proportion of genetic cases of craniosynostosis than any other gene, and are associated with a wide spectrum of severity of clinical problems. Many of these mutations are highly recurrent and their associated features well documented. Crouzon syndrome is typically caused by heterozygous missense mutations in the third immunoglobulin domain of *FGFR2*.

Here we describe two families, each segregating a different, previously unreported *FGFR2* mutation of the same nucleotide, c.1083A>G and c.1083A>T, both of which encode an apparently synonymous change at the Pro361 codon. We provide experimental evidence that these mutations affect normal *FGFR2* splicing and document the clinical consequences, which include a mild Crouzon syndrome phenotype and reduced penetrance of craniosynostosis.

These observations add to a growing list of *FGFR2* mutations that affect splicing and provide important clinical information for genetic counselling of families affected by these specific mutations.

Introduction

Craniosynostosis defines the premature fusion of the cranial sutures and has an overall prevalence of 1 in 2,100–2,300 live births.^{2,3} Nearly one quarter of craniosynostosis has a genetic aetiology,^{59,128} there is considerable genetic heterogeneity and frequent phenotypic overlap between different syndromes. Genes encoding three members of the fibroblast growth factor receptor family (*FGFR1*, *FGFR2* and *FGFR3*) are commonly mutated in individuals with craniosynostosis. Heterozygous mutations in *FGFR2*, which are frequently recurrent, account for ~28% of genetic cases⁵⁹ and cause Crouzon,^{133,134} Pfeiffer,^{149,167,168} Apert,¹³¹ Beare-Stevenson¹⁵⁰ and bent bone dysplasia¹⁶⁹ syndromes. All involve synostosis of the coronal and other cranial sutures, a distinctive “crouzonoid” craniofacial appearance (comprising hypertelorism, exorbitism, prominent nose, and midface hypoplasia), but differ in the presence and extent of abnormalities of the hands and feet, other skeletal manifestations and dermatological features.^{125,170}



FGFR2, like the other members of the *FGFR* family, comprises an extracellular ligand-binding region (composed of three immunoglobulin-like domains), a single transmembrane peptide and a cytoplasmic tyrosine kinase domain. Mutually exclusive alternative splicing of exons IIIb and IIIc gives rise to epithelial and mesenchymal isoforms (*FGFR2b* and *FGFR2c*) respectively.¹⁷¹ These alternative extracellular domains interact with different repertoires of fibroblast growth factors (FGFs) to regulate downstream processes such as proliferation, differentiation and cell migration.¹⁷²

Here we describe two families heterozygous for the same, previously unreported apparently synonymous variant in *FGFR2* [p.(Pro361Pro)], although caused by differing nucleotide substitutions. The mutation carriers in both families exhibit features of mild Crouzon syndrome, and a minority required craniofacial surgery. We propose that this variant is in fact pathogenic and demonstrate the generation of abnormal cDNA products resulting from incorrect splicing of exon IIIc in the mutant allele. This finding highlights the challenges posed in interpreting such synonymous variants when providing genetic counselling for affected families.

Case presentations

Family 1

Individual III-1 (Figure 3.1A) was born after a normal pregnancy and was referred for craniofacial assessment at 2 years of age because prominent eyes and a head tilt. Her father II-1 (Figure 3.1B), grandmother I-1 and two deceased uncles were all said to have a similar appearance with prominent staring eyes, but had not required any surgery. She had an occipitofrontal circumference (OFC) of 50 cm (+1.1 SD) and was noted to have a mildly crouzonoid appearance, with slight exorbitism and midface retrusion. In view

of the mild crouzonoid features, sequencing of *FGFR2* exons IIIa and IIIc was requested. This demonstrated a heterozygous c.1083A>G, p.(Pro361Pro) variant within exon IIIc, which was also present in II-1 and I-1.

Computed tomography (CT) of the skull of individual III-1 at the age of 2.8 years demonstrated right lambdoid and occipitomastoid synostosis, all other major cranial sutures being patent. Ophthalmological review identified slightly reduced visual acuity and a latent divergent squint with slight left hypophoria. The patient is now 4 years old and has not undergone any surgical intervention, as she has a good overall head shape with no major midface retrusion, is making good developmental progress, and has no features to suggest significant intracranial restriction.

Family 2

The male proband (III-2 in Figure 3.1C), born after an uneventful pregnancy, was referred for craniofacial assessment at the age of 3 months. Physical examination showed a mild cloverleaf skull with temporal bulging and reduced OFC (36 cm; -2.2 SD), hypertelorism, and severe exorbitism mainly at the infra-orbital level. Skull X-ray and CT showed pansynostosis and multiple craniolacunae, with no intracerebral anomalies.

Owing to the severe peri-orbital features and the absence of deformations of the upper and lower extremities a clinical diagnosis of Crouzon syndrome was suggested. The patient's mother, grandmother and several cousins were reported to show mild facial features also suggestive of this diagnosis.

The proband underwent fronto-orbital advancement at the age of 5 months. Since the occiput was still severely flattened and both lambdoid sutures were fused, occipital craniotomy and remodelling was performed at the age of 12 months. Clumsiness and motor delay were first noted aged 18 months; psychological testing at the age of 12.8 years gave scores for non-verbal intelligence of 80 (SON-R) and visual-motor integration of 81. Clonidine was prescribed due to high distractibility and he underwent special education. During childhood, the exorbitism increased requiring further orbital advancement and cranial vault remodelling at the age of 8 years. Several deciduous and permanent teeth were extracted because of Class III malocclusion and dental crowding.

Genetic testing of *FGFR2* was performed, identifying the heterozygous point mutation c.1083A>T, p.(Pro361Pro) (Figure 3.2A). This variant was also present in his mother II-1.

Independently of these events, a second patient (III-1) was referred to the same clinic at the age of 10 years with a scaphocephalic head shape. He had previously undergone vault remodelling at the age of 16 months owing to bicoronal synostosis. At the time of referral, he had an occipito-frontal circumference of 48.5 cm (-2.8 SD), hypertelorism and severe exorbitism. In addition, he had mild maxillary hypoplasia and

both second premolars of the lower jaw were absent. Ophthalmic examination showed myopia with divergent strabismus of the right eye associated with reduced visual acuity. A monobloc procedure without distraction (Le Fort III and an advancement of the forehead) was performed.

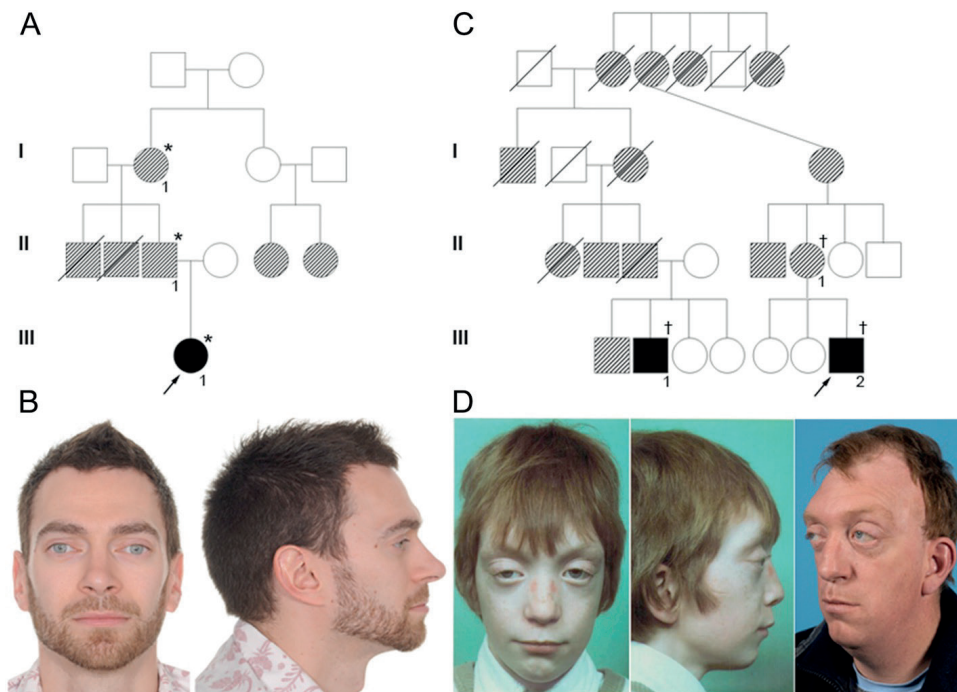


Figure 3.1. Pedigrees and facial features of individuals with *FGFR2* mutations. **A:** pedigree of Family 1; solid symbols represent clinically confirmed craniosynostosis and hatched symbols represent individuals with a similar crouzonoid appearance but without confirmed craniosynostosis. *Confirmed heterozygosity for c.1083A>G. **B:** facial appearance of II-1 from Family 1 aged 33 years. **C:** abbreviated pedigree of Family 2; notation of symbols as in part A. †Confirmed heterozygosity for c.1083A>T. **D:** facial appearance of III-1 from Family 2 aged 8.75 years (left) and 43 years (right).

Due to the severe peri-orbital features a diagnosis of Crouzon syndrome was suggested. Analysis of *FGFR2* identified the heterozygous point mutation c.1083A>T, p.(Pro361Pro). His father, grandmother and great-grandmother had a similar craniofacial appearance. Based on the pedigree analysis, it is evident that III-1 and III-2

are third cousins and that the *FGFR2* mutation present in these two branches is identical by descent (Figure 3.1C). Apart from III-1 and III-2, none of the other affected family members had undergone craniofacial surgery.

Materials and methods

Ethics approval for the study was obtained from NRES Committee London - Riverside (09/H0706/20) and the Medical Ethical Committee of the Erasmus University Medical Centre Rotterdam (MEC-2013-547). Venous blood was collected into PAXgene Blood RNA tubes (Qiagen) from individuals II-1 (Family 1) and III-1 (Family 2), and RNA was extracted according to the associated protocol. cDNA was synthesized using the Fermentas RevertAid First-Strand Synthesis kit with random hexamer primers according to the manufacturer's instructions.

cDNA was amplified using a forward primer in *FGFR2* exon IIIa (5'-TCGGAGGAGACGTAGAGTTTGTCTGC-3') used in combination with a reverse primer in exon 11 (encoding the transmembrane (TM) domain; 5'-TGTTACCTGTCTCCGCAGGGGATA-3'). DNA bands were cut out and gel purified using the Q-Spin gel extraction kit (GeneFlow). Dideoxy sequencing was carried out on the resulting DNA products. The resulting cDNA products were numbered according to NCBI Reference Sequence: NM_000141.4.

Results

The synonymous variants c.1083A>G and c.1083A>T occur at the -2 position of the 5' (donor) splice site of *FGFR2* exon IIIc (Figure 3.2A). The neural network splice site predictor (http://www.fruitfly.org/seq_tools/splice.html) generates a score for the wild type donor of 0.88, which is reduced to 0.37 by the A>G transition, and to 0.19 by the A>T transversion. In these circumstances, use of a cryptic splice site (score 0.84) within exon IIIc, 51 nucleotides upstream from the end of the exon, is expected based on analysis of a previous mutation c.1084+3A>G.¹⁷³ This would lead to an in-frame deletion of 17 amino acids.

Amplification of cDNA from individuals heterozygous for either the *FGFR2* c.1083A>G or the c.1083A>T variants demonstrated the presence of two additional bands, not present in the wild type control, at ~430 bp and 330 bp (Figure 3.2B). Sequencing of the normal 479 bp product from these individuals showed complete absence of the mutant allele (illustrated in Figure 3.2C for II-1 from Family 1), indicating that both mutations abolish use of the normal exon IIIc donor splice site. Sequencing of the ~430 bp product confirmed that the cryptic splice donor within exon IIIc was preferred in the mutant allele (Figure 3.2D), while the ~330 bp product demonstrated complete skipping of exon IIIc (Figure 3.2E).

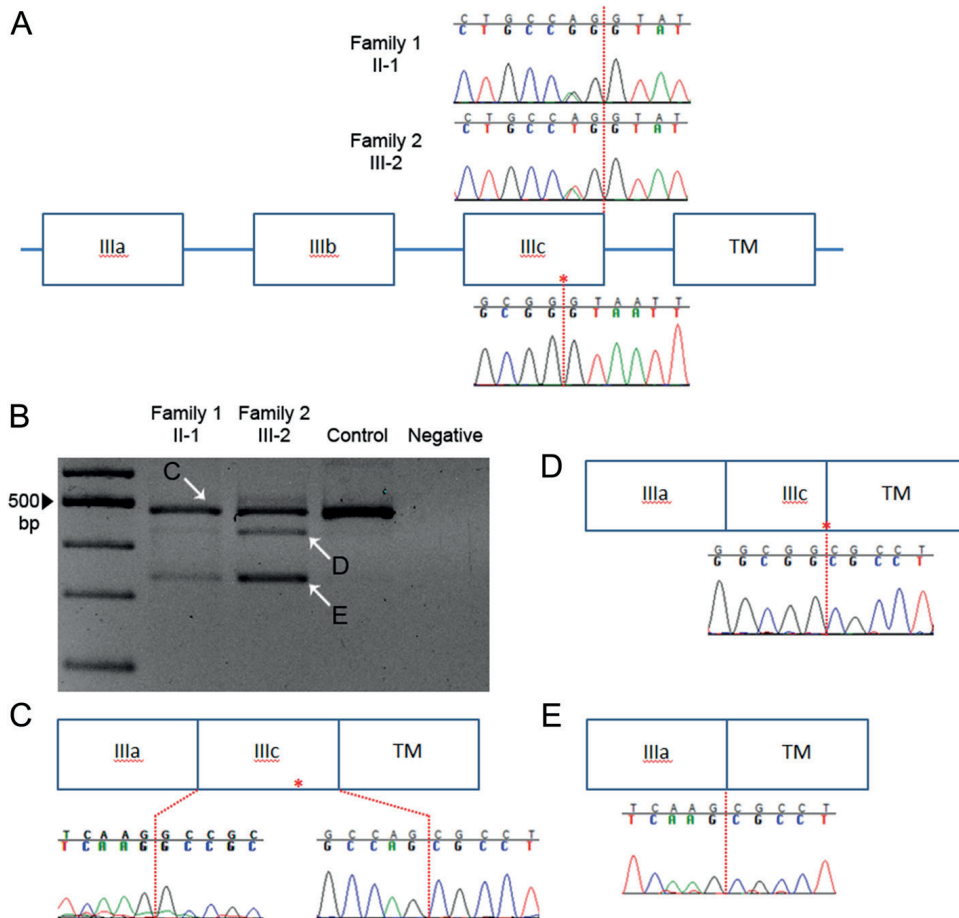


Figure 3.2. Genomic context and consequences of *FGFR2* mutations. **A:** schematic representation of genomic region affected by c.1083A>G and c.1083A>T mutations (not to scale). IIIa, IIIb and IIIc denote exons of *FGFR2* encoding the third immunoglobulin-like domain; note that physiological skipping of exon IIIb normally occurs in blood mRNA. TM, exon encoding transmembrane domain. Sequencing of genomic DNA demonstrates heterozygosity for c.1083A>G (II-1, Family 1) or c.1083A>T (III-2, Family 2) mutation at the -2 position from the end of exon IIIc (indicated by dashed red line; the upper line in each trace shows the wild type sequence). Below the cartoon is shown the genomic sequence around the cryptic donor splice site within exon IIIc (marked with red asterisk). **B:** amplified cDNA corresponding to c.1083A>G and c.1083A>T mutations (same individuals as for genomic analyses), demonstrates two additional smaller products (indicated with white arrows D and E), in addition to the normal (C) product. **C:** in the cDNA product coincident with the wild type band (II-1, Family 1), the mutant allele at the penultimate position of exon IIIc is not represented, indicating complete skipping of normal splicing. **D and E:** the consequences for splicing of the mutant allele (sequence traces illustrated are from III-1, Family 2) are either to activate the cryptic splice donor site within exon IIIc (**D**) or to skip exon IIIc completely (**E**).

Conclusions

In humans there is a consensus sequence around the 5' splice donor site: A, C or T, AG / gtaagt (where / indicates the exon-intron boundary). Mutations of the consensus A at the penultimate nucleotide of the exon have been associated previously with loss of splicing at the donor site.^{140,174} Other mutations near the *FGFR2* exon IIIc splice donor site have also been described (Table 3.1), all associated with a mild Crouzon phenotype. It is likely that the p.(Ala362Ser) substitution¹⁷⁵ in fact exerts its pathogenic effect via the G>T transversion at the –1 position in the exon, rather than as a missense substitution, but this was not tested experimentally.

In the cases reported here, the wild type splice donor site is abolished by the A>G or A>T mutations at the –2 position from the intron, leading to the cryptic site being preferred. The apparently greater amount of mutant cDNA products associated with the A>T mutation appears to correlate both with the greater predicted disruption of the splice site and with the more severe phenotype in clinically affected individuals from Family 2 compared with Family 1. However, since the A>G mutation did not support use of the normal exon IIIc donor splice site (Figure 3.2C), other explanations for these differences are possible, such as differing proportions of cell types in the blood samples analysed, and/or differences in genetic background.

Utilisation of the cryptic donor would lead to an in-frame deletion of the last 17 amino acids of exon IIIc (p.Gly345_Pro361del), including four residues that form specific contacts with the ligand FGF2.¹⁷⁶ However as craniosynostosis-causing *FGFR* mutations function in a constitutively active dominant manner,¹⁷⁷ it is also likely that in these individuals a mutant protein is formed which is prone to forming covalently-linked dimers,¹⁷⁷ leading to variable features of Crouzon syndrome.

Our case reports document the range of phenotypic consequences associated with these particular mutations. Whilst a mild crouzonoid phenotype was generally evident, only a minority of individuals developed overt craniosynostosis requiring calvarial surgery. Orthodontic problems may also occur but these were not fully documented in our study. The causes of the clinical variability are unknown, although one potential factor may be the extent of intrauterine foetal head constraint.¹⁷⁸

In conclusion, mutations near the *FGFR2* exon IIIc splice sites should be carefully evaluated as to whether they may be pathogenic, even if they are synonymous or outside the canonical AG/GT splice acceptor/donor sequences. In particular, the mutations described here are associated with variable Crouzon syndrome features and affected families should be counselled as such.

Table 3.1. Summary of mutations affecting correct splicing of the *FGFR2* exon IIIc donor site.

Mutation	Protein	Proposed effect	Experimental demonstration	Reference
c.1032G>A	p.(Ala344Ala)	Activation of cryptic splice site	Yes	Reardon <i>et al.</i> 1994; ¹³³ Li <i>et al.</i> 1995; ¹⁷⁹ Del Gatto & Breathnach 1995 ¹⁸⁰
c.1083A>G	p.(Pro361Pro)	Loss of normal donor site with use of alternative cryptic splice site	Yes	This study
c.1083A>T	p.(Pro361Pro)	As above	Yes	This study
c.1084G>T	p.(Ala362Ser)	Annotated as missense but likely to affect splicing	No	Everett <i>et al.</i> 1999 ¹⁷⁵
c.1084+3A>G	-	Loss of normal donor site with use of alternative cryptic splice site	Yes	Kan <i>et al.</i> 2004 ¹⁷³
c.1084+3A>C	-	Loss of normal donor site with use of alternative cryptic splice site	No	Cornejo-Roldan, Roessler & Muenke 1999; ¹⁸¹ Kress <i>et al.</i> 2000 ¹⁸²





Phenotypes of craniofrontonasal syndrome in patients with a pathogenic mutation in *EFNB1*

Marijke E.P. van den Elzen, Stephen R.F. Twigg, **Jacqueline A.C. Goos**, A. Jeannette M. Hoozeboom, Ans M.W. van den Ouweland, Andrew O.M. Wilkie, Irene M.J. Mathijssen

European Journal of Human Genetics November 2013

Abstract

Craniofrontonasal syndrome (CFNS) is an X-linked developmental malformation, caused by mutations in the *EFNB1* gene, which have only been described since 2004. A genotype-phenotype correlation seems not to be present. As it is of major importance to adequately counsel patients with *EFNB1* mutations and their parents, and to improve diagnosis of new patients, more information about the phenotypic features is needed. This study included 23 patients (2 male, 21 female) with confirmed *EFNB1* mutations. All patients underwent a thorough physical examination and photographs were taken. If available, radiological images were also consulted. Hypertelorism, longitudinal ridging and/or splitting of nails, a (mild) webbed neck and a clinodactyly of one or more toes were the only consistent features observed in all patients. Frequently observed phenotypic features were bifid tip of the nose (91%), columellar indentation (91%) and low implantation of breasts (90%). In comparison with anthropometric data of facial proportions, patients with CFNS had a significantly different face in multiple respects. An overview of all phenotypic features is shown. Patients with *EFNB1* mutations have a clear phenotype. This study will facilitate genetic counselling of parents and patients, and contribute to the diagnostic and screening process of patients with suspected CFNS.

Introduction

Craniofrontonasal syndrome (CFNS), also known as craniofrontonasal dysplasia, was identified as a specific subpopulation of frontonasal dysplasia, first delineated in a study by Cohen in 1979.¹⁸³ Subsequently, many other studies have focused on the manifestation of this syndrome. Most commonly depicted phenotypic features were coronal synostosis,¹⁸³⁻¹⁹³ hypertelorism,^{183,186-196} bifid nasal tip,^{183,186,187,190-192,194,195} frizzy and curly hair^{190-193,197} and longitudinal ridging and splitting of nails.^{185,186,188,190,191,193-195} It became clear that the majority of CFNS patients were female. In addition, the female patients appeared to be affected more severely than male carriers, who showed only few mild signs or no clear features at all. A genetic basis was likely, because families with multiple affected members were reported.^{184-186,188-191,194} However, there seemed to be a genetic paradox, as all daughters of affected males displayed severe signs of CFNS, but no male-to-male transmission was seen and affected males portrayed only mild or no signs. Therefore, multiple modes for inheritance were proposed; germline mosaicism, autosomal dominant with sex-influenced expression, X-linked dominant and metabolic interference.^{184-186,188-191}



The mystery was unravelled by a combination of results of multiple studies.^{63,198,199} The disease locus was finally claimed to be within Xq13.1 and loss of function mutations in *EFNB1* were proven to cause CFNS.^{63,141,192,200-210} *EFNB1* encodes ephrin-B1, which is a transmembrane ligand for Eph receptor tyrosine kinases. Because of random X-inactivation heterozygous females are uniquely mosaic and by consequence a cell either does or does not produce a functional protein. These proteins are important for cell-cell contact, migration and pattern formation in the developmental process of the embryo.²¹¹ The random pattern of expressing and non-expressing patches therefore leads to an abnormal sorting in cells, and in addition to ectopic tissue boundaries between these zones. The term for this process is called 'cellular interference'.¹⁹² In hemizygous males, all cells are unable to produce a functional protein, and therefore this phenomenon cannot occur. Normal boundaries are probably maintained through an alternative mechanism,²⁰⁵ which could be via an ephrin redundancy²⁰⁵ and promiscuity of the ephrin ligand/receptor system.¹⁹² An explanation for the few severely affected males reported in literature^{188-190,212} could be a mosaicism in these patients, in which the wild type to mutant ratio should be similar to that in heterozygous CFNS females.^{23,206,213} Additional mechanisms were recently added to the phenotypic manifestation. Not only cellular interference, but also an impaired signalling capacity of ephrin-B1 and improper regulation of gap junctional communication could be responsible for the pathogenic process in CFNS expression.^{204,208} A genotype-phenotype correlation has not been proven, and previous studies suggest that this is unlikely.²⁰⁶

Taken together, around 20% of the patients screened for CFNS did not display a mutation in the *EFNB1* gene.^{201,203,205} Multiple explanations have been proposed, one of which is misdiagnosis of some of the included patients.²⁰⁵ Studies following the discovery of the causal gene predominantly describe the location of new mutations, combined with a brief outline of phenotypic features of small families or cohorts.^{63,141,200,202,207,209,210} Detailed overviews of phenotypic features of large cohorts of possible CFNS patients do exist,^{185,186,188-192,194,210} but it is not clear what proportion of these patients carry an *EFNB1* mutation. The reports in the older literature could therefore cause confusion by reporting patients who might be improperly classified as CFNS patients.

As it is of major importance to adequately counsel patients with *EFNB1* mutations and/or their parents and to improve diagnosis of new patients, more information about the phenotypic features of genuine CFNS patients with an *EFNB1* mutation is needed.

Methods

Study population

This study was conducted at the Craniofacial Unit of the Department of Plastic and Reconstructive Surgery of the Erasmus MC, University Medical Centre in Rotterdam, The Netherlands. All patients with a diagnosis of CFNS based on a confirmed *EFNB1* mutation who were currently under treatment, or who were treated in the past, were included in this study. A total of 23 patients (21 female, two male) were selected. Seven of these patients have been described in prior clinical studies, and the mutations of 13 patients have been published before.^{188,212,213}

Design and procedure

A cross-sectional observational study was designed and conducted. Ethical approval was received from the board of the Medical Ethical Committee of the Erasmus MC, University Medical Centre Rotterdam (MEC-2006-121).

Complete series of standardized photographs of all patients were collected, combined with a review of the patient's medical file and physical examinations. If available, radiological images were also consulted. However, as this was a retrospective study, not all images were still available and moreover could not always be used as a source of quantitative data. Patients were asked to participate for an extra physical examination and additional photographs to capture all bodily features. Some short questions on functioning and limitations of their body were asked as well. Patients or parents provided written consent for the use of patient images.

Genotype-phenotype correlation

The *EFNB1* gene was examined by DNA sequence analysis of all coding exons and exon/intron boundaries. Rearrangements of *EFNB1* (deletions or insertions) were sought by multiplex ligation-dependent probe analysis (MLPA). For each patient we classified the type of nucleotide change (point mutation, deletion or duplication) and the type of protein change (missense, nonsense or frameshift mutation). We also indicated in which exons (exons 1-5) the mutations were located and in which regions of the protein the mutations were located (signal peptide, receptor binding domain, ephrin (extracellular domain), transmembrane domain, cytoplasmic domain or PDZ domain).

Measurement of facial proportions

For calculation of facial proportions, standardized (frontal and profile) photographs of all patients were printed. Selected photographs had to be taken prior to major surgical interventions, so genuine dimension could be evaluated. As all evaluated facial proportions were ratios, no scaling or calibration problems existed. Calculated indexes were compared with values derived from anthropometric studies.²¹⁴ As illustrated in Figure 4.1, chosen indexes were: Inter-canthal Index (Inter-canthal width/Biocular width); Upper Face Index (Upper face height/Face width); Nasal Protrusion-Nose Height Index (Nasal tip protrusion/Nose height); Nose-Craniofacial Height Index (Nose height/Craniofacial height); Nose-Upper Face Height Index (Nose height/Upper face height) and Upper Lip-Upper Face Height Index (Upper lip height/Upper face height). Nomenclature of the mentioned indexes and measurements are directly derived from the referred anthropometric studies.²¹⁴



Statistical analyses

As a measure of central tendency, percentages were calculated for categorical variables. For metric variables, the mean was used as measure of central tendency, and the standard deviation was used as a measure of dispersion. For statistical analysis, we used the Statistical Package for the Social Sciences (SPSS) for Windows, version 18.0 (Erasmus University Medical Centre, Rotterdam, The Netherlands).

Results

Twenty-three patients with classical features of CFNS and proven *EFNB1* mutations (Table 4.1, variants reported in this study are submitted to the LOVD database <http://database.lovd.nl/shared/genes/EFNB1>) were included in this study. The single patient excluded was a female originally suspected to have CFNS, but who had no identified *EFNB1* mutation; in retrospect (with the findings of this study) she would clinically not be classified again as having CFNS. A total of 21 female and two male CFNS

patients were identified. Five patients refused to participate for the additional physical examination and photographs. The main reason for not participating was an emotional or psychological problem with their bodily features, and seeing 'no use' in participating. One patient could not be contacted. Patients who did not want to participate however, had had standardized photographs taken during their treatment at least of their face, and sometimes hands, feet and chest. Medical files were available for all selected patients. As a result, the denominator of some of the observed features was lower than the total of 23 patients. Other features (e.g. breast anomalies) could not be scored in all patients, because these individuals were either male or too young to have developed breasts. In addition, one of our patients was a baby aged 6 months, so many features could not be scored. In these cases of incomplete data, fractions are given instead of percentages.

Five patients were heterozygous for the familial mutation identified in the index patient of the family. Regarding the intrafamilial variability, the following most obvious features were found: concerning the patient who was a daughter of a carrier male with a very mild phenotype, no comparison could be made because the daughter obviously showed a very different phenotype. Concerning the affected mother and daughter pair, both patients were equally affected in facial and bodily features. The daughter, however, was born with several cardiac anomalies, dextroposition of the heart, two superior venae cavae, a bidirectional shunt and an atrial septal defect. The two affected sisters differed slightly in facial features, as one of the sisters had more pronounced epicanthic folds, whereas the other had a more obvious orbital dystopia. In addition, one of them had a coloboma of the iris, a strabismus sursoadductorius, and a difference in length of legs (asymmetrical lower limb shortness).

Overall, we scored 107 phenotypic variables in the cohort of 23 patients. We also checked the genotype of our patients and used four variables to describe the genotype (type of nucleotide change, type of protein change, involved exon, and region of protein affected). Many variables consisted of multiple possible values, leading to a large variation of both genotype and phenotype, and no genotype-phenotype correlation could be detected.

General features

The average age of patients at evaluation was 18.0 years (range 0.5-44 years) with 12 adults (age 16 years and above). Analysis of the body mass index revealed that 28% ($n = 5$) were underweight and 11% ($n = 2$) were overweight. The span-length-ratio had a mean of 0.93 (range 0.77-0.99), indicating that in most patients their arm span was not equal to their total height, which is in contrast to the normal population.

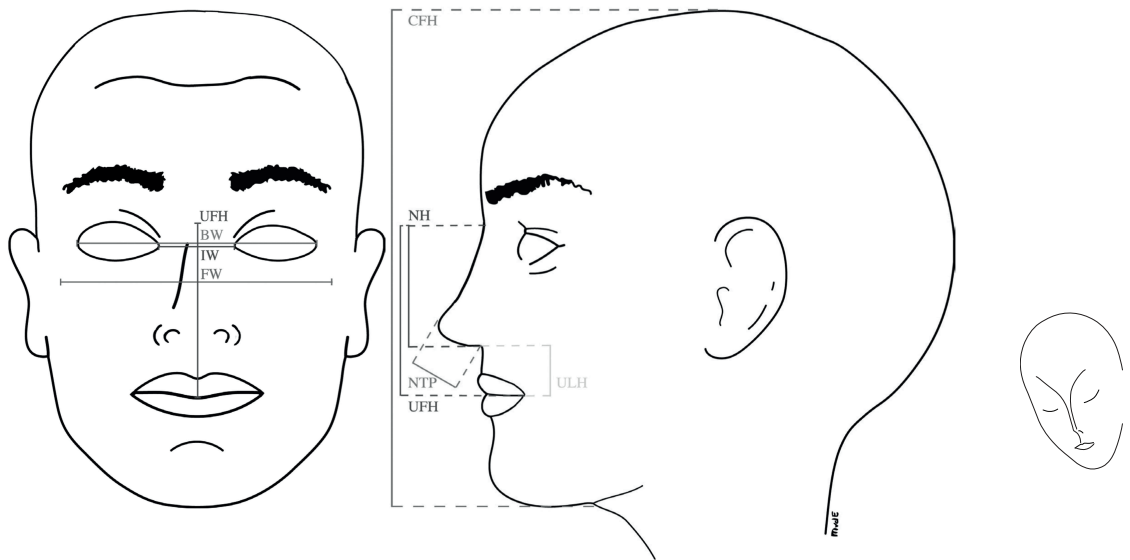


Figure 4.1. Anthropometric facial proportions. BW = Biocular width, CFH = Craniofacial height, FW = Face width, IW = Intercanthal width, NH = Nose height, NTP = Nasal tip protrusion, UFH = Upper face height, ULH = Upper lip height.

Skull and face

As can be seen in Table 4.2 and Figure 4.2, the facial features of CFNS patients differ significantly from the normal population (more than 2 SDs above the mean).²¹⁴ As expected, the intercanthal distance is much greater. The upper face (base of the nose to height of the commissure of the mouth) is relatively small compared to the width of the face (lateral points of zygoma). Compared with the height of the nose, the protrusion of the tip is relatively high in patients. However, the height of the nose itself is significantly shorter, compared with both the total face as well as the upper face. In contrast, the upper lip is larger than normal.

Craniosynostosis was seen in 78% of all patients; 22% ($n = 5$) had a left-sided coronal synostosis, 4% ($n = 1$) had a right-sided coronal synostosis, 48% ($n = 11$) had a bilateral synostosis of the coronal suture and 4% ($n = 1$) had a bilateral coronal synostosis with synostosis of the sagittal suture. One patient had her craniosynostosis corrected abroad before her first presentation, and the exact type of synostosis was unclear. All patients with craniosynostosis needed a surgical correction. A very large anterior fontanelle with delayed closure was present in 6/18. Two patients had agenesis of the corpus callosum, with partial agenesis in another three patients. Facial asymmetry was seen in 19/22 of

all patients, with a degree ranging from mild to severe; three of these patients had no history of craniosynostosis. A diminished development of the maxilla was sometimes observed (4/22), at different ages and of variable degree. In addition, one patient had a groove in the middle of her alveolar ridge.

Hair

In our population, 65% ($n = 15$) of all patients had a widow's peak, and 26% ($n = 6$) had a low anterior hairline. The hair itself was dry and with frizzy curls in 12/22, dry and with loose curls in 8/22, and 2/22 showed normal hair. Parents reported that hair usually changed around 6-12 months, from soft baby hair into dry curly hair.

Table 4.1. Overview of mutations in the *EFNB1* gene^a.

Gender	Nucleotide change	Protein change	Exon	Protein region	Inheritance
1 Female ²¹³	c.[=-95T>C]	p.?	5'UTR	NA	2
2 Male ^{212,213}	c.[=-/412-399_1038+7004del]	p.?	3-5	Ephrin partially, TM and CY	3
3 Female	c.1A>G (mosaic)	p.0?	1	SP	3
4 Female ²⁰³	c.30C>T	p.(Lys11fs) ^b	1	SP	1
5 Female ^{188,203}	c.109T>G	p.(Trp37Gly)	1	RBD	1
6 Female	c.161C>T	p.(Pro54Leu)	2	RBD	0
7 Female	c.196delC	p.(Arg66fs)	2	RBD	2 (daughter)
8 Female	c.228C>G	p.(Tyr76*)	2	RBD	1
9 Female ²⁰³	c.233T>C	p.(Leu78Pro)	2	RBD	2 (mother)
10 Female ²⁰³	c.233T>C	p.(Leu78Pro)	2	RBD	2 (daughter)
11 Female	c.266G>A	p.(Cys89Tyr)	2	RBD	1
12 Female	c.324dupA	p.(Arg109fs)	2	RBD	1
13 Female ^{188,203}	c.339G>C	p.(Lys113Asn)	2	RBD	1
14 Female	c.360C>A	p.(Asn120Lys)	2	RBD	0
15 Female ¹⁸⁸	c.368G>A	p.(Gly123Asp)	2	RBD	1
16 Female ²⁰³	c.407C>T	p.(Ser136Leu)	3	RBD	0
17 Female	c.451G>A	p.(Gly151Ser)	3	RBD	0
18 Female	c.492_499+2del	p.(Gly165fs)	3	Ephrin	1
19 Male ^{188,213}	c.496C>T (mosaic)	p.(Gln166*)	3	Ephrin	3
20 Female ^{188,203}	c.496C>T	p.(Gln166*)	3	Ephrin	2 (Sister)
21 Female ^{188,203}	c.496C>T	p.(Gln166*)	3	Ephrin	2 (Sister)
22 Female	c.543delC	p.(Ser182fs)	4	Ephrin	1
23 Female ²⁰³	c.564dupT	p.(Val189fs)	4	Ephrin	1

CY = Cytoplasmic domain, Ephrin = Ephrin extracellular domain, NA = Not applicable, RBD = Receptor-binding domain (located in the ephrin extracellular domain), SP = Signal peptide, TM = Transmembrane domain, UTR = Untranslated region, 0 = *De novo*, 1 = Sporadic, 2 = Familial, 3 = Mosaic.

Variants submitted to <http://databases.lovd.nl/shared/genes/EFNB1>.

^aReference sequence: NG_008887.1.

^bRNA analysis showed that this synonymous substitution creates a cryptic donor splice site.²⁰³

Zone of the orbits and eyes

All patients, 100% ($n = 23$), displayed hypertelorism, with a variable degree from mild to severe. At the time of evaluation, six patients were still too young to undergo a correction of their hypertelorism, but will probably be operated on in the future. Two adults with a relatively mild form did not require surgical intervention, the other 15 patients underwent a surgical correction. Orbital dystopia was seen in 10/22 of them, five of the patients had no history of craniosynostosis, in seven of them the orbital dystopia was evident before any surgical intervention. Downslanting of the palpebral fissures was present in 35% ($n = 8$), with variable severity, whereas an upslant of the palpebral fissures was present in 48% ($n = 11$), although usually only mild. Epicanthic folds were frequent, and were unilateral in 39% ($n = 9$) cases and bilateral in 39% ($n = 9$) cases. An interrupted hairline of the eyebrow was seen in 70% ($n = 16$) of patients. Rare observations were a coloboma of the iris ($n = 1$) and heterochromia of the iris ($n = 1$).



Table 4.2. Difference of facial proportions of CFNS patients compared with anthropometric means²¹⁴ (expressed in average standard deviations from mean).

	Inter-canthal Index	Upper Face Index	Protrusion–Nose Height Index	Nose–Craniofacial Height Index	Nose–Upper Face Height Index	Upper Lip–Upper Face Height Index
Patients <6 years	+5.3 SD	-2.1 SD	+1.7 SD ^a	-3.4 SD ^b	-4.0 SD ^b	+5.1 SD ^b
Patients >6 years	+4.7 SD	-1.5 SD	+1.6 SD	-1.6 SD	-2.0 SD	+2.8 SD
Total group	+5.0 SD	-1.8 SD	+1.7 SD	-2.5 SD	-3.0 SD	+4.0 SD

^aYoungest age of reference group is 6 years, difference probably slightly bigger if adequate reference would be available.

^bYoungest age of reference group is 6 years, difference probably slightly smaller if adequate reference would be available.

Ocular function

Before a correction of the hypertelorism or orbital dystopia, a substantial number of ophthalmologic abnormalities were observed. The most common anomaly was strabismus (9/22), subdivided into divergent ($n = 3$), sursoadductorius ($n = 4$) and convergent ($n = 2$) types, sometimes in combination with a dissociated vertical deviation ($n = 5$). Nystagmus was also a common finding (9/22 patients): four had congenital nystagmus and four had latent nystagmus. Hypermetropia was present in three, two of them had a very high astigmatism and one had solitary high stigmatism. Amblyopia was identified in two and an absent oblique superior muscle was found in one patient.



Figure 4.2. Patient displaying typical aberrant facial proportions.

Ears

Low set ears were a common finding, 52% ($n = 12$), whereas only two patients had an abnormal shape of the external ear.

Zone of the nose

Nearly all patients (91%, $n = 21$) displayed a bifid tip of the nose. The same can be said for an indentation in the columella, 91% ($n = 21$), although not all patients with a bifid tip also had this indentation. A broad nasal base, 70% ($n = 16$), and flat nasal bridge, 43% ($n = 10$), were frequently observed. One patient had a fistula in the dorsum of her nose with an intracranial connection.

Zone of the mouth, maxilla and mandible

A common observation was a tent-shaped mouth 39% ($n = 9$), and a mild keel-shaped maxilla in 35% ($n = 8$). Crowding of the teeth was seen in 23% ($n = 5$). Hypoplasia of the maxilla was reported in 4/22 patients, whereas 2/22 had a mandibular prognathism. A unilateral right-sided cleft lip and palate was seen in only one patient, whereas one other patient had a very mild notch in the midline of her upper lip.

Zone of the neck, shoulders, chest and back

A true short and webbed neck was present in 12/18 patients and in addition a mild webbing or pseudo-webbing of the neck was present in the other 6/18 patients. Rounded and sloping shoulders, often rather narrow, were observed in 16/18. Sprengel's deformity of the shoulders (defined as one shoulder blade that sits higher on the back than the other) was quite common as well (8/12). Three patients displayed an axillary pterygium; unilateral in two patients, bilateral in one. A low implantation of the breasts was seen in the majority of patients (19/21), and in addition most of them had asymmetrical heights of their nipples (11/19). Patients who were in their adolescence or adulthood also displayed an asymmetry of the breast volume (6/8). Looking at the chest wall itself, revealed a pectus excavatum in 11/17 patients, although mild in most cases. Four patients were affected with both breast asymmetry and a pectus excavatum. All of the above are illustrated in Figure 4.3. Scoliosis was diagnosed in 6/13 patients, but none of the patients needed surgery.



Upper extremity

All patients (100%, $n = 23$) had a longitudinal ridging and/or splitting of nails toward the end, although the number of digits affected and severity differed. Only two patients were born with an extra digit (9%), and only three had a complete or incomplete syndactyly (13%). A clinodactyly of one or more digits was frequent (74%, $n = 17$). A restricted range of motion of the arms, affecting either abduction or elevation above the head, was present in the majority of patients (15/17). This is probably due to the aberrant position of the clavicles, in combination with the earlier mentioned Sprengel's deformity. The available radiological images of the chest revealed that patients had either an aberrant curvature of their clavicles and/or the angle of the clavicles with the sternum was bigger than normal. Either way, this resulted in a typical higher placement of the shoulders.

Lower extremity

As was observed in the hand, all patients (20/20) had a longitudinal ridging and/or splitting of toenails toward the end, whereas both the severity as well as the number of toes affected differed. Duplication of toes was seen in 4/20 patients and syndactyly in 7/20 patients. Clinodactyly of at least one toe, was again a consistent finding (20/20), as illustrated in Figure 4.4. One patient had asymmetrical lower-limb shortness.

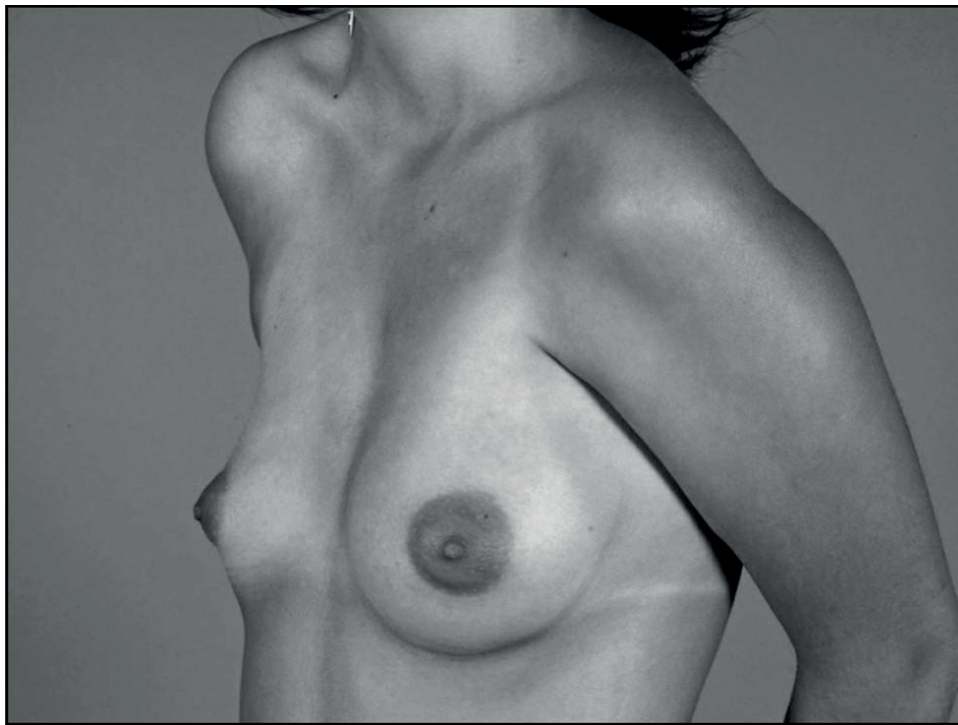


Figure 4.3. Patient with typical chest and breast deformities.

Cardiac abnormalities

Three patients (13%) had problems affecting their heart. One had a patent ductus arteriosus, one had an atrial flutter of unknown origin immediately after birth and one had multiple cardiac problems: dextroposition of the heart, two superior venae cavae, a bidirectional shunt and an atrial septal defect.

Miscellaneous findings

Two patients had psoriasis and another single patient had an umbilical hernia, one male presented with cryptorchidism, another patient had a café-au-lait spot, one patient presented herself with a haemangioma and one patient had an episode with toddler's hypoglycaemia.



Figure 4.4. Patient displaying typical foot and toe deformities.

Discussion

Genuine CFNS patients, with proven *EFNB1* mutations, have a clear and very distinguishable phenotype. However, a detailed overview of the phenotypic features of a large cohort of proven CFNS patients has not previously been presented in the literature. As expected, some of the previous reports can cause confusion by reporting patients who were possibly incorrectly diagnosed with CFNS. This probably explains the majority of the ~20% of apparent CFNS patients without an *EFNB1* mutation.^{201,203,205} The results from this study make the diagnosis of some patients presented in literature therefore doubtful, based on their different facial proportions and dissimilar phenotype.^{189,196,210} In other studies, some patients were classified as having frontonasal dysplasia, whereas they actually match the typical phenotype of CFNS.^{195,212,215}

We included only three families with more than one affected member in this study. One of these comprised a father (a male carrier) and a daughter and therefore we could not draw any conclusions regarding intrafamilial variability. In the other two

families, the clinical features differed highly, suggesting that intrafamilial variability can be significant. A genotype-phenotype correlation seems to be unlikely, based on this intrafamilial variability and a previous study,²⁰⁶ and was not found in this study.

This study leads us to the conclusion that in CFNS patients with an *EFNB1* mutation, consistent features exist: hypertelorism, a certain degree of longitudinal ridging and/or splitting of nails of at least one digit or toe, a certain degree of webbed neck and a clinodactyly of one or more toes. In addition, abnormal facial proportions were observed in all patients.²¹⁴ These proportions are reflected in a relatively small upper face compared with the width of the face, a very short nose, with a relatively high protrusion compared with its length and a relatively long upper lip, compared with the upper face. It must be stressed that the projection of the nose itself in comparison to the whole face is very small, but as the length is about the same as the projection, this ratio is relatively high.

Features that were present in most, but not all patients, can be regarded as 'very suggestive' of the diagnosis. These are: bifid tip of the nose (91%), indentation of the columella (91%), low implant of breasts (90%), rounded, sloping and often rather narrow shoulders (89%) with reduced range of motion of the shoulders (88%), facial asymmetry (86%), craniosynostosis (78%), clinodactyly of at least one digit (74%), aberrant form of eyebrow (70%) and broad nasal bridge (70%). Although similar features have been noted in previously published studies,^{186,188,190,191,193,194} it is not possible to compare frequency data directly because of differences in methodology.

Measurements of facial proportions are seldom reported, which is unfortunate. One study gave a description of the cranio-orbito-zygomatic region, based on CT-scans compared with an age-matched control value. Besides the obvious increased interorbital distance, they also found a degree of horizontal midface retrusion demonstrated by a shortened zygomatic arch length and an expanded interzygomatic buttress distance, suggestive for a brachycephalic morphology.¹⁹⁵ In addition, another study also described a short upper facial height¹⁹⁰ and compared it to anthropometric measurements. However, the short upper facial height seemed to be present in only 66% of their cases. A further study mentions midface hypoplasia,¹⁸⁵ however, they do not support it with objective data or compare it to a normal reference group. These findings are in accordance to our data.

Hopefully, this study will facilitate the diagnosis of CFNS. Based on this study, new patients should be evaluated for facial proportions and hypertelorism, they should be checked for longitudinal ridging and/or splitting of nails of at least one digit or toe, for webbed neck, and for a clinodactyly of one or more toes. Furthermore, other bodily features should be compared with the ones given in this paper.

It is likely that not all possible phenotypic features of CFNS are present within our population. A few other features that were not evaluated in this study are presented in the literature: myoclonus, poor hearing, pelvic kidney, bilateral vesico-ureteral reflux, hip girdle anomalies,¹⁹³ median cleft lip/palate,¹⁹⁰ asymmetric mandible.¹⁹¹ Additional features that have been reported in other studies of patients with *EFNB1* mutations include: diaphragmatic hernia,^{63,141,201,207} dysplastic clavicles and clavicle pseudoarthrosis,^{63,190-194,200,203} accessory nipples,¹⁹² high arched palate,^{186,191-194,212} uterus arcuatus,¹⁹² duplication of uterus, kidneys and ureters,¹⁹² and low posterior hairline.^{190,194,202} Furthermore, some studies state that CFNS patients have a normal intelligence,^{190,192,194,197} whereas others claim that some may have learning difficulties to a variable degree.^{185,186,192,203,212} In this study, intelligence was not measured.

One of the limitations of this study is the low number of males included. Although CFNS manifests particularly in females, and affected males express significantly less features, a clear phenotype of hemizygous males could not be given, as both of the two males evaluated carried mosaic mutations, and as a consequence were as severely affected as the females.³² On the other hand, we believe that the number of clinically evaluated CFNS patients with proven *EFNB1* mutations in this study is unique in its size, and therefore adds value to the current literature. Future research could focus on the psychological and intellectual development and surgical impact.





Mutations in *TCF12*, encoding a basic helix-loop-helix partner of TWIST1, are a frequent cause of coronal craniosynostosis

Vikram P. Sharma,* Aimée L. Fenwick,* Mia S. Brockop,* Simon J. McGowan, **Jacqueline A.C. Goos**, A. Jeannette M. Hoogeboom, Angela F. Brady, Nu Owase Jeelani, Sally Ann Lynch, John B. Mulliken, Dylan J. Murray, Julie M. Phipps, Elizabeth Sweeney, Susan E. Tomkins, Louise C. Wilson, Sophia Bennett, Richard J. Cornall, John Broxholme, Alexander Kanapin, 500 Whole-Genome Sequences (WGS500) Consortium, David Johnson, Steven A. Wall, Peter J. van der Spek, Irene M.J. Mathijssen, Robert E. Maxson,[‡] Stephen R.F. Twigg,[‡] Andrew O.M. Wilkie[‡]

* Equal contributors

[‡]These authors jointly directed this work

Nature Genetics January 2013

Abstract

Craniosynostosis, the premature fusion of the cranial sutures, is a heterogeneous disorder with a prevalence of ~1 in 2,200.^{2,3} A specific genetic aetiology can be identified in ~21% of cases,¹²⁸ including mutations of *TWIST1*, which encodes a class II basic helix-loop-helix (bHLH) transcription factor, and causes Saethre-Chotzen syndrome, typically associated with coronal synostosis.^{138,139,216} Using exome sequencing, we identified 38 heterozygous *TCF12* mutations in 347 samples from unrelated individuals with craniosynostosis. The mutations predominantly occurred in individuals with coronal synostosis and accounted for 32% and 10% of subjects with bilateral and unilateral pathology, respectively. *TCF12* encodes one of three class I E proteins that heterodimerise with class II bHLH proteins such as *TWIST1*. We show that *TCF12* and *TWIST1* act synergistically in a transactivation assay and that mice doubly heterozygous for loss-of-function mutations in *Tcf12* and *Twist1* have severe coronal synostosis. Hence, the dosage of *TCF12*-*TWIST1* heterodimers is critical for normal coronal suture development.

Introduction

Our exome sequencing approach focused on bilateral coronal craniosynostosis (Figure 5.1) because of previous evidence that this pathological group is loaded with cases of monogenic aetiology.¹²⁸ We examined the variant lists from the whole exome data²¹⁷ of seven unrelated Individuals with bilateral coronal synostosis, negative for previously described mutations,¹²⁵ for genes showing nonsynonymous changes in two or more samples. Two samples had different heterozygous frameshift mutations in *TCF12* (encoding transcription factor 12; also known as HEB, HTF4 and ALF1);²¹⁸⁻²²⁰ one (family 19) had a single nucleotide deletion, and the other (family 30) had a four-nucleotide deletion (details in Supplementary Table 5.1). The mutations were confirmed by dideoxy sequencing of the original DNA samples (primary sequence results for all families are shown in Supplementary Figure 5.1). In addition, a text search of the exome sequence data identified a new c.1468–20>A variant in *TCF12* in a third sample (family 22), located 20 nucleotides upstream of the start of exon 17. This variant was predicted to generate a cryptic splice acceptor site that was confirmed experimentally (Supplementary Figure 5.2A). Thus, we had identified different heterozygous disruptive mutations of *TCF12* in three of seven samples from individuals with bilateral coronal synostosis. We interrogated other exome or whole genome sequencing projects on craniosynostosis that we were undertaking concurrently: this analysis identified additional *TCF12* mutations in two siblings with bilateral coronal synostosis and their clinically unaffected mother (family 20, which we had erroneously analysed assuming recessive inheritance) and in two unrelated individuals (from families 11 and 16) with clinical diagnoses of Saethre-Chotzen syndrome who did not have identified mutations in the *TWIST1* gene.^{138,139,216}

To confirm these findings and explore the clinical consequences of *TCF12* mutations, we carried out dideoxy sequencing of *TCF12* in individuals with different types of craniosynostosis in whom mutations had not previously been identified. In the initial panel of 287 unrelated samples, we identified 18 with pathogenic mutations in *TCF12*; all mutation-positive individuals had coronal synostosis. To replicate our findings, we sequenced an independent Dutch cohort of 50 samples with coronal synostosis and identified 14 additional mutations in *TCF12*. Overall, we observed a strong bias for mutations in *TCF12* to occur in association with coronal synostosis (Table 5.1): 22 of 69 (32%) bilateral coronal and 14 of 141 (10%) unilateral coronal cases had mutations, but none of 93 cases with isolated metopic, sagittal or lambdoid synostosis had *TCF12* mutations ($P = 1 \times 10^{-6}$, Fisher's exact test). The remaining two cases positive for *TCF12* mutations had combinations of sagittal and either uni- or bilateral coronal synostosis, such that coronal synostosis was present in all 38 index subjects. In our extended Oxford



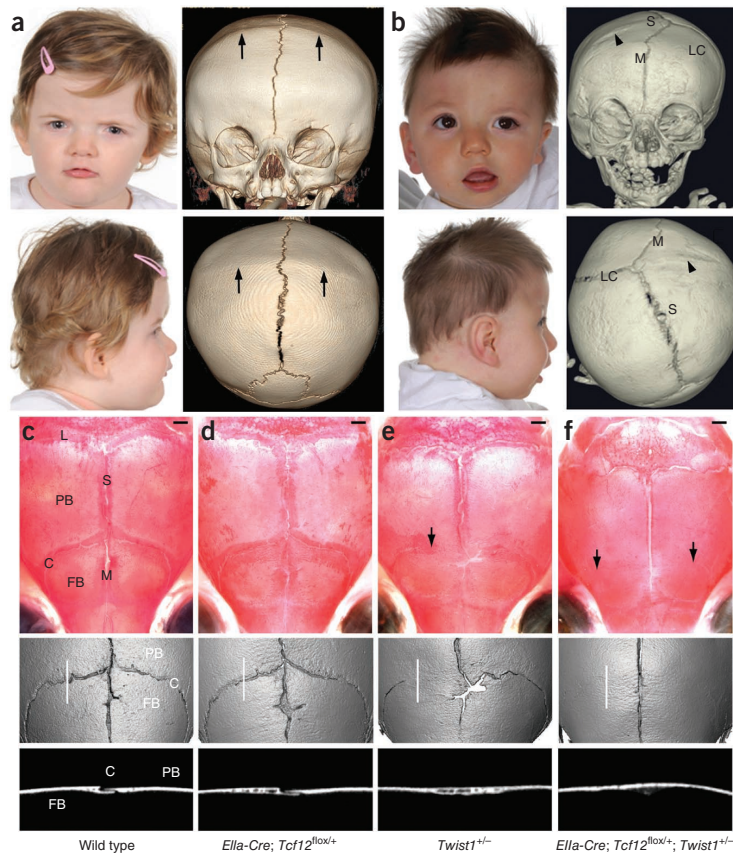


Figure 5.1. Phenotype associated with *TCF12* or *Tcf12* haploinsufficiency in humans and mice. **A and B:** clinical presentation of individuals with *TCF12* mutations, showing facial appearance (left) and computed tomography (CT) images of the head (right). Written permission was obtained to publish the clinical photographs. **A:** bilateral coronal synostosis in the proband from family 30. Note the high forehead and brachycephaly at the age of 13 months. CT images at the age of 4 months show bilateral fusion of the coronal sutures associated with bony ridging (arrows). **B:** right unilateral coronal synostosis in the proband from family 35: at the age of 10 months, note the elevation of the right orbit and shifting of the midface and mandible to the left. CT images at the age of 4 months show complete fusion of the coronal suture on the right (arrowhead), an open coronal suture on the left (LC) and relative angulation of the metopic (M) and sagittal (S) sutures. **C-F:** severe bilateral coronal synostosis in *Ella-Cre; Tcf12^{flax/+}; Twist1^{+/-}* combination mutants. Shown are representative images of postnatal day (P) 21 skulls stained with Alizarin Red S (top), three-dimensional μ CT reconstructions (middle) and two-dimensional μ CT images of sagittal slices (10 μ m) through the coronal suture (bottom; the section planes are indicated by white lines in the three-dimensional images). Note the normal coronal sutures in the wild-type (**C**) and *Ella-Cre; Tcf12^{flax/+}* (**D**) skulls, partial unilateral coronal synostosis in the *Twist1^{+/-}* skull (**E**, arrow) and complete bilateral coronal synostosis in the *Ella-Cre; Tcf12^{flax/+}; Twist1^{+/-}* skull (**F**, arrows). C = Coronal suture, FB = Frontal bone, L = Lambdoid suture, PB = Parietal bone. Scale bars, 1 mm.

birth cohort¹²⁸ with minimum 5-year follow-up (cases born in calendar years 1998–2006), we found *TCF12* mutations in 4 of 402 subjects (1.0%; 95% confidence interval of 0.3–2.5%). Hence, mutations in *TCF12* occur in a measurable fraction of craniosynostosis overall (Supplementary Figure 5.3).

Table 5.1. Identification of *TCF12* mutations in different categories of craniosynostosis.

	Non-syndromic		Syndromic		Combined	
	Total	<i>TCF12</i> mutation positive	Total	<i>TCF12</i> mutation positive	Total	<i>TCF12</i> mutation positive
Metopic	32	0	14	0	46	0
Sagittal	32	0	7	0	39	0
Unilateral coronal	115	9	26	5	141	14
Bilateral coronal	28	5	41	17	69	22
Uni- or bilateral lambdoid	8	0	0	0	8	0
Multisuture	19	1	19	1	38	2
Sutures not specified	2	0	4	0	6	0
Combined	236	15	111	23	347	38



The mutations identified in *TCF12* comprise 14 nonsense, 15 frameshift, 7 splicing and 2 missense changes, suggesting a loss-of-function mechanism (Figure 5.2). This is consistent with previous reports²²¹ of individuals with cytogenetically identified chromosome 15 deletions (predicted to include *TCF12* at 15q21.3) in whom craniosynostosis was present, although no whole exon deletions of *TCF12* were detected in our subject panel using a multiplex ligation–dependent probe amplification (MLPA) assay. In cases with frameshift or splice-site mutations, analyses of mRNA extracted from various cell types showed lower expression of the mutant compared to the wild-type allele, consistent with nonsense-mediated mRNA decay (Supplementary Figure 5.2 and Supplementary Table 5.2). The mutations showed a clear enrichment in the 3' half of *TCF12*, with all but one located between exons 10 and 19. The remaining mutation (c.526+1G>A), which caused skipping of exon 7 (Supplementary Figure 5.2D), is specific to the longer *TCF12* transcript, as the alternative transcription start site²²² lies downstream of this position (exon 9A; Figure 5.2A). The two missense mutations (encoding p.Leu624Pro and p.Gln638Glu substitutions) affect highly conserved residues of the bHLH domain required for dimerization (Supplementary Figures 5.4A and 5.4B); mutations of other bHLH proteins often affect this region, with examples including alterations of the class I protein TCF4 (Pitt-Hopkins syndrome)²²³ and class II protein TWIST1.²¹⁶ Using a transactivation assay with a reporter containing three E-boxes,²²⁴ we found that the combination of native TCF12 and TWIST1 proteins had a synergistic effect

on activation relative to the activity of either protein individually, but this effect was 65–76% lower in the presence of the *TCF12* missense mutations encoding p.Leu624Pro or p.Gln638Glu alterations (Supplementary Figure 5.4C).

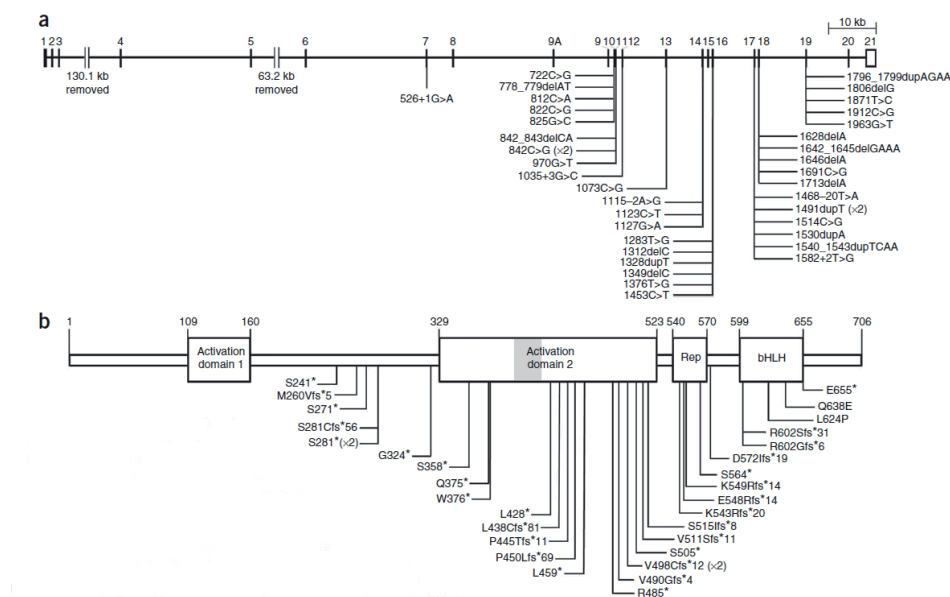


Figure 5.2. Structure of *TCF12* and the encoded protein showing the location of mutations identified in coronal synostosis. A: gene structure. The major transcript comprises 21 exons; inclusion or exclusion of exon 15 by alternative splicing generates proteins of 706 and 682 amino acids, termed HEB β and HEB α , respectively. Alternative transcription starting at exon 9A generates a different protein (HEBAIt) of 512 amino acids.²²² **B:** protein structure. Domains identified in the HEB β protein (portion encoded by exon 15 shaded gray). Functional studies previously defined activation domains 1 and 2²²⁵ and the rep domain.²²⁶ Identical mutations identified in independent families are indicated (x2); note that mutations predicted to affect splicing are omitted from the protein schematic.

Of 36 families from which additional samples were available, the *TCF12* mutation was shown to have arisen *de novo* in 14 (Supplementary Figure 5.1 and Supplementary Table 5.1), providing further evidence that the *TCF12* mutations are causative of the coronal synostosis phenotype. In 23 of the families, cascade testing identified 34 additional mutation-positive individuals, only 16 of whom had craniosynostosis or other relevant clinical features, indicating substantial (53%) non-penetrance (Supplementary Table 5.1; see Supplementary Figure 5.5 for representative clinical photographs). There was no evidence to implicate somatic mosaicism in any of the non-penetrant cases, but

preliminary analysis of haplotypes around *TCF12* (which resides in a region of strong linkage disequilibrium) suggested that the allelic backgrounds of both non-mutant and mutant copies of *TCF12* contribute to variability in the phenotype (data not shown). Of 14 mutation-positive relatives diagnosed with craniosynostosis involving specific sutures, 12 had coronal synostosis, and 2 had sagittal synostosis.

The clinical features associated with *TCF12*-related craniosynostosis are detailed (Supplementary Table 5.3), and representative subjects with bilateral coronal synostosis (Figure 5.1A) or unilateral coronal synostosis (Figure 5.1B) are shown. In 15 probands (39%), a genetic cause was suspected because of a positive family history. In another seven probands (18%), clinical features (including dysmorphic appearance of the face and external ears and minor limb anomalies) were suggestive of Saethre-Chotzen syndrome, which had been excluded by negative *TWIST1* mutation testing. The remaining subjects (16/38 = 42%) presented sporadically with apparently non-syndromic synostosis (Supplementary Table 5.1). No genotype-phenotype correlation was detected. For affected individuals recruited at Oxford, we compared the surgical trajectory¹²⁸ of *TCF12*-positive individuals with those of individuals falling into other clinical and genetic categories. The individuals with *TCF12* mutations had a more benign course compared with individuals with either p.Pro250Arg *FGFR3* or *TWIST1* alterations (Supplementary Figure 5.6), and no individuals positive for *TCF12* mutations were documented to have an interval onset of raised intracranial pressure after their initial surgical procedure(s). Most individuals had normal developmental attainment, but ten (14%) had developmental delay or learning disability, which in two cases was associated with autism (clinical features are summarized in Supplementary Table 5.4). Previous genetic data derived from homozygous mutant mice identified key roles for the orthologous *Tcf12* gene in the development of the immune system,^{222,227} but we found no history of infection susceptibility in individuals heterozygous for *TCF12* mutations, and there was no detectable reduction in monocyte, natural killer (NK), T-cell or B-cell subsets or lower amounts of immunoglobulin in 11 mutation-positive individuals.

Supporting our transactivation data (Supplementary Figure 5.4), it was previously reported that *TCF12* forms heterodimers with *TWIST1*²²⁸ and that *TWIST1* haploinsufficiency causes Saethre-Chotzen syndrome.^{138,139,216} Our observation that haploinsufficiency of *TCF12* in humans leads specifically to coronal synostosis suggests that the total quantity of *TCF12*-*TWIST1* heterodimers is a critical factor in coronal suture development.

To test this hypothesis, we compared the phenotypes of the previously constructed individual heterozygous null mutant mice (*Ella-Cre; Tcf12^{flox/+}* and *Twist1^{+/-}*)^{227,229,230} to that of the compound heterozygotes (*Ella-Cre; Tcf12^{flox/+}; Twist1^{+/-}*). At three weeks of age, the *Ella-Cre; Tcf12^{flox/+}* animals ($n = 14$) had normal coronal sutures, indicating



that the coronal suture is less sensitive to *Tcf12* dosage in mice than in humans (Figure 5.1C,D); *Twist1*^{+/-} mice (*n* = 4) showed variable coronal synostosis, as previously reported (Figure 5.1E).^{139,231} However, the *Ells-Cre; Tcf12*^{fllox/+}; *Twist1*^{+/-} compound heterozygotes (*n* = 6), which were born at a frequency close to the expected Mendelian ratio (25%), consistently showed severe coronal synostosis (Figure 5.1F).

The discovery that haploinsufficiency of *TCF12* causes coronal synostosis in humans and that severe bilateral coronal synostosis occurs in mice with 50% of the wild-type dosage of both the *Tcf12* and *Twist1* genes highlights the key role of TCF12 acting with TWIST1, probably as a heterodimeric complex, in the normal development of the coronal sutures. The TCF12-TWIST1 heterodimer is likely to regulate specification of the boundary between the neural crest and cephalic mesoderm^{231,232} and/or inhibit osteogenic differentiation via actions on RUNX2²³³ and bone morphogenetic protein²³⁴ or fibroblast growth factor receptor²²⁸ signalling.

URLs

ANNOVAR, <http://www.biobase-international.com/product/annovar>;

GBrowse2, <http://gmod.org/wiki/GBrowse>;

MRC-Holland, <http://www.mrc-holland.com/>;

PolyPhen-2, <http://genetics.bwh.harvard.edu/pph2>;

SAMtools, <http://samtools.sourceforge.net>.

Accession codes

All cDNA numbering of *TCF12* follows NCBI reference NM_207037.1, starting with A of the ATG initiation codon (+1). We used NM_207040.1 to design primers to the alternatively spliced first exon (9A). The genomic reference sequence is available under accession NC_000015.9.

Supporting information

Samples

The clinical studies were approved by Oxfordshire Research Ethics Committee B (reference C02.143), Riverside Research Ethics Committee (reference 09/H0706/20) and the Medical Ethical Committee of the Erasmus University Medical Centre Rotterdam (MEC-2012-140). Written informed consent to obtain samples for genetics research was obtained from each child's parent or guardian. The clinical diagnosis of craniosynostosis was confirmed by CT scan, and evidence of associated syndromic features was sought by clinical examination. Venous blood was obtained for DNA and RNA extraction (collected into PAXgene Blood RNA tubes (Qiagen) for the latter procedure). Fibroblast cultures were established from skin biopsies obtained from the scalp incision at the time of surgical

intervention. When clinically indicated, samples were tested for mutation hotspots in *FGFR2*, *FGFR3* and *TWIST1*,¹²⁵ and significant chromosome aneuploidy was investigated using aCGH; samples with identified mutations known to cause craniosynostosis were excluded. Seven samples from unrelated individuals with bilateral coronal synostosis were chosen for exome sequencing. These comprised five subjects who were clinically non-syndromic with negative family history, one subject who was clinically non-syndromic but reported to have two children with coronal synostosis and one subject who was the only individual in the family affected with craniosynostosis but who had short thumbs that were also present in several additional family members from the two previous generations.

Exome sequencing

We used an Agilent SureSelect Human All Exon Kit (v.2; 44 Mb) to capture exonic DNA from a library prepared from 3 µg of each proband's genomic DNA (extracted from whole blood). The enriched DNA was sequenced on an Illumina Genome Analyzer IIx platform with 51-bp paired-end reads. We generated between 3.98 and 4.56 Gb of sequence for each sample that, after mapping with Novoalign (Novocraft Technologies) to the hg19 genome and removal of artefacts using custom Perl scripts, resulted in an average coverage of exons of between 33- and 44-fold. Variants were called using SAMtools and annotated using ANNOVAR and PolyPhen-2. We removed all variants annotated in dbSNP132 and manually examined the gene lists for overlaps of two or more variants. Sequence data were visualized using GBrowse2.



Analysis of *TCF12*

After the identification of candidate *TCF12* mutations in the exome sequence, we confirmed and extended this analysis by direct sequencing of genomic PCR amplification products, MLPA and analysis of cDNA products. Details of the oligonucleotides and experimental conditions are provided in Supplementary Table 5.5. Our initial screening panel mostly comprised samples recruited in Oxford¹²⁸ and other craniofacial units within the UK, and the replication panel comprised samples obtained in Rotterdam, the Netherlands. PCR amplification was performed in a volume of 20 µl, containing 15 mM Tris-HCl (pH 8.0), 50 mM KCl, 2.5 mM MgCl₂, 100 µM each dNTP, 0.4 µM primers and 0.5 units of Amplitaq Gold polymerase (Applied Biosystems), with or without 10% DMSO, as indicated. Cycling conditions consisted of an 8-min denaturation step at 94 °C, followed by 35 cycles of 94 °C for 30 s, annealing at 65 °C (unless otherwise indicated in Supplementary Table 5.5) for 30 s and extension at 72 °C for 30 s, with a final extension at 72 °C for 10 min. Amplification products were sequenced using the BigDye Terminator v3.1 cycle sequencer system (Applied Biosystems). All mutations were reconfirmed, either by restriction digestion of 5 µl of PCR product or by repeat dideoxy sequencing

of an independent PCR product. In addition to the mutations listed in Supplementary Table 5.1, we identified two previously unreported variants in single individuals that are currently of uncertain pathogenic significance, c.630T>G, p.(Ser210Arg) and c.982A>G, p.(Asn328Asp).

Copy-number variation was analysed by MLPA performed using synthetic oligonucleotide probes designed to *TCF12* according to protocols available from MRC-Holland. Fragments were analysed by capillary electrophoresis using an ABI 3130 containing POP-7 polymer. Peaks were visualized using Gene Mapper v3.7 (Applied Biosystems). Normal MLPA results were obtained in 226 craniosynostosis samples negative for intragenic *TCF12* mutations. For studies of splicing and mRNA stability, RNA was extracted from whole blood and fibroblasts using TRIzol reagent. cDNA was synthesized using the Fermentas RevertAid First-Strand Synthesis kit with random hexamer primers according to the manufacturer's instructions. The microsatellites used to confirm sample relationships were *D3S1311*, *D4S403*, *D5S2027*, *D6S1610*, *D7S519*, *D9S158*, *D10S548*, *D11S898*, *D13S1265*, *D14S280*, *D16S415* and *D18S474*.

Immune function tests

Peripheral blood mononuclear cells (PBMCs) were isolated from whole blood by density gradient centrifugation in cell separation tubes (Sigma), washed three times in sterile PBS and rested overnight in RPMI 1640 medium supplemented with 10% FCS, 1% L-glutamine, 1% penicillin/streptomycin solution and 50 μ M β -mercaptoethanol (all from Sigma) and 1% HEPES buffer (GibcoBRL). Monocytes, NK cells and naive, effector and memory T- and B-cell subsets were enumerated by flow cytometry of PBMCs stained with human-specific antibodies against CD3, CD4, CD19, CD14, CCR7, CD45RO, CD62L, CD16, CD56, CD25, IgD, IgM, CD10 and CD27 (Supplementary Table 5.6). Total IgM, IgA and IgG antibody titres were measured by ELISA.

Transactivation analysis of missense mutations

We obtained a full-length *TCF12* cDNA clone (pCMV6-XL5, encoding HEB β) from OriGene and synthesized the *TWIST1* clone (pCMV-Twist) in house. The pCaSpeR-*Tinman::lacZ* (pTinE1/E2/E3) construct (containing three *Tinman* E-boxes comprising two 5'-CATGTG-3' and one 5'-CATATG-3') was used as a bHLH protein-responsive reporter, and placZ (containing no E-boxes) was used as a control (both constructs were gifts from E.M. Füchtbauer).²²⁴ PCR mutagenesis was used to introduce the c.1871T>C and c.1912C>G mutations into the *TCF12* cDNA using the primers indicated in Supplementary Table 5.5; mutated cDNAs were fully verified by sequencing.

The HT1080 human cell line was cultured in high-glucose DMEM (Invitrogen) supplemented with 10% FCS. Cells were transfected in triplicate with 1 μ g of reporter plasmid, 1 μ g each of *TWIST1* and *TCF12* constructs or the corresponding empty

expression vectors using Promega FuGENE 6 transfection reagent according to the manufacturer's protocols. Transfections were carried out when cells were ~50% confluent in 6-well plates. Cells were harvested after 48 h, and β -galactosidase assays were performed in triplicate on 5 μ l of cellular extract using the Galacto-Star system (Applied Biosystems). The missense mutations were modelled in Protein Workshop onto the structure of mouse E47/NeuroD1 (Protein Data Bank (PDB) accession 2QL2).²³⁵

Analysis of mouse mutants

The mouse mutants analysed were *Tcf12*^{fl^{ox}} (obtained on a mixed C57BL/6/129 background as a gift of Y. Zhuang),²²⁷ *Ella-Cre* (purchased from The Jackson Laboratory (B6.FVB-Tg(Ella-cre) C5379Lmgd/J)²²⁹ and *Twist1* (C57BL/6 background).²³⁰ The *Ella-Cre* transgene was detected using primers Cre-F and Cre-R (Supplementary Table 5.5); *Tcf12*^{fl^{ox}} and *Twist1* were genotyped as described.^{227,230} Heads of P21 mice were skinned and stained for mineralized bone with Alizarin Red S (80 mg/l in 1% KOH) for 3 days. Skulls were then cleared and stored in 100% glycerol. P21 mouse skulls were scanned using a μ CT system (SCANCO μ CT 50, Scanco Medical AG) and analysed using Amira software (Visage Imaging). All scans were conducted at an energy setting of 70 kVp, current intensity of 200 μ A, integration time of 500 ms/projection, 0.24 degree rotational step (DRS) and a field of view (FOV) of 15.1 mm. Scans were performed at a 10- μ m isotropic resolution.





Identification of intragenic exon deletions and duplication of *TCF12* by whole genome or targeted sequencing as a cause of *TCF12*-related craniosynostosis

Jacqueline A.C. Goos,* Aimée L. Fenwick,* Sigrid M.A. Swagemakers, Simon J. McGowan, Samantha J.L. Knight, Stephen R.F. Twigg, A. Jeannette M. Hoozeboom, Marieke F. van Dooren, Frank J. Magielsen, Steven A. Wall, Irene M.J. Mathijssen, Andrew O.M. Wilkie, Peter J. van der Spek, Ans M.W. van den Ouweland

* Equal contributors

Human Mutation June 2016

Abstract

TCF12-related craniosynostosis can be caused by small heterozygous loss-of-function mutations in *TCF12*. Large intragenic rearrangements, however, have not been described yet. Here, we present the identification of four large rearrangements in *TCF12* causing *TCF12*-related craniosynostosis. Whole genome sequencing was applied on the DNA of 18 index-cases with coronal synostosis and their family members (43 samples in total). The data were analysed using an autosomal-dominant disease model. Structural variant analysis reported intragenic exon deletions (of sizes 84.9, 8.6 and 5.4 kb) in *TCF12* in three different families. The results were confirmed by deletion-specific PCR and dideoxy-sequence analysis. Separately, targeted sequencing of the *TCF12* genomic region in a patient with coronal synostosis identified a tandem duplication of 11.3 kb. The pathogenic effect of this duplication was confirmed by cDNA analysis. These findings indicate the importance of screening for larger rearrangements in patients suspected to have *TCF12*-related craniosynostosis.

Introduction

Craniosynostosis is a condition in which the calvarial sutures are fused prematurely. Fusion of the coronal sutures has the highest chance of having a specific genetic cause. In patients with coronal synostosis, mutations are often found in *FGFR2* [MIM: 176943], *FGFR3* [MIM: 134934], *TWIST1* [MIM: 601622] and *EFNB1* [MIM: 300035]. Recently, however, another disease gene for coronal synostosis, *TCF12* [MIM: 600480], has been identified.⁵⁹ The product of this gene is a member of the basic helix-loop-helix E-protein family and forms heterodimers with *TWIST1*.^{59,228}

In 32% and 10%, respectively, of patients with bicoronal and unicoronal synostosis in whom other genetic testing was negative, a pathogenic heterozygous mutation could be identified in *TCF12* by dideoxy-sequencing.⁵⁹ In addition to coronal synostosis, patients can have craniofacial features suggestive of Saethre-Chotzen syndrome, and a minority has developmental delay and/or learning disabilities. On the other hand, a substantial proportion (>50%) of individuals heterozygous for a pathogenic *TCF12* mutation are non-penetrant.⁵⁹

In patients with *TCF12*-related craniosynostosis, point mutations are predominantly found.^{59,236,237} A few patients with craniosynostosis and intellectual disability have been reported with large chromosome 15q deletions including *TCF12*.^{221,238,239} Recently, Le Tanno *et al.* have described a heterozygous *de novo* deletion of 3.64 Mb due to an unbalanced maternally inherited translocation in a patient with coronal craniosynostosis and intellectual disability.²⁴⁰ In addition, a 72-year-old patient has been identified with intellectual disability (without clear signs of craniosynostosis) and a *TCF12* microdeletion of 84-121 kb, removing exons 19-21 and extending 3' from the end of the gene.²⁴¹ Gross rearrangements with both breakpoints lying within *TCF12*, however, have not been described to date; in the original report of *TCF12* mutations, an assay for deletions using multiplex ligation-dependent probe amplification (MLPA) found no rearrangements in 226 mixed craniosynostosis samples negative for intragenic *TCF12* mutations.⁵⁹

In this study, we describe the identification of three large inherited intragenic exon deletions in *TCF12* using whole genome sequencing and one large inherited duplication using targeted *TCF12* sequencing.

Within the framework of a broader study into the genetic causes of craniosynostosis, whole genome sequencing was applied to DNA of 18 Dutch index cases with coronal synostosis and negative testing for *FGFR2*, *FGFR3* and *TWIST1*, and their family members (43 samples in total), by Complete Genomics, a BGI company (Mountain View, CA, USA), as described by Drmanac *et al.*¹⁰⁴ The data were analysed using an autosomal-dominant disease model. Structural variant analysis using a custom made Python script¹⁴³ reported different large intragenic exon deletions of *TCF12* in three families



(families 1, 2 and 3). The clinical features of the families are summarized in Table 6.1 and full subject descriptions and pedigrees are provided in the Supporting Information and Supplementary Figure 6.1 respectively.

A heterozygous 84,949 bp deletion was reported in family 1, starting at chr15:57478485 and ending at chr15:57563433 (c.391-5871_1746-1795del) in DNA of the index patient and his mother (using reference NM_207037.1 on GRCh37). Exons 7 through 18 were deleted. In family 2, a heterozygous deletion of 8,580 bp was reported, starting at chr15:57560034 and ending at chr15:57568613 (c.1745+4562_1978+3153del) in DNA of the index patient, the clinically unaffected father and affected paternal aunt. The deletion removed exon 19. In family 3, a heterozygous 5,363 bp deletion was reported, starting at chr15:57571496 and ending at chr15:57576858 (c.1979-3147_*12-1497del) in DNA of the index patient and his clinically unaffected mother. This deleted exon 20. The three deletions were not seen in control samples (i.e. Structural Variation Baseline Genome Set comprising 52 baseline genomes used by Complete Genomics and 588 Welllderly samples [Scripps Welllderly Genome Resource, The Scripps Welllderly Study, La Jolla, CA [December, 2015]], funding provided by Scripps Health and NIH/NCATS UL1 TR00114).

Deletion-specific PCRs were designed to confirm the findings by whole genome sequencing (Figure 6.1A-E). In family 1, the mutant PCR product of 644 bp was present in II.2 and III.1 (Figure 6.1B lanes 2-4, and 6.1C). An analysis of the normal sequence showed that the proximal breakpoint resided in an *AluJb* element, whereas the distal breakpoint was located in a *L1P2* repetitive element. The sequences of the breakpoints showed no significant similarity except for a shared 4 bp GAGC motif. In family 2, the mutant PCR product of 556 bp was present in II.1, II.2 and III.1 (Figure 6.1B lanes 5-8, and 6.1D). The proximal breakpoint was located in an *MIRb* element and the distal breakpoint in a *HAL1* element. The sequences showed no significant similarity, except for a shared cytosine. In family 3, the mutant PCR product of 646 bp was present in II.2 and III.2 (Figure 6.1B lane 9-11, and 6.1E). The proximal breakpoint also resided in a *HAL1* element; the distal breakpoint was not located in a repetitive element. However, an *AluSz* repeat was located 151 bp centromeric of the distal breakpoint and an *MIRb* 789 bp telomeric. The sequences of the breakpoints showed no significant similarity. Amplification of patient cDNA of family 3 with primers located in exon 18 and 3' UTR (exon 21) showed an extra smaller product, absent in control cDNA. Sequencing of the smaller-sized product indicated skipping of exon 20 (Supplementary Figure 6.2).

Table 6.1. Clinical features of families harbouring *TCF12* rearrangements.

	Family 1	Family 2	Family 3	Family 4
cDNA position of rearrangement	c.391–5871_1746–1795del	c.1745 + 4562_1978 + 3153del	c.1979–3147_12–1497del	c.1746–1697_11 + 65dup
Size of rearrangement (kb)	84.9	8.6	5.4	11.3
Exons involved	7–18	19	20	19 and 20
Type of rearrangement	Deletion	Deletion	Deletion	Duplication
Gender of index patient	Male	Female	Male	Male
Gestational age (weeks)	37+6	42+4	39+4	38
Birth weight (grams)	3,075	3,620	3,365	NA
Cranial suture fusion	RC	BC	All except M	BC
Major craniofacial procedures	Fronto-supraorbital remodelling @ 10 months	Supraorbital advancement @ 9 months	Fronto-biparietal remodelling @ 8 months, parieto-occipital decompression @ 2 years	FOAR @ 10.5 months
Development	Mild learning problems VIQ 82, PIQ 64, GIQ 74	Normal	Normal	Normal
Limbs	Fifth finger camptodactyly	Normal	Normal	Fifth finger clinodactyly
Other major clinical features	Divergent strabismus, recurrent infections, febrile seizures	Myopia, crowding of teeth, divergent growth pattern	Increased ICP	Class II.1 malocclusion, small ears with prominent helical crura
Family history	Mother LC	Sister of father brachycephaly	Negative	Flattened foreheads in maternal half-brother and his daughter
Previous genetic diagnostics	Karyotyping, <i>FGFR2</i> , <i>FGFR3</i> , <i>TWIST1</i> , <i>TCF12</i>	<i>FGFR2</i> , <i>FGFR3</i> , <i>TWIST1</i> , <i>TCF12</i>	<i>FGFR2</i> , <i>FGFR3</i> , <i>TWIST1</i>	<i>FGFR2</i> , <i>FGFR3</i> , <i>TWIST1</i> , <i>TCF12</i>
Subjects sequenced	II.1, II.2 and III.1	II.1, II.2, II.3 and III.1	II.1, II.2 and III.2	III.1

BC = Bicoronal, FOAR = Fronto-orbital advancement and remodelling, GIQ = Global IQ, LC = Left coronal, M = Metopic, PIQ = Performal IQ, RC = Right coronal, VIQ = Verbal IQ.



In parallel to this work, targeted sequencing of DNA samples of 160 British unrelated subjects with craniosynostosis, including the coronal suture, and previously negative testing of the *FGFR2*, *FGFR3*, *TWIST1* and *TCF12* genes, was carried out by capturing the *TCF12* genomic region (chr15: 57,029,979-57,670,037) using the SeqCap EZ Choice Library system (Roche-Nimblegen, Inc., Madison, WI, USA). Using analysis with Pindel,²⁴² a heterozygous tandem duplication was called in the index patient of family 4 (pedigree in Supplementary Figure 6.1D (II.1)).

Breakpoint spanning PCR (using primers orientated in opposite directions in the wild-type sequence, shown in Supplementary Table 6.1) showed a mutant PCR product from genomic DNA of both the index patient and his clinically unaffected mother (Figure 6.1F). Dideoxy-sequencing confirmed a tandem duplication of 11,331 base pairs, starting at chr15:57563531 and ending at chr15:57574861 (c.1746-1697_*11+65dup) in the DNA of the index patient of family 4. The duplication included *TCF12* exons 19 and 20.

An analysis of the normal sequence showed that the proximal breakpoint was located in an *L1P2* repetitive element, whereas the distal breakpoint did not reside in a repetitive element. Further sequence analysis revealed the presence of an *MER1A* DNA sequence 678 bp centromeric of the distal breakpoint, and the presence of an *AluSx* element and a simple tandem repeat at 597 bp and 1,165 bp, respectively, telomeric of the distal breakpoint. The sequences of the breakpoints shared an AG dinucleotide (Figure 6.1G).

Amplification of patient cDNA with primers located in exon 18 and 3' UTR (therefore spanning the duplication) showed only a single product corresponding to the wild-type allele (data not shown). This suggested that the product from the duplicated allele might be expressed at a relatively low level, although bias in PCR amplification favouring the smaller wild-type product could not be excluded. We therefore designed a pair of primers in exon 19, orientated in opposite directions, predicted to generate a product only from the duplicated allele. Electrophoresis of PCR products revealed two relatively weak fragments in the patient cell line, absent in two controls (Figure 6.1I). Sequencing of the smaller-sized product indicated splicing from exon 20 to the duplicated exon 19, whereas the larger product contained additional neo-exon sequence of 35 bp, originating from within the intron 18-19 sequence (Figure 6.1J).

In summary we have identified the first intragenic duplication and deletions within *TCF12* in patients with craniosynostosis. These findings demonstrate the importance of screening, not only for point mutations and small indels in *TCF12*, but also for larger rearrangements.

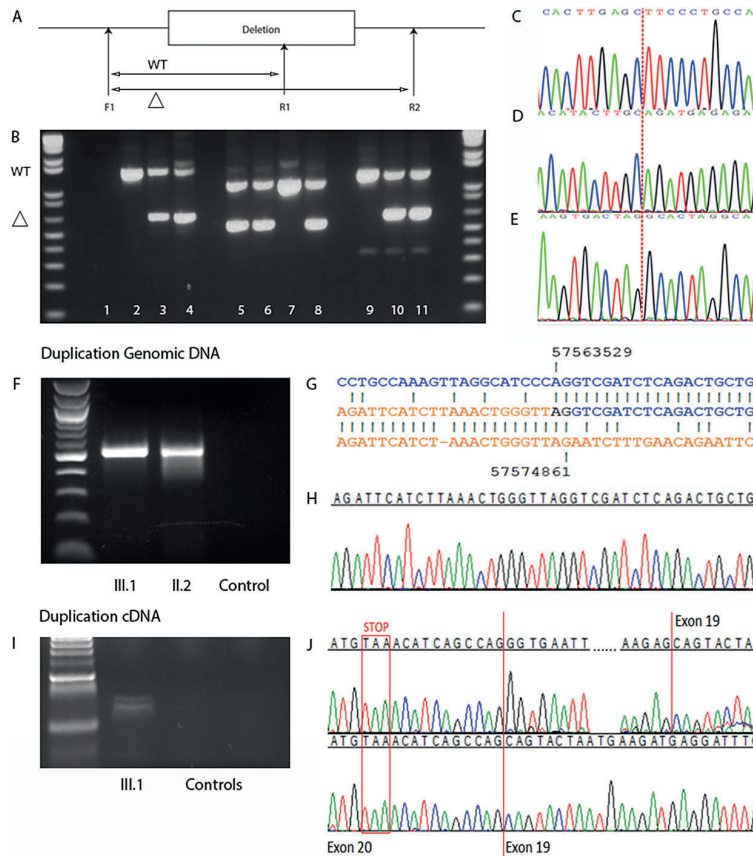


Figure 6.1. Rearrangements identified in *TCF12*. **A–E:** confirmation of deletions. **A** primer design. F1, forward primer; R1, reverse primer 1; R2, reverse primer 2. F1+R1, wild-type allele (WT); F1+R2, mutant allele (Δ). **B:** results of mutation-specific deletion PCR analysis. Lane 1, negative control. Lanes 2–4, family 1; wild-type fragment 1,455 bp, mutant fragment 644 bp; lane 2, II.1; lane 3, II.2; lane 4, III.1. Lanes 5–8, family 2; wild-type fragment 1,107 bp, mutant fragment 556 bp; lane 5, II.1; lane 6, II.2; lane 7, II.3; lane 8, III.1. Lanes 9–11, family 3; wild-type fragment 1,303 bp, mutant fragment 646 bp; lane 9, II.1; lane 10, II.2; lane 11, III.2. **C–E:** electropherograms of dideoxy sequence analysis. **C:** mutant allele in family 1, exons 7–18 deleted. **D:** mutant allele in family 2, exon 19 deleted. **E:** mutant allele in family 3, exon 20 deleted. Dashed lines indicate where deletions occurred. **F–J:** confirmation of duplication. **F:** PCR from genomic DNA confirming the presence of duplication in index patient of family 4 (III.1), which was inherited from the index patient's clinically unaffected mother (II.2). **G:** the sequence at the duplication breakpoint is sandwiched between the normal proximal (above) and distal (below) sequences, with the electropherogram underneath (**H**). **I:** cDNA amplified from the index patient (III.1) with primers specific to the mutant allele. Two different products were visible on the gel (but absent in two control cDNA samples). **J:** sequencing of these products indicated splicing from exon 20 to the duplicated exon 19 in the smaller-sized product (lower electropherogram). The larger product (upper electropherogram) contains an additional 35 nucleotide neo-exon between exons 20 and 19. The normal stop codon in exon 20 is highlighted.

In patients with non-syndromic and syndromic bicoronal or unicoronal synostosis, *FGFR2*, *FGFR3* and *TWIST1* are often tested routinely for mutations. In approximately 28% of the craniosynostosis patients (with any combination of sutures fused) having a genetic cause, a pathogenic mutation can be identified in *FGFR2*, in 19% of the patients in *FGFR3*, and in 16% in *TWIST1*. *TCF12* intragenic mutations cause approximately 4% of these cases.⁵⁹

To date, we have tested, by dideoxy-sequencing of *TCF12*, 105 Dutch syndromic and non-syndromic coronal craniosynostosis index patients with negative results for *FGFR2*, *FGFR3* and *TWIST1* testing. This led to the identification of 22 *TCF12* mutation-positive index cases (including 14 cases that were previously described by Sharma *et al.*)⁵⁹ We now report the identification of gross deletions of *TCF12* in three out of 18 index cases that were analysed by whole genome sequencing (in five cases a mutation was found in another gene). Furthermore, we describe a gross *TCF12* duplication in a further patient with coronal synostosis, using targeted sequencing of the *TCF12* genomic region.

The identification of *TCF12* deletions in two of the Dutch patients (families 1 and 2) was a particular surprise, because these patients had been included in the negative MLPA analysis (zero positive from 226 samples) previously reported by Sharma *et al.* (2013).⁵⁹ Re-examination of the raw MLPA data revealed that the analysis had not been performed correctly, and both deletions were in fact evident. Further scrutiny of the remaining MLPA data revealed an Oxford sample that harboured a deletion of exons 5-19, which was independently found in the *TCF12* capture sequencing data (not shown). Hence, it is evident that *TCF12* deletions contribute more frequently to coronal synostosis than previously thought; combining the results of whole genome sequencing (3/13) and the reanalysed MLPA dataset (1/95), 4 of 108 (3.7%) individuals with this diagnosis and previously negative for standard genetic testing, were found to have deletions. Overall, three out of 25 Dutch cases of *TCF12*-related craniosynostosis were caused by large, intragenic *TCF12* rearrangements.

Analysing the breakpoint sequences, it appears that the rearrangements occur in, or in the proximity of, repeat sequences (family 1 *AluJb* SINE and *L1P2* LINE element; family 2 *MIRb* SINE and *HAL1* LINE; family 3 *HAL1* LINE and in proximity of *AluSz* SINE/*MIRb* SINE; family 4 *L1P2* LINE and in proximity of *MER1A/AluSx* SINE). Furthermore, the sequences of the breakpoints show no significant similarity (family 1 four-nucleotide homology; family 2 one shared nucleotide; family 3 none; family 4 two shared nucleotides). The nonobligatory presence of terminal microhomology and repeat sequences indicates classical nonhomologous end joining as the most likely mechanism.²⁴³⁻²⁴⁵

All but one previously described pathogenic mutations are located in the 3' half of *TCF12* (exons 9-19).⁵⁹ The first two deletions also include this region of the gene (family 1 exons 7-18 and family 2 exon 19). The deletion in family 1 contains regions of *TCF12*

encoding the activation domain 2 and the rep domain. In family 2, the region encoding the functionally important basic helix-loop-helix domain is included.^{225,226,246} These domains are still present in the mutant alleles in families 3 and 4. cDNA studies indicate skipping of exon 20 in family 3 (Supplementary Figure 6.2). Although the duplicated allele in family 4 should retain the capacity to translate the full-length protein, the cDNA studies (Figure 6.1G) indicate that this transcript is likely unstable, causing functional haploinsufficiency. The rearrangements in families 3 and 4 are the first mutations described that lie 3' of the region that encodes the bHLH domain.

While the deletion in family 1 is 10-fold larger than that in family 2 and removes two functional domains of *TCF12*, the clinical craniofacial features of the index patient of family 1 are not more severe than the features of the index patient of family 2. The index patient of family 1 has unicoronal synostosis, whereas the index patient of family 2 and her aunt have bicoronal synostosis. The index patient of family 1, however, does have mild learning disability. The most severe phenotype in our study is seen in the index patient of family 3 (synostosis of almost all sutures and increased intracranial pressure), though the smallest deletion is present in this family. Although the index patient of family 4 has a duplication partially overlapping the deleted regions of both family 2 and the more severely affected family 3, he only shows bicoronal synostosis and minor anomalies like fifth finger clinodactyly. Clinodactyly and brachydactyly (present in his mother), have previously been described in association with *TCF12* mutations.^{59,236} Overall, the findings do not reveal any genotype-phenotype correlation.

The index patient of family 3 does not exhibit the classical clinical phenotype of *TCF12*-related craniosynostosis, since all vault sutures were fused except for the metopic suture. Only two patients have been described previously with synostosis of the coronal sutures combined with synostosis of the sagittal suture.⁵⁹ Also, the patient had papilledema postoperatively, indicating increased intracranial pressure. To our knowledge, this is the first patient described with *TCF12*-related craniosynostosis and increased intracranial pressure postoperatively.

In conclusion, the clinical features of the index patients of family 1, 2 and 4 fit the phenotype of *TCF12*-related craniosynostosis as described by Sharma *et al.*⁵⁹ The reduced penetrance described previously is seen in three of our families as well. Our study demonstrates that *TCF12*-related craniosynostosis can also be caused by large intragenic rearrangements and that there is no indication of a genotype-phenotype correlation. Therefore, mutation analysis of *TCF12* should also include a search for larger rearrangements.



Supporting information

Materials and methods

Ethical approval was given for whole genome sequencing by the board of the Medical Ethical Committee Rotterdam (MEC-2012-140) and for targeted *TCF12* sequencing by the Oxfordshire Research Ethics Committee B (reference C02.143) and London Riverside Research Ethics Committee (reference 09/H0706/20). Informed consent was received from the study participants.

Within the framework of a broader study into the genetic causes of craniosynostosis, whole genome sequencing was applied on the DNA of 18 Dutch index-cases with coronal synostosis and negative testing for *FGFR2*, *FGFR3* and *TWIST1*, and their family-members (43 samples in total), by Complete Genomics, a BGI company (Mountain View, CA, USA), as described by Drmanac *et al.*¹⁰⁴ Data were analysed using cga tools version 1.6.0.43. An autosomal dominant disease model was tested. The analysis was restricted to novel non-synonymous variants, variants disrupting a splice site (± 2 bp), and insertions or deletions in the coding sequence (± 50 bp). Because there were no obvious mutations in known craniosynostosis genes (list of variants available on request), a structural variant analysis was performed using a custom-made Python script. Structural variant calling was performed using uniquely mapped discordant read pairs as described by Gilissen *et al.*,¹⁴³ and filtering was based on scrutinizing regions with a known association with craniosynostosis. In three families, large intragenic exon deletions were identified in *TCF12*. Variants of family 1 and 2 were annotated using NCBI build 36.3/hg18 and dbSNP build 130, variants of family 3 were annotated using GRCh37/hg19. Annotations of the deletions of family 1 and 2 were lifted over to hg19 by using Human BLAT search on the UCSC website (Kent Informatics, Inc., Santa Cruz, CA, USA).

The deletions identified by whole genome sequencing were confirmed by deletion specific PCR. Primers used for the deletion PCR are given in Supplementary Table 6.1. For each specific deletion PCR, one forward and one reverse primer were designed outside the deletion. The third primer was designed in the deleted region in such a way that the PCR product resulting from the mutant allele was smaller than the PCR product produced from the wild-type allele.

In parallel to this, targeted sequencing of DNA samples of 160 British unrelated subjects with craniosynostosis, including the coronal suture, and previously negative testing of the *FGFR2*, *FGFR3*, *TWIST1* and *TCF12* genes, was carried out by capture of the *TCF12* genomic region (chr15: 57,029,979-57,670,037) using the SeqCap EZ Choice Library system (Roche-Nimblegen, Inc., Madison, WI, USA). Samples were multiplexed and two pools of 80 samples were each run on a single lane of the HiSeq2500 platform

(Illumina, Inc., San Diego, CA, USA) run in rapid mode. The resulting data were aligned using Novoalign (<http://www.novocraft.com/products/novoalign/>) to the human reference genome GRCh37/hg19, and indels were detected by Pindel v0.2.4.²⁴²

The duplication was confirmed on genomic DNA by breakpoint spanning PCR (primers shown in Supplementary Table 6.1). The effect of the duplication and the deletion in family 3 were studied by cDNA analysis. RNA was extracted from a lymphoblastoid cell line obtained from individual III.1 (family 4) using Trizol reagent (Invitrogen, Carlsbad, CA, USA) and the RNeasy kit (Qiagen Ltd., Crawley, UK). cDNA was synthesized using the RevertAid First Strand cDNA kit (Thermo Scientific Inc., Waltham, MA, USA), with random hexamer primers according to the manufacturer's instructions.

All amplification reactions were performed according to standard procedures. Products were electrophoresed on agarose gels in TBE buffer. To confirm the exact position of the breakpoints, the PCR products were sequenced. PCR products were purified with ExoSAP-IT (USB, Affymetrix, Cleveland, OH, USA). Dideoxy-sequencing of both strands was performed using Big Dye terminator version 3.1 (Applied Biosystems, Foster City, CA, USA) as recommended by the manufacturer. Dye terminators were removed using SephadexG50 (GE Healthcare, Pittsburgh, PA, USA) and loaded on an ABI 3130XL Genetic Analyzer or ABI 3730 (Applied Biosystems).

The pathogenic mutations were described according to HGVS nomenclature,¹⁴⁸ using reference NM_207037.1 consisting of 21 exons, protein coding from exon 2 through 20, on GRCh37 and submitted to the Leiden Open Variation Database (<http://www.lovd.nl/TCF12>).

Subject descriptions

Family 1

The index patient was a boy, born by caesarean section due to breech position at 37+6 weeks of gestation, weighing 3,075 grams (Supplementary Figure 6.1A, III.1). He had non-consanguineous parents. Directly after birth, a progressive skull malformation was observed. Physical examination at the age of 4.5 months showed a frontal plagiocephalic head shape and a closed fontanel. The skull circumference was 42.5 cm (-0.41 SD). Apart from bilateral camptodactyly of the fifth fingers, no hand or foot anomalies were present. Skull radiographs and 3-dimensional computed tomography (3D-CT) showed synostosis of the right coronal suture. A fronto-supraorbital remodelling was performed at the age of 10 months. Furthermore, a tenotomy was performed at the age of 4 years because of divergent strabismus and an adenoidectomy was performed because of recurrent airway infections. In addition to this, he suffered from febrile seizures. He had mild learning problems (Verbal IQ 82, Performance IQ 64, Global IQ 74). Karyotyping was normal and *FGFR2*, *FGFR3*, *TWIST1* and *TCF12* were tested negative by dideoxy-



sequencing. The family history was positive; his mother (II.2) was born with a left-sided plagiocephaly, requiring a surgical correction early in life. The DNA of subjects II.1, II.2 and III.1 was sequenced.

Family 2

The index patient was a girl born as the third child of non-consanguineous unaffected parents at 42+4 weeks of gestation, weighing 3,620 grams (Supplementary Figure 6.1B, III.1). Physical examination at the age of 5 months showed a frontal brachycephalic head shape. The skull circumference was 41 cm (-0.87 SD). Her hands and feet were normal. Skull radiograph and 3D-CT showed bicoronal synostosis. At the age of 9 months, a supraorbital advancement was performed. Later, the girl was seen by an ophthalmologist because of myopia. Furthermore, she was seen by an orthodontist because of a divergent growth pattern and crowding of teeth. She had normal development. The family history was positive; a sister of the father (II.1) had an un-operated brachycephalic head shape. The father of the patient was clinically unaffected. Learning disabilities were not mentioned in the family. In the index patient, no mutations were found in *FGFR2*, *FGFR3*, *TWIST1* and *TCF12* by dideoxy-sequencing. The DNA of subjects II.1, II.2, II.3 and III.1 was sequenced.

Family 3

The index patient was a boy born as a second child at 39+4 weeks of gestation, weighing 3,365 grams (Supplementary Figure 6.1C, III.2). Physical examination at the age of 6 months showed an asymmetrical skull shape, with frontal bossing (predominantly on the left side), right-sided supra-orbital retrusion and an asymmetrical occiput. The skull circumference was 45 cm (+0.62 SD). Hands and feet were normal. Skull radiographs and 3D-CT showed premature fusion of all calvarial sutures, except for the metopic suture. Clinically, the patient was suspected to have Crouzon syndrome. A fronto-biparietal remodelling was performed at the age of 8 months. At the age of 2 years, the patient had a skull circumference of 51 cm (+1.07 SD), a bony defect occipitally, and mild fingerprinting on the skull radiograph. No other symptoms of increased intracranial pressure were noticed. However, fundoscopy showed papilledema of 1.5-2 dpt. Thus, a parieto-occipital decompression was performed. During the subsequent four-year follow-up, papilledema was absent. The family history was negative. No mutations were found in *FGFR2*, *FGFR3* or *TWIST1*. The DNA of subjects II.1, II.2 and III.2 was sequenced.

Family 4

The index patient was a boy born at 38 weeks' gestation following an uneventful pregnancy (Supplementary Figure 6.1D, III.1). At birth he was noted to have hypertelorism and brachycephaly. The head circumference was 43 cm at the age of 8 months (-1.9 SD). At the age of 10.5 months a CT head scan showed bicoronal synostosis with a very shallow anterior cranial fossa and small facial skeleton, and a fronto-orbital advancement and remodelling procedure was performed. Physical examination at the age of 6 years revealed relatively small ears with prominent helical crura and marked bilateral 5th finger clinodactyly. He attended a normal school without additional help up to the age of 15 years. He was receiving treatment for Class II.1 dental malocclusion on a mild Class II skeletal base. His mother had a normal craniofacial examination but was noted to have generalized brachydactyly. A maternal half-brother and his daughter were reported to have flattened foreheads.





Gain-of-function mutations in *ZIC1* are associated with coronal craniosynostosis and learning disability

Stephen R.F. Twigg, Jennifer Forecki,* **Jacqueline A.C. Goos**,* Ivy C.A. Richardson, A. Jeannette M. Hoogeboom, Ans M.W. van den Ouweland, Sigrid M.A. Swagemakers, Maarten H. Lequin, Daniel van Antwerp, Simon J. McGowan, Isabelle Westbury, Kerry A. Miller, Steven A. Wall, WGS500 Consortium, Peter J. van der Spek, Irene M.J. Mathijssen, Erwin Pauws, Christa S. Merzdorf, Andrew O.M. Wilkie

*Equal contributors

American Journal of Human Genetics September 2015

Abstract

Human *ZIC1* (zinc finger protein of cerebellum 1), one of five homologs of the *Drosophila* pair-rule gene *odd-paired*, encodes a transcription factor previously implicated in vertebrate brain development. Heterozygous deletions of *ZIC1* and its nearby paralog *ZIC4* on chromosome 3q25.1 are associated with Dandy-Walker malformation of the cerebellum, and loss of the orthologous *Zic1* gene in the mouse causes cerebellar hypoplasia and vertebral defects. We describe individuals from five families with heterozygous mutations located in the final (third) exon of *ZIC1* (encoding four nonsense and one missense change) who have a distinct phenotype in which severe craniosynostosis, specifically involving the coronal sutures, and variable learning disability are the most characteristic features. The location of the nonsense mutations predicts escape of mutant *ZIC1* transcripts from nonsense-mediated decay, which was confirmed in a cell line from an affected individual. Both nonsense and missense mutations are associated with altered and/or enhanced expression of a target gene, *engrailed-2*, in a *Xenopus* embryo assay. Analysis of mouse embryos revealed a localized domain of *Zic1* expression at embryonic days E11.5–12.5 in a region overlapping the supraorbital regulatory centre, which patterns the coronal suture. We conclude that the human mutations uncover a previously unsuspected role for *Zic1* in early cranial suture development, potentially by regulating *engrailed 1*, which was previously shown to be critical for positioning of the murine coronal suture. The diagnosis of a *ZIC1* mutation has significant implications for prognosis and we recommend genetic testing when common causes of coronal synostosis have been excluded.

Introduction

Among the varied causes of craniosynostosis (premature fusion of one or more sutures of the skull vault), a monogenic aetiology is most commonly identified in individuals with fusion of the coronal sutures, the major pair of transverse sutures crossing the vertex of the skull.¹²⁸ Coronal synostosis, which can be present bilaterally (bicoronal) or unilaterally (unicoronal), affects approximately 1 in 10,000 children² and is the type most commonly associated with an identifiable syndrome. Common monogenic disorders that characteristically present with coronal synostosis are Muenke [MIM: 602849] and Apert [MIM: 101200] syndromes, caused by localized gain-of-function mutations encoded by *FGFR3* [MIM: 134934] and *FGFR2* [MIM: 176943], respectively; Saethre-Chotzen syndrome [MIM: 101400] (*TWIST1* [MIM: 601622] haploinsufficiency); *TCF12*-related craniosynostosis [MIM: 600480 and 615314] (also a haploinsufficiency); and craniofrontonasal syndrome [MIM: 304110] (cellular interference involving variants in the X-linked *EFNB1* gene [MIM: 300035]).^{59,125}

Even in the absence of an obvious syndromic diagnosis, a specific mutation can be identified in about 60% of individuals with bicoronal and 30% with uniconal synostosis.^{59,128} The high monogenic load in coronal synostosis can be accounted for by the specific developmental origin of the coronal suture, which lies at an embryonic tissue boundary between neural-crest-derived frontal bone and mesoderm-derived parietal bone.^{29,30} Based on analysis of mouse models,¹²⁷ coronal synostosis is frequently caused by disruption in the maintenance of the population of stem cells within the suture during early development (typically, embryonic days E12.5–14.5), caused, for example, by abnormalities in migration of neural crest cells²³² or abnormal paracrine signalling through fibroblast growth factor receptors.^{247,248}

An alternative possibility is that coronal synostosis could be caused by a primary failure of the suture to develop. Lineage tracing demonstrates that the cells of the future coronal suture originate from paraxial cephalic mesoderm at E7.5 and migrate laterally to locate above the developing eye.³⁷ This region constitutes the supraorbital regulatory centre and during E11.5–E13.5, cells from this zone migrate apically to form and populate the coronal suture.^{24,30,37} One of the genes characteristically expressed by these cells is *engrailed 1* (*En1*), a homolog of the *Drosophila engrailed* segment polarity gene. Mice with homozygous loss of *En1* function have generalized calvarial bone hypoplasia and persistent widening of the sutural gaps, which is associated with a posterior shift in the boundary between cells of neural crest and mesodermal origin.^{37,249} An orthologous mutation has not yet been described in humans.

Here, we report an additional genetic aetiology for coronal synostosis, caused by heterozygous variants in the final exon of *ZIC1* (zinc finger protein of cerebellum 1 [MIM: 600470]), identified in four simplex case subjects and a three-generation pedigree. *ZIC1*,



located on chromosome 3q25.1, belongs to a family of five genes encoding Zn-finger transcription factors, which are arranged as one unpaired and two paired paralogs in the human and mouse genomes;²⁵⁰ *ZIC* genes are homologous to the *Drosophila* pair-rule gene *odd-paired*, which is required for activation of embryonic *engrailed* expression.²⁵¹ Vertebrate *ZICs* have important roles in multiple developmental processes, including neurogenesis, left-right axis formation, myogenesis, and skeletal patterning.^{252,253} Heterozygous complete deletions of *ZIC1* were previously associated with Dandy-Walker malformation (DWM; hypoplasia and upward rotation of the cerebellar vermis and cystic dilatation of the fourth ventricle [MIM: 220200]);²⁵⁴ we now show that mutations affecting the highly conserved C terminus of the protein, which are likely to be associated with a gain of function, lead to a distinct phenotype of coronal suture fusion and learning disability. In addition to its previously established importance for neurogenesis,^{255,256} this work shows that *ZIC1* is required for normal coronal suture development. We find that murine *Zic1* is expressed in the supraorbital regulatory centre, suggesting that this gene acts at a very early stage of coronal suture development,¹²⁷ potentially (reflecting a similar epistatic relationship to that in *Drosophila*) by regulating *En1*.

Subjects and methods

Subjects

The clinical studies were approved by Oxfordshire Research Ethics Committee B (reference C02.143), London Riverside Research Ethics Committee (reference 09/H0706/20), and the Medical Ethical Committee of the Erasmus University Medical Centre Rotterdam (MEC-2012-140 and MEC-2013-547). Written informed consent to obtain samples for genetics research was obtained from each child's parent or guardian. Venous blood was used for DNA extraction and fibroblast cultures were established from skin biopsies taken from scalp incisions during surgical intervention. Intracranial pressures in subject 1 were documented by 24–48 h direct recording with an intraparenchymal Codman Microsensor.²⁵⁷ The screening panel comprised samples from 307 individuals with syndromic or non-syndromic craniosynostosis. All DNA samples were previously tested for mutation hotspots in *FGFR2*, *FGFR3*, *TWIST1*, and *TCF12*.^{59,125} Significant chromosome aneuploidy in individuals with *ZIC1* mutations was excluded by karyotyping and/or array comparative genomic hybridisation. Where necessary, correct biological relationships were confirmed by segregation analysis of a panel of 13 microsatellites (D1S2868, D3S1311, D4S403, D5S2027, D6S1610, D7S519, D9S158, D10S548, D11S898, D13S1265, D14S280, D16S415, and D18S474).

Whole genome/exome sequencing and mutation screening of *ZIC1*

Whole genome sequencing of the male proband subject 1 and his parents was performed as part of the WGS500 clinical genome sequencing initiative.²⁵⁸ In brief, 3–5 µg DNA was used to prepare libraries for 100 bp paired-end sequencing to generate a mean coverage of 30x using the Illumina HiSeq2000 platform. Sequence reads were mapped to the human reference GRCh37d5 using Stampy (v1.0.12–1.0.22) and variants called with Platypus (v.0.2.4).^{259,260} To identify *de novo* mutations, we prioritized variants within coding regions that were called as absent in both parents and in dbSNP135, generating a list of 203 variants in 177 genes, of which 39 were classified as protein altering. Visualization of the trio read alignments revealed a single bona fide change in *ZIC1* (12 of 27 reads), which was absent in both the paternal (19 reads) and maternal (31 reads) samples; the other 38 variants were either in fact present in one of the parents or were artefactual (Supplementary Table 7.1). Possible recessive inheritance was analysed with an in-house perl script to list homozygous, compound heterozygous, and hemizygous X chromosomal variants in subject 1, with a frequency cut-off of 0.003 in either 1000 Genomes or Exome Variant Server; variants in two genes fitted the criteria (Supplementary Table 7.1). Whole genome sequencing of genomic DNA from four subjects in family 5 (affected: 5:II.2, 5:III.3, 5:III.6; unaffected: 5:II.3) was performed by BGI Complete Genomics.^{104,108} Filtering based on a list of genes mutated in craniosynostosis identified a predicted missense substitution encoded by *ZIC1*, present only in the three affected individuals. Exome sequencing of subject 3 was performed on genomic DNA (extracted from whole blood) using an Agilent SureSelect Human All Exon Kit (v.5; 50 Mb) on the Illumina HiSeq2000 platform. Reads were mapped to hg19 with Novoalign (Novocraft Technologies) and variants called with SAMtools and annotated by ANNOVAR.

To investigate further the significance of the *ZIC1* mutations, primers were designed for amplification of genomic DNA (GenBank: NT_005612.17) and cDNA (GenBank: NM_003412.3), for multiplex ligation-dependent probe amplification (MLPA) analysis, and for deep sequencing (Supplementary Table 7.2, which provides details of experimental conditions). Variant screening of all three exons of *ZIC1* was performed by dideoxy sequencing on PCR amplification products from genomic DNA by BigDye Terminator v3.1 (Applied Biosystems). Copy-number variation was analysed by MLPA using probes to each exon, according to the manufacturer's instructions (MRC Holland). RNA was extracted from fibroblasts (Trizol, Invitrogen), cDNA synthesized with RevertAid first strand cDNA kit (Thermo Scientific), and the samples analysed by agarose gel electrophoresis after digestion with BfaI. To quantify the proportions of wild-type to mutant allele in cDNA, an amplification product spanning exons 2–3 was used as a template for PCR to add Ion Torrent P1 and A adapters, and the resulting product was purified with AMPure beads (Beckman Coulter). Emulsion PCR and enrichment were performed with the Ion PGM Template OT2 200 Kit (Life Technologies) according to the



manufacturer's instructions and sequencing of enriched templates performed on the Ion Torrent PGM (Life Technologies) for 125 cycles with the Ion PGM Sequencing 200 kit v2. Data were processed with Ion Torrent platform-specific pipeline software v.4.2.1.

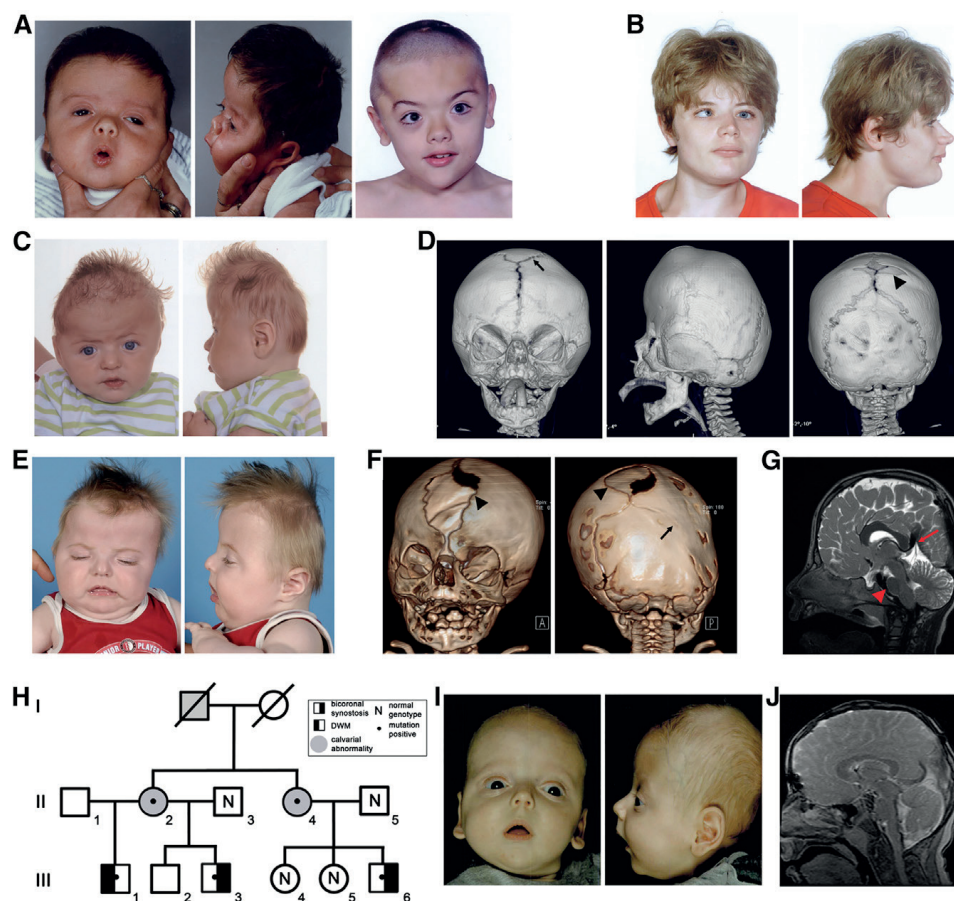


Figure 7.1. Clinical and radiological phenotype of individuals with *ZIC1* mutations.

A: subject 1, age 7 weeks (left) and 8 years (right). **B:** subject 2, age 23 years. **C:** subject 3, age 5 months. **D:** CT head scan of subject 3 (age 5 months) showing biconal synostosis, a large wormian bone (arrow) in the position of the anterior fontanelle, and an ossification defect in the sagittal suture (arrowhead). **E:** subject 4, age 7 months. **F:** CT head scan of subject 4 (age 2.5 months). Note asymmetric skull shape associated with bilateral coronal and right lambdoid suture fusion (arrow). Sections of the metopic and sagittal sutures remain widely patent (arrowheads). **G:** MRI brain scan (T2 image) of subject 4, age 16 months. Note short, broad corpus callosum, peaked tentorium cerebelli (arrow), and hypoplasia of the pons (arrowhead), cerebellar vermis, and cerebellar hemispheres. **H:** pedigree of family 5. **I:** subject 5:III.6, age 2 months. **J:** MRI brain scan (T2 image) of subject 5:III.6, age 13 years. Abnormal features show a similar pattern to those present in subject 4.

***Xenopus* assays**

All experiments using *Xenopus* were approved by the Institutional Animal Care and Use committee of Montana State University. *Xenopus* full-length *zic1*²⁶¹ and *zic1ΔC*²⁶² cDNA constructs were described previously (*zic1ΔC* was originally termed *oplΔC*). The *zic1ΔC2* construct was made by PCR amplification of the portion of *zic1* cDNA encoding the N terminus and zinc finger domains, including four amino acids of the C-terminal region, followed by cloning into the EcoR1 and Xba1 sites of pCS2+ATG.²⁶¹ The human *ZIC1* cDNA pCR4-Topo-ZIC1 (ThermoFisher) was subcloned into pcDNA3 and six different nucleotide substitutions— c.895G>T, p.(Glu299*), c.1163C>A, p.(Ser388*), c.1198G>C, p.(Gly400Arg), c.1204G>T, p.(Glu402*), c.1240A>G, p.(Thr414Ala), and c.1309_1310GC>TA, p.(Ala437*)—were introduced by PCR mutagenesis using the primer sequences and experimental conditions provided in Supplementary Table 7.2. The human *ZIC1* constructs were subsequently digested with EcoR1 and Xba1 and ligated into the pCS2+ plasmid. Capped sense RNAs for microinjection were synthesized from the *Xenopus* and human pCS2+ constructs by SP6 transcription of NarI linearized plasmids. *Xenopus laevis* eggs were collected and fertilized as previously described²⁶² and embryos were staged according to Nieuwkoop and Faber.²⁶³ Embryos at the two-cell stage were injected into a single cell with 200 pg sense RNA synthesized from cDNA constructs, together with 25 pg *lacZ* RNA as tracer. After β-galactosidase staining,²⁶⁴ wild-type embryos were bleached by exposing the embryos to fluorescent light in hybridisation buffer containing 1% H₂O₂. Expression of *en-2* was determined in neurula stage 15–17 albino and wild-type embryos by *in situ* hybridization²⁶⁵ with digoxigenin-labelled antisense RNA *en-2* probe as described.²⁶⁶ An anti-digoxigenin alkaline phosphatase-conjugated antibody (Roche) and the alkaline phosphatase substrate NBT/BCIP (Fisher Scientific) were used for colour detection. Embryos were scored double-blind to determine changes in *en-2* expression in comparison to the uninjected side. Results using wild-type and mutant constructs were compared by Fisher's exact tests with Bonferroni correction for multiple comparisons (*n* = 9).



RNA *in situ* hybridisation of mouse embryos

Experimental procedures were performed in accordance with UK Animals (Scientific Procedures) Act, 1986 (PPL 70/7194). For whole-mount embryo *in situ* hybridisation, embryos were dissected, fixed overnight in 4% paraformaldehyde in phosphate-buffered saline, and dehydrated through graded methanol solutions. Non-radioactive RNA *in situ* hybridisation was performed as described²⁶⁷ before vibratome sectioning. RNA probes for *Zic1*²⁶⁸ and *En1*²⁶⁹ were digoxigenin labelled with the In Vitro Transcription kit (Roche Applied Science) followed by anti-digoxigenin-AP antibody (1:1,000) (Roche Applied Science) and NBT/BCIP (Sigma) staining to detect the hybridisation signals.

Results

Identification of *ZIC1* mutations

The proband (subject 1) presented at birth with severe brachycephaly (Figure 7.1A), which was shown by three-dimensional computed tomographic reconstruction (3D-CT) to be caused by bicoronal synostosis. He required three major craniofacial surgical procedures (at the ages of 7 months, 2.4 years, and 4.8 years), the latter two because of raised intracranial pressure. In addition he had autistic traits and moderate-severe learning disability, features that are rarely associated with coronal synostosis. Genetic testing for mutations known to be associated with coronal synostosis was negative; his phenotype is summarized in Table 7.1 and more detailed descriptions of all subjects are provided in the Case Reports.

We undertook whole genome sequencing of the parent-child trio and analysed the data for variants consistent with either (1) autosomal or X-linked recessive inheritance or (2) a new dominant mutation (Supplementary Table 7.1). After filtering, variants in two genes were consistent with the recessive disease model, but these genes, *CNGA3* [MIM: 600053] and *NEB* [MIM: 161650], are associated with achromatopsia 2 [MIM: 216900] and nemaline myopathy 2 [MIM: 256030], respectively, disorders without a craniofacial phenotype, and thus were not considered further. The single dominant candidate was a heterozygous c.1163C>A mutation in *ZIC1* (GenBank: NM_003412.3), predicting the nonsense change p.Ser388*. This variant was absent in the parental samples and was confirmed by dideoxy sequencing (Figure 7.2A).

The significance of this *de novo* *ZIC1* mutation was initially uncertain. Contiguous heterozygous deletions of *ZIC1* and its adjacent paralog *ZIC4* were previously described in DWM,²⁵⁴ although a few deletion cases have lacked this characteristic phenotype.²⁷⁰ Review of the CT scan in subject 1 showed no brain malformation, and on a later magnetic resonance imaging (MRI) scan, only minor abnormalities of configuration of the ventricles and corpus callosum were evident (not shown).

Nonsense mutations of *ZIC1* have not previously been reported, but the location of the nucleotide substitution in the terminal (third) exon (Figure 7.2A) predicted that it would escape nonsense-mediated decay.²⁷¹ We digested *ZIC1* cDNA generated from scalp fibroblasts with the restriction enzyme Bfal, which cuts the mutant allele, and found that the expected mutant fragments were readily visualized (Figure 7.2B); we then used deep sequencing for accurate quantification and found that 7,175 of 13,088 reads (55%) represented mutant alleles, confirming escape from nonsense-mediated decay (not shown). A prematurely truncated translation product could be associated with dominant-negative or gain-of-function mechanism, distinct from the previously described deletions.²⁷¹ Support for a gain-of-function mechanism was provided by previously published work on the *Xenopus zic1* ortholog, formerly known as *opl*

Table 7.1. Phenotypic features of individuals with *ZIC1* mutations.

Subject ID	Reference ID	Gender	Mutation (cDNA) and alteration (Protein)	Cranial sutures	Number of major craniofacial procedures	Other brain abnormalities on CT/MRI scanning	Strabismus/ptosis	Learning disability	Other major clinical features
1	4447	M	c.1163C>A, p.(Ser388*)	bicoronal synostosis	3	abnormal configuration of ventricles and corpus callosum	–	moderate-severe	scoliosis, foreskin stricture
2	4098	F	c.1204G>T, p.(Glu402*)	bicoronal synostosis	0	agenesis of corpus callosum, dilated lateral ventricles	divergent strabismus	moderate	scoliosis
3	4133/5847	M	c.1204G>T, p.(Glu402*) ^a	bicoronal synostosis, bony defect of sagittal suture	2	normal on CT scan	–	mild	–
4	12D11570	M	c.1165C>T, p.(Gln389*)	bicoronal synostosis, partial R lambdoid synostosis, bony defect of metopic and sagittal sutures	1	mildly enlarged lateral ventricles, shortened corpus callosum, hypoplastic pons, enlarged foramen magnum	strabismus sursoadductorius	moderate-severe	–
5:II.2	12D15615	F	c.1198G>C, p.(Gly400Arg)	brachycephaly, delayed closure anterior fontanelle	0	atrophy of the rostral part of the cerebellum and pons	–	mild	–
5:II.4	08D1850	F	c.1198G>C, p.(Gly400Arg)	plagiocephaly	0	reduced dorsum of pons, minor posterior fossa abnormalities	strabismus correction, ptosis L eye	below average	–
5:III.1	14D6457	M	c.1198G>C, p.(Gly400Arg)	delayed closure anterior fontanelle (4 years)	0	DWM	–	mild	50 dB sensorineural hearing loss R; spina bifida occulta; LHRH deficiency



5:III.3	12D15613	M	c.1198G>C, p.(Gly400Arg)	bicoronal synostosis, patent metopic, bilateral bony defect of lambdoid sutures	0	normal on CT scan	bilateral convergent strabismus + ptosis	mild	-
5:III.6	10D5797	M	c.1198G>C, p.(Gly400Arg)	bicoronal synostosis, bilateral parietal foramina	1	reduced dorsum of pons, minor posterior fossa abnormalities	bilateral divergent strabismus + ptosis R eye	below average	-

*Mutation present in mosaic state.

(*odd-paired-like*), in which it had been shown that a cDNA construct, *zic1ΔC*, containing a shorter truncation missing the C-terminal 36 amino acids (see Figure 7.2C), had enhanced activity compared to full-length cDNA, in transactivation, and *Xenopus* animal cap, and other *in vivo* assays.^{261,272,273}

To search for further evidence that *ZIC1* mutations cause craniosynostosis, we screened a panel comprising 307 unrelated subjects with synostosis affecting any combination of sutures (including 45 and 112 with exclusively bilateral and unilateral coronal synostosis, respectively) and for whom no genetic diagnosis had been made. Initially we identified a single heterozygous nonsense mutation in this panel (subject 2: c.1204G>T encoding p.Glu402*); neither parent had the mutation, indicating that it had arisen *de novo* (sample relationships were confirmed by microsatellite analysis). We did not identify any *ZIC1* copy-number changes in this craniosynostosis panel by MLPA (data not shown). Later, we discovered by exome sequencing that a second individual included on the panel (subject 3) had the identical mutation, but present in mosaic state (see legend to Figure 7.2A for details). Strikingly, review of the phenotypes of subjects 2 and 3 revealed that both had bicoronal synostosis with severe brachycephaly (Figures 7.1B–D); in addition, both had learning disability, which was milder in subject 3 who had the mosaic mutation. Review of CT brain scans showed that subject 2 had agenesis of corpus callosum and dilated lateral ventricles, but neither subject 2 or 3 had DWM (not shown).

In an attempt to further replicate these findings, we examined DNA samples collected at a second craniofacial unit (Rotterdam), specifically where the combination of both coronal synostosis and significant learning disability was present. Only three samples were available for analysis, which reflects the rarity of this combination of phenotypes; remarkably, however, dideoxy sequencing showed that one of these samples harboured a heterozygous nonsense mutation in *ZIC1* (c.1165C>T encoding p.Gln389*) at the codon adjacent to that affected in subject 1 (Figure 7.2A). This child had presented with bicoronal and unilateral lambdoid synostosis (Figures 7.1E and 7.1F) and had significant learning problems (Table 7.1). An MRI scan identified several cerebral anomalies including a short corpus callosum, mildly enlarged lateral ventricles, peaked tentorium, hypoplastic pons, and cerebellum with prominent cerebellar folia and enlarged foramen magnum with signal void near the cervical cord (Figure 7.1G).

The final family (family 5) consisted of six affected individuals in three generations (Figure 7.1H). Two cousins (subjects 5:III.3 and 5:III.6) had bicoronal synostosis (Figures 7.1I and 7.1J) and a further individual (subject 5:III.1, a half-brother of 5:III.3) had a DWM but no craniosynostosis (not shown). All three, and their respective mothers (5:II.2 and 5:II.4), had mild learning disability. Whole genome sequencing of four individuals (subjects 5:II.2, 5:II.3, 5:III.3, 5:III.6) identified a heterozygous variant in *ZIC1*, c.1198G>C



encoding p.Gly400Arg, present in the three affected individuals (5:II.2, 5:III.3, 5:III.6) but not in the unaffected spouse (5:II.3). These results were confirmed by dideoxy sequencing, which showed that the variant was also present in 5:III.1 (the individual with DWM) and in 5:II.4 (the obligate transmitting mother) but not in her two unaffected children (5:III.4 and 5:III.5). This variant is absent from more than 120,000 alleles in the Exome Aggregation Consortium (ExAC). The combination of phenotypic features, the segregation of the variant, its location in the region where the previously identified nonsense mutations all clustered (Figure 7.2A), and absence in large databases of variation suggest that this variant is causative of the phenotype.

Functional consequence of *ZIC1* mutations in *Xenopus* embryo assay

The function of the *Xenopus zic1* ortholog has been studied in detail, where it was shown to act together with Pax3 as a key transcription factor required for the initiation of neural crest formation.²⁷⁴ In *Xenopus* embryos, a signalling cascade has been proposed in which inhibition of bone morphogenetic proteins (Bmps) activates *zic1*, which in turn activates members of the Wnt family including *wnt1*, which in turn activates the transcription factor *engrailed-2* (*en-2*).^{261,272} A previously designed assay had shown that injection of *zic1*ΔC RNA encoding a truncated ZIC1 into a single cell of 2-cell stage embryos led to increased *en-2* expression in stage 15–17 *Xenopus* embryos, whereas injection of wild-type *zic1* construct had no effect.²⁶¹ We next examined the activity of human *ZIC1* and various mutant constructs with this assay.

In initial experiments, we replicated the previously reported results of the *Xenopus* assay. Although very few (3%) embryos were disrupted by injection of the wildtype *zic1* construct, this increased to 31% using the previously published *zic1*ΔC. Moreover, a construct deleting almost the entire region C-terminal to the zinc fingers (*zic1*ΔC2; Figure 7.2C) showed an even higher proportion (61%) of disrupted embryos (Figure 7.3). Using constructs encoding human ZIC1, injection of full-length *ZIC1* RNA yielded only 8% disrupted embryos, but this was increased to 79% and 68% with constructs corresponding to two of the observed truncations, p.Ser388* (subject 1) and p.Glu402* (subjects 2 and 3), respectively. Strikingly, a similar magnitude of effect (66%) was found with the most C-terminal truncation construct (p.Ala437*, which does not correspond to an observed mutation), highlighting the importance of the terminal 11 amino acids, which includes a 5-amino-acid motif (NEWYV) of unknown function that is conserved in human ZIC2, ZIC3 (isoform A), and ZIC5 (Figure 7.2C) but is not present in any other human protein. Two constructs encoding missense substitutions were studied with the same assay: p.Gly400Arg present in family 5 and p.Thr414Ala, corresponding to a rare SNP (dbSNP rs143292136), present in 104/121,380 alleles in ExAC, which we had identified in a child with bicoronal synostosis and her unaffected father (data not shown);

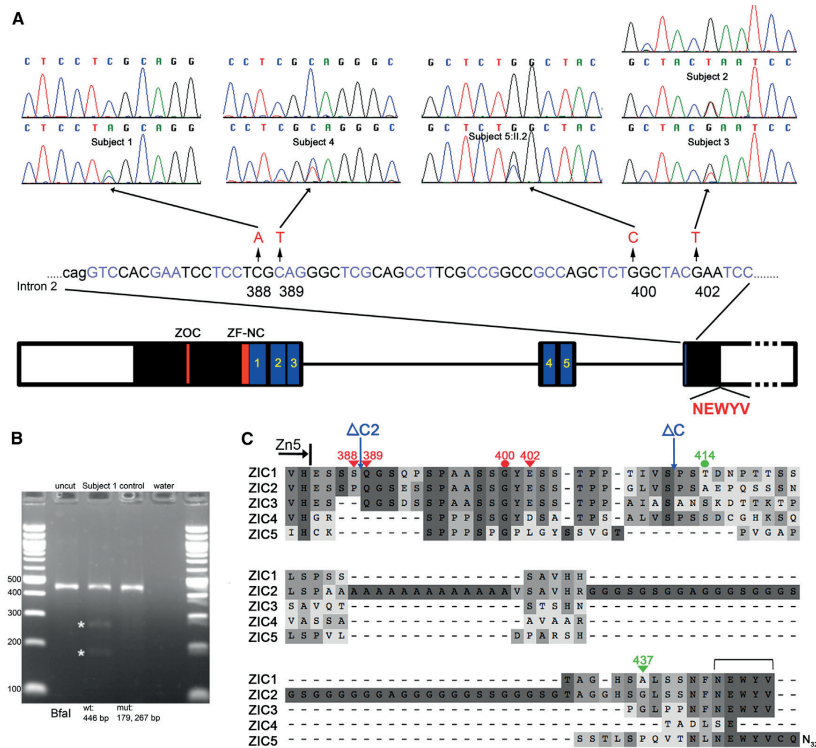


Figure 7.2. Molecular genetic analysis of individuals with *ZIC1* mutations.

A: cartoon showing exon organization (white boxes denote non-coding regions) and previously identified conserved domains (Zic opa conserved motif [ZOC], zinc finger N-flanking conserved region [ZF-NC], and five zinc fingers [1–5, blue boxes]) of human *ZIC1*.²⁵² Also indicated is the C-terminal NEWYV motif conserved in all family members except *ZIC4*. Above the cartoon are the positions of the five independent *ZIC1* mutations described in this report, and dideoxy-sequence traces showing comparison of normal sequence (above) and mutant sequence (below). Note, in the case of subject 3, the mutation was not evident in the DNA sample (sourced from scalp fibroblasts; not shown) originally analysed; however, in the exome sequence of DNA sourced from blood of the same individual, 63 of 183 (34%) reads showed the c.1204G>T mutation, which is also readily apparent on the dideoxy sequence. The relative heights of mutant and wild-type peaks differ between samples from subject 3 and subject 2, who is constitutionally heterozygous for the identical mutation, corroborating that in subject 3 the mutation is present in high-level mosaic state. **B:** agarose gel analysis of *ZIC1* cDNA obtained from RNA extracted from scalp fibroblasts of subject 1 and digested with *BfaI*. The fragments yielded by digestion of the mutant allele are indicated with asterisks. **C:** amino acid sequence encoded by 30-terminal exon of *ZIC1* and comparison with the paralogous human proteins *ZIC2*–*ZIC5*, showing conservation including the NEWYV motif (bracket). The end of the fifth zinc finger (Zn5) is shown above the sequence, as are the positions of the four different pathogenic variants (red symbols) (triangle, nonsense; circle, missense) identified in this study. The positions at which the *Xenopus* constructs *zic1*ΔC2 and *zic1*ΔC are truncated, relative to the human sequence, are indicated by blue arrows (note *zic1*ΔC2 is equivalent to p.Gln389*). Additional human constructs tested in the *Xenopus* assay are indicated by green symbols.



60% of embryos were disrupted in both cases. Although producing a slightly milder effect than the nonsense mutations, these results suggest that residues in the C-terminal domain in addition to the NEWYV motif contribute to function. Importantly, using a truncated control construct (p.Glu299*) missing the last three of the five zinc fingers, a much lower proportion of embryos (20%) was disrupted, which did not differ significantly from the full-length *ZIC1* RNA (Figure 7.3C). This indicates that intact zinc fingers are required to induce consistently abnormal *en-2* expression in this assay.

***Zic1* expression in mouse embryos**

Of note in the above experiments, the effect of the *ZIC1* C-terminal mutants was to increase the expression of the *Xenopus* target gene *en-2* (Figures 7.3B and 7.3C). Given previous evidence that the paralogous gene *En1* is critical for early biogenesis of the murine coronal suture,³⁷ we asked whether *Zic1* might also be expressed in relevant cells. Although the neural pattern of *Zic1* expression^{256,275} and loss-of-function phenotypes^{255,256} were previously described in the mouse, no evidence has linked *Zic1* expression to coronal suture development. Therefore, we analysed expression patterns of *Zic1* in embryonic mouse heads between E11.5 and E17.5. Between E11.5 and E12.5, a distinct domain of *Zic1* expression was observed in the supraorbital region and cephalic mesoderm, which appeared to precede and partly overlap *En1* expression (Figure 7.4). By contrast, no *Zic1* expression was observed in the calvaria at E14.5 and E17.5 (not shown).

Discussion

Given the homology to one of the classical early patterning genes of the *Drosophila* embryo, the function of the vertebrate Zic family has been the focus of sustained interest. Highlighting their importance for development, mutations in the related genes *ZIC2* [MIM: 603073] and *ZIC3* [MIM: 300265] were previously described in holoprosencephaly [MIM: 609637]²⁷⁶ and X-linked visceral heterotaxy [MIM: 306955],²⁷⁷ respectively. In the case of *ZIC1*, the observation that heterozygous deletions in tandem with *ZIC4* cause DWM^{254,270} has supported work in *Xenopus*^{261,272,274} and mouse,^{256,275} indicating key roles for the Zic1 ortholog in neurogenesis (in the mouse, deficiency of *Zic1* and *Zic4* contribute additively to cerebellar hypoplasia).²⁵⁶ Our data now highlight a previously unsuspected subsidiary role for *ZIC1* in early patterning events in the coronal suture.

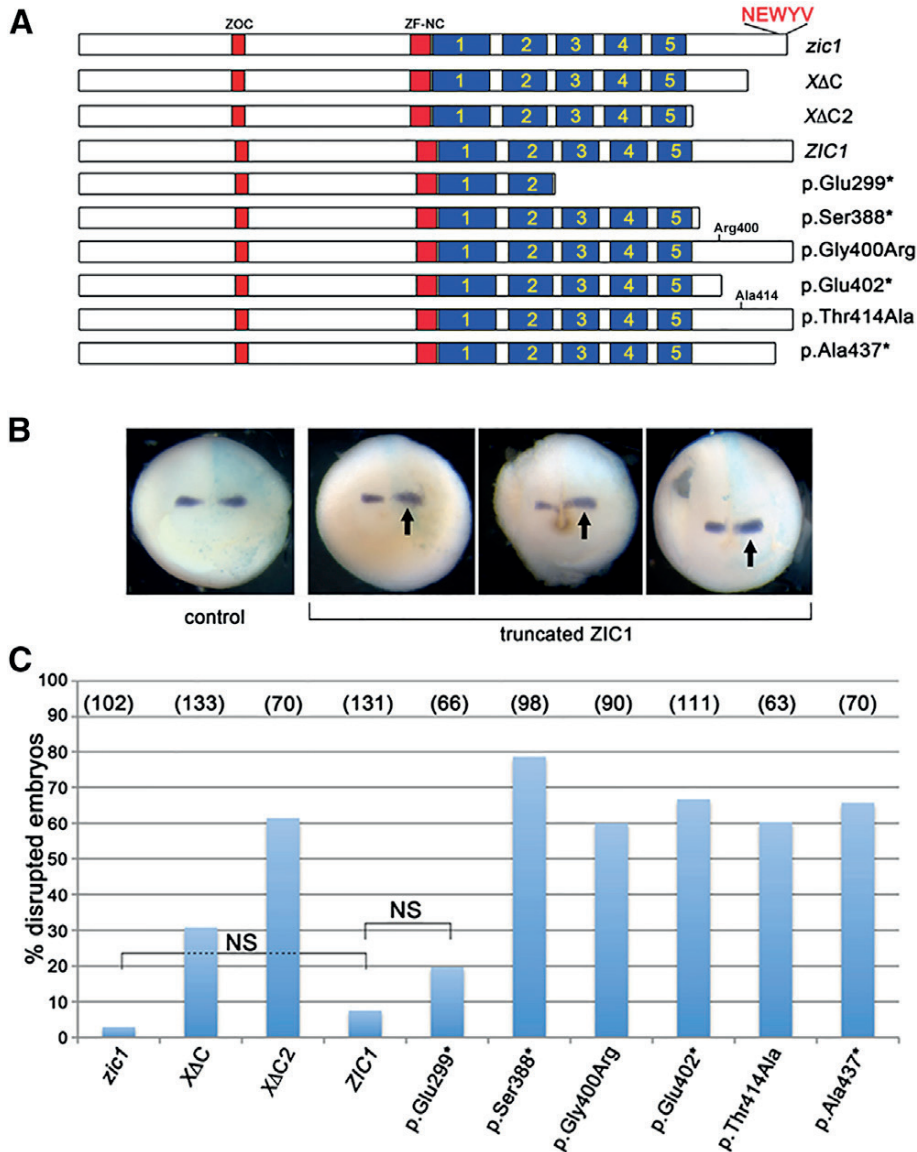


Figure 7.3. Analysis of consequences of *ZIC1* mutations in *Xenopus* embryos. **A:** cartoon showing the structure and nomenclature of the cDNA constructs used in the experiment. The five zinc finger domains are highlighted in blue. **B:** *Xenopus en-2* expression after microinjection of *ZIC1* construct RNA (right side of each embryo). Arrows indicate widened, increased, or shifted *en-2* expression in three representative embryos. **C:** quantification of effects of *ZIC1* mutations on *en-2* expression. The numbers of embryos used in each experiment are indicated in parentheses. Statistical comparisons between full-length *Xenopus zic1* and human *ZIC1* and between *ZIC1* and *ZIC1*-p.Glu299* were not significant (NS), whereas comparisons between all other mutants and corresponding full-length constructs were highly significant ($p < 10^{-8}$).

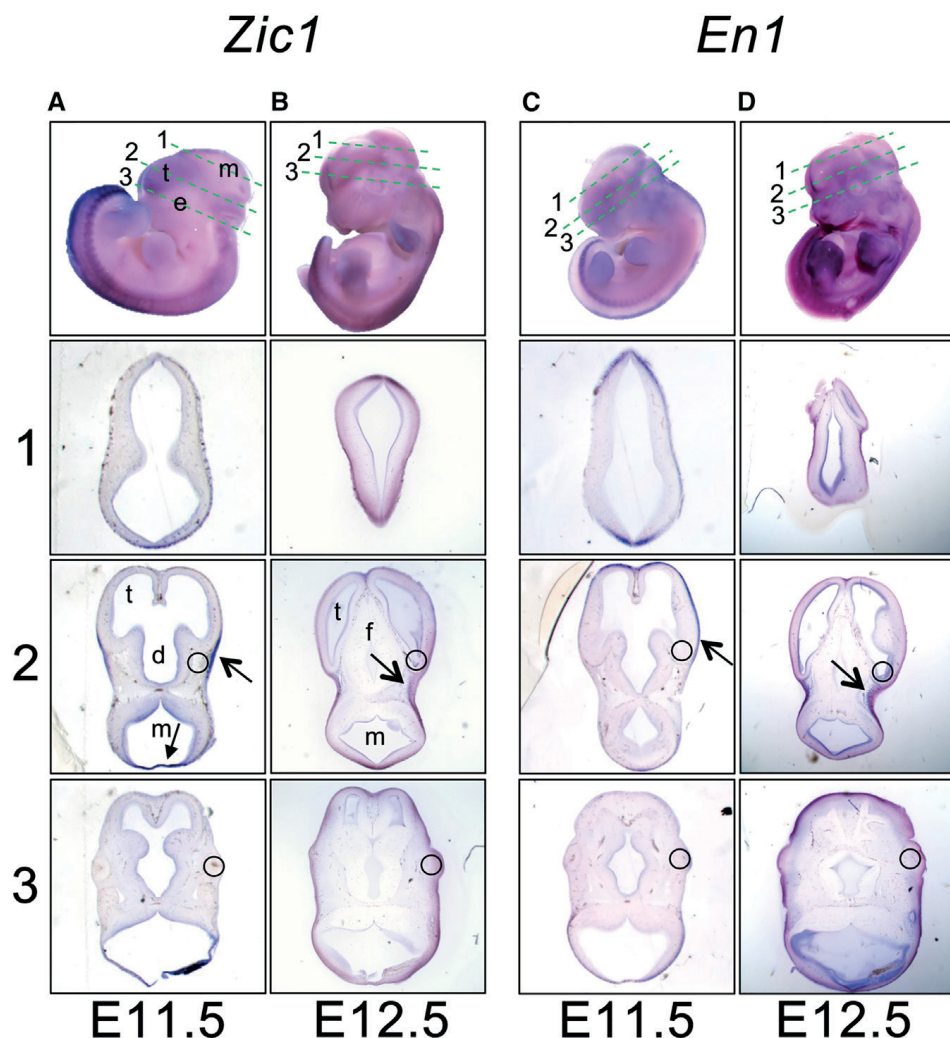


Figure 7.4. Expression of *Zic1* in E11.5–E12.5 mouse embryos analysed by RNA *in situ* hybridisation and comparison with *En1*. A–D: panels show comparison of *Zic1* (A,B) and *En1* (C,D) expression at E11.5 (A,C) and E12.5 (B,D). In each case the top panel shows the whole embryo and plane of sections 1, 2, and 3, which are illustrated in the three respective lower panels (e = eye, t = telencephalon, d = diencephalon, m = mesencephalon, f = forebrain, circles indicate relative position of the eye). Note strong expression of *Zic1* in supraorbital region (open arrow) at E11.5; other areas of expression are midbrain-hindbrain boundary (closed arrow), neural tube, and limb mesenchyme (A). At E12.5 *Zic1* expression is seen mainly in the cephalic mesenchyme, just posterior to the eye (B). By comparison, at E11.5 the expression of *En1* expression is relatively weak in the supraorbital region (stronger expression is seen in the apical ectodermal ridge of the limb and in the somitic mesoderm). By E12.5 *En1* expression has increased in the cephalic mesoderm.

The nonsense mutations of *ZIC1* present in subjects 1 to 4 all arose *de novo* (post-zygotically in the case of subject 3, who has an attenuated phenotype) and are associated with consistent features comprising bicoronal synostosis, moderate to severe learning disability, and subtle abnormalities in brain anatomy including variable deficiency of the corpus callosum and abnormal conformation of the ventricles and posterior fossa. The progressive scoliosis in two of these individuals is likely to be causally related to the mutation, because vertebral and thoracic defects were also observed in mouse mutants homozygous for the null mutation in *Zic1*.²⁷⁸ In family 5, a heterozygous missense variant p.Gly400Arg, present in the same C-terminal region of the *ZIC1* protein, segregated through three generations in six affected individuals. The phenotype in this family was variable, with two individuals having documented bicoronal synostosis and another a DWM. Associated learning disabilities were less severe than in subjects with truncations. Interestingly, MRI scans showed that several individuals from this family not formally diagnosed with DWM nevertheless had more subtle abnormalities in the conformation of the posterior fossa (Figure 7.1J). Hence the cerebral features were reminiscent of, but milder than, the malformations described in the previous cases with contiguous *ZIC1*-*ZIC4* deletions. In contrast to many craniosynostosis syndromes, no diagnostic limb anomalies were apparent in any of the affected individuals.

In assessing the association of *ZIC1* mutations with craniosynostosis, two features are particularly striking: the highly localized distribution of the mutations and the severity of the phenotype. All five mutations predict protein alterations within a 15-residue stretch encoded by the final exon. The occurrence of distinct phenotypes and/or patterns of inheritance associated with truncations localized to the terminal exon is a well-recognized indication that escape from nonsense-mediated decay might be responsible.²⁷¹ Indeed, we were able to demonstrate that the transcript carrying the nonsense mutation was stable in a fibroblast cell line from the individual (subject 1) with the most N-terminal truncation (Figure 7.2B). The qualitative difference in phenotype associated with heterozygous truncating mutations, compared to previously reported heterozygous deletions,^{254,270} supports a gain-of-function mechanism (see also below). In the four case subjects with truncating mutations, the coronal synostosis was always bilateral and associated with marked brachycephaly (Figures 7.1A–G), consistent with a severe, early effect on cranial suture formation; localized sutural ossification defects also occurred frequently. Craniosynostosis accompanied by DWM is rare, although an association with sagittal synostosis was reported previously.²⁷⁹

To investigate the mechanism by which these mutations could disturb coronal suture biogenesis, we first explored their functional effect in a previously established *Xenopus* assay. Injection of several constructs truncated at different positions in the C-terminal region led to disrupted *en-2* expression in a majority of treated embryos,



provided that the zinc finger domain remained intact (Figure 7.3). Mostly the disrupted expression pattern involved combinations of upregulation, shifting, and expansion of *en-2* expression (for examples see Figure 7.3B), although with the larger truncations retaining all Zn fingers, some embryos showed reduced *en-2* expression. The *zic1* Δ C construct has been used previously in *Xenopus* to obtain enhanced biological responses to *zic1* in several assays in which sensitization of the ectoderm to Bmp inhibition led to activation of genes expressed in the neural crest and neural tube; this was interpreted as showing that the C-terminal region has negative regulatory activity.²⁷² The biological basis of this activity remains unknown; based on the enhanced *en-2* expression associated with both the very C-terminal truncation p.Ala437* and the two missense substitutions, this might involve protein interaction over several parts of the ZIC1 C-terminal region, which shows several patches that are conserved between multiple ZIC paralogs (Figure 7.2C). Although the *Xenopus* assay supports the genetic evidence that the c.1198G>C, p.(Gly400Arg) substitution is causative of the phenotype in family 5, a cautionary note is provided by the finding that p.Thr414Ala also disrupted *en-2* expression, because this variant occurs too frequently (at 1 in 1,167 alleles) to be penetrant for craniosynostosis in more than a small proportion of individuals who carry this variant.

In a second approach to understand the pathogenic mechanisms, we asked whether the pattern of *Zic1* expression was consistent with a specific role in coronal suture biogenesis. We found a previously undescribed, transient zone of *Zic1* expression in the supraorbital region at E11.5 (Figure 7.4) that is spatially and temporally overlapping with that of *En1* (Figure 7.4) and is consistent with an early instructive role for *Zic1* in the supraorbital regulatory centre; combining these observations with the finding of increased *en-2* expression driven by mutant ZIC1 constructs in the *Xenopus* experiments, we propose that the coronal synostosis phenotype associated with the human mutations might be attributable to alteration of *EN1* expression in the supraorbital regulatory centre, thus disrupting the patterning of the coronal suture at a very early stage in its development. The induction of *engrailed* expression by ZIC1 orthologs is well characterized in both *Drosophila*^{251,280} and *Xenopus*²⁷² and is thought to act through the *Wnt* signalling pathway.²⁶¹ A further component of this signalling network is likely to be *Lmx1b*, which encodes a LIM-homeodomain protein and is upregulated in early neural crest of *Xenopus*.²⁸¹ In the mouse, *Lmx1b* is prominently expressed in the supraorbital region at E11.5, and homozygous mutants have severely abnormal cranial sutures.²⁸² In humans, heterozygous mutations in *LMX1B* usually cause nail-patella syndrome [MIM: 161200],²⁸³ but a specific missense mutation in the N-terminal arm of the homeodomain has been associated with craniosynostosis.¹²⁸

Putting the evidence together, we propose that the *ZIC1* mutations we have described serendipitously uncover an important role for this transcription factor in early lineage commitment at the supraorbital regulatory center¹²⁷ and that *En1* is likely to represent a key target gene. This will stimulate further work to define more precisely the role of *Zic1* in the coronal suture and to delineate the function of the conserved C-terminal domain. In *ZIC2*, constructs with holoprosencephaly-associated mutations C-terminal to the zinc fingers showed variable loss of transactivation activity,²⁸⁴ whereas in *ZIC3*, the single missense mutation beyond the zinc fingers reported to date (in a simplex case subject with congenital heart disease) was uniquely associated with increased transactivation activity.²⁸⁵ Collectively these data highlight the distinct properties of the C-terminal domain of ZIC proteins. The sequence conservation identified in this region (Figure 7.2C) suggests that a shared but currently unexplored mechanism exists for their regulatory function. Finally, although *ZIC1* mutations are rare because the genetic target is localized, the complications for intellectual and skeletal development are more serious than is usually the case with coronal synostosis; therefore, genetic testing is recommended when the more common diagnostic possibilities (involving mutations in *TWIST1*, *FGFR3*, *FGFR2*, and *TCF12*)^{59,125} have been excluded.



Supporting information

Case reports

Subject 1

This male was the first child born to a healthy unrelated couple, aged 38.9 years (father) and 28.5 years (mother) at the time of birth. The mother had four healthy children by a previous relationship. A brother born subsequently had metopic synostosis but this is presumed to be coincidental since he had normal development and was negative for the *ZIC1* mutation.

During the pregnancy, renal dilatation had been noted at 22 weeks' gestation; a foetal blood sample showed a normal karyotype. The proband was born at 37 weeks' gestation by Caesarean section owing to persistent transverse lie, weighed 2.98 kg and was noted to have an abnormal head shape at birth. On assessment aged 20 weeks, his occipito-frontal circumference (OFC) was 38.5 (-3.5 SD). He was noted to have severe brachycephaly, a high forehead, downslanting palpebral fissures and an open posterior fontanelle. The remainder of the examination was normal except for a transverse palmar crease on the right hand. The computed tomography (CT) head scan showed bilateral coronal synostosis and no identifiable cerebral abnormality. He underwent a fronto-orbital advancement and remodelling procedure at the age of 7 months. By the age of 8 months he was noted to have developmental delay, with age-equivalent development at 4-5 month level. On formal assessment at 29 months using Bayley Scales of Infant Development (2nd Ed), his motor development was equivalent to 17 months and mental development to 12 months. Hearing and vision assessments were normal, although he previously required insertion of grommets. At 2.5 years his intracranial pressure (ICP) was measured because of concerns about slow head growth and delayed development, this was markedly increased (baseline 25-30 mm Hg, peaks up to 50 mm Hg) and he underwent a posterior release and remodelling procedure. By 3 years he was showing hyperactive behaviour, with sleep disturbance and head-banging. A repeat ICP measurement aged 4.6 years was again elevated with episodes of abnormal pressure in the 25-35 mm Hg range, and he underwent a posterior release and advancement procedure.

At the age of 5 years he was noted to have a stricture of his foreskin and was developing a scoliosis. By 8 years, the left sided thoraco-lumbar curve measured 50°, and he had extensive spina bifida occulta in his lower lumbar spine; he subsequently had spinal surgery at the age of 10 years. He started to develop intermittent outbursts of aggressive behaviour, but several measurements of ICP were normal. A magnetic resonance imaging (MRI) brain scan showed abnormal configuration of the ventricles and corpus callosum. His developmental progress was slow and he attended a school for children with special educational needs. Genetic testing for causes of learning disability

including repeat karyotype, telomere screen, *FRAX* and *PW71B* methylation (for Prader-Willi/Angelman syndrome) were normal. Testing for craniosynostosis mutations in the research laboratory (*FGFR2*, *FGFR3*, *TWIST1*) was normal. On assessment at the age of 13 years, he continued to have violent outbursts and poor sleeping routine. He had no language and only limited communication using signs, but his gross motor skills and comprehension were less severely delayed. He showed autistic features, being dependent on routines and focused on individual tasks.

Subject 2

This female was the only child of healthy unrelated parents aged 34.4 years (father) and 31.7 years (mother). She was born at term by forceps delivery following a normal pregnancy and weighed 3.23 kg. Although well at birth she fed poorly and was referred at the age of 4 months for assessment of an unusual head shape and dysmorphic appearance with “almond shaped eyes” and down-slanted palpebral fissures, when a skull radiograph showed craniosynostosis. A clinical geneticist noted a high forehead, large open anterior fontanelle, flat occiput, maxillary hypoplasia and normal extremities, and suggested a diagnosis of Crouzon syndrome. Her development was moderately delayed; she walked unsupported at 2 years and had a vocabulary of 30 words at 2.8 years. She attended special schools for children with moderate to severe learning disability. She had surgery for divergent strabismus aged 3 years. CT head scan at 9 years showed dilated lateral ventricles and agenesis of the corpus callosum. At the age of 13 years she was noted to have a kyphoscoliosis. Plain radiographs showed multiple abnormalities of the thoracic spine and ribs and spondylolisthesis at L5/S1. MRI scan aged 17 years confirmed the previous findings and demonstrated a retroverted odontoid peg impinging on the cranio-cervical junction. There was no deterioration on orthopaedic follow-up to the age of 21 years.

She was referred for craniofacial assessment at the age of 23 years. Her head circumference was 48.5 cm (-5 SD) and height 149 cm (-2.2 SD). She was noted to be markedly brachycephalic with a high, flat brow and low frontal hairline. The remainder of the examination was normal and did not reveal diagnostic features of any craniosynostosis syndrome. Genetic testing (*FGFR1*, *FGFR2*, *FGFR3*, *TWIST1*) was negative and the karyotype was normal. CT scanning was consistent with bicoronal synostosis and demonstrated dilatation of the trigone and temporal regions of the ventricles. No surgical intervention was undertaken in view of her stable state. Currently aged 36 years, she lives in supervised residential accommodation, is able to communicate in short sentences and wash, dress and feed herself, but requires help with cooking.



Subject 3

This boy was the first child born to healthy unrelated parents after a normal pregnancy and weighed 3.34 kg (-0.1 SD). He was noted to have brachycephaly shortly after birth and was referred for craniofacial assessment aged 6 weeks. At 19 weeks his OFC was 39.0 cm (-2.8 SD) and cephalic index was 1.24. He had a low frontal hairline and normal extremities; on clinical genetic assessment his appearance was considered consistent with either Muenke or Saethre-Chotzen syndrome, but genetic testing of *FGFR3* and *TWIST1* was normal. The CT scan at the age of 5 months showed bicoronal synostosis, a patent metopic suture, a large wormian bone in the position of the anterior fontanelle, and an ossification defect in the sagittal suture. He developed progressive turricephaly and underwent a posterior distraction procedure aged 8 months followed by fronto-orbital advancement and remodelling aged 2.4 years.

He had mild developmental delay with speech dysfluency, and occasional tantrums with changes in routine. Tests of vision and hearing were normal. At the age of 8 years he was attending a normal school but was receiving 1:1 educational support because of delayed learning. Array comparative genomic hybridisation was normal except for a 140 kb deletion on chromosome 17 that was inherited from the mother and therefore presumed to be coincidental to the phenotype.

Subject 4

This boy was the fourth child of healthy unrelated parents aged 41 years (father) and 36 years (mother); an older sibling had trisomy 18. The proband was born at 38 weeks' gestation, weighing 4.27 kg. An altered skull shape was immediately apparent; on assessment by the plastic surgery department at the age of 2.5 months, this was clinically consistent with bilateral coronal synostosis and microcephaly (OFC 36 cm; -2.1 SD), but without significant exorbitism, ptosis or malformations of the extremities. 3D CT scan showed bilateral coronal synostosis and a partial right lambdoid synostosis; the metopic and mid-part of the sagittal suture were widely patent. A clinical diagnosis of Muenke or Saethre-Chotzen syndrome was considered, but appropriate genetic testing was negative. Fronto-orbital and supraorbital rim remodelling, and osteotomy of the right lambdoid suture were performed at the age of 7 months.

On reassessment at the age of 1 year, delayed development was apparent. An MRI brain scan at 16 months showed a short corpus callosum, mildly enlarged lateral ventricles, a peaked tentorium cerebelli, enlarged foramen magnum with hypoplastic pons and cerebellum with prominent cerebellar folia and signal void near the cervical cord. The left transverse and sigmoid sinuses, together with the jugular foramen were enlarged, whereas on the right the transverse and sigmoid sinuses were underdeveloped. Ophthalmological assessment at the age of 18 months showed exotropia of the right

eye, latent nystagmus, strabismus sursoadductorius with V motility and bilateral granular pigmented retinæ. Metabolic testing was normal. Adenotonsillectomy was performed at the age of 2 years because of recurrent tonsillitis and otitis media.

Development continued to be delayed and was formally assessed at the age of 34 months. Motor development was at 15 months equivalent, but no formal testing of mental development or speech was possible. His back was hyperpigmented and pedes plano valgi were present. At 4 years, speech and gait were noted to be ataxic and autistic spectrum disorder and attention deficit hyperactivity disorder were diagnosed. Optic nerve hypoplasia was noted, worse in the right eye in which vision was reduced to 30% of normal; the left eye was myopic (-2.25 dpt).

Subject 5:III.3 (proband)

This male was the second child born at 38 weeks' gestation to unrelated parents. His grandfather (I.1), mother (II.2) and half-brother (III.1) had a similar head shape (see below). He weighed 2.94 kg and was well except for neonatal jaundice. At 30 months a brachycephalic head shape was noted with OFC of 46 cm (-2.5 SD), associated with patent posterior fontanelle (3.3 cm), an asymmetrical face, beaked nose, a high palate, and downslant and ptosis of the eyes. No hearing deficits or malformations of the upper or lower extremities were present. A clinical diagnosis of Saethre-Chotzen syndrome was suggested.

His development was generally delayed; he started walking at the age of 2.5 years and had delayed speech. He was generally hypotonic with joint laxity. An electroencephalogram (EEG) showed an irregular and diffuse disordered background pattern with accentuated frontal dysfunction. He had a bilateral convergent strabismus.

He was referred for plastic surgical assessment at the age of 3.5 years. The craniofacial features were as noted previously. Vision was normal with glasses. Skull radiographs showed bicoronal synostosis with increased thumb printing of the frontal bones. CT head scanning demonstrated in addition a patent metopic suture, bilateral bony defect of the lambdoid suture, and normal ventricles and posterior fossa. No surgery was performed because of his age.

His most recent review was at the age of 19 years. He still complained of headaches. He had a mildly delayed development and lived under social supervision. His communication was normal. Mild flattening of the left supra-orbital region, mild asymmetry of the skull, and downslant and exorbitism of the eyes were present.



Subject 5:III.1

The older half-brother of the proband was born at 40 weeks' gestation with a weight of 4.00 kg and a length of 52 cm. He was well during infancy but was clumsy with mildly delayed developmental milestones (walked at 3 years, rode a bicycle at 6 years, swimming certificate at 12 years). He had a large anterior fontanelle that did not close until 4 years of age. Attention deficit disorder was diagnosed.

At the age of 8 years he was investigated for suspected hearing loss. He had persisting central hypotonia, was dysarthric, mildly dysphasic and dyspraxic, and was unable to heel-toe walk. Hyperpigmentation was noted over his back. He was found to have a 50 dB left-sided sensorineural hearing loss; auditory evoked potentials suggested a sensorineural cause. CT head scan showed cystic dilatation of the 4th ventricle communicating with the cisterna magna, and hypoplasia of the cerebellar vermis. The third and lateral ventricles and the foramina of Luschka and Magendi were normal. These features were consistent with a variant of Dandy-Walker malformation. Visual evoked potentials were normal and a radio-iodinated serum albumin brain scan suggested obstruction of drainage of the left lateral ventricle. Radiology of the spine showed hypolordosis of the cervical spine and spina bifida occulta with absent arches of the L4, L5 and S1 vertebrae.

During the latter part of childhood his symptoms persisted. At the age of 15 years LHRH deficiency was diagnosed because of pubertal delay and he was started on pulsatile LHRH therapy. On further assessment aged 16 years, his OFC was 53 cm (-1.96 SD) and hyperpigmentation of his back was present. An MRI scan confirmed the earlier CT findings and showed atrophy of the cerebellum, the brachium pontis and temporo-basal lobes with widened sulci.

Subject 5:II.2

Little detailed information is available on the mother of III-1 and III-3. She reported that as a child she had an enlarged late-closing fontanel, and had learning disability requiring her to repeat classes in both primary and secondary school. She suffered from vertigo and had a clumsy tandem gait. MRI scan showed atrophy of the rostral part of the cerebellum and pons, similar to, but less severe than, III-1.

The family was investigated for a suspected autosomal dominant cerebellar atrophy, but relevant genetic testing (*SCA1*, *SCA2*, *SCA3* and *SCA6*) was negative in both 5:II.2 and 5:III.1.

Subject 5:III.6

The proband's male cousin, the third child in the sibship (the two older siblings were healthy) was born at 37 weeks' gestation after an uneventful pregnancy, weighing 3.35 kg. He was referred for a plastic surgery opinion at 1 month of age because of concerns about his head size. He was microcephalic (OFC 38.5cm at 3.5 months; -1.9 SD) and noted to have brachycephaly, hypoplastic supraorbital ridges, hypertelorism, mild ptosis of the right eye, downslanting palpebral fissures, divergent strabismus, a high narrow palate, normal ears and symmetrical defects palpable over the occipito-parietal region. Additional features noted were axial hypotonia (but with increased muscle tone of the upper extremities), mild tapering of the fingers, clinodactyly of the 4th and 5th toes and a sacral dimple. A clinical diagnosis of Saethre-Chotzen syndrome was suggested. 3D CT scanning at the age of 2 months showed bilateral coronal synostosis with bilateral large parietal foramina. Ultrasound of the brain was normal. A fronto-orbital advancement was performed at the age of 11 months. The divergent strabismus persisted and posterior tenotomies were performed at the age of 3 years and 5 months.

At the age of 13 years an MRI brain scan was performed. The fourth ventricle and both superior cerebellar peduncles were mildly enlarged, with a prominent great cerebral vein and inferior sagittal sinus. The posterior fossa was small with a peaked tentorium cerebelli, short and steep straight sinus with mild hypoplasia of the dorsal part of the pons and inferior part of the cerebellar vermis. There was no Chiari or Dandy-Walker malformation.

His schooling history is not documented. Formal psychological testing was performed at the age of 16 years. The WISCIII scores were full scale IQ 89, verbal IQ 96, performance IQ 84. The Child Behaviour Checklist 6-18, Social Communication Questionnaire, and Children's Communication Checklist-2 NL were normal. The OFC was 55 cm (0 SD). He had small teeth and wore orthodontic braces.

**Subject 5:II.4**

This individual is the sister of II.2 and mother of III.6. As a child she had a strabismus correction, but no other surgery. She had mildly delayed development with attention deficit, aberrant fine motor skills and clumsiness, but attended a normal school. Her hearing and balance were normal. Currently aged 53 years, she complains of persistent severe headaches, forgetfulness and dental problems. On examination her height was 1.62 m (-0.3 SD), she had brachymicrocephaly (OFC 51 cm, -2.9 SD), vertical orbital dystopia, ptosis of the left upper eyelid, midface hypoplasia, nasal deviation, and facial and occlusal asymmetry with narrow maxilla, crowding of the upper front teeth, absence of the lower right first molar and upper right canine, and prominent crura of both ears. The hands and feet were normal. MRI brain scan showed asymmetry of the skull base

and head shape, an enlarged foramen magnum, a peaked tentorium cerebelli, mildly hypoplastic inferior part of the cerebellar vermis and possibly a small defect of the hiatus tentorium cerebelli.

Subject 5:I.1

The deceased father of II.2 and II.4 (I.1) had a high forehead, facial asymmetry and hearing deficits, suggesting that the *ZIC1* mutation present in his two daughters had been transmitted from him.



Identification of causative variants in *TXNL4A* in Burn-McKeown syndrome and isolated choanal atresia

Jacqueline A.C. Goos, Sigrid M.A. Swagemakers,* Stephen R.F. Twigg,* Marieke F. van Dooren, A. Jeannette M. Hoogeboom, Christian Beetz, Sven Günther, Frank J. Magielsen, Charlotte W. Ockeloen, Maria A. Ramos-Arroyo, Rolph Pfundt, Helger G. Yntema, Peter J. van der Spek, Philip Stanier, Dagmar Wieczorek, Andrew O.M. Wilkie, Ans M.W. van den Ouweland, Irene M.J. Mathijssen, Jane A. Hurst

*Equal contributors

European Journal of Human Genetics July 2017

Abstract

Burn-McKeown syndrome (BMKS) is a rare syndrome characterized by choanal atresia, prominent ears, abnormalities of the outer third of the lower eyelid, structural cardiac abnormalities, conductive and sensorineural hearing loss, and cleft lip. Recently, causative compound heterozygous variants were identified in *TXNL4A*. We analysed an individual with clinical features of BMKS and her parents by whole genome sequencing and identified compound heterozygous variants in *TXNL4A* (a novel splice site variant (c.258-2A>G, (p.?.)) and a 34 bp promoter deletion (hg19 chr18:g.77748581_77748614del (type 1Δ) in the proband). Subsequently, we tested a cohort of 19 individuals with (mild) features of BMKS and 17 individuals with isolated choanal atresia for causative variants in *TXNL4A* by dideoxy-sequence analysis. In one individual with BMKS unrelated to the first family, we identified the identical compound heterozygous variants. In an individual with isolated choanal atresia, we found homozygosity for the same type 1Δ promoter deletion, whilst in two cousins from a family with choanal atresia and other minor anomalies we found homozygosity for a different deletion within the promoter (hg19 chr18:g.77748604_77748637del (type 2Δ)). Hence, we identified causative recessive variants in *TXNL4A* in two individuals with BMKS as well as in three individuals (from two families) with isolated choanal atresia.

Introduction

Burn-McKeown syndrome (BMKS) was first described in five children by Burn *et al.*²⁸⁶ It is a rare disorder characterized by choanal atresia, prominent ears, hypertelorism with short palpebral fissures and abnormalities of the outer third of the lower eyelids. Other features that can be observed are structural cardiac abnormalities, conductive and sensorineural hearing loss, and unilateral cleft lip.²⁸⁶ There is clinical overlap with both Treacher Collins and CHARGE syndromes.

Burn *et al.*²⁸⁶ advised counselling a high recurrence risk in families with BMKS, but the inheritance pattern remained unclear until recently. As the syndrome was repeatedly described in siblings and mainly in males, an autosomal recessive²⁸⁶ or X-linked inheritance pattern was suggested.²⁸⁷ However, the identification of a chromosomal rearrangement, 46,XX,r(18)(p14q23), in an isolated female case with features of BMKS suggested terminal 18p or 18q as the locus for the disorder.²⁸⁶ This was borne out by the detection of causative compound heterozygous variants in *TXNL4A* (located on chromosome 18q23), identified more than 20 years after the initial description of BMKS.⁶¹

TXNL4A is a member of the U5 spliceosomal complex that is critical for pre-mRNA splicing.²⁸⁸ It has been suggested that reduced expression of *TXNL4A* influences the splicing of a specific subset of pre-mRNAs, resulting in the tissue-specific phenotypic spectrum of BMKS.^{61,289} In the present study, we describe new causative variants in *TXNL4A* and expand the associated phenotypic spectrum.

Subjects and methods




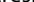


Subjects

Ethical approval from the board of the Medical Ethical Committee of the Erasmus MC, University Medical Centre Rotterdam, the Netherlands, was given for whole genome sequencing (MEC-2012-140) and for retrospective data collection (MEC-2013-547). UK samples were collected following approval from the Great Ormond Street Hospital for Children NHS Trust Ethics Committee (REC No. 08H0713/46). Informed consent was received from the individuals and parents.

Whole genome sequencing was performed on DNA of the members of family 1 (see Figure 8.1).





  choanal atresia,   prognathism,   maxillary hypoplasia.

1Δ = Promoter deletion type 1Δ (hg19 chr18:g.77748581_77748614del), 2Δ = Promoter deletion type 2Δ (hg19 chr18: g.77748604_77748637del), NA = Not available, Spl = splice site variant, -/- = no causative variant in *TXNL4A*.

To identify further mutation-positive individuals, dideoxy-sequence analysis of the promoter region, the exons and the exon/intron boundaries of *TXNL4A* was performed using DNA of 19 individuals who have clinical features that overlap with (mild) BMKS. In addition, 17 individuals with isolated choanal atresia were also tested for mutations in *TXNL4A*. In addition, 29 of the DNA samples were analysed for copy number variations in *TXNL4A* using a multiplex ligation-dependent probe amplification (MLPA) assay as described by Wiczorek *et al.*⁶¹

The variants identified were described according to HGVS nomenclature,¹⁴⁸ using the reference sequences NM_006701.2, ENST00000269601 and ENSG00000141759, on GRCh37/hg19 and were submitted to the Leiden Open Variation Database (<http://www.lovd.nl/TXNL4A>).

Whole genome sequencing

Before publication of the paper of Wieczorek *et al.*,⁶¹ whole genome sequencing was performed on DNA of the proband of family 1 (III.2) and her parents (see Figure 8.1) by Complete Genomics, a BGI company (Mountain View, CA, USA) as described by Drmanac.¹⁰⁴ Variants were annotated using NCBI build 36.3/hg18 and dbSNP build 130. Data were analysed using cga tools version 1.6.0.43 and TIBCO Spotfire 7.0.0 (TIBCO Software Inc., Boston, MA, USA). The annotations were converted to GRCh37/hg19 by using Human BLAT search on the UCSC website (Kent Informatics, Inc., Santa Cruz, CA, USA) as described previously.¹⁴⁶

An autosomal dominant disease model was tested in family 1. The analysis was restricted to novel non-synonymous variants, variants disrupting a splice site (± 2 bp), and insertions or deletions in the coding sequence (± 50 bp).

The remaining variants were analysed with Annovar,²⁹⁰ to get an indication of the pathogenicity and the ESP frequency as given in Exome Variant Server (EVS, NHLBI GO Exome Sequencing Project (ESP), Seattle, WA (URL: <http://evs.gs.washington.edu/EVS/>) [April 2014 accessed]). We focused on variants that were located in genes without loss-of-function mutations in EVS.

Confirmation by dideoxy-sequence analysis

The variants identified by whole genome sequencing were validated by dideoxy-sequence analysis (all primer sequences are provided in Supplementary Table 8.1). Amplification reactions were performed according to standard procedures. PCR products were purified using Agencourt AMPure (Agencourt, Beckman Coulter Inc., Brea, CA, USA). Direct sequencing of both strands was performed using Big Dye terminator version 3.1 (Applied Biosystems, Foster City, CA, USA) as recommended by the manufacturer. Dye terminators were removed using Agencourt CleanSeq (Agencourt) and loaded on an ABI 3130XL Genetic Analyzer (Applied Biosystems). The sequences were analysed using SeqPilot version 4.1.2 build 507 (JSI Medical Systems GmbH, Kippenheim, Germany).



Confirmation of effect of the variants on RNA expression

To analyse the effect of the variants on RNA expression, cDNA was analysed by restriction enzyme digestion and deep sequencing. First, RNA was extracted according to the manufacturer's protocol from venous blood collected into PAXgene Blood RNA tubes (Qiagen N.V., Venlo, The Netherlands) from individuals II.1, II.2 and III.2 (Figure 8.1, family 1). cDNA was synthesized using the RevertAid First Strand cDNA kit (Thermo Scientific Inc., Waltham, MA, USA), with random hexamer primers according to the manufacturer's instructions. Primers were designed for all exons and intron two to screen for truncations and intron retention (Supplementary Table 8.1). cDNA was amplified and products were electrophoresed on agarose gels and DNA was visualized by staining with ethidium bromide (EtBr).

Digestion with PshAI and AhdI and electrophoresis of digests

To assess the effect of the paternal variant on RNA expression in family 1, cDNA amplification products were digested with PshAI or AhdI (New England Biolabs Inc., Ipswich, MA, USA) and analysed by agarose gel electrophoresis. The forward primer was mutated to allow digestion with AhdI (underlined and bold 'a' in Supplementary Table 8.1).

Deep sequencing by Ion PGM Sequencing

To distinguish between the wild-type and mutant allele, two heterozygous SNPs in the 3'-UTR of *TXNL4A* that were identified in the WGS data from the parents of the family 1 proband were used. To quantify the effect of the maternal variant, deep sequencing covering the SNP was performed on cDNA of the proband. Primers are given in Supplementary Table 8.1. The cDNA amplification products were diluted 1/100 and 2 µl was used in a second round PCR, with a reverse primer including the Ion PGM P1 adapter, and a forward primer with the Ion PGM A adapter sequence and a barcode sequence (reaction conditions available on request). Amplification products (roughly equal amounts as judged by EtBr staining by agarose gel electrophoresis) were combined and then purified with AMPure beads (Beckman Coulter). Emulsion PCR and enrichment was performed with the Ion PGM Template OT2 200 Kit (Life Technologies) according to the manufacturer's instructions. Sequencing of enriched templates was performed on the Ion Torrent PGM (Life Technologies) for 125 cycles using the Ion PGM Sequencing 200 kit v2 and Ion 316 chips. Data were processed with Ion Torrent platform-specific pipeline software v4.2.1.

Results

Whole genome sequencing of family 1

The proband of family 1 and her parents were analysed by WGS. Variants remaining after the various filtering steps are available on request. By testing the expected autosomal dominant disease model, we identified a novel splice site variant upstream of the last exon in *TXNL4A* (c.258-2A>G, (p.?)), that was inherited from the father. According to both cga tools and ANNOVAR, the splice site variant was predicted to be deleterious. As this variant was present in the 3' splice site consensus sequence, it was highly conserved with a PhyloP score of 1.824×10^{-5} . The variant was not present in ESP, 1000 Genomes (The 1000 Genomes Project Consortium, 2012, URL: <http://www.1000genomes.org/>¹⁵⁴), Ensembl,²⁹¹ nor in our in-house Huvariome database.¹⁵³ However, it did have an allele frequency of 7.31×10^{-6} in gnomAD.¹¹¹ During the analysis, the phenotype was recognized as suspected BMKS. Therefore, recessive variants on chromosome 18 were implicated and the DNA sequence of *TXNL4A* was scrutinized manually. Based on the

publication of Wieczorek et al,⁶¹ the likely significance of a 34 bp deletion within the promoter became apparent (hg19 chr18:g.77748581_77748614del, referred to as type 1Δ and inherited from the mother).⁶¹ The presence of both variants was confirmed by dideoxy sequencing (Figure 8.2).

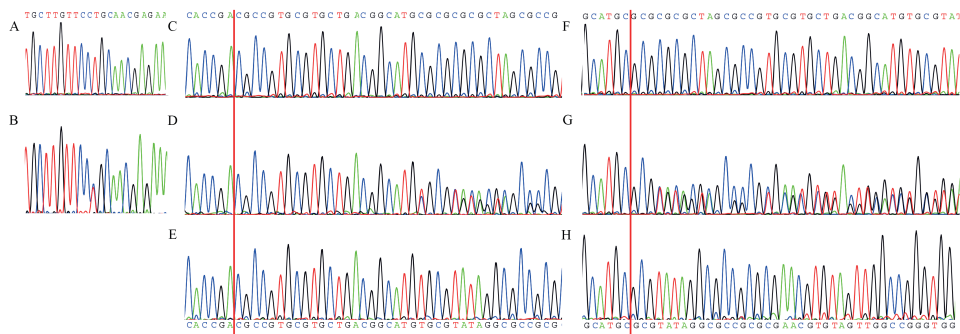


Figure 8.2. Electropherograms of dideoxy-sequence analyses. Red line indicates the start of the deletion. **A:** control DNA. **B:** splice site variant in DNA of III.2 of family 1. **C:** region of type 1Δ deletion in control DNA. **D:** heterozygous type 1Δ deletion in DNA of III.2 of family 1. **E:** homozygous type 1Δ deletion as seen in DNA of III.1 of family 3. **F:** region of type 2Δ deletion in control DNA. **G:** heterozygous type 2Δ deletion as seen in DNA of IV.6 of family 4. **H:** homozygous type 2Δ deletion as seen in DNA of V.4 of family 4.

cDNA analysis of *TXNL4A*

RT-PCR analysis of the proband of family 1 and her parents, followed by agarose gel electrophoresis, did not show any aberrantly spliced products in any of the samples, despite the presence of the predicted splice site variant in both the proband and her father. WGS data indicated that both parents each carried a different sequence change within the 3' UTR of *TXNL4A* that was not inherited by their daughter (thus located on the reference alleles): the father was heterozygous for hg19 chr18:g.77733297dupC (rs77355432, dbSNP build 146) and the mother for hg19 chr18:g.77733273C4T (rs4798931). Primers were designed to amplify both SNPs in one amplicon.

The effect of the 3' acceptor variant c.258-2A>G on splicing, was assessed using the restriction enzymes AhdI and PshAI. AhdI was specific for the 3' UTR dupC (reference allele, not passed to the proband), while PshAI was specific for the mutant allele in cDNA from the father (passed to the proband). The primer was designed to amplify the alleles equally, had they both been present in the cDNA. Using AhdI, the cDNA of the father



was digested almost to completion (Figure 8.3), and using PshAI the cDNA remained undigested (data not shown), indicating that there was no or extremely reduced mature transcript from the mutant allele.

Deep sequencing of maternal cDNA demonstrated reduced expression from the allele with the type 1Δ: in a total of 36,924 reads, 8,636 reads (23%) were of the reference C (the allele with the promoter variant), and 28,283 reads (77%) contained the variant T (wildtype promoter allele).

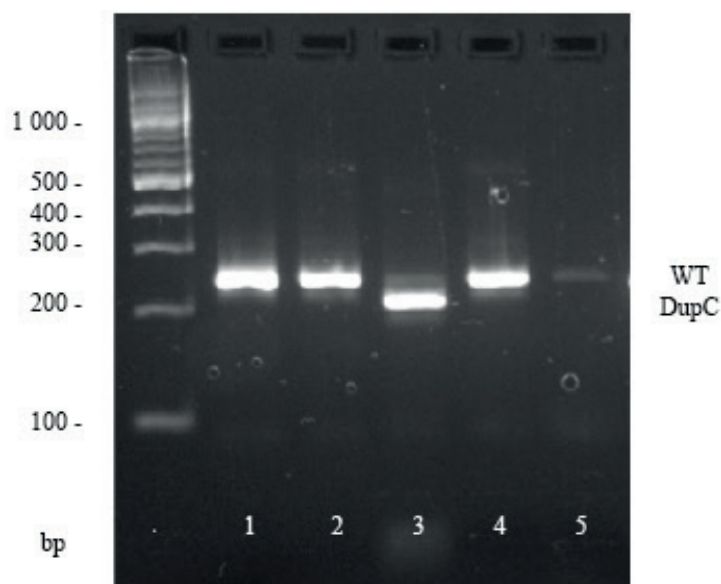


Figure 8.3. Restriction enzyme digest analysis of rs77355432 SNP in cDNA from family 1. Expected fragment sizes reference allele 249 bp (WT), alternative allele 215+34 bp (dupC). Lane 1, uncut DNA. Lane 2, cDNA from the proband is not digested with AhdI. Lane 3, cDNA of the father is cut almost to completion with AhdI. Lane 4, cDNA of the mother is uncut with AhdI. Lane 5, negative control.

Expansion of the mutation spectrum

Dideoxy sequencing of *TXNL4A* was performed on DNA obtained from 19 index cases with (mild) features of BMKS. The proband of family 2 (Figure 8.1, III.1 of family 2) was found to carry the identical variants to those of the family 1 proband. Analysis of parental samples showed that they were present in compound heterozygous state with the type 1 Δ deletion inherited from the father and the splice site variant inherited from the mother. In addition, 17 index cases with choanal atresia were tested for mutations in *TXNL4A*. In two probands, homozygosity for a promoter deletion was identified. The proband of family 3 (Figure 8.1, III.1 of family 3) had a uniparental disomy of chromosome 18p11.32q23, leading to homozygosity for the type 1 Δ deletion. The family 4 proband (Figure 8.1, V.4 of family 4) was homozygous for a slightly different promoter deletion: hg19 chr18:g.77748604_77748637del corresponding to type 2 Δ in Wieczorek *et al.*⁶¹ The same genotype was also present in his first cousin (Figure 8.1, V.6 of family 4).

MLPA analysis was performed on the 29 samples with sufficient DNA available. This included samples of both families 3 and 4 (Table 8.2). Large rearrangements were not identified in any of these samples.

Subjects

Nineteen individuals with clinical features overlapping with BMKS syndrome and 17 individuals with isolated choanal atresia were tested for mutations in *TXNL4A*. Causative variants were identified in five individuals. An overview of the clinical phenotype of these individuals is given in Table 8.1. The proband of family 4 and his first cousin (Figure 8.1, V.4 and V.6 of family 4) were previously described as patients 1 and 3 in the paper of Ramos-Arroyo *et al.*²⁹² All individuals had choanal atresia and normal development. In three out of five, their pregnancy was complicated by polyhydramnios. The same three had a prominent nasal bridge. Maxillary hypoplasia was also seen in the same three individuals, and micrognathia was seen in two out of them. Two out of five individuals had defects of the lower eyelids. The proband of family 4 and his first cousin had oligodontia, however, due to the high prevalence of this condition,²⁹³ we cannot rule out that this is a separate condition that is segregating within this family.²⁹²



Discussion

In two out of 20 unrelated individuals with clinical features of BMKS, we identified compound heterozygosity in *TXNL4A* for a novel splice site variant, c.258-2A>G, (p.?) and the type 1Δ promoter variant, hg19 chr18:g.77748581_77748614del. Our findings support the idea that causative *TXNL4A* variants do not completely ablate function in BMKS.⁶¹

In nine out of 11 affected families, Wieczorek *et al.*⁶¹ found a rare loss-of-function variant (nonsense, frameshift or microdeletion) on one allele in conjunction with a promoter deletion on the other allele. In our deep sequencing analysis of RNA isolated from blood, expression of the type 1Δ mutant allele was reduced by ~ 69%. This is in keeping with a luciferase reporter gene assay, where the promoter activity of constructs containing type 1Δ deletion was reduced by 59% compared to a wild-type construct.⁶¹ The presence of the splice-site variant on the other *TXNL4A* allele of the family 1 proband most likely leads to loss-of-function, since analysis of paternal cDNA based on the closely adjacent SNP rs77355432, indicated no evidence of transcription of this allele (Figure 8.3). Wieczorek *et al.*⁶¹ have shown that deletion of exon three combined with type 1Δ causes BMKS. Hence, we can conclude that the variants identified in the probands of families 1 and 2 are the underlying causes of the clinical phenotype.

In the paper of Wieczorek *et al.*⁶¹ the allele frequency of the promoter deletions in German control samples was estimated at 0.76%. A single homozygous type 1Δ deletion was identified in 3,343 population-based German and South Asian samples. Unfortunately, data about the craniofacial phenotype in that individual were not available. In this study, we sequenced a cohort of 17 individuals with choanal atresia and also identified a homozygous type 1Δ deletion (family 3). Although the predicted frequency of homozygous type 1Δ deletions was estimated at 1:17,300, which seemed to exclude this genotype as a cause for BMKS, Wieczorek *et al.*⁶¹ stated that this genotype might lead to a mild phenotype. It seems likely that the isolated bilateral choanal atresia identified in the proband of family 3 might be part of this mild phenotype, especially since choanal atresia is one of the major anomalies of BMKS. As isolated choanal atresia is a feature of the *Tbx22* knock-out mouse,²⁹⁴ the individuals with isolated choanal atresia were screened for mutations in *TBX22*, but causative variants were not found.

In family 4, homozygosity for the pathogenic promoter variant type 2Δ was found to segregate in the affected individuals. Wieczorek *et al.*⁶¹ also found a homozygous type 2Δ case in an individual with true BMKS and showed that promoter activity of a construct containing type 2Δ was reduced by 72% compared to wild-type, indicating a stronger reduction of *TXNL4A* expression than type 1Δ. However, individuals with the type 2Δ (family 4) seem to be less severely affected than the compound heterozygotes; only choanal atresia, hypodontia and some minor anomalies were seen (Table 8.2).

Further screening of family 4 identified eight members who were heterozygous for type 2 Δ , and interestingly minor anomalies were present in two of them (Figure 8.1 and Table 8.2). Our data support the proposed dosage-specific effect.^{61,289}

Wieczorek *et al.*⁶¹ identified causative variants in nine out of 11 families, compared to two out of 18 in this study. This may be attributed to the fact that in this work individuals were included with only mild features of BMKS and may overlap with other conditions such as bilateral craniofacial microsomia, CHARGE phenotype, and asymmetrical Treacher-Collins like phenotype. Recently, it has been shown that ribosomopathies, such as Treacher Collins syndrome, and spliceosomopathies can have similar craniofacial phenotypes.²⁸⁹ In contrast to CHARGE and Treacher Collins syndrome, individuals with BMKS tend to have a normal intellectual development, however, there is otherwise significant clinical overlap. Therefore, we suggest it will be important to test for mutations in *TXNL4A* if the clinical phenotype is indicative of BMKS, but also if the clinical phenotype is indicative of these other conditions should their appropriate gene tests report negative.

Conclusion

We describe the finding of the splice site variant c.258-2A>G, combined with promoter deletion type 1 Δ , in *TXNL4A* as the genetic cause of BMKS in two unrelated individuals. Homozygosity for the type 1 Δ deletion was identified in a third individual with isolated choanal atresia. Homozygosity for the type 2 Δ deletion was identified in a family with choanal atresia and other minor anomalies. These results confirm that variants affecting function of *TXNL4A* are the cause of BMKS and possibly a cause of isolated choanal atresia, underlining the tissue-specific nature of craniofacial disorders caused by spliceosomal defects.²⁸⁹



Table 8.1. Clinical phenotype of individuals with causative variants using the features mentioned by Wieczorek *et al.*^[6] that are associated with BMKS.

Clinical phenotype of individuals with causative variants						
ID in pedigree	III.2 family 1	III.1 family 2	III.1 family 3	V.4 family 4	V.6 family 4	
Gender	Female	Male	Male	Male	Female	
Age at examination	37 years			7 years		
Genetic testing	TCOF1 CHD7 SNP array WGS MLPA	Affymetrix 750K microarray TXNL4A MLPA	Affymetrix 750K microarray → 18p11.32q23 (136,300- 77,997,592) hmz uniparental disomy for chromosome 18 TXNL4A MLPA	Karyo TXNL4A MLPA	TXNL4A MLPA	
Variant carried by father	c.258-2A>G, (p.?)	hg19 chr18:g.77748581_77748614del (type 1Δ)	hg19 chr18:g.77748581_77748614del (type 1Δ)	hg19 chr18:g.77748604_77748637del (type 2Δ)	hg19 chr18:g.77748604_77748637del (type 2Δ)	
Variant carried by mother	hg19 chr18:g.77748581_77748614del (type 1Δ)	c.258-2A>G, (p.?)	hg19 chr18:g.77748581_77748614del (type 1Δ)	hg19 chr18:g.77748604_77748637del (type 2Δ)	hg19 chr18:g.77748604_77748637del (type 2Δ)	
Positive family history	Y father scleral show	N	N	Y	Y	
Normal pregnancy	Y	Polyhydramnios	IVF ICSI Failure to progress	Polyhydramnios	Polyhydramnios	
Asymmetry of the face	Y			N	N	
Hypertelorism	N			N	N	
Short palpebral fissures	Y			N	N	
Defect of lower eyelids	Y	Y (B)		N	N	
Aplasia of puncta lacrimalis	Y (L)					
Prominent nasal bridge	Y	Y		Y	Y	
Short philtrum	N			Y	Y	
Thin lips	Y			Y	N	
Cleft lip or palate	N	Y (L)		N	N	

Bilateral choanal atresia/ stenosis	Bilateral (bony)	Bilateral	Bilateral (bony)	Bilateral
Prominent ears	Y			
Preauricular tags	Y (R)	Y (R)		Y
Maxillary hypoplasia	Y (R)			
Micrognathia	Y (R)	Y		Y
Cardiac defect	N	Asymptomatic ASD and VSD		
Hearing loss	N			N
Normal psychomotor development	Y	Y		Y
Short stature	Y			N
Other	Hypoplasia infra-orbital rim (R) Upslanting palpebral fissures Eyelashes were longer laterally than medially Choroid coloboma (L) Microstrabismus Amblyopia	Dimple on the cheek Hypermetropia	Downslanting palpebral fissures Prognathism High arched narrow palate Absence of the upper and lower deciduous premolars Hypodontia of four permanent premolars	Cowlick Downslanting palpebral fissures Prognathism Dental malocclusion Narrow palate Unilateral absence of the permanent upper lateral incisor

ASD = Atrial septal defect, B = Bilateral, Hom = Homozygous, ICSI = Intracytoplasmic sperm injection, IVF = *In vitro* fertilization, Karyo = Karyotype, L = Left, M = Maternal, N = No, P = Paternal, R = Right, VSD = Ventricular septal defect, WGS = Whole genome sequencing, Y = Yes. Blank entries indicate that information was not available.



Table 8.2. Overview of testing done for 41 affected and 19 unaffected individuals.

Family	Sample	Gender	Genetic testing	Variants identified	MLPA	Clinical features	BMKS/ isolated choanal atresia
Family 1	III.2	F	TCOF1, CHD7, SNP array, WGS	hg19 chr18:g.77748581_77748614del (1Δ) (M), c.258-2A>G, (p.?) (P)	Y	Normal pregnancy, facial asymmetry, short palpebral fissures, defect of lower eyelids, aplasia of puncta lacrimalis L, hypoplasia infra-orbital rim R, upslanting palpebral fissures, longer eyelashes laterally than medially, choroid coloboma L, microstrabismus, amblyopia bilateral choanal atresia, preauricular tag R, maxillary hypoplasia R, micrognathia R, normal psychomotor development	BMKS
	II.1	M	WGS	c.258-2A>G, (p.?)	Y	Scleral show	
	II.2	F	WGS	hg19 chr18:g.77748581_77748614del (1Δ)	Y		
	Uncle	M	TXNL4A		Y		
Family 2	Husband	M	TXNL4A		Y		
	III.1	M	Affymetrix 750K microarray, TXNL4A	hg19 chr18:g.77748581_77748614del (1Δ) (P), c.258-2A>G, (p.?) (M)	Y	Polyhydramnios, bilateral defect of lower eyelids, hypermetropia, prominent nasal bridge, cleft lip and palate L, bilateral choanal atresia, preauricular tag R, micrognathia, normal psychomotor development, dimple on the cheek, asymptomatic ASD and VSD	BMKS
	II.2	F	TXNL4A	c.258-2A>G, (p.?)	N		
	II.1	M	TXNL4A	hg19 chr18:g.77748581_77748614del (1Δ) (het)	N		
Family 3	III.1	M	Affymetrix 750K microarray -> isodisomy of chr18 TXNL4A	hg19 chr18:g.77748581_77748614del (1Δ) (hom)	Y	IVF ICSI, failure to progress, bilateral choanal atresia	Choanal atresia
	II.2	F	TXNL4A	hg19 chr18:g.77748581_77748614del (1Δ) (het)	N		

Family 3	II.1	M	TXNL4A	hg19 chr18:g.77748581_77748614del (1Δ) (het)	N		
Family 4	V.4	M	TXNL4A, TBX22	hg19 chr18:g.77748604_77748637del (2Δ) (hom)	Y	Polyhydramnios, downslanting palpebral fissures, prominent nasal bridge, bilateral choanal atresia, maxillary hypoplasia, prognathism, high arched narrow palate, absence of the upper and lower deciduous premolars, hypodontia of four permanent premolars, normal psychomotor development	Choanal atresia
	V.6	F	Karyo, TXNL4A, TBX22	hg19 chr18:g.77748604_77748637del (2Δ) (hom)	Y	Polyhydramnios, prominent nasal bridge, bilateral choanal atresia, maxillary hypoplasia, cowlick, downslanting palpebral fissures, prognathism, dental malocclusion, narrow palate, unilateral absence of the permanent upper lateral incisor	Choanal atresia
	III.1	F	TXNL4A		N		
	III.2	F	TXNL4A	hg19 chr18:g.77748604_77748637del (2Δ) (het)	N		
	IV.1	F	TXNL4A		N		
	IV.2	M	TXNL4A	hg19 chr18:g.77748604_77748637del (2Δ) (het)	N	Prognathism	
	IV.3	F	TXNL4A		N		
	IV.4	M	TXNL4A	hg19 chr18:g.77748604_77748637del (2Δ) (het)	N		
	IV.5	M	TXNL4A	hg19 chr18:g.77748604_77748637del (2Δ) (het)	N	Prognathism	
	IV.6	M	TXNL4A	hg19 chr18:g.77748604_77748637del (2Δ) (het)	N		



Table 8.2. (continued)

Family	Sample	Gender	Genetic testing	Variants identified	MLPA	Clinical features	BMKS/ isolated choanal atresia
Family 4	IV.7	F	TXNL4A	hg19 chr18:g.77748604_77748637del (2Δ) (het)	N		
	V.1	F	TXNL4A		N		
	V.2	M	TXNL4A		N		
	V.3	M	TXNL4A		N		
	V.5	M	TXNL4A	hg19 chr18:g.77748604_77748637del (2Δ) (het)	N		
	V.7	M	TXNL4A	hg19 chr18:g.77748604_77748637del (2Δ) (het)	N		
Family 5	II.1	M	WGS, TXNL4A		Y	Prosis, shallow orbits, prominent beaked nose, micrognathia	BMKS
	I.2 (mother)	F	WGS, TXNL4A		Y		
	6	M	WGS, TXNL4A, TCOF1, POLR1C, POLR1D, POLR1A, array		Y	Polyhydramnios, prematurity, respiratory distress, macroglossia, micrognathia, retrognathia, cleft palate, bilateral microtia, preauricular fistula, short downslanting palpebral fissures, shallow orbits, hearing loss	BMKS
	7	M	TXNL4A, array; TCOF1, SALL1, POLR1C, POLR1D		Y	Small for gestational age, conductive hearing loss, bilateral ear tags, downslanting palpebral fissures, hypertelorism, micrognathia, perianal tag, patent foramen ovale	BMKS
	8	F	TXNL4A, CHD7		Y	Bilateral choanal atresia	Choanal atresia
	9	F	TXNL4A		Y	Bilateral Tessier 7 cleft, dental crowding, bilateral ear tags, hearing loss based on absent cochlear nerves, coloboma of the left papilla, retina and pupil, amblyopia, oesophageal atresia with tracheoesophageal fistula, hemivertebrae, hypoplastic thumbs L>R, bilateral hemifacial macrosomia, hypotonia, OSA, mild PMR	BMKS

10	M	Karyo, <i>TXNL4A</i>		Y	Micrognathia, retrognathia, narrow maxilla, bilateral ear tags, hearing loss, epibulbar dermoid (R), dental crowding, OSA	BMKS
11	F	All TCS genes, WES, BOR syndrome genes		Y	Asymmetry of the face, hearing loss, normal stature, dysplastic ears, amblyopia, aberrant facial nerve	BMKS
12	F	<i>TCOF1</i> , <i>POLR1C</i> , <i>POLR1D</i> , WES, <i>TXNL4A</i>	deletion of <i>POLR1D</i>	Y	Asymmetry of the face, hypertelorism, short palpebral fissures, prominent nasal bridge, cleft lip and palate, microtia, maxillary hypoplasia, micrognathia, hearing loss, normal psychomotor development, short stature	BMKS
13	M	all TCS genes, <i>TXNL4A</i>		Y	Unilateral cleft lip and palate, maxillary hypoplasia, micrognathia, normal psychomotor development	BMKS
14	M	<i>TCOF1</i> , array, BOR syndrome genes, <i>TXNL4A</i>		Y	Renal cysts, microtia (unilateral)	BMKS
15	F	<i>TCOF1</i> , SNP array, <i>POLR1C</i> , <i>POLR1D</i> , <i>TXNL4A</i>		Y	Bilateral preauricular tags, bilateral Tessier 7 cleft, microtia R and anal atresia	BMKS
16	M	<i>TCOF1</i> , <i>TXNL4A</i>		Y	Maxillary hypoplasia, micrognathia, microtia R, hypoplasia zygomatic (mild)	BMKS
17	M	<i>TCOF1</i> , <i>TXNL4A</i>		Y	Maxillary hypoplasia, micrognathia, unilateral hearing loss	BMKS
18		<i>TXNL4A</i> , <i>TBX22</i>		Y	Hypertelorism, hypoplastic uvula, right sided choanal atresia, Mum Carbimazole treatment, blue eyes, ear pit (cochlear implant)	Choanal atresia
19		<i>TXNL4A</i> , <i>TBX22</i>		Y	Choanal atresia R	Choanal atresia
20		<i>TXNL4A</i> , <i>TBX22</i>		Y	Choanal atresia B	Choanal atresia
21		<i>TXNL4A</i> , <i>TBX22</i>		Y	Choanal atresia R	Choanal atresia
22		<i>TXNL4A</i> , <i>TBX22</i>		Y	Bifid uvula, choanal atresia R, ASD	Choanal atresia
23		<i>TXNL4A</i> , <i>TBX22</i>		Y	Choanal atresia R	Choanal atresia
24		<i>TXNL4A</i> , <i>TBX22</i>		N	Choanal atresia R	Choanal atresia
25		<i>TXNL4A</i> , <i>TBX22</i>		N		Choanal atresia
26		<i>CHD7</i> , <i>TXNL4A</i> , <i>TBX22</i>	R157X in <i>CHD7</i> p.(Arg157*)	N	CHARGE	Choanal atresia



Table 8.2. (continued)

Family	Sample	Gender	Genetic testing	Variants identified	MLPA	Clinical features	BMKS/ isolated choanal atresia
	27		TXNL4A, TBX22		N		Choanal atresia
	28		TXNL4A, TBX22		N		Choanal atresia
	29		TXNL4A, TBX22		N		Choanal atresia
	30		TXNL4A, TBX22		N		Choanal atresia
	31		TXNL4A, TBX22		N	Choanal atresia L, ID, syngnathia	Choanal atresia
	32		TXNL4A		N		BMKS
	33	F	TXNL4A		N		BMKS
	34	M	TXNL4A		N		BMKS
	35	M	TXNL4A		N		BMKS
	36	M	TXNL4A		N		BMKS

ASD = Atrial septal defect, B = Bilateral, f = Female, Hom = Homozygous, ICSI = Intracytoplasmic sperm injection, ID = Intellectual disability, IVF = *In vitro* fertilization, karyo = Karyogram, L = Left, m = Male, M = Maternal, N = No, OSA = Obstructive sleep apnoea, P = Paternal, PMR = Psychomotor retardation, R = Right, VSD = Ventricular septal defect, WES = Whole exome sequencing, WGS = Whole genome sequencing, Y = Yes.



Diagnostic value of exome and whole genome sequencing in craniosynostosis

Kerry A. Miller, Stephen R.F. Twigg, Simon J. McGowan, Julie M. Phipps, Aimée L. Fenwick, David Johnson, Steven A. Wall, Peter Noons, Katie E.M. Rees, Elizabeth A. Tidey, Judith Craft, John Taylor, Jenny C. Taylor, **Jacqueline A.C. Goos**, Sigrid M.A. Swagemakers, Irene M.J. Mathijssen, Peter J. van der Spek, Helen Lord, Tracy Lester, Noina Abid, Deirdre Cilliers, Jane A. Hurst, Jenny E.V. Morton, Elizabeth Sweeney, Astrid Weber, Louise C. Wilson, Andrew O.M. Wilkie

Journal of Medical Genetics November 2016

Abstract

Craniosynostosis, the premature fusion of one or more cranial sutures, occurs in ~1 in 2,250 births, either in isolation or as part of a syndrome. Mutations in at least 57 genes have been associated with craniosynostosis, but only a minority of these are included in routine laboratory genetic testing.

We used exome or whole genome sequencing to seek a genetic cause in a cohort of 40 subjects with craniosynostosis, selected by clinical or molecular geneticists as being high-priority cases, and in whom prior clinically-driven genetic testing had been negative.

We identified likely associated mutations in 15 patients (37.5%), involving 14 different genes. All genes were mutated in single families, except for *IL11RA* (2 families). We classified the other positive diagnoses as follows: commonly mutated craniosynostosis genes with atypical presentation (*EFNB1*, *TWIST1*); other core craniosynostosis genes (*CDC45*, *MSX2*, *ZIC1*); genes for which mutations are only rarely associated with craniosynostosis (*FBN1*, *HUWE1*, *KRAS*, *STAT3*); and known disease genes for which a causal relationship with craniosynostosis is currently unknown (*AHDC1*, *NTRK2*). In two further families, likely novel disease genes are currently undergoing functional validation. In 5 of the 15 positive cases, the (previously unanticipated) molecular diagnosis had immediate, actionable consequences for either genetic or medical management (mutations in *EFNB1*, *FBN1*, *KRAS*, *NTRK2*, *STAT3*).

This substantial genetic heterogeneity, and the multiple actionable mutations identified, emphasises the benefits of exome/whole genome sequencing to identify causal mutations in craniosynostosis cases for which routine clinical testing has yielded negative results.

Introduction

Accurate molecular classification is critical for the clinical management, counselling and prognosis of individuals with suspected monogenic diseases, particularly where early diagnosis and intervention would substantially influence decision-making by the clinician or family. Traditional phenotypically guided genetic testing may fail to identify rarer causes of disease, as many conditions have a highly variable clinical presentation. The use of next-generation sequencing technologies to interrogate the exome sequence or whole genome sequence may circumvent some of these difficulties since these approaches are agnostic to the underlying genetic cause.^{143,145,258}

Craniosynostosis, a condition that affects ~1 in 2,250 births,^{2,3} is defined as the premature fusion of one or more of the normally patent cranial sutures, a consequence of the disruption in the coordinated patterning, proliferation and differentiation of these tissues.²⁹⁵ It has a highly heterogeneous and complex aetiology with contributions from monogenic, chromosomal, polygenic and environmental factors all playing a role.^{125,127} Craniosynostosis most commonly occurs in isolation, but a minority of cases are associated with additional clinical features as part of a syndrome, probably reflecting the co-option of pleiotropic signalling pathways to pattern and maintain the suture; association with over 100 human syndromes has been reported.¹²⁹ An underlying genetic cause can be identified in ~24% of cases, with mutations in just six genes (in decreasing order of frequency: *FGFR2*, *FGFR3*, *TWIST1*, *TCF12*, *ERF* and *EFNB1*) together accounting for over three-quarters of monogenic diagnoses.^{59,63,128,131,133,134,136,138-140} At least 52 other genes have been identified as recurrently mutated in craniosynostosis,^{127,296} but these rarer targets do not tend to be included in molecular testing panels unless indicated by specific clinical features. Craniosynostosis may also present as a low-frequency association with intellectual disability syndromes, possibly related to disturbed maintenance of suture patency.¹²⁷

To evaluate the utility of exome sequencing and whole genome sequencing in this context, we used these technologies to search for a molecular diagnosis in 40 patients with craniosynostosis who had previously been evaluated using existing routine molecular testing, without a diagnosis being made. Cases were identified as being of high priority for further investigation, either by craniofacial clinical geneticists or by laboratory scientists specialising in craniofacial molecular diagnostics. From this cohort, we identified an underlying molecular lesion in 15 (37.5%) families. We document several cases where the mutation identified either did not obviously fit with the original clinical diagnosis, or where identification of the causal mutation would have proved difficult using traditional methods of molecular testing. We highlight five families for



which diagnosis has immediately impacted on clinical management or counselling. This work illustrates the molecular diversity of causes of craniosynostosis and the added value that can be gained by a comprehensive diagnostic approach in difficult cases.

Subjects and methods

Ethics statement and prior clinical investigation

Written, informed consent for genetic research and publication of clinical photographs was obtained by the referring clinicians and their research teams. DNA was extracted from whole blood. Genetic testing by a clinically accredited laboratory was guided by the judgement of the referring clinician and diagnostic laboratory but usually included dideoxy sequencing of *TWIST1*, *TCF12* and *ERF* (entire gene), *FGFR2* and *FGFR3* (regions enriched for craniosynostosis-associated mutations) and multiplex-ligation dependent probe amplification of *TWIST1* to exclude heterozygous deletions.^{59,125,140} Since chromosomal abnormalities account for 13-15% of genetic diagnoses in craniosynostosis,^{59,128} a karyotype or array comparative genomic hybridisation was undertaken in the majority of cases.

Cohort description

Subjects with craniosynostosis, who had previously been investigated by molecular genetic testing with normal findings, were identified either by four clinical geneticists with specialist expertise in craniosynostosis ($n = 36$) or by clinical laboratory scientists working in a specialist genetic diagnostic service ($n = 20$), for further investigation. Clinical geneticists were asked to prioritise cases thought most likely to have a genetic diagnosis (based on presence of syndromic features, multiple sutures affected, consanguinity or positive family history, and lack of any obvious environmental predisposition), particularly where there were active issues with genetic counselling. Twelve of the cases initially identified by clinical geneticists were excluded, either because further targeted genetic testing identified a monogenic cause (one case each with mutations in *ERF*,¹⁴⁰ *FGFR2*,¹³³ and *FLNA*,²⁹⁷ and two with *IL11RA* mutations),⁶⁰ where enrolment into the Deciphering Developmental Disorders study¹⁴⁵ was considered more appropriate ($n = 5$), or where samples were not available for analysis ($n = 2$). The remaining cases ($n = 24$), together with parental samples (where available) were enrolled into the craniofacial research study following informed consent. Sequencing comprised 12 singletons, one parent-child duo, ten parent-child trios and one trio comprising three affected individuals. Similar criteria were used by clinical laboratory scientists to prioritise 20 cases for exome sequencing, however clinical information tended to be more limited and availability of sufficient stored DNA sample was often a decisive factor for case inclusion. For the laboratory samples, consent for research

investigation was sought secondarily to enable the entire exome to be interrogated; two cases were excluded because consent was not obtained. In 16 of the remaining 18 laboratory diagnostic cases, exome sequencing was performed on the proband only; in one instance the exome of an affected sibling was already available and in another the family trio subsequently had whole genome sequencing. Two duplicate families (29, 34) identified by both clinicians and laboratory scientists are listed under the latter category in Table 9.1, which summarises the patterns of cranial suture involvement and syndromic features of the final total of 40 patients/families analysed, with further details in Supplementary Table 9.1. In general, cases referred by clinical geneticists exhibited higher proportions of multisuture involvement and syndromic features (Table 9.1). The significance of differences between two groups was calculated using Fisher's exact test.

Table 9.1. Cranial suture involvement in patients recruited for exome sequence/whole genome sequence.

	Non-syndromic		Syndromic		Combined	
	Total	Mutation positive	Total	Mutation positive	Total	Mutation positive
Clinical genetic cases						
Metopic	0	0	2	2	2	2
Sagittal	0	0	0	0	0	0
Unicoronal	0	0	1	0	1	0
Bicoronal	2	0	2	2	4	2
Multisuture	3	1	12	5*	15	6
Total	5	1	17	9	22	10
Molecular genetic cases						
Metopic	0	0	0	0	0	0
Sagittal	0	0	2	0	2	0
Unicoronal	5	1	1	1	6	2
Bicoronal	2	0	2	1*	4	1
Multisuture	1	0	5	2	6	2
Total	8	1	10	4	18	5

*Includes likely novel disease gene, still undergoing validation.



Exome and whole genome sequencing

Exome capture of DNA from patients was carried out using the TruSeq v2 (Illumina), SureSelect Human All Exon Kit v4/v5 (Agilent) or SeqCap EZ Human Exome Library v2.0 (NimbleGen) following the manufacturer's instructions. We generated a library for each sample using DNA extracted from whole blood; usually we employed 3 µg DNA, except for SureSelect v5 processed samples from families 8, 16 and 17 only, for which we used 200 ng DNA. Exome sequencing was performed on an Illumina HiSeq 2000 or 4000, with

75 bp or 100 bp paired-end reads. Whole genome sequencing was performed on 5 µg DNA extracted from blood by Complete Genomics (a BGI Company) and analysed as previously described.¹⁰⁴

Bioinformatic analysis

Exome sequencing reads were mapped to the GRCh38 reference genome with Bowtie 2²⁹⁸ and removal of artefacts (unmapped sequences, duplicate PCR products and likely pseudogene sequences) using custom Perl scripts.¹⁴⁰ Variants were called using SAMtools v1.1²⁹⁹ and Platypus v0.5.2.²⁵⁹ Sequence reads from whole genome sequencing were mapped to the GRCh37 reference genome and analysed as previously described.¹⁰⁴ The pathogenicity of each variant was given a custom deleterious score based on a 6-point scale,³⁰⁰ calculated using output from ANNOVAR.²⁹⁰ Variants predicted to affect splicing were assigned a deleterious score based on MaxEntScan score differences,³⁰¹ and the relationship of variants present in known disease-causing genes analysed for pathogenicity using ClinVar.³⁰² Variants with minor allele frequency (MAF) >1% in dbSNP or ExAC were removed, and remaining variants examined manually by visualisation in GBrowse (hg37/hg38).³⁰³

In families comprising parent-child trios with a sporadic affected individual, we evaluated variants based on all likely modes of inheritance; *de novo* mutation, recessive (homozygous and compound heterozygous), and X-linked hemizygous variants (in males). For cases in which the parents were known to be related, the proband was usually sequenced as a singleton and the data interrogated for homozygous changes. For all samples, data were analysed for variants in 57 genes recurrently mutated in craniosynostosis¹²⁷ and 1,313 genes curated as being mutated in developmental disorders.¹⁴⁵

Variant validation

Confirmation of variants was carried out by dideoxy sequencing or restriction digest of genomic PCR amplification products. Primer sequences and conditions are detailed in Supplementary Table 9.2. Amplification products were sequenced using the BigDye Terminator v3.1 cycle sequencer system (Applied Biosystems) and visualised using BioEdit Sequence Alignment Editor (Ibis Biosciences) and Mutation Surveyor Software (SoftGenetics).

Where a previously undescribed *de novo* variant was identified in a singleton sample (i.e. *HUWE1*), correct sample relationships of the trio were checked by demonstrating consistent inheritance of nine microsatellite loci (*D1S2826*, *D3S1311*, *D5S2027*, *D6S1610*, *D9S158*, *D10S548*, *D13S1265*, *D14S280* and *D18S474*), labelled with 6-FAM fluorescent tags.

Results

Overview of molecular findings

We used either exome sequencing ($n = 37$) or whole genome sequencing ($n = 3$) to seek a causative mutation in the two patient cohorts. In the cases from clinical geneticists ($n = 22$), interpretation was often assisted by sequencing samples from unaffected parents or affected first-degree relatives; 23 additional samples were sequenced in this group (Supplementary Table 9.1). For most cases from the diagnostic laboratory, samples from relatives were either unavailable or not consented for analysis of exome sequencing/whole genome sequencing (as described above) and, with two exceptions (total of three additional samples sequenced), these cases were analysed as singletons.

Mutations considered to be clinically significant (for the diagnosis of craniosynostosis and/or another genetic disorder) were identified in 15 of the 40 patients (37.5%), including two cases associated with putative novel disease genes that are still undergoing validation (Table 9.2). Significantly more positive diagnoses were found in syndromic (13/27) than non-syndromic (2/13) patients (one-tailed $p = 0.046$). The number of mutations identified in patients recruited via clinical geneticists (including the two duplicate ascertainties) was higher (11/24; 46%) compared with those recruited via the diagnostic laboratory (5/18; 28%), likely a consequence of more rigorous clinical selection and inclusion of sequencing data from a greater number of additional family members in these cases; however the difference was not significant (one-tailed $p = 0.19$). A positive diagnosis was obtained in a higher proportion of families in which multiple individuals were sequenced (6/14; 43%) than when singletons were sequenced (9/26; 35%), but this difference was also not significant. When the case solution rate was analysed in terms of total samples sequenced, sequencing of multiple individuals in a family appeared less cost-effective (six solved using a total of 40 exome sequencing/whole genome sequencing; an efficiency of 0.43 per exome/genome sequenced compared with singleton sequencing).

Table 9.2 summarises the 13 cases or families with mutation in a validated disease gene. Seven of the mutations identified (in *AHDC1*, *EFNB1*, *FBN1*, *IL11RA*, *KRAS*, *MSX2*, *STAT3*) were previously reported; in two instances (*CDC45* and *HUWE1*), the patients contributed to the first reported disease gene identification;^{258,304} and in four cases, the mutations are newly identified and help to extend the genotype-phenotype spectrum (mutations in *IL11RA*, *NTRK2*, *TWIST1*, *ZIC1*). The associated phenotypes are summarised in Table 9.2 and complete details are provided in Supplementary Table 9.1. Aside from the importance of a molecular diagnosis to end the diagnostic odyssey and to enable precise genetic counselling (with appropriate estimation of recurrence risk and testing of at-risk family members), in five families the diagnosis had unexpected, actionable consequences for immediate clinical management. Details of these latter cases are



Table 9.2. Summary details of patients with a positive genetic diagnosis.

Family	Sex	Gene	Mutation	Inheritance	Ref	CRS	Clinical features [†]
3	F	CDC45	c.[226A>C];[469C>T]	Compound heterozygous	304	BC	Short stature, thin eyebrows, anteriorly placed anus
4	M	IL11RA	c.[886C>T];[886C>T]	Homozygous	60	P	Exorbitism, intellectual disability, atopy, ?Crouzon syndrome
7	F	Novel [‡]		Homozygous		P	Midface hypoplasia, corneal ulceration, scoliosis, severe respiratory tract infections/bronchiectasis, mild–moderate developmental delay
9	M	IL11RA	c.[98dupC];[98dupC]	Homozygous	–	S, BC	Crouzonoid facies, mild developmental delay, dental anomalies, patent ductus arteriosus, atrial septal defect, umbilical hernia
10	M	MSX2	c.443C>T	Heterozygous (from affected mother)	305, 306	BC	Mild learning difficulties, short, broad thumbs, fifth finger clinodactyly, thick hair, squint and hydrocele
11	M	FBN1	c.8226+5G>A	Splice	307	S, M	Exorbitism, ligamentous laxity, recurrent inguinal hernia, tall stature, lens subluxation and mild aortic dilatation aged 8 years
14	M	HUWE1	c.328C>T	De novo	258	M	Facial dysmorphism, dental anomalies, pectus excavatum, scoliosis, long palms, Chiari malformation, moderate–severe intellectual disability
16	M	ZIC1	c.1101C>A	Suspected de novo [§]	–	S, BL	Microcephaly, asymmetric ventriculomegaly, possible abnormalities on MRI brain imaging
18	M	TWIST1	c.350A>T	De novo	–	M	Hypertelorism, wide anterior fontanelle, upper eyelid colobomas, pseudoptosis, dysplastic cupped ears, syndactyly of fingers, bilateral talipes, bilateral undescended testes, imperforate anus, hypertrichosis
21	F	KRAS	c.40G>A	De novo	308	P	Exorbitism, cloverleaf skull
23	F+M	Novel [‡]		Compound heterozygous		BC	Bilateral superior vena cava, dilated cardiomyopathy, rudimentary right thumb, duplex kidney, anterior anus, bilateral inguinal hernia, growth deficiency
24	F	AHDC1	c.2373_2374delTG	De novo	309	BC, M	Moderate developmental delay, hoarse cry

25	F	EFNB1	c.325C>T	p.(Arg109Cys)	Paternal	²⁰⁵	RC	Hypertelorism
29	M	STAT3	c.1915C>T	p.(Pro639Ser)	De novo	³¹⁰	P	Crouzonoid appearance, mild global developmental delay, necrotising pneumonia and bronchopleural fistula aged 3 years
37	F	NTRK2	c.1330G>T	p.(Gly444*)	Suspected de novo ⁵	–	LC	Facial asymmetry, progressive onset of aggressive outbursts, ritualised behaviours and language delay, hyperphagic obesity, streak ovaries

⁵See Supplementary Table 9.1 for detailed information. ⁶Gene identity confirmed by functional testing (manuscript submitted). ⁷Father's sample not available for analysis. ⁸Gene identity supported by similar case found on GeneMatcher; functional testing ongoing. CRS = Sutures fused in craniosynostosis; BC = Bicoronal, BL = Bilambdoid, LC = Left coronal, LL = Left lambdoid, M = Metopic, P = Pansynostosis, RC = Right coronal, RL = Right lambdoid, S = Sagittal.



provided as brief case reports to illustrate the range of diagnostic and management issues encountered; more complete descriptions are provided as Case Reports in the Supporting Information.

Case reports

Family 11: *FBN1* mutation

This boy (II-3 in Figure 9.1A) was initially diagnosed with Shprintzen-Goldberg syndrome (based on the combination of sagittal synostosis, blue sclerae, micrognathia, ligamentous laxity, bilateral recurrent inguinal hernia, tall stature and mildly abnormal aortic contour on echocardiography. However sequencing of *SKI*, in addition to *TGFBR1* and *TGFBR2*, did not reveal any mutations.³¹¹

Exome sequencing was performed on the proband only. Concomitantly, the referring clinician reported that the patient, now aged 8 years, had presented with subluxed lenses; together with the aortic findings, this suggested possible Marfan syndrome (MFS). Scrutiny of the exome sequencing data revealed two rare heterozygous variants in the *FBN1* (Fibrillin 1) gene, c.2615A>G, p.(Lys872Arg) and c.8226+5G>A. Dideoxy sequencing of parental samples showed that whereas the p.Lys872Arg substitution had been inherited from the unaffected father (not shown), the c.8226+5G>A variant had arisen *de novo* (Figure 9.1A). The c.8226+5G>A variant, which was re-confirmed in a diagnostic laboratory, has been identified previously in a patient with a progeroid variant of MFS;³⁰⁷ a different mutation of the same splice site (c.8226+1G>A) was shown to cause skipping of the upstream exon, introducing a frameshift and premature stop codon.³¹²

Confirmation of the molecular diagnosis of MFS has triggered a program of lifelong monitoring owing to the association with progressive aortic dilatation; aged 10 years, mild aortic root dilatation was observed (Z score = 3.02). Of note, craniosynostosis is an extremely rare, but previously recognised association of MFS.^{313,314}

Family 21: *KRAS* mutation

This girl presented neonatally with a cloverleaf skull appearance. 3D-CT revealed synostosis of multiple cranial sutures. There were no additional syndromic features and cardiac examination was normal. Raised intracranial pressure (ICP) was documented, requiring a posterior vault expansion with springs, performed at the age of 3 months, and insertion of a right parieto-occipital ventriculo peritoneal shunt.

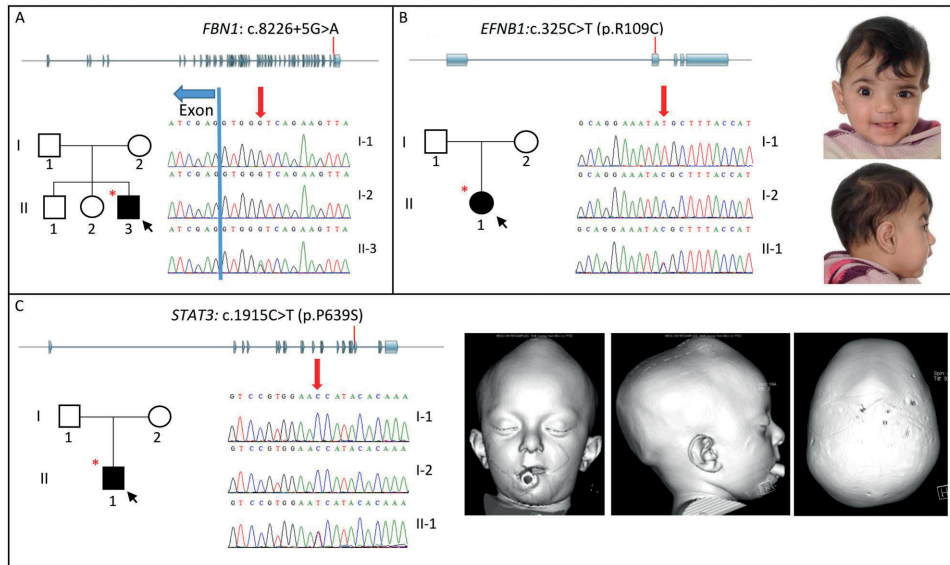


Figure 9.1. Family pedigrees, clinical photographs/3D-CT scans and sequencing traces of families with mutations identified in *FBN1* (A), *EFNB1* (B) and *STAT3* (C). Each panel shows the location of the mutation (red line) within the gene structure (exons in blue), family pedigree (affected individuals are in black, black arrow depicts the proband and individuals selected for exome sequence/whole genome sequence are indicated with a red asterisk), sequence traces of indicated individuals (red arrow indicates position of mutation) and clinical photographs (B) and 3D-CT scans (C) of affected individuals. Note facial asymmetry associated with right unicoronal synostosis in patient with *EFNB1* mutation (B); there is moderate hypertelorism, but the grooving of the nasal tip usually observed in craniofrontonasal syndrome is absent. In the patient with the *STAT3* mutation (C), images with soft tissue windows (left and centre) show exorbitism, midface hypoplasia and vertex bulge; image with bone windows (right) shows fusion of all sutures of the skull vault.

Whole genome sequencing of the parent-child trio identified a heterozygous *de novo* mutation (c.40G>A encoding p.Val14Ile) in *KRAS*, which has been reported previously in patients with Noonan syndrome.³⁰⁸ In the light of the exome results, an echocardiogram was performed, which was normal at almost 3 years of age, but she will continue cardiac surveillance. A coagulation screen has been normal but recommendations have been made to repeat it prior to any future surgery. Craniosynostosis is a rare but previously recognised complication of Noonan syndrome, being particularly associated with *KRAS* mutations.³¹⁵



Family 25: *EFNB1* mutation

The female proband (II-1 in Figure 9.1B), the first-born child to healthy parents with no relevant family history, was noted to have facial asymmetry at birth. Physical examination showed hypertelorism and ridging over the right coronal suture. A 3D-CT scan confirmed right coronal synostosis. She underwent a fronto-orbital advancement and remodelling (FOAR) procedure aged 15 months.

Exome sequencing identified a heterozygous mutation (c.325C>T, p.(Arg109Cys)) in the X-linked *EFNB1* (ephrin-B1) gene, previously reported in a patient with craniofrontonasal syndrome (CFNS).²⁰⁵ Dideoxy sequencing of the parents showed that the clinically unaffected father (I-1) was hemizygous for the same variant (Figure 9.1B). CFNS presents a paradoxical pattern of severity for an X-linked disorder, with heterozygous females more severely affected than hemizygous males, who can be non-penetrant.³¹⁶ The result predicts that 100% of female children of the father would be expected to exhibit CFNS and/or craniosynostosis, and the couple have elected to enrol in a programme of pre-implantation genetic diagnosis (PGD), selecting only male embryos for uterine transfer.

Family 29: *STAT3* mutation

This boy (II-1 in Figure 9.1C), presented to the craniofacial unit at 2 years of age with mild midfacial hypoplasia, a short nose with a convex ridge, exorbitism and mild global development delay; 3D-CT scan demonstrated fusion of all of the cranial sutures with convexity of the closed anterior fontanelle, prominent ventricles and crowded basal cisterns. At the age of 2 years 2 months, ophthalmological assessment showed bilateral papilledema and invasive monitoring demonstrated significantly raised ICP. He underwent a posterior vault expansion with insertion of springs at the age of 28 months.

Exome sequencing of the proband was performed. This identified a heterozygous c.1915C>T, p.(Pro639Ser) mutation in the SH2 domain encoded by *STAT3* (signal transducer and activator of transcription 3), which was previously reported in a case of hyper-IgE/Jobs syndrome (HIES).³¹¹ Dideoxy sequencing of the parents showed that the mutation had arisen *de novo* (Figure 9.1C).

Upon feedback of this finding it transpired that the proband had more recently presented at the age of 3 years 3 months with an upper respiratory tract infection, progressing to severe necrotising pneumonia with a pulmonary abscess and pneumatocele. He developed a pneumothorax and bronchopleural fistula; following two unsuccessful attempts at surgical resection, he required a right lower lobe segmentectomy. A large secundum atrial septal defect required patch closure at 5 years of age. Further immunological assessment demonstrated a markedly elevated total IgE of 3091 kU/L (normal range 0-52). He commenced prophylactic azithromycin and

itraconazole and is awaiting a suitably matched donor for stem cell transplantation. Bone mineral density assessment was normal but he takes multivitamin supplements including vitamin D and is under enhanced dental and skeletal surveillance.

Family 37: *NTRK2* mutation

The female proband presented with an asymmetric face at 12 months of age and left coronal synostosis was diagnosed on 3D-CT scan; there were no syndromic features. She underwent a FOAR procedure aged 17 months. On clinical follow-up at the age of 2 years 8 months she was noted to have episodes of temper tantrums and was exhibiting speech and language delay. By the age of 6 years she required a school statement indicating moderate learning difficulties. Exome sequencing identified a heterozygous nonsense mutation (c.1330G>T, p.(Gly444*)) in *NTRK2*, encoding neurotrophic tyrosine receptor kinase, type 2, with a predicted loss of the entire intracellular tyrosine kinase domain. The proband's mother did not carry the mutation and the father was not available for analysis. Dominant mutations of *NTRK2* have been described in association with hyperphagic obesity associated with developmental delay (OBHD), and functional studies have pointed to haploinsufficiency as the likely pathogenic mechanism of a previously identified p.Tyr722Cys substitution.^{317,318}

The discovery of the *NTRK2* mutation prompted a further endocrinology assessment at the age of 7 years 6 months. Her height was 135.2 cm (+2.04 SD), weight 46.2 kg (+3.19 SD), and body mass index 25.3 kg/m² (+3.1 SD), consistent with a diagnosis of OBHD. She was noted to have a long-standing history of hyperphagia. The oral glucose tolerance test was normal; streak ovaries and uterus were evident on ultrasound scan. Management implications have included referral to a clinical psychologist and dietician to address her eating behaviours, and regular monitoring for secondary complications including cardiovascular disease and diabetes.



Discussion

We present, to our knowledge, the first investigation of the added value provided by exome sequencing or whole genome sequencing in molecular genetic diagnosis of craniosynostosis, applied to two cohorts of patients (total of 40) identified as high-priority cases by clinical or laboratory geneticists following negative results from routine molecular genetic testing. We identified 13 mutations in 12 confirmed disease genes that we considered to be pathogenic. Seven of the particular DNA sequence changes found were previously reported, whereas an additional six are currently unique to the patients described here. The newly identified variants were considered pathogenic using evidence from population MAF data, predictive computational data and studies of aberrant function (either performed ourselves or published in the literature),

according to guidelines from the Association for Clinical Genetic Science.³¹⁹ In addition, we identified at least two likely novel disease-associated genes; further studies to corroborate these findings are ongoing, so details are not presented here. Including these latter cases, our overall success rate in identifying pathogenic mutations was 15/40 (37.5%), which is towards the upper end of the range usually quoted in exome sequencing/whole genome sequencing analysis of other diseases with a major genetic component.^{143,145,258} We used a mixed strategy of sequencing both singletons and multiple family members; the latter strategy was associated with a higher success rate per family, but the former with a 2.3-fold higher success rate per sample sequenced. Although trio sequencing is the favoured design in many other exome sequencing/whole genome sequencing studies because complete bioinformatic analysis of the data is more straightforward,^{143,145,258} singleton sequencing appears more cost-effective in a diagnostic setting.

Craniosynostosis comprises a very diverse group of disorders and its causes are correspondingly heterogeneous, with intrauterine foetal head constraint, reduced transduction of stretch forces from the growing brain owing to poor intrinsic growth, and polygenic background all likely to play substantial roles, in addition to monogenic causes.¹²⁷ Since a major motivation of this work was to use next generation sequencing to identify novel disease genes in craniosynostosis, we selected cases suspected to have a genetic cause, based on positive family history, presence of additional syndromic features or multiple suture fusions, and for which clinically guided genetic testing had been normal. Although this strategy was successful, with at least four newly recognised disease genes for craniosynostosis being identified as part of this study (*CDC45*³⁰⁴ and *HUWE1*,²⁵⁸ and two awaiting further corroboration), the major finding presented here is that next generation sequencing is very valuable for diagnosis of a long “tail” of rare genetic associations with craniosynostosis. All of these positive diagnoses have made a critical difference to genetic counselling, with some having broader management implications.

To understand why a genetic diagnosis in craniosynostosis may elude standard molecular diagnostic testing, we categorised each additional diagnosis in terms of the molecular genetic framework recently presented by Twigg and Wilkie.¹²⁷ These authors identified 57 genes as recurrently mutated in craniosynostosis, of which they categorised 20 as “core genes” (craniosynostosis present in >50% of patients with specific categories of mutation in that gene), whilst mutations in the remaining 37 genes were associated with craniosynostosis in only a minority of cases. The core genes could be further subdivided into six with mutations each accounting for over 0.5% of all craniosynostosis, and 14 more rarely mutated genes. Figure 9.2 summarises how the 13 identified mutations are classified according to this framework. While, not surprisingly,

the number of mutations identified, as a proportion of total genes in the category, rose progressively as the pathogenic hierarchy was ascended, there were multiple genes in each category. This includes two genes (*NTRK2*, *AHDC1*), for which we are unaware of any previous association with craniosynostosis; it is unclear whether the co-occurrence of the mutation and sentinel phenotype is causally linked (potentially through the adverse effect of the mutation on brain development),¹²⁷ or simply coincidental.

In the cases found to have mutations in the “core” genes, the question arises why these were not identified by testing within the routine diagnostic service. In the patients with *EFNB1* and *TWIST1* mutations, the diagnosis was missed because analysis of the relevant gene had not been requested by the clinician; either because of an unusually mild presentation (*EFNB1*, Figure 9.1B), or a severe, atypical presentation (*TWIST1*). Of the other core genes, homozygous mutations in *IL11RA*, first described in 2011,⁶⁰ are increasingly recognised, especially in consanguineous families from the Indian subcontinent, and clinical diagnostic testing has now been introduced in the UK (http://ukgtn.nhs.uk/uploads/tx_ukgtn/CRSDA_IL11RA_GD_Sept_14.pdf). Although a specific heterozygous mutation of *MSX2* encoding Pro148His was the first molecular lesion to be described in craniosynostosis in 1993,¹³⁰ only two further families (both segregating p.Pro148Leu) have subsequently been reported worldwide,^{305,306} and the family described here (also with p.Pro148Leu) is the first known in the UK. Finally, the *CDC45* patient contributed to the recent identification of mutations in this gene,³⁰⁴ and the patient with the *ZIC1* mutation extends the currently described genotype phenotype correlation,⁶⁵ being the first with a mutation in exon 2 and also the first with involvement of the sagittal suture instead of the originally described presentation with bilateral coronal synostosis.

As in any branch of genetic medicine, achieving a precise molecular diagnosis has immediate implications for genetic counselling, both in terms of recurrence risk and for targeted preventive measures. The common craniosynostosis syndromes all show dominant patterns of inheritance, so that when parents are clinically unaffected, empiric recurrence risks are low (around 5%).^{125,126} Our cohort illustrates two scenarios where providing the standard genetic advice would substantially underestimate recurrence risks. In family 25 (*EFNB1* mutation), the clinically unaffected father was shown to be hemizygous for the mutation originally identified in his daughter, indicating that the risk of CFNS in future female children is 100%. In family 3 (*CDC45* mutation), the autosomal recessive inheritance of this disorder raises the recurrence risk for children of the unaffected parents to 25%. Both findings have affected reproductive decision-making; one family is seeking PIGD, whereas in the other, the option not to have further children is being considered.



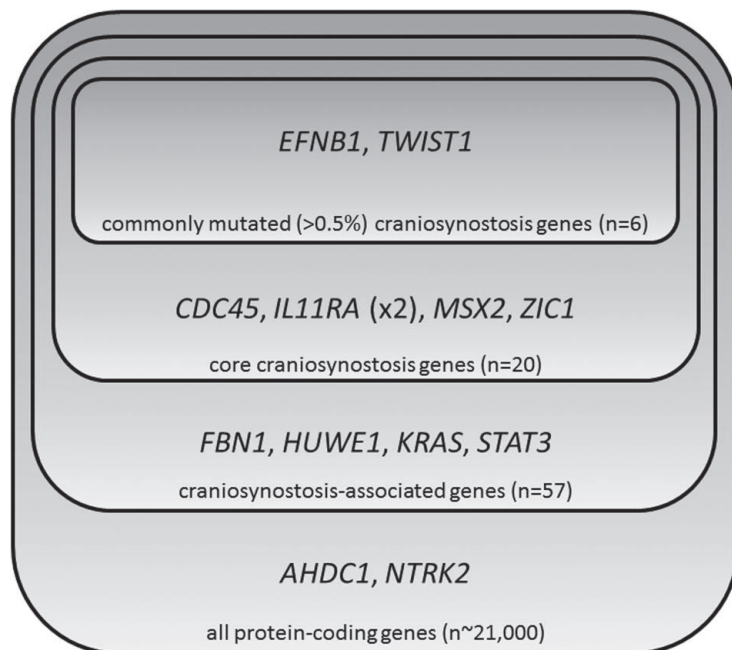


Figure 9.2. Identified mutations and their association within the classification of craniosynostosis-associated genes proposed by Twigg and Wilkie.¹²⁷

In addition to the genetic implications, in several cases (mutations in the *FBN1*, *KRAS*, *NTRK2* and *STAT3* genes), the molecular diagnosis has had immediate implications for clinical management, as described in the case reports, so genetic diagnosis was additionally important. Mutations in each of these genes are only infrequently associated with craniosynostosis; indeed, the presence of the craniosynostosis may have delayed correct diagnosis by laying a confusing trail. As a result of the molecular diagnosis, appropriate, potentially life-saving monitoring has been instigated. The high apparent rate of rare actionable mutations identified in complex craniosynostosis without an obvious diagnosis may reflect developmental pleiotropy of signalling in the cranial sutures, with multiple pathways, co-opted from more ancient uses in embryogenesis, implicated at different stages of suture development.¹²⁷

In summary, our findings illustrate the considerable added value provided by exome sequencing/whole genome sequencing to the precise diagnosis of patients with craniosynostosis suspected to have a genetic cause, but where routine testing has failed to elucidate this. As technologies improve, a strategic question in molecular diagnostics is whether it is preferable to extend panel tests to more genes, or whether to opt directly for exome sequencing/whole genome sequencing. Aside from the

most common disease-associated mutations, for which targeted testing currently remains cost-effective, we propose, based on the distribution of mutations identified (Figure 9.2), together with the substantial burden of actionable findings (case reports), a low threshold for implementing exome sequencing/whole genome sequencing. An additional benefit of this strategy is that it may identify new disease loci,^{258,304} enabling improved diagnostic and management strategies in the future.

Gene accession numbers

AHDC1 (NM_001029882), *CDC45* (NM_003504), *EFNB1* (NM_004429), *FBN1* (NM_000138), *HUWE1* (NM_031407), *IL11RA* (NM_001142784), *KRAS* (NM_033360), *MSX2* (NM_002449), *NTRK2* (NM_001007097), *TWIST1* (NM_000474), *STAT3* (NM_139276), *ZIC1* (NM_003412).

Web resources

MaxEntScan (http://genes.mit.edu/burgelab/maxent/Xmaxentscan_scoreseq.html)

NNSPLICE/BDGP (http://www.fruitfly.org/seq_tools/splice.html)

dbSNP (<http://www.ncbi.nlm.nih.gov/SNP/>)

ExAC (<http://exac.broadinstitute.org/>)

GeneMatcher (<https://genematcher.org/>)

ClinVAR (<http://www.ncbi.nlm.nih.gov/clinvar/>)

LOVD (<http://databases.lovd.nl/shared/genes/ZIC1>)

Supporting information

Case Reports

Family 11: *FBN1* mutation

This boy (II-3 in Figure 9.1A) is the third child of healthy parents from the Middle East, with no prior family history of craniosynostosis. He was born at 37 weeks' gestation (birth weight 2,830 g (-0.25 SD); length 52 cm (+1.76 SD); OFC 33.4 cm (-0.03 SD)) and needed neonatal care for treatment of amniotic fluid aspiration. A clinical genetics opinion was requested because of dysmorphic features, a large fontanelle, and stridor caused by left vocal cord palsy. A skeletal survey and ophthalmology assessment were normal, and no unifying diagnosis was made.

On further evaluation at the age of 10 months, he was noted to have a long narrow face, scaphocephaly, large (3 cm x 4 cm) anterior fontanelle, blue sclerae, vertical dimple on the chin and hypermobility of his small joints. His length was 75 cm (75th centile), and developmental milestones were normal. A skeletal survey was repeated, and craniofacial investigation confirmed sagittal synostosis. A total calvarial remodelling procedure was performed at the age of 3 years 10 months. A diagnosis of Shprintzen-Goldberg syndrome (SGS)[MIM: 182212] was proposed, based on the combination of



sagittal synostosis, exorbitism, downslanting palpebral fissures, blue sclerae, prominent nasal bridge, midface hypoplasia, micrognathia, syndactyly of the fingers, ligamentous laxity, recurrent inguinal hernia and tall stature. Targeted sequencing of the *SKI* gene,³¹¹ in addition to *TGFBR1* and *TGFBR2*, did not reveal any mutations. Echocardiography, when initially performed at 2 years 9 months, was normal; on repeat examination at the age of 4 years, requested because of the phenotypic overlap with Marfan syndrome (MFS)[MIM: 154700], the cardiologist considered that the shape of the aorta was mildly abnormal (although the dimensions were within normal limits), and he continued to be followed up.

We performed whole exome sequencing of the proband as a singleton; concomitantly, the referring clinician reported that the patient, by now aged 8 years, had recently presented with subluxed lenses, a mild scoliosis and a mildly dilated aorta. His modified Ghent score was 7/20, suggesting a possible diagnosis of Marfan syndrome. Scrutiny of the whole exome sequencing data revealed two rare heterozygous variants in the *FBN1* (Fibrillin 1) gene, c.2615A>G encoding p.Lys872Arg and the splice site variant c.8226+5G>A; Figure 9.1A). Dideoxy-sequencing of parental samples showed that whereas the p.Lys872Arg variant had been inherited from the unaffected father (not shown), the c.8226+5G>A had arisen *de novo* (Figure 9.1A). The c.8226+5G>A variant, which was re-confirmed in a diagnostic laboratory, has been identified previously in a patient with a progeroid variant of MFS;³⁰⁷ a different mutation of the same splice site (c.8226+1G>A) caused skipping of the associated exon, introducing a frameshift and premature stop codon.³¹²

Confirmation of the molecular diagnosis of MFS has triggered a program of lifelong monitoring owing to the association with progressive aortic dilatation; aged 10 years, he has mild aortic root dilatation (Z score = 3.02). Of note, craniosynostosis is an extremely rare, but previously recognized association of MFS.^{313,314}

Family 21: KRAS mutation

This girl, born to healthy unrelated parents, presented neonatally with a cloverleaf skull appearance. Computed tomography (CT) scanning revealed synostosis of both coronal sutures, the posterior part of the sagittal, both lambdoids and partial sphenoidal synostosis. There were no additional syndromic features and cardiac examination was normal. Due to CT and ophthalmological evidence of raised intracranial pressure (ICP), a posterior vault expansion with springs was performed at 3 months of age; the springs were removed 3 weeks later owing to infection. Due to persisting raised ICP, a right parieto-occipital ventriculo-peritoneal shunt was inserted aged 7 months which has required a number of revisions. She was suspected to have Crouzon syndrome but targeted sequencing of *FGFR2*, *FGFR3*, *TWIST1*, *TCF12* and *ERF* was normal, as was *TWIST1*

multiplex ligation-dependent probe amplification (MLPA) and array-CGH chromosome testing. Whole genome sequencing of the parent-child trio identified a heterozygous *de novo* mutation (c.40G>A encoding p.Val141Ile) in *KRAS*. This mutation has been reported previously in patients with Noonan syndrome.³⁰⁸ Although *KRAS* mutations only account for ~7% of the Noonan syndrome spectrum,³²⁰ craniosynostosis has been reported in 6 patients with *KRAS* mutations to date.^{308,315,320,321}

Prior to the exome result a diagnosis of Noonan syndrome had not been suspected as the patient did not have typical antenatal findings, facial features or significant cardiac or feeding abnormalities, and cloverleaf skull has not been reported previously in Noonan syndrome or related disorders. In light of the exome results the proband had an echocardiogram at almost 3 years of age; this was normal but she will continue cardiac surveillance. A coagulation screen has been normal but recommendations have been made to repeat it prior to any future surgery. Her development has been moderately delayed and her parents and community paediatricians have been given information about the spectrum of neurodevelopmental and behavioural phenotypes occurring in Noonan syndrome. In addition the finding of a *de novo* mutation accounting for her phenotype has facilitated accurate genetic counselling. A more complete account of this family will be published elsewhere.

Family 25: *EFNB1* mutation

The female proband (II-1 in Figure 9.1B), the first born child to healthy parents, with no relevant family history, was noted to have facial asymmetry at birth. Clinical assessment showed hypertelorism, orbital dystopia and ridging over the right coronal suture, but there were no additional dysmorphic features; in particular examination for signs of craniofrontonasal syndrome (CFNS [MIM: 304110] associated with grooving of the nasal tip, longitudinal splits of the finger- or toenails and cutaneous syndactyly) was negative (Figure 9.1B). A 3D-CT scan confirmed right coronal synostosis. She underwent a fronto-orbital advancement and remodelling (FOAR) procedure aged 15 months. On preoperative developmental assessment (Bayley Scales of Infant and Toddler Development, 3rd edition), composite scores ranged from 86 (language) to 100 (cognitive). Targeted sequencing of *FGFR2*, *FGFR3*, *TWIST1* and *TCF12* was normal.

Exome sequencing identified a heterozygous mutation (c.325C>T, p.(Arg109Cys)) in the X-linked *EFNB1* (ephrin-B1) gene, previously reported in a patient with CFNS.²⁰⁵ Dideoxy-sequencing of the parents showed that the clinically unaffected father (I-1) was hemizygous for the same variant (Figure 9.1B). CFNS presents a paradoxical pattern of severity for an X-linked disorder, with heterozygous females more severely affected than hemizygous males, who can be non-penetrant.³¹⁶ This phenomenon is accounted for by cellular interference.¹⁹² This result predicts that 100% of female children of the



father would be expected to exhibit CFNS and/or craniosynostosis, and the couple have elected to enrol in a programme of pre-implantation genetic diagnosis (PGD), selecting only male embryos for uterine transfer.

Family 29: *STAT3* mutation

This boy (II-3 in Figure 9.1C), the only child of unrelated parents of Sri Lankan ethnicity, presented to the craniofacial unit at 2 years of age. His parents had been concerned about his head shape at 6 months but he was not investigated until the age of 1 year 6 months. He had a history of recurrent ear infections and minor eczema behind his ears for which only emollients had been required. There was no relevant family history, except that his mother was recorded as having a large uterine fibroid. On examination he had mild midfacial hypoplasia, a short nose with a convex ridge, exorbitism and mild global development delay; 3D-CT scan demonstrated fusion of all of the cranial sutures with convexity of the closed anterior fontanelle, prominent ventricles and crowded basal cisterns. At the age of 2 years 2 months, ophthalmological assessment, which had previously been normal, showed progression to bilateral papilledema and ICP bolt insertion with 48 hour monitoring confirmed significantly raised ICP. A sleep study did not show any obstructive sleep apnoea. A clinical diagnosis of Crouzon syndrome [MIM: 123500] was suspected but targeted sequencing of *FGFR2*, *FGFR3*, *TWIST1*, *TCF12* and *ERF* was normal. He underwent a posterior vault expansion with insertion of springs at the age of 28 months, with spring removal 8 months later. Formal dental review at 5 years of age found established primary dentition with a class III incisor relationship due to midfacial hypoplasia.

Exome sequencing of the proband identified a heterozygous c.1915C>T, p.(Pro639Ser) mutation in the SH2 domain encoded by *STAT3* (signal transducer and activator of transcription 3), which was previously reported in a case of Hyper-IgE/Jobs syndrome (HIES) [MIM: 147060].³¹⁰ Dideoxy sequencing of the parents showed that the mutation had arisen *de novo* (Figure 9.1C). Non-immunological manifestations of HIES can include distinctive facial features, hyperextensibility of the joints, bone fractures and in rare cases, craniosynostosis.^{60,322,323}

Upon report of this finding to the referring clinician it transpired that the proband had presented to his local hospital at the age of 3 years 3 months with an upper respiratory infection, progressing to severe necrotising pneumonia associated with a pulmonary abscess and pneumatocele. Methicillin-resistant *Staphylococcus aureus* was initially isolated and subsequently he grew a *Stenotrophomonas maltophilia*. Despite intravenous antibiotics he developed a pneumothorax and bronchopleural fistula. Due to persistence of the fistula after two surgical resections, he was admitted to a specialist cardiothoracic unit at 3 years 7 months of age where he required a further thoracotomy

with right lower lobe segmentectomy, resection of the sixth rib and an intercostal muscle pedicle to reinforce the repaired area. He was found to have a large secundum atrial septal defect for which he had a patch closure at 5 years of age.

In view of the identification of the *STAT3* mutation a detailed immunology assessment was undertaken. Of note, he had suffered a perforating otitis media with purulent discharge from which *Staphylococcus aureus* was isolated, and a single skin abscess on his neck at 3 years of age. As a baby he had had some cradle cap but no wider rash. There had been no significant gastrointestinal symptoms, sinusitis, tonsillitis or fractures. He had a molluscum contagiosum skin infection which was mild. His total IgE was 3091 kU/L (normal range 0-52). Other salient findings were a good response to tetanus vaccination but a very poor response to pneumococcal conjugate vaccination, and relatively normal lymphocyte subsets but with raised levels of $\gamma\delta$ T cells indicating immune dysregulation. He was found to have EBV (IgE-VCA and IgM positive) and CMV (IgM negative, IgG positive) viremias, of which the former has become chronic. Varicella zoster serology was negative and eosinophil counts have been consistently normal. He commenced prophylactic azithromycin and itraconazole and is currently awaiting a suitably matched donor for stem cell transplantation. Bone mineral density assessment was normal but he takes multivitamin supplements including vitamin D.

HIES is a multisystem immunodeficiency syndrome associated with a clinical triad of recurrent staphylococcal skin boils, cyst-forming pneumonias and extremely elevated IgE, usually manifesting in the first years of life. Typically it presents with a pustular rash in the new-born period which evolves into an eczematous dermatitis. Other features include mucocutaneous candidiasis, osteopenia with recurrent fractures, scoliosis, craniosynostosis which is said rarely to require surgery,³²⁴⁻³²⁶ and failure to exfoliate the primary dentition. Vascular abnormalities include tortuosity of medium sized arteries and aneurysms. Gastro-intestinal features include gastro-oesophageal reflux disease, oesophageal dysmotility, and colonic diverticulae and perforations. There is also a predisposition to lymphoma. Management is directed at prevention and early aggressive treatment of pneumonia, abscesses and other infections using antibiotics, antifungal agents and skin antiseptics, treatment of eczema and optimisation of calcium and vitamin D intake. Surveillance for chest infections, scoliosis and retained primary dentition is indicated. A small number of patients have had stem cell transplantation with marked reduction in infections and significantly improved quality of life. Current recommendations in children with HIES associated with serious respiratory complications are to proceed to stem cell transplant once the child is clinically stabilised if there is a well matched donor available.



The proband had an atypical neonatal course and presented with a Crouzon-like facial appearance and pansynostosis prior to developing the more characteristic clinical features that might have pointed to a diagnosis of HIES. Demonstration of a *de novo* *STAT3* mutation accelerated referral for specialist immunological assessment and management allowing relatively early optimisation of treatment. As a result of the diagnosis closer dental and skeletal surveillance has been arranged. The findings have facilitated genetic counselling confirming that the parents have just a low germ-line mosaic recurrence risk for future pregnancies with prenatal testing available should they wish.

Family 37: *NTRK2* mutation

The female proband was the first born child to unrelated parents, with no relevant family history. Her birth weight was 3.2 kg (-0.57 SD) and she had a normal neonatal course. She presented with an asymmetric face at 12 months of age and left coronal synostosis was diagnosed on 3D-CT scan; there were no syndromic features and the head circumference at the age of 15 months was 47.0 cm (-0.28 SD). She underwent a FOAR procedure aged 17 months and has also required a strabismus correction. Formal testing at 17 months indicated low average attainment (composite scores on sub-tests 85-88, percentile rank 16-21).³²⁷ Targeted sequencing of *FGFR2*, *FGFR3*, *TWIST1* and *TCF12*, MLPA of *TWIST1*, karyotype and array CGH were all normal.

By the age of 2 years 8 months she was noted to have episodes of temper tantrums and was exhibiting speech and language delay. On formal assessment at the age of 3 years 8 months, her standard scores for understanding and speaking language were 82 and 97, respectively.³²⁸ Concerns about aggressive outbursts, ritualised behaviours, and language delay persisted at the age of 6 years and she required a school statement indicating moderate learning difficulties. In addition she was tall for her age with disproportionate weight gain, at the age of 6 years 8 months her height was 127.2 cm (+1.56 SD) and weight was 38.6 kg (+3.08 SD). Exome sequencing identified a heterozygous nonsense mutation (c.1330G>T, p.(Gly444*)) in *NTRK2*, encoding neurotrophic tyrosine receptor kinase, type 2, with a predicted loss of the intracellular tyrosine kinase domain. The proband's mother did not carry the mutation and the father was not available for analysis. Dominant mutations of *NTRK2* have previously been described in association with hyperphagic obesity associated with developmental delay (OBHD) [MIM: 613886].³¹⁷

The discovery of the *NTRK2* mutation prompted a further endocrinology assessment at the age of 7 years 6 months. Her height was 135.2 cm (+2.04 SD), weight 46.2 kg (+3.19 SD), and body mass index 25.3 kg/m² (+3.1 SD). She was noted to have a long-standing history of hyperphagia. The oral glucose tolerance test was normal; streak ovaries and

uterus were evident on ultrasound scan. Management implications have included referral to a clinical psychologist and dietician to address her eating behaviours, and regular monitoring for secondary complications including cardiovascular disease and diabetes.³²²





Chapter 10

General discussion

The merits of this thesis

The aim of this thesis was to obtain more insight into the genetic alterations that cause congenital craniofacial malformations, to improve genetic counselling and to gain further knowledge about the development of the head and face. Novel mutations have been identified in genes known to be associated with craniofacial malformations. Also, new craniofacial genes have been identified. Finally diagnostics have been improved by new genetic techniques, facilitating genetic counselling.

New mutations have been identified in *FGFR2*. Expanding the analysis of *FGFR2* to all coding exons and exon/intron junctions has demonstrated once again that pathogenic mutations predominantly occur in the well-conserved functional regions of *FGFR2*.³²⁹ Also, we have shown that apparently synonymous substitutions in *FGFR2* can affect splicing and result in Crouzon syndrome.⁵⁸ Therefore, we recommend that synonymous substitutions and variants outside the canonical AG/GT splice acceptor/donor sequences are carefully evaluated as to whether they may have an effect on RNA splicing and therefore are pathogenic.⁵⁸

Using next generation sequencing, we have identified novel genetic causes of craniofacial malformations. One of these genes is *TCF12*.⁵⁹ Presumably, the TCF12/TWIST1 heterodimer protein complex plays an important role in coronal suture development by specifying the neural crest and cephalic mesoderm boundary,^{231,232} and/or inhibiting osteogenic differentiation via actions on RUNX2,²³³ bone morphogenetic protein²³⁴ and/or fibroblast growth factor receptor signalling.²²⁸ Therefore, if a patient has isolated coronal suture synostosis and gene-specific testing of *FGFR3* and *TWIST1* is negative, *TCF12* should be checked.

We identified deletions in *TCF12* in 4 of 108 (3.7%) individuals with coronal suture synostosis and previously negative genetic testing.¹⁴⁶ Hence, screening for larger rearrangements in *TCF12* seems essential if *TCF12*-related craniosynostosis is suspected.

We also identified mutations in *ZIC1* in patients with coronal suture synostosis.⁶⁵ Learning disabilities are frequently seen in these patients. The function of *ZIC1* has been studied in the *Xenopus* by injecting several truncated constructs, leading to disrupted *en-2* expression. Using *in situ* hybridisation, a transient zone of *Zic1* expression was identified in the supraorbital region that overlaps that of *En1*. From this region, cells migrate and populate the coronal suture,^{24,30,37} indicating an early instructive role for *Zic1* in the supraorbital regulatory centre. Combining these results, it seems likely that the coronal synostosis phenotype is attributable to alteration of EN1 expression in the supraorbital regulatory centre. Hence, if coronal suture synostosis in combination with learning disabilities is seen, *ZIC1* should be tested.



Additionally, compound heterozygous point mutations were identified in *TXNL4A* in patients with Burn-McKeown syndrome (BMKS).³³⁰ Reduced expression of *TXNL4A* is assumed to cause reduced tri-snRNP assembly, hypothetically influencing splicing of a specific subset of pre-mRNAs.⁶¹ Furthermore, homozygous 34 bp deletions in *TXNL4A* were identified in patients with (isolated) choanal atresia. Choanal atresia is a key feature of BMKS. This demonstrates the importance of screening for mutations in *TXNL4A* in patients with (mild) clinical features of BMKS.

The last part of this thesis has focused on the use of next generation sequencing as a diagnostic tool in patient cohorts. First, we tested 40 patients with whole exome or whole genome sequencing. In 15 out of 40 patients (37.5%) a mutation was identified; 13 mutations in confirmed disease genes and at least two in novel disease-associated genes.

Many of the pathogenic mutations identified were in genes rarely associated with craniosynostosis. In some of these cases, achieving a precise molecular diagnosis has had immediate implications for genetic counselling and for clinical management.

Since phenotypes are getting less specific and single-gene tests are therefore getting less efficient, it seems worthwhile to apply next generation sequencing more frequently. An additional benefit of this strategy is the potential identification of new disease loci.

Barriers of this thesis

Whole genome sequencing by Complete Genomics

We have used Complete Genomics' whole genome sequencing to search for pathogenic mutations in the genomes of patients with craniosynostosis. The strengths and weaknesses of this technique can be assessed by looking at both practical and technical parameters.

Practical parameters include the required amount of DNA, the sequencing costs and the running time.³³¹ When the samples were shipped, between 2012 and 2015, Complete Genomics required a large amount of DNA (at least 5 µg of DNA was required and more than 10 µg was strongly recommended). At the time of writing this thesis, Complete Genomics was a service provider and DNA was sent to the US to be sequenced in an external core facility. Therefore, the costs per genome were relatively high. However, there were no acquisition costs associated with the sequencing machine, all other materials and equipment. The turnaround time from shipping to receiving a full annotated genome was 3 months.

Technological parameters include coverage of the genome, distribution of reads across different genomic regions, and SNV calling sensitivity and specificity. Several studies have compared these parameters between different sequencing technologies.

In one study Complete Genomics shows a high coverage distribution (<2% of bases not covered).³³¹ However, another study found that Illumina covers more bases.³³² The coverage at genomic positions corresponding to SNPs on the SNP array is on average 40x and therefore lower than the overall average.³³¹ Because Complete Genomics requires a higher average coverage in order to cover a similar fraction of the genome, we used Complete Genomics 80x sequencing in our samples (hypothetically 40x paternal and 40x maternal allele). Also, a considerable degree of sample-to-sample variation in coverage distribution is observed, which is not seen by other platforms.³³¹ Complete Genomics performs well in GC rich regions (the least GC bias, leading to good coverage of CpG islands), but in GC poor regions Complete Genomics performs worst, and simple repeat regions are covered worst in comparison to other platforms.³³¹ Comparing Complete Genomics with Illumina, it seems that Complete Genomics is slightly less sensitive, but does have fewer false positive calls.³³² Nonetheless, both methods missed variants that were clearly called by the other technology,³³² and each platform detected a large quantity of indels missed by the other.³³²

In summary, every sequencing platform has its strengths and weaknesses and each platform is likely to miss some true functional rare variants.³³³ Therefore, several studies have suggested to sequence genomes with two platforms if budget permits³³¹⁻³³³ until these weaknesses are solved.

Incidental findings

While analysing the whole genome or exome, there is an inevitable risk of discovering so-called “incidental findings”. Incidental findings are secondary genetic findings that are unrelated to the indication for obtaining the genetic test, but they may cause another disease. For example, the identification of a variant in a breast cancer gene like *BRCA1*, while trying to identify the genetic cause of a craniofacial malformation. All incidental findings combined are called the “incidentalome.”³³⁴

The question arises what to do with these incidental findings. Should they be communicated to a patient or shouldn't they? Compromising between the ethical principles of “duty to warn” versus “do no harm”. Especially since the findings can be irrelevant in childhood, such as findings concerning adult-onset diseases or information about carrier status. Also, one might state that the child's autonomy should be respected and a child shouldn't be burdened by these findings. Especially since only a few incidental findings are actionable, one recent study showed that 23 out of 1,000 exomes (~2%) carried actionable pathogenic SNPs.³³⁵

For years, guidelines didn't exist on how to communicate incidental findings. Returning of incidental findings differed per country, city and even per department. In our study design, incidental findings were not communicated.



Fortunately, the ACMG has released recommendations for returning incidental findings,³³⁶ and currently patients who participate in whole exome sequencing can give their preference on the reporting of their incidental findings.

Genetic discrimination

One of the drawbacks of participating in genetic research is concern about genetic discrimination, i.e. being treated differently based on genetic background, especially in cases of social necessities like healthcare, insurance, housing and employment.³³⁷

In Europe, genetic discrimination is prohibited by the Convention on Biomedicine (1997), the Charter of Fundamental Rights of the European Union (2000), and the national legislation of many individual countries.³³⁷ In the Netherlands the Act on Medical Examinations was approved in 1998.³³⁸ This act protects individuals who want to obtain a civil employment contract, a pension, life insurance or disability insurance, by stating that below predefined sums no questions may be asked about untreatable hereditary diseases or about the results of genetic tests for such diseases in the applicant and his/her relatives.³³⁹ Insurance companies are legally obliged to disregard available genetic test results for insurance below predefined sums, except in cases of manifest disease.³³⁹ Applicants in turn are legally obliged to report any manifest disease.³³⁹

Despite this legislation, individual cases of genetic discrimination have been described. A systematic review on genetic discrimination in the life insurance sector shows that between 1991 and 2012 33 studies were performed concerning genetic discrimination.³³⁷ Six of these studies took place in Europe, two of which were in the Netherlands.³³⁷ These two studies addressed genetic screening on familial hypercholesterolemia³⁴⁰ and hypertrophic cardiomyopathy respectively.³³⁹ The latter suggested that the insurance companies' risk assessment of hypertrophic cardiomyopathy mutation carriers is most often correct (95%). However, 5% of mutation carriers do encounter potentially unjustified problems at obtaining insurance.³³⁹

Overall one might conclude that genetic discrimination exists. However, research on genetic discrimination in the context of omics studies remains absent in literature.³³⁷ But it might be stated that the application of the Act on Medical Examination should be monitored, and the public should be informed and educated about the existing legislation when participating in genetic testing.^{337,339}

Recent developments in craniofacial genetics

Craniosynostosis

According to Twigg *et al.* in 2015,¹²⁷ 57 human genes have been described for which there is evidence that mutations are causally related to craniosynostosis (based on at least two affected individuals with congruent phenotypes). These genes were divided into two broad groups: 1. occurrence of craniosynostosis in >50% of independent mutations ("core genes", 20 in total); 2. occurrence of craniosynostosis in only a minority of cases with the mutation.¹²⁷ The latter group includes many genes that represent perturbations in osteogenesis rather than in the biology of cranial suture development per se (such as filaminopathy, hypophosphatasia, mucopolysaccharidoses, osteosclerosis, and pycnodysostosis).¹²⁷ During the following years, a further 32 genes were identified that cause craniosynostosis (16 in multiple patients and 16 in single patients). An overview of these genes is given in Tables 10.1 and 10.2. Most of the genes are involved in previously described pathways: Sonic hedgehog pathway, WNT-signalling, NOTCH/EPH pathway, the RAS/MAPK pathway, Indian hedgehog, Retinoic acid and/or the STAT3 pathway.

However, more and more mutations are being identified in genes that are involved in brain development or that are shown to be mutated in intellectual disability and/or behavioural anomalies. In these cases, craniosynostosis does not occur in all affected individuals.

Mutations have also been identified in genes that were previously shown to be pathogenic in mouse models (*FUZ*, *BCL11B*) and in *SMAD6* (an inhibitor of BMP), with striking incomplete penetrance.³⁴¹ Genotypes of a common variant near *BMP2* explain nearly all the phenotypic variation in these kindreds.³⁴¹ This interaction of rare and common variants has implications for variant filtering using frequencies.

The phenotypes associated with these newly identified mutations are less specific and some are very rare. This, in combination with the increasing number of potential genetic causes, indicates the importance of next generation sequencing.

Craniofacial clefting

As craniofacial clefts are very rare and aetiologically heterogeneous³⁴² only a subset of genetic causes are known, varying from homeobox gene mutations to mutations in genes involved in vesicle trafficking. Strikingly, an overlap is seen with the genetic causes of craniosynostosis. First *EFNB1* was identified to cause CFNS, a phenotype comprising of both craniosynostosis and frontonasal dysplasia.⁶³ Recently, localized *TWIST1* mutations were shown to cause a severe form of frontonasal dysplasia (Sweeney-Cox syndrome).¹⁴² In contrast, *TWIST1* haploinsufficiency is known to cause Saethre-Chotzen syndrome.^{138,139} Both *EFNB1* and *TWIST1* are involved in the NOTCH/EPH pathway. Although few genetic causes of craniofacial clefting in humans are



known, several mouse models have been described that suffer from severe craniofacial clefting. One of these is the *brachyrrhine* mouse, which exhibits frontonasal dysplasia and renal hypoplasia.³⁴³ Linkage analysis has mapped the mutation in the *brachyrrhine* mouse to a critical region that contains only one gene, *Six2*.³⁴³ Direct sequencing of the gene has not identified any mutations,³⁴³ but expression of the gene was reduced.³⁴³ Therefore, it is likely that a regulatory sequence upstream or downstream of the *Six2* gene is involved.³⁴³ The identification of a patient with a deletion of the *SIX2* gene and its surrounding noncoding DNA, exhibiting frontonasal dysplasia³⁴⁴ is further evidence that regulatory elements may play a key role in the occurrence of craniofacial clefting, and underlining the importance of whole genome sequencing in these disorders (see table 10.3 for an overview).

Facial dysostosis

Recently, Terrazas *et al.* gave an overview of the aetiology of the most well-known facial dysostoses (Treacher Collins syndrome, Acrofacial Dysostosis-Cincinnati type, Mandibulofacial Dysostosis with Microcephaly, Nager, and Miller syndrome).³⁴⁵ Many other subtypes are known (as reviewed by Wieczorek *et al.* in 2013).¹¹ Since 2013, new genetic causes have been identified, and some subtypes have been shown to be allelic (see table 10.4 for an overview). However, the genetic cause of several subtypes remains unknown. Lehalle *et al.* mention that many facial dysostoses are caused by spliceosomal defects (hence called spliceosomopathies), whilst others are caused by ribosomal dysfunction (ribosomopathies).²⁸⁹ It would be of great interest to further screen the genes of these pathways.

Next generation sequencing

For years dideoxy sequencing was the gold standard for genetic testing. More recently, whole exome sequencing has been adopted as a standard approach within genetic research. Clinical implementation, however, needs robust data and high quality,³⁴⁶ therefore questions arise about which method should be used in the clinic.

In particularly, the reduced sensitivity of whole exome sequencing at certain regions (especially GC-rich),³⁴⁷ is a major concern.³⁴⁸ The quality of the data depends on the sequencing platform used, as well as on the sensitivity of the bioinformatic pipeline.³⁴⁹ This has been demonstrated by Gilissen *et al.* in 2014,¹⁴³ who reanalysed whole exome sequencing parent-patient trios that had been described by De Ligt *et al.* in 2012.³⁵⁰ Using more sensitive analysis pipelines they revealed many additional *de novo* variants.¹⁴³

To achieve better capture performance, clinical laboratories have developed custom gene panels.³⁴⁶ Recently published studies show that these gene panels are generally sequenced much deeper than whole exome sequencing and whole genome

sequencing.³⁴⁶ As gene-panels are hypothesis-driven, they can be designed with care to provide consistent coverage of the targets if the number of candidates is limited. However, as new disease genes are being discovered at a fast pace, gene panels need to be updated frequently.³⁵¹

The major advantage of whole genome sequencing is the possibility identifying non-coding pathogenic variations. Whole genome sequencing has the potential to detect all types of genomic variants, including structural variants.¹⁴³ whole genome sequencing is also expected to be more powerful for detecting potential disease-causing mutations within whole exome sequencing regions³⁵² as it has a more even coverage, no strand bias, and a higher proportion of transcripts covered completely.^{143,346,349} However, a comparison of two whole genome sequencing platforms for 56 genes concluded that current whole genome sequencing platforms are unable to cover 10-19% of genes to acceptable standards for SNV discovery.^{346,353} A comparison of whole exome sequencing and whole genome sequencing for variant calling showed that both whole exome sequencing as well as whole genome sequencing were unable to identify all variants.^{346,354} Moreover, whole exome sequencing is still considerably cheaper than whole genome sequencing and analysis time still seriously limits implementation of whole genome sequencing in routine diagnostics.³⁴⁹ Currently, little benefit can be expected from the identification of deep-intronic *de novo* variants since these are still very difficult to interpret³⁵¹ and validate.¹⁴³ Whole exome sequencing is unlikely to miss confident calls made by whole genome sequencing, provided that the position is covered by whole exome sequencing.³⁴⁹ For these reasons, whole exome sequencing remains the preferred choice for diagnostic laboratories for now. However, with sequencing costs further declining and techniques and analysis improving, whole genome sequencing has the potential to entirely replace whole exome sequencing.³⁴⁸

Future directions of craniofacial genetics

Multiplex ligation-dependent probe amplification (MLPA)

Using next generation sequencing, we have identified gross rearrangements in *TCF12* causing *TCF12*-related craniosynostosis. Previous to this, dideoxy sequencing has been used to identify mutations in *TCF12*. Gross rearrangements, however, cannot be identified by this sequence technology, but they can be identified using MLPA. Instead of preparing an in-house MLPA kit, negotiation with MRC Holland (MRC Holland BV, Amsterdam, NL) has been undertaken to develop an MLPA kit for *TCF12* including the genes *ZIC1* and *ERF*. In this way a certified test can be performed in a diagnostic setting both in a prospective and a retrospective way.



Table 10.1. Genes recently associated with craniosynostosis. Incidence in >1 patient with craniosynostosis.

Gene	Location	Clinical disorder	OMIM gene #	Major phenotypic features	Inheritance pattern	Prevalence of craniosynostosis with mutation	First reference
1	3q13.1-q13.2	Opitz trigonocephaly C syndrome	606037	Trigonocephaly, unusual facies, wide alveolar ridges, multiple oral frenula, limb defects, visceral anomalies, redundant skin, PMR, hypotonia	AR (bi-allelic)	1 balanced translocation that disrupted CD96 and 1 missense mutation	355,356
2	17p13.3	3C syndrome like phenotype	603527	ID, short stature, craniofacial and ectodermal anomalies, scaphocephaly	AR	2 families with deviated skull shape with or without craniosynostosis	357
3	16q12.2		610966	Multiple malformation syndrome: postnatal growth retardation, microcephaly, severe psychomotor delay, functional brain deficits, characteristic facial dysmorphisms (craniosynostosis, microcephaly, macrotia, cataract, cryptorchidism)	AR	1 patient with craniosynostosis, others have microcephaly or an asymmetrical skull	358
4	19q13.33		610622	Single bone pair encases the forebrain in mice. Trigonocephaly and plagiocephaly in human.	AR	2 monozygotic twins	359
5		Kabuki syndrome/ Aukline syndrome	600712	PMR, ADD, dolichocephaly, ridged metopic suture, long face, long palpebral fissures, ptosis, broad or sparse lateral eyebrows, underdeveloped ear helices, wide nasal bridge with dip at the nasal tip, open downturned mouth, high palate, prominent midline tongue groove, missing molars, and excess nuchal skin, cryptorchidism, skeletal anomalies, cardiac defects, hypotonia, hyporeflexia, and high pain tolerance	AD	3 patients	360

6	<i>IFT140</i>	16p13.3	Opitz trigonocephaly C syndrome	614620	Trigonocephaly, unusual facies, wide alveolar ridges, multiple oral frenula, limb defects, visceral anomalies, redundant skin, PMR, hypotonia	AR (bi-allelic)	3 patients: 1 trigono, 2 scaphocephaly	361,362
7	<i>IGF1R</i>	15q26.3		147370	Isolated sagittal or coronal craniosynostosis	AD	3 patients (associated with)	363
8	<i>MASP1</i>	3q27.3	3MC syndrome 1	600521	Blepharophimosis, blepharoptosis, epicanthus inversus, developmental defect of the anterior segment of the eye leading to corneal stromal opacities, limitation of upward gaze, cleft lip/palate, minor skeletal abnormalities	AR	At least 2 with mutation in <i>MASP1</i>	364,365
9	<i>NF1A</i>	1p31.3		600727	Cloverleaf skull, metopic synostosis, macrocephaly, renal and central nervous system malformations, cleft palate, severe ocular anomalies, upslanting palpebral fissures, cutis laxa, developmental delay, seizures, round face with prominent nose, anteverted nares, microretrognathia, half-opened mouth, short neck, hand/foot malformations, abnormal external genitalia	AD	4 patients with a microdeletion	366-368
10	<i>P4HB</i>	17q25.3	Cole-Carpenter syndrome	176790	Osteogenesis imperfecta with craniosynostosis	AD	2 patients	369
11	<i>RSPRY1</i>	16q13	Spondyloepimetaphyseal dysplasia, Faden-Alkuraya type	616585	Progressive Spondyloepimetaphyseal dysplasia, short stature, facial dysmorphism, short fourth metatarsals, ID, craniosynostosis	AR	4 Saudi sibs, but not in Peruvian patient	370
12	<i>SCN4A</i>	17q23.3	Congenital myopathy with "corona" fibres, selective muscle atrophy, and craniosynostosis	603967	Lower facial weakness, highly arched palate, metopic and sagittal suture synostosis, axial hypotonia, proximal muscle weakness, mild scoliosis, and unusual muscle biopsy: myofibres with internalized nuclei, myofibrillar disarray, and "corona" fibres	AR	2 brothers	371
13	<i>SMAD6</i> /14 + <i>BMP2</i>	15q22.31	Susceptibility to craniosynostosis	602931	Nonsyndromic midline craniosynostosis	AD	frequent	341
		20p12.3	Susceptibility to craniosynostosis	112261	Nonsyndromic midline craniosynostosis			341



Table 10.1. (continued)

	Gene	Location	Clinical disorder	OMIM gene #	Major phenotypic features	Inheritance pattern	Prevalence of craniosynostosis with mutation	First reference
15	<i>SFO</i>	7q32.1	Curry-Jones syndrome	601500	Coronal craniosynostosis, cutaneous syndactyly, bilateral preaxial polydactyly of the feet, streaky skin lesions, ectopic hair growth, abnormalities of brain development, coloboma and/or microphthalmia, intestinal malrotation and/or obstruction, mild ID	Mosaic mutations	multiple patients	²⁹⁶
16	<i>SOX6</i>	11p15.2		607257	Brachycephaly, proptosis, midfacial hypoplasia, low set ears, lambdoid suture synostosis, sagittal suture synostosis, gaping anterior fontanelle	AD	1 balanced translocation; 1 SNP	³⁷²

AD = Autosomal dominant, ADD = Attention deficit disorder, AR = Autosomal recessive, CFNS = Craniofrontonasal syndrome, ID = Intellectual disability, PMR = Psychomotor retardation, SNP = Single nucleotide polymorphism, XLD = X-linked dominant.

Table 10.2. Genes recently associated with craniosynostosis. Incidence in 1 patient with craniosynostosis.

Gene	Location	Clinical disorder	OMIM gene #	Major phenotypic features	Inheritance pattern	Prevalence of craniosynostosis with mutation	First reference	
1	ABCC9	12p12.1	Cantu syndrome	601439	congenital hypertrichosis, neonatal macrosomia, macrocephaly, coarse facial features, distinct osteochondrodysplasia: thickened calvarium, narrow thorax, wide ribs, flattened or ovoid vertebral bodies, coxa valga, osteopenia, enlarged medullary canals, and metaphyseal widening of long bones. Cardiac manifestations: cardiomegaly, patent ductus arteriosus, ventricular hypertrophy, pulmonary hypertension, and pericardial effusions. Motor and speech delay.	AD	1 patient	373
2	AHDC1	1p36.1–p35.3	Xia-Gibbs syndrome	615790	ID, failure to thrive hypotonia, absent expressive language, OSA, bicoronal suture and metopic suture synostosis, moderate developmental delay, hoarse cry	AD	1 patient with CSO	4
3	BCL11B	14q32.2		606558	Coronal suture synostosis and increased intracranial pressure	AD	1 patient	###
4	CHST3	10q22.1	Larsen	603799	Short long bones, bilateral clubfeet, micrognathia, scaphocephaly, genu valga, internal rotation of the hips, subluxed hips and elbows, coronal clefting of several vertebral bodies in the lumbar spine and prominent angulation of the lumbar sacral junction, phalangeal bones appeared slightly thickened and spade-like, prominent anterior slip of C2 on C3, lumbar lordosis, mild hypertelorism, slightly prominent metopic ridge, mild temporal hollowing, an anterior placed bregma and a pinched appearance of the upper ear helix	AR	1 patient	374
5	CRTAP	3p22.3	Cole-Carpenter syndrome	605497	Osteogenesis imperfecta with craniosynostosis	AR	1 patient with CSO, others with OI	375
6	GLIS3	9p24.2		610192	Neonatal diabetes, thyroid disease, hepatic and renal disease with liver dysfunction, renal cysts, craniosynostosis, hiatus hernia, atrial septal defect, splenic cyst, choanal atresia, sensorineural deafness, exocrine pancreatic insufficiency	AR (bi-allelic)	1 patient	376



Table 10.2. (continued)

Gene	Location	Clinical disorder	OMIM gene #	Major phenotypic features	Inheritance pattern	Prevalence of craniosynostosis with mutation	First reference
7	IFT43	14q24.3	Sensenbrenner syndrome	614068	Sensenbrenner syndrome: skeletal abnormalities (craniosynostosis, narrow rib cage, short limbs, brachydactyly), ectodermal defects, renal failure, hepatic fibrosis, heart defects and retinitis pigmentosa	AR	1 patient 377
8	KANSL1	17q21.31	Chromosome 17q21.31 deletion syndrome/ Koolen-de Vries syndrome/ KANSL1 haploinsufficiency syndrome	612452	highly distinctive facial features, moderate-to-severe intellectual disability, hypotonia and friendly behaviour, epilepsy, heart defects, kidney anomalies, sagittal suture synostosis, macrocephaly, microcephaly	AD	1 patient CSO 378
9	MED13L	12q24.21	MED13L haploinsufficiency syndrome	608771	ID, developmental delay, congenital heart defects, dysmorphic features, 1x craniosynostosis, and microcephaly and macrocephaly	AD	1 patient CSO 379
10	NTRK2	9q21.33	Hyperphagic obesity associated with developmental delay	600456	Hyperphagia, streak ovaries and uterus, coronal suture synostosis, temper tantrums, speech and language delay	AD	1 patient CSO 4
11	OSTEM1	6q21	Osteopetrosis	607649	Osteopetrosis, craniosynostosis, Chiari I, progressive irritability, abnormal movements, progressive visual loss, global developmental delay, lower motor neuron facial palsy, hydrocephalus	AR	1 patient triad of OP, CSO and Chiari 380
12	PPP1CB	2p23.2	PPP1CB-related Noonan syndrome with loose anagen hair	600590	Sparse, thin, and slow growing hair, relative or absolute macrocephaly, prominent forehead, dolichocephaly, ocular hypertelorism, low-set posteriorly angulated ears, developmental delay, learning/behaviour problems, short stature, cardiac anomalies, ventriculomegaly, Chiari I, Dandy Walker, craniosynostosis	AD	1 patient CSO 381

13	<i>PTPRD</i>	9p24.1p23	<i>PTPRD</i> microdeletion syndrome	601598	Trigonocephaly, scaphocephaly, growth retardation, hearing loss, ID, midface hypoplasia, flat nose, depressed nasal bridge, hypertelorism, long philtrum, drooping mouth	AR	1 patient	382
14	<i>SEC24D</i>	4q26	Cole-Carpenter syndrome 2	616294	Phenotype closely resembling Cole-Carpenter syndrome: severely disturbed ossification of the skull, multiple fractures with prenatal onset, short stature, macrocephaly, midface hypoplasia, micrognathia, frontal bossing, down- slanting palpebral fissures	AD	1 patient CSO	383
15	<i>SHOC2</i>	10q25.2	Noonan-like syndrome with loose anagen hair	602775	Noonan-like syndrome: foetal hydrops, atrial tachycardia, foetal pleural effusion, short stature, developmental delay, macrocephaly, severe craniostenosis	AD	1 patient CSO	384
16	<i>WDR19</i>	4p14	Cranioectodermal dysplasia	608151	Sensenbrenner/Jeune syndrome: nephronophthisis- like nephropathy, skeletal abnormalities (narrow rib cage, pectus excavatum, short limbs, brachydactyly), ectodermal defects, renal failure, hepatic fibrosis, heart defects, retinitis pigmentosa, sagittal suture synostosis	AR	1 patient CSO	385

AD = Autosomal dominant, AR = Autosomal recessive, CSO = Craniostenosis, C2/3 = 2nd and 3rd vertebrae of the spinal cord, ID = Intellectual disability, OP = Osteopetrosis, OSA = Obstructive sleep apnoea.



Table 10.3. Genes recently associated with craniofacial clefting.

	Gene	Location	Clinical disorder	OMIM gene #	Major phenotypic features	Inheritance pattern	First reference
1	<i>ALX1</i>	12q21.31	FND type 3	601527	Bilateral extreme microphthalmia, bilateral oblique facial cleft, complete cleft palate, hypertelorism, wide nasal bridge with hypoplasia of the ala nasi and low-set posteriorly rotated ears	AR	386
2	<i>ALX3</i>	1p13.3	FND type 1	606014	Hypertelorism, wide nasal bridge, short nasal ridge, bifid nasal tip, broad columella, widely separated slit-like nares, long philtrum with prominent bilateral swellings, midline notch in the upper lip and alveolus, upper eyelid ptosis, midline dermoid cysts	AR	387
3	<i>ALX4</i>	11p11.2	FND	605420	Isolated symmetrical parietal ossification defects at the intersection of the sagittal and lambdoid sutures (enlarged parietal foramina)	AR, AD	388-390
			Parietal foramina		Enlarged parietal foramina, abnormalities of the corpus callosum and cerebellum (meningoencephalocele)	AR	391
4	<i>ARFGF2</i>	20q13.13	Periventricular heterotopia with microcephaly	605371	Bilateral periventricular nodular heterotopia with microcephaly and severe mental retardation	AR	392
5	<i>EFNB1</i>	Xq13.1	CFNS	300035	Frontonasal dysplasia and coronal craniosynostosis (hypertelorism in hemizygous males)	XLD	63
6	<i>FLNA</i>	Xq28	Frontometaphyseal dysplasia 1	300017	Bilateral periventricular nodular heterotopia, mega cisterna magna, cardiovascular malformations and epilepsy	XLR	393
7	<i>FREM1</i>	9p22.3	Manitoba-oculo-tricho-anal syndromes	608944	Bifid nose, anorectal and renal anomalies	AR	394
8	<i>FOXC1</i>	6p25.3	Axenfeld-Rieger syndrome	601090	Malformations of the eyes and craniofacial malformations	AD	395
9	<i>GLI2</i>	2q14.2	Holoprosencephaly-like	165230	Defective anterior pituitary formation and pan-hypopituitarism, forebrain cleavage abnormalities, midface hypoplasia	AD	396
10	<i>L1CAM</i>	Xq28	Hydrocephalus, CRASH syndrome, MASA syndrome	308840	Hydrocephalus, Hirschsprung disease, agenesis of the corpus callosum	XLR	397
11	<i>PITX2</i>	4q25	Axenfeld-Rieger syndrome	601542	Malformations of the eyes and craniofacial malformations	AD	398
12	<i>SHH</i>	7q36	Holoprosencephaly	600725	Holoprosencephaly: cyclopia, proboscis, midfacial clefting, microcephaly, hypertelorism, single maxillary incisor	AD	399

13	<i>SIX2</i>	2p21	Frontonasal dysplasia and renal dysplasia	604994	Frontonasal dysplasia and renal dysplasia	AD	344
14	<i>SIX3</i>	2p21	Holoprosencephaly	603714	Holoprosencephaly, single central incisor, hypotelorism, microcephaly, midline clefting of both the lip and palate	AD	400
15	<i>SMAD3</i>	15q22.33	Loeys-Dietz syndrome 3	603109	Hypertelorism, abnormal palate and/or uvula, dental malocclusion, aneurysms, arterial tortuosity, heart diseases, osteoarthritis, umbilical/inguinal hernias, velvety skin and striae	AD	401
16	<i>TDGF1</i>	3p21.31	Holoprosencephaly	187395	Developmental delay, dysplastic forebrain, absence of the septum pellucidum, hypoplastic corpus callosum,	AD	402
17	<i>TGIF</i>	18p11.31	Holoprosencephaly 4	602630	FND and eye anomalies, midline cleft lip and palate, agenesis of the corpus callosum, basal encephalocele, holoprosencephaly	AD	403
18	<i>TGFBR1</i>	9q22.33	Loeys-Dietz syndrome 1	190181	Hypertelorism, bifid uvula, arterial and/or aortic aneurysms, arterial tortuosity, craniofacial, neurodevelopmental, skeletal and skin abnormalities, joint laxity, arachnodactyly, pectus deformity, scoliosis	AD	404
19	<i>TGFBR2</i>	3p24.1	Loeys-Dietz syndrome 2	190182	Arterial tortuosity, aneurysms, hypertelorism, bifid uvula, cleft palate, craniostenosis, high rate of pregnancy-related complications, food allergies, asthma, rhinitis, and eczema	AD	405
20	<i>TWIST1</i>	7p21.1	Sweeney-Cox syndrome	601622	Facial dysostosis, hypertelorism, deficiency of the eyelids and facial bones, cleft palate, velopharyngeal insufficiency, low set cupped ears	AD p.(Glu117Val) and p.(Glu117Gly)	142
21	<i>TWIST2</i>	2q37.3	Ablepharon-macrostomia Barber-Say syndrome	607556	Sparse hair, absent or reduced eyelids	p.(Glu75Lys)	406
					Excess hair, bulbous nose, large mouth, small ears	AD p.(Glu75Ala) and p.(Glu75Gln)	406
			Setleis syndrome/ Type III focal facial dermal dysplasia		Bilateral temporal marks, an aged-leonine appearance, absent eyelashes on both lids or multiple rows on the upper lids, absent Meibomian glands, slanted eyebrows, chin clefting, and other nonfacial manifestations	AR	407
22	<i>ZIC2</i>	13q32	Holoprosencephaly	603073	Brain anomalies, holoprosencephaly, exencephaly, digital anomalies (absent thumbs)	AD	276
23	<i>ZSWIM6</i>	5q12.1	Acromelic frontonasal dysostosis	615951	Dysostosis: frontonasal dysplasia, interhemispheric lipoma, agenesis of the corpus callosum, tibial hemimelia, preaxial polydactyly of the feet, ID	AD	408

AD = Autosomal dominant, AR = Autosomal recessive, CFNS = Craniofrontonasal syndrome, FND = Frontonasal dysplasia, ID = Intellectual disability, XLD = X-linked dominant, XLR = X-linked recessive.



Table 10.4. Genes recently associated with facial dysostosis.

	Gene	Location	Clinical disorder	OMIM gene #	Major phenotypic features	Inheritance pattern	First reference
1	<i>ACTB</i>	7p22.1	Barraitser-Winter syndrome	102630	Congenital ptosis, high-arched eyebrows, hypertelorism, ocular colobomata, anterior predominant lissencephaly, short stature, microcephaly, ID, seizures and hearing loss	AD	409
2	<i>ACTG1</i>	17q25.3	Barraitser-Winter syndrome 2	102560	Congenital ptosis, high-arched eyebrows, hypertelorism, ocular colobomata, anterior predominant lissencephaly, short stature, microcephaly, ID, seizures and hearing loss	AD	409
3	<i>COG1</i>	17q25.1	CCMS-like syndrome	606973	CCMS with only one having posterior rib gaps	AR	410
4	<i>DHODH</i>	16q22.2	Miller syndrome	126064	AFD characterized by postaxial limb defects and MFD, micrognathia, cleft lip and/or palate, hypoplasia or aplasia of the postaxial elements of the limbs, coloboma of the eyelids, and supernumerary nipples	AR (bi-allelic)	217
5	<i>EDN1</i>	6p24.1	Auriculocondylar syndrome type 3	131240	Micrognathia, temporomandibular joint and condyle anomalies, microstomia, prominent cheeks and question-mark ears	AR	411
6	<i>EDN1</i>	6p24.1	Question-mark ears		Isolated question-mark ears	AD	411
7	<i>EDNRA</i>	4q31.22-q31.23	Mandibulofacial dysostosis with alopecia/Johnson-McMillin syndrome	131243	Mandibulofacial dysostosis, micrognathia, cleft palate, limited jaw mobility, glossoptosis, upper airway obstruction, irregular placement of primary teeth, delayed eruption of primary teeth, agenesis of permanent teeth, everted lower lip, short nose with squared nasal tip, small/cupped/dysplastic ears with ectopic tissue, conductive hearing loss, sparse eyelashes, hypoplasia of the eyelids, eyelid coloboma, alopecia	AD	412
8	<i>EFTUD2</i>	17q21.31	Mandibulofacial dysostosis, Guion-Almeida type (MFDGA)	603892	Mandibulofacial dysostosis, microcephaly, external ear malformations and intellectual disability less frequent features include hearing, loss, cleft palate, choanal atresia, oesophageal atresia, congenital heart defects and radial ray defects	AD	413
9	<i>EIF4A3</i>	17q25.3	Richieri-Costa-Pereira syndrome	608546	Microstomia, midline mandibular cleft, Robin sequence, absence of lower incisors, cleft palate, laryngeal anomalies, limb reductions (radial, tibial, thumb, thenar, fifth finger and hallux hypoplasia), club feet, intellectual disabilities	AR nucleotide repeat expansion	414

10	<i>EVC</i>	4p16.2	Ellis-van-Creveld syndrome	604831	Frenula, peg or misshaped maxillary incisors, enamel hypoplasia, oligodontia, malocclusion, premature teeth eruption, congenital cardiac malformations (ASD, AVSD), genu valga, strabismus, epi- and hypospadias, cryptorchidism, pulmonary malformation, renal anomalies, dwarfism, postaxial polydactyly, short limbs, short ribs, bilateral postaxial polydactyly of hands and feet, nail dystrophy, dental anomalies	AR	415
11	<i>EVC2</i>	4p16.2	Ellis-van-Creveld syndrome	607261	Disproportionate chondrodysplasia, dwarfism, postaxial polydactyly, short limbs, short ribs, bilateral postaxial polydactyly of hands and feet, nail dystrophy, dental abnormalities, multiple frenula, peg or misshaped maxillary incisors, enamel hypoplasia, oligodontia, malocclusion, premature teeth eruption, V-notch, congenital cardiac malformations (ASD, AVSD), genu valgum, strabismus, epi- and hypospadias, cryptorchidism, pulmonary malformations, renal anomalies	AR	416
12	<i>GNAI3</i>	1p13.3	Weyer acrocardental dysostosis	607261	Dental anomalies, nail dystrophy, postaxial polydactyly, and mild short stature	AD	417
13	<i>MRE11A</i>	11q21	Auriculocondylar syndrome	139370	Variable micrognathia, temporomandibular joint ankylosis, cleft palate, question-mark ears	AD	418
14	<i>NBS1</i>	8q21.3	Ataxia-Teleangiectasia like disorder	600814	Early-onset, slowly progressive, ataxia plus ocular apraxia, small jaw and chin, short palpebral fissures, microcephaly	AR	419
15	<i>PLCB4</i>		Nijmegen breakage syndrome	602667	Microcephaly, growth retardation, immunodeficiency, predisposition to cancer	AR, hypomorphic	420
16	<i>POLR1A</i>	2p11.2	Auriculocondylar syndrome	600810	Variable micrognathia, temporomandibular joint ankylosis, cleft palate, question-mark ears	AD	418
17	<i>POLR1C</i>	6p21.1	Acrofacial dysostosis, Cincinnati type	616404	Mandibulofacial dysostosis and limb anomalies	AD	421
18	<i>POLR1D</i>	13q12.2	Treacher Collins syndrome 3	610060	Treacher Collins syndrome	AR (bi-allelic)	422
19	<i>PRRX1</i>	1q24.2	Treacher Collins syndrome 2	613715	Treacher Collins syndrome	AD, AR	422
			Agnathia-otocephaly complex	167420	Otocephaly: absent/underdeveloped mandible, microstomia, hypoglossia/aglossia, variable anterior midline fusion of the auricles	AD, AR	423,424



Table 10.4. (continued)

	Gene	Location	Clinical disorder	OMIM gene #	Major phenotypic features	Inheritance pattern	First reference
20	<i>PQBP1</i>	Xp11.23	Renpenning syndrome	300463	Microcephaly, short stature, small testes, dysmorphic facies, including tall narrow face, upslanting palpebral fissures, long bulbous nose, overhanging columella, cupped ears, and short philtrum, ocular colobomata, cardiac malformations, cleft palate, and anal anomalies	XLR	425
21	<i>RPL5</i>	1p22.1	Diamond-Blackfan Anaemia 6 with Mandibulofacial Dysostosis	603634	Red blood cell aplasia, macrocytic anaemia, growth retardation, hydrocephalus, hypertelorism, cleft lip and palate, bifid uvula, micrognathia, retrognathia, mandibular hypoplasia, tracheomalacia, hypoplastic/triphalangeal thumbs, congenital heart defects, hypospadias, hip dysplasia, rib anomalies	AD	426
22	<i>RPS26</i>	12q13.2	Diamond-Blackfan Anaemia 10	603701	Diamond Blackfan anaemia and TCS-like phenotype: microtia with absent external auditory canals and abnormal middle ears, malar hypoplasia, choanal atresia, micrognathia, (submucous) cleft palate, downslanting palpebral fissures, midface hypoplasia, short stature, renal anomalies	AD	427/428
23	<i>RPS28</i>	19p13.2	Diamond-Blackfan Anaemia 15 with Mandibulofacial Dysostosis	603685	Diamond Blackfan anaemia and TCS-like phenotype: microtia with absent external auditory canals and abnormal middle ears, malar hypoplasia, choanal atresia, micrognathia, (submucous) cleft palate, downslanting palpebral fissures, midface hypoplasia	AD	428
24	<i>SALL1</i>	16q12.1	Townes-Brocks syndrome	602218	Anal, renal, limb (pre-axial polydactyly), and ear anomalies and sensorineural hearing loss with a conductive component, mental retardation	AD	429
25	<i>SF3B4</i>	1q21.2	Acrofacial dysostosis 1, Nager syndrome	605593	Malar and mandibular hypoplasia, down-slanting palpebral fissures, lower eyelid and eyelash anomalies, external ear dysplasia and cleft palate (5, 61, 62). The most frequent limb abnormalities involve the thumbs, which can be hypoplastic, absent, or triphalangeal; less commonly seen are radioulnar synostosis, phocomelia, or lower limb defects. Psychomotor development can be mildly delayed; however the occipito-frontal circumference is usually within normal ranges. Other visceral malformations are rare.	AD	430

26	SNRPB	20p13	Cerebrocostomandibular syndrome (CCMS)	182282	Frequently leading to death in the early post-natal period due to respiratory distress, while some individuals have been reported with intellectual disability and/or microcephaly, scoliosis, decreased height, conductive hearing loss and down-slanting palpebral fissures and neurologic and cognitive defects	AD	431
27	TCOF1	5q32-q33	Treacher Collins syndrome 1	606847	Treacher Collins syndrome	AD	399
28	TFAP2A	6p24.3	Branchio-oculo-facial syndrome	107580	Cutaneous anomalies (cervical, infra-auricular/supra-auricular defects, dermal thymus, ocular anomalies, malformed pinnae, oral clefts, renal and ectodermal anomalies)	AD	432
29	TSR2	Xp11.22	Diamond-Blackfan Anaemia 14 with Mandibulofacial Dysostosis	300945	Diamond Blackfan anaemia and TCS-like phenotype: microtia with absent external auditory canals and abnormal middle ears, malar hypoplasia, micrognathia, (submucous) cleft palate, downslanting palpebral fissures, midface hypoplasia, cryptorchidism	XLR	428
30	TXNLA	18q23	Burn-McKeown syndrome	611595	Bilateral choanal atresia, hearing loss, cleft lip/palate, cardiac defects, narrow palpebral fissures, coloboma of the lower eyelids, prominent nose with high nasal bridge, short philtrum, large and protruding ears	AR (bi-allelic)	61
31	ZEB2	2q22.3	Mowat-Wilson syndrome	605802	Microcephaly, mental retardation, hypertelorism, submucous cleft palate, congenital heart disease and short stature	AD	433

AD = Autosomal dominant, AR = Autosomal recessive, ASD = Atrial septum defect, AVSD = Atrioventricular septal defect, ID = Intellectual disability, TCS = Treacher Collins Syndrome, XLR = X-linked recessive.



Incidental findings

Patient material used in our whole genome sequencing study was send to us from several physicians and/or laboratories situated in several countries. When starting, discussions were on-going concerning communicating incidental findings. A consensus had not been reached; each country, each university and even each department in our own hospital had different views on this subject. Therefore we have chosen not to communicate the incidental findings. We plan to offer parents and patients the possibility to opt open. In this way, we can test preferences concerning incidental findings, as well as meeting the recommendations of the ACMG.³³⁶

Next generation sequencing

This thesis has shown that next generation sequencing contributes to genetic testing of patients with craniofacial malformations. With whole exome sequencing, all genes are tested in a single experiment, increasing the chance of identifying the genetic cause, especially if the mutation is located in a gene that otherwise would not have been tested (for example in the case of an atypical presentation or rarely associated gene). Hence, next generation sequencing increases the efficiency of identifying the genetic causes of craniofacial malformations, as it has been shown to do for other rare diseases, intellectual disability¹⁴³ and cardiovascular diseases.⁴³⁴

Moving from gene-specific testing to next generation sequencing can lead to a reduction of costs. In patients with syndromic craniosynostosis for example, *FGFR2*, *FGFR3* and *TWIST1* are routinely screened and an array has been performed routinely. By increasing the numbers of genes that are tested, these costs can rise even further. Although the costs of massively-parallel sequencing are high (originally US \$2.7 billion during the Human Genome Project), they are decreasing. Furthermore, the competition for the breakthrough leading to the 1000-dollar genome is still on. Therefore, it seems cost-effective to switch to next generation sequencing.

It has been hypothesized that next generation sequencing data can be re-used for other diagnostics, for example to test the response to certain medication (prevention of severe side effects and avoidance of ineffective therapy),⁴³⁵ to screen for hereditary cancer, carrier testing,⁴³⁶ and instead of blood type testing, possibly leading to a cost reduction and efficiency gain. Also, stored data can be reused as reference material for other indications. However, the increased amount of data produced by next generation sequencing leads to higher storage costs, therefore, time will tell if genetic data is stored and re-used or if resequencing is performed.

Whole genome sequencing

As more and more genes are found to be involved in the occurrence of congenital craniofacial malformations, and the associated phenotypes become less specific, the focus shifts from single-gene tests to multiplex testing of all genes (i.e. next generation sequencing). In case of whole genome sequencing, the complete genome is tested.

To date, we have sequenced (whole genome) 317 DNA samples of patients with craniofacial malformations and their family members, comprising one sextet, two quintets, eleven quartets, seventy-eight trios, six duos and eleven singletons. Based on clinical appearance, samples were expected to be affected or not-affected. Eighty probands had craniosynostosis, eleven had a form of craniofacial clefting, two had a combination of craniosynostosis and craniofacial clefting, three had facial dysostosis, two had another facial phenotype and eleven were sent by another craniofacial centre and their exact phenotype was unknown (see table 10.5 for an overview). Appropriate genes and, if indicated, metabolic tests were tested with negative results prior to sequencing.

Filtering of the data was based on inheritance pattern, frequency, the predicted effect of the mutation and using lists of genes of interest (manually curated lists of genes that were mentioned in literature, were associated with a “craniofacial” phenotype in the Mouse Genome Database [Mouse Genome Informatics website, The Jackson Laboratory, Bar Harbor, Maine, USA] and POSSUMweb database [Pictures of Standard Syndromes and Undiagnosed Malformations, Murdoch Children’s Research Institute, Royal Children’s Hospital, Melbourne, Australia], that did not have a loss-of-function mutation in the Exome Variant Server [Exome Variant Server, NHLBI GO Exome Sequencing Project (ESP), Seattle, WA (URL: <http://evs.gs.washington.edu/EVS/>)], as well as all genes that had a *de novo* mutation in DDD). Variants were classified according to ACMG guidelines into Benign, likely Benign, variant of unknown significance, Likely Pathogenic, and Pathogenic.¹⁴⁷ All putatively causative variants were confirmed by an independent sequencing technology.

When a previously described mutation was observed it was assumed to be pathogenic. If a mutation was observed in a previously described gene with a phenotype similar to the proband in question, the phenotype of the patient was re-evaluated for the syndrome (like the *ANKRD11* mutation). If candidate mutations were found in the same gene in more than one case with a similar phenotype, this was suggestive of a pathogenic effect. Therefore, all 317 samples were checked for the repeated occurrence of mutations in candidate genes. To confirm pathogenicity, candidate genes were screened in our patient cohort and an additional cohort in Oxford. If possible, the biological consequence of a candidate was validated.



Using the above-mentioned gene lists and various filtering techniques we identified mutations in 30 out of 109 proband samples. Fourteen mutations were identified in “core craniofacial genes” (*BMP2/SMAD6*, *TCF12* deletion (3x), *TCF12* (2x), *ERF* (2x), *TWIST1*, *IL11RA* (2x), *MSX2*, *ZIC1*, *TXNL4A*), four in genes that were only rarely associated with craniosynostosis, craniofacial clefting or facial dysostosis (*ANKRD11*, *IDS*, *KRAS*, *JAG1*) and one known disease gene for which a causal relationship with craniosynostosis, craniofacial clefting or facial dysostosis was currently unknown (*AHDC1*). In eight patients, mutations were identified in novel genes (*TLK2* (2x), *BCL11B*, *PRRX1*, *LUZP1*, *FUZ*, *CDK8*, *ZFH4*). In three, a chromosomal rearrangement was identified (del1p31.3, UPD chromosome 5, del10p13). Hence, our overall success rate in identifying pathogenic mutations was 30/109 (27.5%), compared to 37.5% when a combined approach (whole exome and whole genome sequencing) was performed on samples with craniosynostosis exclusively.⁴

Novel causative gene identification

Using next generation sequencing, we have identified a number of interesting candidate genes. Currently, validation of these genes is ongoing by using mouse-models and also resequencing the genes in patient cohorts. The confirmation of the pathogenicity of these genes cannot be established without our close (international) collaborations. Also, these collaborations are essential to be able to identify novel genetic causes in the unsolved cases where these strategical partnerships offer the possibility to have large test and validation cohorts.

Additional strategies to identify even more novel genetic causes are: 1. identifying mosaic causes (mosaicism has been seen in craniofrontonasal syndrome²⁰³ and *ZIC1*-related craniosynostosis⁶⁵ for example), 2. searching for complex causes (as shown in the *SMAD6/BMP2* case³⁴¹), 3. searching in regulatory elements (as shown by the *SIX2* case³⁴⁴), 4. using pathway analysis to identify other causative genes (as shown by the ribosomopathies and spliceosomopathies that underlie many facial dysostoses²⁸⁹), 5. studying epigenetic factors (differentially methylated sites have been associated with non-syndromic cleft lip and/or palate⁹⁷ for example).

Best care

A molecular diagnosis has implications for genetic counselling and for clinical management. With respect to genetic counselling, an accurate recurrence risk can be given. Concerning clinical management, one could think of preventive measures like early hearing tests in patients with a P250R mutation in *FGFR3* (Muenke syndrome) at a younger age. Also, therapy can be adjusted to the genetic diagnosis. Nowadays, patients with Muenke syndrome undergo a fronto-orbital advancement, while patients

with Apert and Crouzon syndrome undergo occipital remodelling. Moreover, because of the mild phenotype of *TCF12*-related craniosynostosis, an adjusted protocol is used in these patients (unpublished data). Hence, personalized medicine seems within reach.

Therapy

Due to the prenatal onset, true treatment options remain poor. However, Shukla *et al.* were able to reverse coronal synostosis in mice by intraperitoneal injection of the pregnant mother⁴³⁷, Wang *et al.* ameliorated the associated skin disorder in Beare-Stevenson mice⁴³⁸ and the late onset of craniosynostosis in *ERF*-related craniosynostosis seems to provide a therapeutic goal. In mice with Treacher-Collins syndrome, p53-inhibition^{439,440} or dietary supplementation with N-acetylcysteine⁴⁴¹ (an antioxidant) substantially ameliorated the phenotype. Additionally, with the introduction of CRISPR/Cas9, treatment of congenital craniofacial malformations seems within reach.⁴⁴² Obviously, designing therapy requires detailed knowledge of the development of the head and neck and the involved genetic pathways. Improving this knowledge has been the aim of this thesis as it can lead to a future with improved diagnostic and therapeutic strategies.



Table 10.5. Overview of sequenced samples (whole genome).

Family number	Sample ID	Gender	Sample	Hg	Phenotype	Key feature	Additional information	Clinical appearance	Family history	Genes tested previously	Mutation positive			
											Gene/ location	Nucleotide	Protein	Inheritance
01	JAC29	m	Father	19	CSO			A						
	JAC28	f	Mother	19				NA						
	JAC16	m	Proband	19		S, RC	Developmental delay, autism	A		FGFR2, FGFR3, TWIST1, karyo	TLK2	c.907C>T	p.(Arg303*)	de novo
02	JAC26	m	Father	19	CSO			NA						
	JAC25	f	Mother	19				NA						
	JAC4	m	Proband	19		S, BL (part)	Increased ICP Chiari malformation, papilledema, asthma, eczema, OSA, GAF score 51-60, class II/1, narrow v-shaped maxilla, dental crowding	A		FGFR1, FGFR2, FGFR3, ERF, FISH TWIST1, karyo				
03	JAC32	m	Father	19	CSO			NA						
	JAC31	f	Mother	19				NA						
	JAC24	m	Proband	19		S, RC	Ptosis	A		FGFR2 (Leu770Leu), FGFR3, TWIST1 + FISH, TCF12				
	JAC1	m	Brother	19		S		A		FGFR1, FGFR2 (Leu770Leu), FGFR3, TWIST1 + FISH, karyo				
04	JAC20	m	Father	19	CC and CSO			NA						
	JAC21	f	Mother	19				NA						
	JAC19	m	Proband	19		M	Nasal tip, dysplastic ears, ectropion lower lip, retrognathia maxilla and mandible, single umbilical artery, exorbitism, VSD	A		FGFR2, EFNB1, SNP array, karyo				

Table 10.5. (continued)

Family number	Sample ID	Gender	Sample	Hg	Phenotype	Key feature	Additional information	Clinical appearance	Family history	Genes tested previously	Mutation positive			
											Gene/ location	Nucleotide	Protein	Inheritance
10	JAC38	m	Father	19	CC	Rugose		NA						
	JAC39	f	Mother	19		Rugose		NA						
	JAC13	f	Proband	19		Rugose	Telecanthus, hypertelorism, infantile exotropia, dissociated vertical deviation, nystagmus latens, strabismus sursoadductorius B, V-motility, excyclotropia	A		EFNB1, karyo (9ph)				
11	JAC73	m	Father	19	CSO	S		A						
	JAC67	f	Mother	19				NA						
	JAC3	m	Proband	19		S	Father and grandfather S, PT, fructose intolerance	A		FGFR1, FGFR2, FGFR3, TWIST1 + FISH, karyo				
12	JAC225	m	Father	19	CC			NA						
	JAC211	f	Mother	19				NA						
	JAC23	f	Proband	19			Microtia L, macrostomia L, hypoplastic mandible L, hypoplastic hand L, four finger hand, hemivertebrae, anteriorly positioned anus, Pruzansky class II	A						

207

Table 10.5. (continued)

Family number	Sample ID	Gender	Sample	Hg	Phenotype	Key feature	Additional information	Clinical appearance	Family history	Genes tested previously	Mutation positive			
											Gene/location	Nucleotide	Protein	Inheritance
17	JAC74	m	Father	19	FD			NA			ZFX4	c.7781-7783del	p.(Glu2594del)	
	JAC75	f	Mother	19				A			ZFX4	c.7781-7783del	p.(Glu2594del)	
	JAC47	m	Proband	19	TCL	Bilateral ptosis, hypoplasia of mandible		A	Consanguineous parents, brother and mother same phenotype	TCOF1, POLR1C, POLR1D, TXNL4A, meta	ZFX4	c.[7781-7783del]; [7781-7783del]	p.[Glu2594del]; [Glu2594del]	
18	JAC57	m	Father	19	CSO			NA						
	JAC56	f	Mother	19				NA						
	JAC44	m	Proband	19	S, BC (part), BL (part)	Intermittent papilledema, supernumerary finger, metatarsus adductus, abducted 5th metatarsal B, MRI: tonsillar herniation, PT, ST		A		FGFR1, FGFR2, FGFR3, TWIST1, ERF, karyo (21ps+)				
19	JAC63	m	Father	19	CSO			NA						
	JAC64	f	Mother	19				A +/-	2 brothers of mother hydrocephalus					
	JAC18	m	Proband	19	BC, M, S	Chiari, papilledema, microstrabismus L, anisohypermetropia, amblyopia L, laxity		A		FGFR2, FGFR3, TWIST1, ERF, karyo (Yq21)				

20	JAC58	m	Father	19	CSO														
	JAC62	f	Mother	19															
	JAC60	f	Proband	19															
	JAC61	f	Sister	19															
21	JAC65	m	Father	19	CSO														
	JAC66	f	Mother	19															
	JAC42	f	Proband	19															
22	JAC96	m	Father	19	CSO														
	JAC95	f	Mother	19															
	JAC43	m	Proband	19															
23	JAC213	m	Father	19	CSO														
	JAC46	f	Mother	19															
	JAC80	f	Proband	19															
	28	F	Grand Mother	18															



Table 10.5. (continued)

Family number	Sample ID	Gender	Sample	Hg	Phenotype	Key feature	Additional information	Clinical appearance	Family history	Genes tested previously	Mutation positive			
											Gene/ location	Nucleotide	Protein	Inheritance
24	JAC55	m	Father	19	CC			NA						
	JAC176	f	Mother	19				NA						
	JAC45	m	Proband	19			Small anterior fossa, panhypopit postoperatively, eczema, ID, ADHD, autism, PT, ST, OSA (anamnestic). CT: basal encephalocoele, agenesis of callosal body, bony defect, cleft	A		Karyo				
25	JAC48	m	Father	19	CSO			NA						
	JAC49	f	Mother	19				NA						
	JAC41	f	Proband	19		RC	Headaches	A		FGFR1, FGFR2, FGFR3, TWIST1				
26	JAC77	m	Father	19	CSO			NA						
	JAC78	f	Mother	19				NA						
	JAC76	m	Proband	19		RC	PMR, attention deficit, ptosis, hearing deficit, short stature	A		FGFR3, TWIST1 + FISH, karyo	ANKRD11	c.7606C>T	p.(Arg253GTrp)	de novo
27	JAC50	m	Father	19	CSO	S		A						
	JAC51	f	Mother	19				NA						
	JAC52	m	Proband	19		S	Headaches, attention deficit	A	Brother of father also S					

211

Table 10.5. (continued)

Family number	Sample ID	Gender	Sample	Hg	Phenotype	Key feature	Additional information	Clinical appearance	Family history	Genes tested previously	Mutation positive			
											Gene/location	Nucleotide	Protein	Inheritance
32	JAC109	m	Father	19	CSO			NA						
	JAC110	f	Mother	19				NA						
	JAC108	f	Proband	19		BC	Large big toes, axial hypotonia (PT) underdevelopment nVIII, intermittent exotropia, hypermetropia B, central apnoea, correction of hernia epigastrica, mild bilateral genua valga and pes planus, autism and ADHD, ID (special education)	A		FGFR2, FGFR3, TWIST1, ZIC1, SNP array, WES (Ala7Val RPS6KA3 (+/-), His114Arg PQBP1 (+/-), Gln186His TRIM32 (+/+))				
33	JAC106	m	Father	19	CSO			A +/-						
	JAC105	f	Mother	19				NA						
	JAC107	f	Proband	19		BC	Class II, cross bite, premature loss of 64, ATE due to snoring	A		FGFR1, FGFR2, FGFR3, TWIST1, NSD1 (c.1792T>C, Leu598Leu (Father), karyo				
34	JAC114	m	Father	19	CC			NA						
	JAC113	f	Mother	19				NA						
	JAC112	f	Proband	19		bifid nose	Additional subcutaneous tissue, lactose intolerance	A		ALX3, karyo				

35	JAC99	m	Father	19	CSO	S	3x correction	NA									
	JAC98	f	Mother	19		S, LC, BL	Headache, papilledema, increased ICP, MRI: more CSF	A									
	JAC97	m	Proband	19			optic nerve, empty sella, occipital collaterals, special education, PT, ADHD	A									
36	JAC104	f	Mother	19	CSO			A									
	JAC103	f	Proband	19		S, BL (part)	ID, PT, otitis media with effusion	A									
37	JAC100	m	Father	19	CSO			A									
	JAC102	f	Mother	19				NA									
	JAC101	f	Proband	19		S (part), M, BC		A									
	MC1	f	Grand Mother	18		M		A									
	MC2	f	Aunt	18		M		A									
	MC3	m	Cousin	18		M		A									
38	JAC116	m	Father	19	CSO			NA									
	JAC117	f	Mother	19				NA									
	JAC115	m	Proband	19		LC	Cardiac malformation (double inlet ventricle L, small atrium R, transposition large arteries, aorta ascends from R ventricle, large VSD, small ASD), strabismus OD, torticollis	A									



Table 10.5. (continued)

Family number	Sample ID	Gender	Sample	Hg	Phenotype	Key feature	Additional information	Clinical appearance	Family history	Genes tested previously	Mutation positive			
											Gene/location	Nucleotide	Protein	Inheritance
39	JAC227	m	Father	19	CC			NA						
	JAC118	f	Mother	19				NA						
	JAC120	m	Proband	19		Hemi L	Absent maxillary sinus	A	Several cousins with hydrocephalus, kidney malformations and visual disability					
40	JAC125	m	Father	19				UK						
	JAC126	f	Mother	19				UK						
	JAC124	m	Proband	19				UK						
	JAC128	m	Father	19				UK						
	JAC129	f	Mother	19				UK						
42	JAC127	f	Proband	19				UK			AHDC1	c.2373_2374delTG	p.(Cys791fs*)	de novo
	JAC132	m	Father	19				UK						
	JAC131	f	Mother	19				UK			JAG1	c.2449T>C	p.(Cys817Arg)	AD UK
	JAC130	f	Proband	19				UK			JAG1	c.2449T>C	p.(Cys817Arg)	AD iMother
43	JAC134	m	Father	19				UK						
	JAC135	f	Mother	19				UK						
	JAC133	f	Proband	19				UK			UPD chrom 5			maternal
44	JAC137	m	Father	19				UK						
	JAC138	f	Mother	19				UK						
	JAC136	m	Proband	19				UK						

215

Table 10.5. (continued)

Family number	Sample ID	Gender	Sample	Hg	Phenotype	Key feature	Additional information	Clinical appearance	Family history	Genes tested previously	Mutation positive			
											Gene/ location	Nucleotide	Protein	Inheritance
51	JAC181	m	Father	19	CSO			NA						
	JAC182	f	Mother	19				NA						
	JAC162	m	Proband	19		S, BL	Syndactyly 3rd and 4th finger L, incomplete syndactyly of 3rd and 4th finger R and both feet, Chiari with syrinx leading to clumsiness and progressive bipyramidal syndrome, rheumatoid arthritis, OMA L, ADHD, CGAS 51-60, underdeveloped chin, asymmetrical occlusion, dental crowding	A		<i>FGFR2, FGFR3, TWIST1 + FISH, ERF</i> , karyo				
52	JAC184	m	Father	19	CSO			NA						
	JAC185	f	Mother	19				A			<i>ERF</i>	c.1392dupT	p.(Lys465*)	AD UK
	JAC165	m	Proband	19		S	Hypertelorism, bifid nose, speech and language delay (ST), attention deficit, increased ICP, tubes	A	Brother of mother S and speech and language delay	<i>FGFR2, IL11RA, FISH 22q11</i> , karyo, meta	<i>ERF</i>	c.1392dupT	p.(Lys465*)	AD iMother
	JAC195	m	Uncle	19		S		A			<i>ERF</i>	c.1392dupT	p.(Lys465*)	AD UK

217

Table 10.5. (continued)

Family number	Sample ID	Gender	Sample	Hg	Phenotype	Key feature	Additional information	Clinical appearance	Family history	Genes tested previously	Mutation positive			
											Gene/ location	Nucleotide	Protein	Inheritance
56	JAC189	m	Father	19	CSO			NA						
	JAC190	f	Mother	19				NA						
	JAC175	m	Proband	19		M	Constriction ring syndrome, deformation foot L, amputation lower leg R, underdeveloped midphalanges and distal phalanges 2nd and 3rd ray foot L, eczema, BPD	A						
57	JAC186	m	Father	19	CSO	S		A						
	JAC177	f	Mother	19				NA						
	JAC178	m	Proband	19		S		A						
58	JAC192	m	Father	19	CSO	S		A						
	JAC188	f	Mother	19				NA						
	JAC187	m	Proband	19		S	Bregma, headaches, MRI: prominent superior sagittal sine and falxiform sine and collaterals, no Chiari, parents choose not to perform ICP measurement	A						
	JAC249	m	Uncle	19				UK						

58	JAC250	f	Cousin	19	CSO	LC	ASD, VSD, dysplasia of tricuspid valve, short fingers, WISC-III-NI: VIQ 109, PIQ 81, TIQ 95, VB 110, PO 76, VS 108, cGAS 70, ADHD	A		FGFR2, FGFR3, TWIST1, TCF12						
59	JAC193	m	Father	19	CSO			A								
	JAC191	f	Mother	19				NA								
	JAC194	m	Proband	19		LC	Alternating convergent strabismus, dissociated vertical deviation, amblyopia, nystagmus, anisohypermetropia and astigmatism, malocclusion, agenesis 72, crowding, narrow maxilla, ID, Asperger syndrome	A		FGFR1, FGFR2, FGFR3, TWIST1, TCF12						
60	JAC143	m		19				UK								
	JAC144	f	Mother	19				UK								
	JAC142	f	Proband	19				UK								
61	JAC207	f	Mother	19	CSO			NA				ERF	c.652C>T	p.(Arg218*)	AD UK	
	JAC201	m	Proband	19		PAN	Increased ICP, ID	A		FGFR2, TWIST1, karyo		ERF	c.652C>T	p.(Arg218*)	AD iMother	
62	JAC212	m	Father	19	CSO			NA								
	JAC206	f	Mother	19				NA								
	JAC202	m	Proband	19		S, BC (part), BL (part)	Mild ID, supernumerary incisor, broad thumbs and halluces, IQ 70-80, hypotonic (PT)	A		FGFR1, FGFR2, TWIST1 + FISH, ERF, karyo (15q11), FISH 15q						



Table 10.5. (continued)

Family number	Sample ID	Gender	Sample	Hq	Phenotype	Key feature	Additional information	Clinical appearance	Family history	Genes tested previously	Mutation positive			
											Gene/ location	Nucleotide	Protein	Inheritance
63	JAC223	m	Father	19	CSO		Same head shape as child	NA						
	JAC222	f	Mother	19				A +/-						
	JAC203	f	Proband	19		S	Malformed crus helices, bifid nasal top, speech therapy	A		FGFR2, FGFR3, TWIST1, karyo				
64	JAC216	m	Father	19	CSO			NA						
	JAC217	f	Mother	19				A +/-			TWIST1	c.416C>T	p.(Pro139Leu)	AD UK
	JAC204	m	Proband	19		BC, S, M	ATE	A	mother, grand-mother, uncle and cousin head malformation	FGFR2, FGFR3, ERF, SNP array (arr 10p15.3(357,094-873,639) x3;10p15.3(1,193,561-1,389,623)x3 (18))	TWIST1	c.416C>T	p.(Pro139Leu)	AD iMother
65	JAC205	m	Father	19	CSO			NA						
	JAC228	f	Mother	19				NA						
	JAC226	f	Proband	19		RC	Hypermotropia, Crohn	A		FGFR2, FGFR3, TWIST1, ERF, TCF12, SNP array	TLK2	c.779A>G	p.(Lys260Arg)	de novo
66	JAC208	m	Father	19	CC			NA						
	JAC209	f	Mother	19				NA						
	JAC210	f	Proband	19		bilateral cleft and encephalocele	Multiple hand and foot malformations (syndactyly) leading to multiple surgeries	A						

67	JAC251	m	Father	19	CSO														
	JAC215	f	Mother	19															
	JAC214	m	Proband	19		BL, S	Chiari, narrow callosal body, tubes	A											
68	JAC218	m	Father	19	CSO	S	No surgery	A											
	JAC220	f	Mother	19				NA											
	JAC219	m	Proband	19		S	Headache and decreased growth, no papilledema, ICP measurement normal	A											
69	JAC229	m	Father	19	CSO			NA			TCF12	c.1035+5G>C	(p.?)				AD UK		
	JAC306	f	Mother	19				NA											
	JAC221	f	Proband	19		BC and BL (part)	Delayed tooth eruption, mild dental crowding	A			TCF12	c.1035+5G>C	(p.?)				AD if Father		
70	JAC233	m	Father	19	FD			NA											
	JAC232	f	Mother	19				NA											
	JAC311	m	Proband	19		TCL	Tracheostomy, macroglossus, micrognathia, retrognathia, cleft palate, bilateral microtia, preauricular fistula, downslant, small palpebral fissures, choanal atresia, shallow orbits and zygoma	A			TXNL4A, POLR1A, WES								
71	JAC238	m	Father	19				UK											
	JAC237	f		19				UK											
	JAC236	f		19				A											
72	JAC244	f	Mother	19	CSO			NA											
	JAC242	f	Proband	19		LC	Strabismus sursoadductorius L, hypermetropia, mild astigmatism L, mild amblyopia L	A			TCF12, SNP array (arr Xp22.2(16,819,778-17,027,099)x3 (18))								



Table 10.5. (continued)

Family number	Sample ID	Gender	Sample	Hg	Phenotype	Key feature	Additional information	Clinical appearance	Family history	Genes tested previously	Mutation positive			
											Gene/ location	Nucleotide	Protein	Inheritance
73	JAC265	m	Father	19	CSO			NA						
	JAC266	f	Mother	19				NA						
	JAC245	m	Proband	19		RC	PTSS	A		FGFR3, TCF12, ERF				
74	JAC246	m	Father	19	CSO	asymmetry		A +/-						
	JAC247	f	Mother	19		ptosis		NA						
	JAC248	f	Proband	19	RC	RC	Strabismus sursoadductorius R, astigmatism R>L, mild hypermetropia R>L, amblyopia R	A	father, uncle and grand-mother possibly vertical orbital dystopia	TCF12, SNP array (arr Xp22.2(16,819,778-17,027,099)x3 (18))				
75	JAC308	m	Father	19	CSO			NA						
	JAC299	f	Mother	19				NA						
	JAC327	f	Proband	19	LC		Class II/1, agenesis 12 and 22	A		FGFR2, FGFR3, FISH TWIST1, karyo (9ph)				
76	JAC276	f	Mother	19	CSO			NA						
	JAC256	m	Proband	19	M		Papilledema, hypermetropia, astigmatism B	A		FGFR1, FGFR2, FGFR3, TWIST1, karyo				

Table 10.5. (continued)

Family number	Sample ID	Gender	Sample	Hq	Phenotype	Key feature	Additional information	Clinical appearance	Family history	Genes tested previously	Mutation positive			
											Gene/location	Nucleotide	Protein	Inheritance
82	JAC318	m	Father	19	CSO			NA						
	JAC297	f	Mother	19				A						
	JAC286	f	Proband	19		RC	Mild learning difficulties, amblyopia, supernumerary canine	A		FGFR2, FGFR3, TWIST1, TCF12				
83	JAC324	m	Father	19	CSO			NA						
	JAC323	f	Mother	19				A +/-						
	JAC287	f	Proband	19		LC	Hypermetropia B, brain tumour	A		FGFR2, FGFR3, TWIST1, TCF12, SNP array				
84	JAC294	m	Father	19	CSO			NA						
	JAC293	f	Mother	19				NA						
	JAC305	m	Proband	19		BC	Open bite, backache, dyslexia	A		FGFR2, FGFR3, FISH TWIST1 FISH, karyo				
85	JAC296	m	Father	19	CSO			NA						
	JAC295	f	Mother	19				NA						
	JAC289	m	Proband	19		S	Bulging vertex, mild ID, reflux, tracheomalacia, recurrent upper respiratory tract and ear infections, papilledema leading to second surgery, PTSS, eczema, speech and language delay (ST), PDD-NOS, GAF 41-50	A	Cousin (mother's side) S and midface hypoplasia	IL11RA, ERF, array (10p13(13,420,074-13,667,593)x1 dn), WES (c.1163T>C, p.(Leu388Pro) DISC1 (+/-), c.825T>A, p.(Asn275Lys) AMT (+/-), c.1545C>G, p.(Ser515Arg) POMT1 (+/-), c.665G>A, p.(Arg222Gln) LAMA1 (+/-)	del 10p13			

225

Table 10.5. (continued)

Family number	Sample ID	Gender	Sample	Hq	Phenotype	Key feature	Additional information	Clinical appearance	Family history	Genes tested previously	Mutation positive			
											Gene/ location	Nucleotide	Protein	Inheritance
88	JF1	m	Father	18	CSO			A			MSX2	c.443C>T	p.(Pro148Leu)	AD ifather
	JF2	f	Mother	18				NA						
	JF3	m	Proband	18		M, BC	Hypotelorism, maxillary hypoplasia	A	father, uncle, cousins affected	FGFR1, FGFR2, FGFR3, TWIST1, karyo	MSX2	c.443C>T	p.(Pro148Leu)	AD ifather
	JF4	m	Grandfather	18				A			MSX2	c.443C>T	p.(Pro148Leu)	AD UK
	JF5	f	Grandmother	18				NA						
89	JG1	m	Grand Father	18	CC			A		EFNB1				
	JG2	f	Mother	18				A		EFNB1				
	2	f	Aunt	18				NA						
	8	m	Father	18	CSO			NA						
90	7	f	Mother	18			Enlarged late-closing fontanel, mild ID, vertigo, clumsy tandem gait, MRI: atrophy of the rostral part of the cerebellum and pons, similar to, but less severe than son	A			ZIC1	c.1198G>C	p.(Gly400Arg)	AD UK
	6	m	Proband	18		BC	Beaked nose, high palate, downslant and ptosis of the eyes, mild ID, hypotonia with joint laxity, convergent strabismus B, headaches, EEG: irregular and diffuse disordered background pattern with accentuated frontal dysfunction, MRI: atrophy of the cerebellum, branchium pontis and temporo-basal lobes with widened sulci	A			ZIC1	c.1198G>C	p.(Gly400Arg)	AD IMother

90	5	m	Cousin	18	CSO	BC + parietal foramina	Microcephalic, brachycephalic, ptosis R, downslanting palpebral fissures, divergent strabismus (tenotomy), high narrow palate, symmetrical defects palpable over the occipito-parietal region, mild ID, axial hypotonia, mild tapering of the fingers, clinodactyly of the 4th and 5th toes, sacral dimple, small teeth, WISCIII: TIQ 89 VIQ 96 PIQ 84. CBCL 6-18, MRI: fourth ventricle and both superior cerebellar peduncles mildly enlarged, a prominent great cerebral vein and inferior sagittal sinus, small posterior fossa, tent-shaped tentorium cerebelli, short and steep straight sinus, mild hypoplasia of the dorsal part of the pons and inferior part of the cerebellar vermis	A		FGFR1, FGFR2, FGFR3, MSX2, karyo	ZIC1	c.1198G>C	p.(Gly400Arg)	AD (Mother)
91	10	m	Father	18	FD		Scleral show	A			TXNL4A	c.258-2A>G	(p.?)	
	11	f	Mother	18				NA			TXNL4A	chr18:g.77748581_ 77748614del (type 1Δ)		
	9	f	Proband	18		TCL	Bilateral choanal atresia, asymmetry of the face, ear tags R, hypoplasia of the mandible R, maxilla R and infra-orbital rim R, short palpe- bral fissures, upslant of the eyes, eyelashes at the outer parts of the lower eyelids longer than on the inner parts, dimple at 1/3 of the outer canthus of both eyes, small choroid coloboma L, aplasia of the puncta lacrimalis, microstrabismus, amblyopia	A		TCOF1, CHD7, karyo, SNP array	TXNL4A	c.[258-2A>G];[type 1Δ]		AR (bi- allelic)



Table 10.5. (continued)

Family number	Sample ID	Gender	Sample	Hg	Phenotype	Key feature	Additional information	Clinical appearance	Family history	Genes tested previously	Mutation positive			
											Gene/location	Nucleotide	Protein	Inheritance
92	12	m	Father	18	CSO			NA			TCF12 del	c.1745 + 4562_1978 + 3153del		AD UK
	13	f	Mother	18	CSO			NA						
	14	f	Proband	18		BC	Myopia, divergent growth pattern and crowding of teeth	A		FGFR1, FGFR2, FGFR3, TWIST1 + FISH, TCF12, karyo	TCF12 del	c.1745 + 4562_1978 + 3153del		AD fFather
	45	f	Aunt	18		BC		A			TCF12 del	c.1745 + 4562_1978 + 3153del		AD UK
93	15	m	Father	18	CSO			NA						
	16	f	Mother	18		LC		A			TCF12 del	c.391 – 5871_1746 – 1795del		AD UK
	17	m	Proband	18		RC	Bilateral camptodactyly of the fifth fingers, divergent strabismus (tenotomy), recurrent airway infections (adenoidectomy), febrile seizures, mild learning problems VIQ 82, PIQ 64, GIQ 74	A		FGFR1, FGFR2, FGFR3, TWIST1 + FISH, TCF12, karyo	TCF12 del	c.391 – 5871_1746 – 1795del		AD iMother
94	18	m	Father	18	CSO			NA						
	19	f	Mother	18				NA						
	20	m	Proband	18		LC		A		FGFR2, FGFR3, TWIST1 + FISH, karyo (9ph)				
	21	m	Brother	18		LC	Short frenulum lingualis, micro strabismus R, mild hypermetropia, amblyopia R	A		FGFR1, FGFR2, FGFR3, TWIST1, karyo				

Table 10.5. (continued)

Family number	Sample ID	Gender	Sample	Hg	Phenotype	Key feature	Additional information	Clinical appearance	Family history	Genes tested previously	Mutation positive			
											Gene/ location	Nucleotide	Protein	Inheritance
S4	JAC252	m	Proband	19	CC	Hemi L	Proboscis, choanal atresia L, coloboma, tear duct aplasia	A						
S5	JAC254	m	Proband	19	CSO	S	Tubes, ATE, papilledema, increased ICP on measurement, leading to 2nd surgery, developmental delay, social delay, GAF 61–70, conductive hearing loss R, MRI: Chiari and increased CSF surrounding both optic nerves	A		FGFR1, FGFR2, FGFR3, ERE, TWIST1 + FISH, karyo				
S6	JAC281	f	Proband	19	CSO	RC, LC (part) and NSOP	Tenotomy St. elsewhere	A	father ptosis	FGFR3, TWIST1, TCF12				
S7	JAC282	f	Proband	19	CSO	RC		A		FGFR1, FGFR2, FGFR3 (1959+22G>A), FISH TWIST1, karyo, TCF12				
S8	JAC283	f	Proband	19	CSO	RC	Anisohypermetropia and astigmatism L>R	A		FGFR1, FGFR2, FGFR3 (1535-29insGCC), TWIST1 + FISH, TCF12				
S9	JAC284	m	Proband	19	CSO	LC	Strabismus sursoaductorius L (tenotomy), V motility, torticollis, special education, behavioural deficit, circumcised	A		FGFR1, FGFR2 (1673-12 C>T), FGFR3, TWIST1, TCF12, karyo				
S10	JAC285	f	Proband	19	CSO	RC + NSOP R		A		FGFR2, FGFR3, TWIST1, TCF12, karyo				

A = Affected, A +/- = Probably affected, AD = Autosomal dominant, ADD = Attention deficit disorder, ADHD = Attention deficit hyperactivity disorder, AR = Autosomal recessive, ASD = Atrial septal defect, ATE = Adenotonsillectomy, B = Both, BC = Bicornual, BL = Bilateral lambdoid, BPD = Bronchopulmonary dysplasia, CC = Craniofacial cleft, CSO = Craniosynostosis, dig = Digit, EEG = Electroencephalogram, f = Female, FD = Facial dysostosis, FISH = Fluorescent *in situ* hybridisation, FND = Frontonasal dysplasia, Hemi = Heminose, ICP = Increased intracranial pressure, ID = Intellectual disability, iFather = Inherited from father, iMother = Inherited from mother, karyo = Karyotype, L = Left, LC = Left coronal, LFIll = Le Fort III, LL = Left lambdoid, m = Male, M = Metopic, meta = Metabolic tests, MPS II = Mucopolysaccharidosis type II, na = Not applicable, NA = Not affected, NSOP = Nonsynostotic occipital plagiocephaly, n VIII = 8th cranial nerve, OMA = Acute otitis media, OME = Otitis media with effusion, OSA = Obstructive sleep apnoea, PAN = Pansynostosis, (part) = Suture partially fused, PDD-NOS = Pervasive developmental disorder-not otherwise specified, PMR = Psychomotor retardation, PT = Physical therapy, PTSS = Post traumatic stress syndrome, R = Right, RC = Right coronal, RL = Right lambdoid, S = Sagittal, ST = Speech therapy, TCL = Treacher-Collins like, TMJ = Temporomandibular joint syndrome, UK = Unknown, UPD = Uniparental disomy, VSD = Ventricular septal defect, WES = Whole exome sequencing, Y = Years, +FISH = Gene sequenced and fluorescent *in situ* hybridisation performed.





Chapter 11

Summary

In this era of rapidly developing next generation sequencing, the aim of this thesis is to study the genetic alterations that cause congenital craniofacial malformations with a special emphasis on the use of next generation sequencing.

Chapter 1 is an introduction to craniofacial genetics. It describes the subdivision of craniofacial malformations in:

1. Craniosynostosis: the premature fusion of calvarial sutures.
2. Craniofacial clefts: a disturbed bone outgrowth or a fusion defect of various embryologic facial prominences.
3. Facial dysostosis: underdevelopment of structures derived from the first and second pharyngeal arches.

To gain a better understanding of these malformations, knowledge of the anatomy of the human head and face and its embryological development is essential. The embryological development is driven by the genetic code, which is written in DNA. Errors in the DNA can occur during mitosis (normal cell division), but also during meiosis (the formation of germ cells). These errors can lead to heritable diseases. Until now, most of the identified causes of heritable craniofacial malformations are dominant. However, more and more causes are identified that are showing a recessive mode of inheritance. And even polygenic causes are implied. So besides the current targeted gene specific tests, new clever sequencing and analyses techniques are needed that test all genes and modes of inheritance at the same time. Next generation sequencing provides the answer to this. One of these next generation sequencing techniques is whole genome sequencing, offered by Complete Genomics for example, studying the complete human genome. Using whole genome sequencing, a huge amount of data is produced that need to be filtered cleverly to identify the genetic cause of a craniofacial malformation. Knowing the precise molecular diagnosis is essential for genetic counselling, especially concerning recurrence risk for the parents and inheritance for the proband. Also, the molecular diagnosis has implications for clinical management.

Therefore, the following aims were defined for this thesis:

1. Identify new genetic causes in genes that have been previously associated with craniofacial malformations.
2. Use next generation sequencing to identify novel genetic causes in genes that have not previously been associated with craniofacial malformations.
3. Study the use of next generation sequencing as a diagnostic tool in patient cohorts.



The first part of this thesis studies genes that have been previously associated with craniofacial malformations. We focus predominantly on mutations in *FGFR2*, a Fibroblast Growth Factor Receptor, that cause Crouzon syndrome if mutated.

Chapter 2 describes the identification of a novel missense mutation in *FGFR2* (c.812G>T, p.(Gly271Val)) in two individual patients with Crouzon syndrome. The first patient had bicoronal and sagittal suture synostosis and exorbitism directly after birth. The second patient was first referred at the age of 20 years with mild retrusion of the forehead, exorbitism, mild orbital dystopia, and maxillary hypoplasia. No information was available regarding the presence of craniosynostosis. In addition, a *de novo* mutation in *FGFR2* (c.1851G>C, p.(Leu617Phe)) was described that had been identified once before. This mutation occurred in a patient with sagittal suture synostosis, bilateral undescended testes, OSA and maxillary hypoplasia. In the same chapter, the results of a sequencing study of *FGFR2* are described. In 124 patients with syndromic craniosynostosis, all coding exons and exon/intron junctions of *FGFR2* have been analysed. By expanding the analysis, two previously described mutations have been identified and four unclassified variants, that are considered non-pathogenic. Hence, new mutations are still identified in *FGFR2*.

Chapter 3 describes the identification of apparently synonymous variants in *FGFR2* (c.1083A>G, p.(Pro361Pro) and c.1083A>T, p.(Pro361Pro)) in two families. The mutation carriers in both families exhibit features of mild Crouzon syndrome. The synonymous variants occur at the donor splice site of exon IIIc of *FGFR2*. Due to these variants the use of a cryptic splice site in exon IIIc is expected that leads to an in-frame deletion of 17 amino acids. Amplification and sequencing of cDNA from the patients shows the use of the cryptic splice donor within exon IIIc in the mutant allele and also complete skipping of exon IIIc. These results demonstrate that these sequence changes are pathogenic mutations.

In the first part of this thesis we have also focused on *EFNB1*. It has been demonstrated that mutations in this gene cause craniofrontonasal syndrome (CFNS). **Chapter 4** studies the phenotype of 23 patients with a pathogenic mutation in *EFNB1* by a cross-sectional observational study. Patients with CFNS have consistent features like hypertelorism, a certain degree of longitudinal ridging and/or splitting of nails of at least one digit or toe, a certain degree of webbed neck and a clinodactyly of one or more toes. Also, abnormal facial proportions have been observed in all patients (relatively small upper face compared to the width of the face, short nose, and a relatively long upper lip).

The second part of this thesis studies the identification of novel genetic causes of craniofacial malformations using next generation sequencing and describes the phenotype of these malformations.

Chapter 5 discusses the identification of mutations in *TCF12* as a frequent cause of coronal craniosynostosis by whole exome sequencing. Dideoxy sequencing of 340 samples, has led to the identification of another 35 heterozygous mutations. Analysis of the phenotype of the index patients shows that mutations predominantly occur in patients with coronal synostosis. The clinical features are suggestive of Saethre-Chotzen syndrome. And most of the patients have a benign clinical course. Analysis of the family members of the index patients has led to the identification of another 35 mutation-positive individuals. Only 16 of them have craniosynostosis or other suspicious clinical features, indicating a substantial non-penetrance. *TCF12* encodes a class I E protein that heterodimerises with class II basic Helix-Loop-Helix proteins such as *TWIST1*. Functional analysis has shown that *TCF12* and *TWIST1* act synergistically in a transactivation assay, but this effect is lower in the presence of *TCF12* missense mutations. Mouse models have shown that mice heterozygous for both *Tcf12* and *Twist1* suffer from severe coronal synostosis. This suggests that the total quantity of *TCF12*/*TWIST1* heterodimers plays an important role in coronal suture development. So if a patient suffers from coronal suture synostosis and gene-specific testing of *FGFR3* and *TWIST1* is negative, *TCF12* should be tested.

TCF12-related craniosynostosis can also be caused by small heterozygous loss-of-function mutations in *TCF12*. The identification of large intragenic rearrangements causing *TCF12*-related craniosynostosis is described in **Chapter 6**. Using whole genome sequencing, three large (84.9, 8.6 and 5.4 kb) intragenic exon deletions are identified in *TCF12*. Deletion-specific PCRs have confirmed these deletions. The deletions co-segregate with the disorder and non-penetrance has been shown (as has been described in chapter 5). One of the deletions lies 3' of the region that encodes the bHLH domain. cDNA analysis of this deletion indicates skipping of exon 20. This patient is the first patient described with increased intracranial pressure and synostosis of all vault sutures (except for the metopic suture). In parallel, a heterozygous tandem duplication (11.3 kb) has been identified that includes exons 19 and 20 of *TCF12*. Analysis of the cDNA reveals two relatively weak fragments, indicating splicing from exon 20 to the duplicated exon 19 in one fragment and an additional neo-exon in the other. Analysis of the normal sequences of the rearrangements indicates nonhomologous end joining as the most likely cause. Since 4 of 108 (3.7%) individuals with coronal synostosis and previously negative genetic testing have deletions in *TCF12*, screening for larger rearrangements in *TCF12* seems essential, if *TCF12*-related craniosynostosis is suspected.

Chapter 7 discusses the identification with next generation sequencing of five gain-of-function mutations in *ZIC1* that are associated with coronal craniosynostosis and learning disabilities. All mutations identified in *ZIC1* are located in the highly conserved C-terminus of the protein. Four nonsense mutations have arisen *de novo*



(post-zygotically in one case) and one missense mutation has been identified in a family consisting of six affected individuals in three generations. Analysis of the phenotype shows bicoronal synostosis with severe brachycephaly, sometimes lambdoid synostosis, and mild to severe learning disabilities. Also, progressive scoliosis is seen. CT and MRI brain scans show agenesis of the corpus callosum, dilated lateral ventricles, peaked tentorium, hypoplastic pons, cerebellum with prominent cerebellar folia and enlarged foramen magnum. Functional analysis of *ZIC1* indicates escape from nonsense-mediated decay and suggests a gain-of-function mechanism. Also, the function of *Xenopus zic1* has been studied by injecting several truncated constructs, leading to disrupted *en-2* expression. Using *in situ* hybridisation, a transient zone of *Zic1* expression is identified in the supraorbital region that overlap with *En1*. This indicates an early instructive role for *Zic1* in the supraorbital regulatory centre that constitutes the zone from which cells migrate and populate the coronal suture. Combining these results, it seems likely that the coronal synostosis phenotype might be attributable to alteration of EN1 expression in the supraorbital regulatory centre. If coronal suture synostosis in combination with learning disabilities is seen, *ZIC1* should be tested.

Lastly, **chapter 8** focuses on the identification by whole genome sequencing of mutations in *TXNL4A* as a cause of Burn-McKeown syndrome (BMKS) and choanal atresia. A patient with clinical features of BMKS and her parents have been analysed by whole genome sequencing, identifying a splice-site mutation and a 34 base pair promoter deletion in *TXNL4A*. Analysis of the cDNA indicates that the allele carrying the splice-site mutation is not expressed, while the expression of the allele carrying the promoter deletion has been reduced. Dideoxy-sequence analysis of a cohort of 19 patients with clinical features of BMKS and 17 patients with isolated choanal atresia identified the same splice-site mutation and promoter deletion in a patient with BMKS. Additionally, a homozygous promoter deletion has been identified in a patient with isolated choanal atresia and another homozygous promoter deletion has been identified in two cousins with BMKS. This demonstrates the importance of screening for mutations in *TXNL4A* in patients with (mild) clinical features of BMKS.

The third part of this thesis studies the use of next generation sequencing as a diagnostic tool in patient cohorts.

Chapter 9 describes the use of next generation sequencing (both exome and whole genome sequencing) in craniosynostosis. Subjects with craniosynostosis have been enrolled where previous molecular genetic testing has been negative. A total of 40 cases and, if available, parental samples, have been enrolled. Thirty-seven samples have been exome sequenced and 3 samples by whole genome sequencing. Data have been analysed based on all likely modes of inheritance and for variants in 57 genes

recurrently mutated in craniosynostosis. Variants have been confirmed by dideoxy sequencing. Mutations have been identified in 15 of the 40 cases (37.5%); 13 mutations in confirmed disease genes and at least two in novel disease-associated genes. Many of the mutations are found in genes that are rarely associated with craniosynostosis. In some of these cases, achieving a precise molecular diagnosis has had immediate implications for genetic counselling and for clinical management.

Therefore, it seems worthwhile to apply next generation sequencing. As shown by the findings of mutations in at least two likely novel craniosynostosis-genes, an additional benefit of this strategy is that new disease loci may be identified.

Taking these findings together we may conclude that:

1. Novel mutations are still found in genes known to be associated with craniofacial malformations.
2. Using next generation sequencing, more genes are associated with craniofacial malformations.
3. The use of next generation sequencing is appropriate not only in genetic research but also as a diagnostic tool.

Improving the knowledge concerning craniofacial genetics can lead to a future with improved diagnostic and therapeutic strategies.





Chapter 12

Dutch summary

Nu next generation sequencing zich heel snel ontwikkelt, is het doel van dit proefschrift om de genetische oorzaken van aangeboren schedel- en aangezichtsafwijkingen verder te onderzoeken en dan in het bijzonder door middel van next generation sequencing.

Hoofdstuk 1 geeft een introductie in de craniofaciale genetica. Het beschrijft de onderverdeling van aangeboren schedel- en aangezichtsafwijkingen in:

1. Craniosynostose: het te vroeg sluiten van de schedelnaden.
2. Schedel- en aangezichtsspleten (clefts): waarbij sprake is van bijvoorbeeld een verstoorde bot uitgroei of een mislukte fusie van verschillende embryologische prominentia.
3. En faciale dysostose: waarbij sprake is van een onderontwikkeling van de structuren die hun oorsprong vinden in de eerste en tweede kieuwboog.

Om een beter begrip te krijgen van deze aandoeningen, is kennis van de normale anatomie en de embryologische ontwikkeling van het hoofd en aangezicht essentieel. De embryologische ontwikkeling wordt aangestuurd door DNA. Foutjes in het DNA kunnen ontstaan tijdens de mitose (de normale celdeling), maar ook tijdens de meiose (de vorming van kiemcellen). Deze foutjes kunnen leiden tot erfelijke aandoeningen. Tot nu toe zijn de meeste geïdentificeerde oorzaken van schedel- en aangezichts-aandoeningen dominant, echter meer en meer worden ook recessief overervende oorzaken geïdentificeerd en er wordt zelfs gespeculeerd over polygene oorzaken. Dus naast de huidige gen specifieke diagnostiek, waarbij slechts 1 gen per test wordt onderzocht, zijn sequencing en analyse technieken nodig, die alle genen en overervingsmanieren in 1 keer kunnen testen. Met next generation sequencing kan dit. Een van deze next generation sequencing technieken is whole genome sequencing, een techniek waarbij het gehele genoom wordt onderzocht in 1 test. Deze techniek wordt onder andere aangeboden door Complete Genomics. Door middel van whole genome sequencing worden grote hoeveelheden data geproduceerd die op een slimme manier gefilterd moeten worden om de genetische oorzaak van bijvoorbeeld schedel- en aangezichts-aandoeningen te kunnen identificeren.

Als de exacte moleculaire oorzaak bekend is, kunnen patiënten beter gecounseld worden, vooral over het herhalingsrisico voor de ouders en de erfelijkheid voor de patiënt. Ook kan de moleculaire diagnose gevolgen hebben voor de behandeling.

De volgende doelen zijn gesteld voor dit proefschrift:

1. Identificeren van nieuwe genetische oorzaken in genen die eerder al geassocieerd zijn met schedel- en aangezichts-aandoeningen.
2. Door middel van next generation sequencing nieuwe genetische oorzaken identificeren in genen die nog niet geassocieerd zijn met schedel- en aangezichts-aandoeningen.



3. Het gebruik van next generation sequencing voor de genetische diagnostiek van schedel- en aangezichtsafwijkingen bestuderen in een patiënten cohort.

Het eerste gedeelte van dit proefschrift gaat over genen die eerder al geassocieerd zijn met aangeboren schedel- en aangezichtsafwijkingen. We focussen met name op mutaties in *FGFR2*, een Fibroblast Growth Factor Receptor. Indien hier een mutatie in optreedt, kan het klinisch beeld van Crouzon syndroom ontstaan.

Hoofdstuk 2 beschrijft de identificatie van een nieuwe missense mutatie in *FGFR2* (c.812G>T, p.(Gly271Val)) in twee patiënten met Crouzon syndroom die geen familie van elkaar zijn. De eerste patiënt heeft sinds zijn geboorte synostose van beide coronanaden, synostose van de sagittaal naad en exorbitisme. De tweede patiënt is pas op latere leeftijd doorverwezen (20 jaar) met milde retrusie van het voorhoofd, exorbitisme, milde orbitale dystopie en hypoplasie van de maxilla. Het is onduidelijk of eerder sprake is geweest van craniosynostose. Daarnaast wordt een *de novo* mutatie in *FGFR2* (c.1851G>C, p.(Leu617Phe)) beschreven die 1 keer eerder is aangetoond. Deze mutatie komt voor bij een patiënt met synostose van de sagittaal naad, niet-ingedaalde testes, OSAS en hypoplasie van de maxilla. In hetzelfde hoofdstuk, worden de resultaten gepresenteerd van een sequencing studie van *FGFR2* waarbij alle coderende exonen en ook de exon/intron overgangen worden geanalyseerd in het DNA van 124 patiënten met syndromale craniosynostose. Door deze uitbreiding van de analyse, zijn twee mutaties gevonden en vier (niet-pathogene) unclassified variants. Kortom, er worden nog steeds nieuwe mutaties geïdentificeerd in *FGFR2*.

Hoofdstuk 3 beschrijft de identificatie van twee ogenschijnlijk synonieme varianten in *FGFR2* (c.1083A>G, p.(Pro361Pro) en c.1083A>T, p.(Pro361Pro)) in patiënten met milde kenmerken van Crouzon syndroom. De varianten liggen ter plaatse van de donor splice site van exon IIIc van *FGFR2*. Door analyse van het cDNA van de twee patiënten wordt aangetoond dat het gehele exon IIIc wordt overgeslagen (exon skipping), wat aannemelijk maakt dat deze varianten de pathogene mutaties zijn.

Naast *FGFR2* kijken we in het eerste deel van dit proefschrift ook naar *EFNB1*. Eerder is aangetoond dat mutaties in dit gen kunnen leiden tot het craniofrontonasaal syndroom (CFNS). **Hoofdstuk 4** bestudeert het fenotype van 23 patiënten met een pathogene mutatie in *EFNB1* door middel van een cross-sectioneel observationeel onderzoek. Patiënten met CFNS kunnen kenmerken vertonen zoals hypertelorisme, longitudinale ribbels op de nagels of zelfs gespleten nagels van minstens 1 vinger of teen, enige webbing van de nek en clinodactylie van 1 of meer tenen. Daarnaast blijken de proporties van het aangezicht afwijkend in alle patiënten (waarbij het bovenste deel van het gezicht relatief klein is in vergelijking met de breedte van het gezicht, de neus korter is en er een relatief lange bovenlip bestaat).

Het tweede deel van dit proefschrift beschrijft de identificatie door middel van next generation sequencing van nieuwe genetische oorzaken van schedel- en aangezichtsafwijkingen en het fenotype van deze aandoeningen.

Hoofdstuk 5 beschrijft de ontdekking, door middel van whole exome sequencing, van mutaties in *TCF12* als een frequente oorzaak van synostose van de corona naden. Door daarna dideoxy sequencing van *TCF12* te verrichten op 340 andere DNA monsters zijn nog eens 35 mutaties in *TCF12* gevonden. Analyse van het fenotype van de index patiënten toont aan dat er vooral sprake is van synostose van de corona naden. De klinische kenmerken lijken enigszins op Saethre-Chotzen syndroom. Verder hebben de meeste patiënten een redelijk goede kliniek. Analyse van de familieleden van de index patiënten heeft geleid tot de identificatie van nog eens 35 mutatie-positieve personen. Slechts 16 van hen hebben craniosynostose of andere verdachte kenmerken, wat verminderde penetrantie aannemelijk maakt. *TCF12* codeert voor een klasse I E eiwit dat heterodimeren vormt met klasse II basic Helix-Loop-Helix eiwitten zoals TWIST1. Een transactivatie assay toont dat TCF12 en TWIST1 synergistisch werken, maar dat dit synergistische effect lager is wanneer er missense mutaties zitten in *TCF12*. Een muizenmodel toont aan dat muizen die zowel heterozygoot zijn voor een mutatie in *Tcf12* als in *Twist1* ernstige coronale synostose hebben. Dit alles suggereert dat de totale hoeveelheid heterodimeren van TCF12/TWIST1 een belangrijke rol speelt in de ontwikkeling van coronale synostose. Als een patiënt coronale synostose heeft en gen-specifieke testen voor mutaties in *FGFR3* en *TWIST1* negatief zijn, dan moet *TCF12* getest worden.

Waar in hoofdstuk 5 wordt beschreven dat *TCF12*-gerelateerde craniosynostose veroorzaakt kan worden door kleine heterozygote loss-of-function mutaties in *TCF12*, wordt in **hoofdstuk 6** de identificatie van grote rearrangements in het *TCF12*-gen als oorzaak van *TCF12*-gerelateerde craniosynostose beschreven. Door middel van whole genome sequencing zijn drie grote intragene exon deleties gevonden (84.9, 8.6 en 5.4 KB). De deleties zijn bevestigd door middel van deletie-specifieke PCRs. De deleties cosegregeren met de aandoening, terwijl verminderde penetrantie ook wordt gezien (net als in hoofdstuk 5). Een van de deleties ligt 3' van de regio die codeert voor het bHLH domein. cDNA analyse toont aan dat deze deletie skipping van exon 20 veroorzaakt. De patiënt met deze deletie is de eerste patiënt met TCF12-gerelateerde craniosynostose en verhoogde intracranieële druk en synostose van alle schedelnaden (behoudens de metopica naad). Tevens wordt een heterozygote tandem duplicatie (11.3 KB) beschreven die zowel exon 19 als 20 dupliceert. cDNA analyse toont twee relatief zwakke fragmenten, wat doet suggereert dat zowel sprake is van splicing van exon 20 naar het gedupliceerde exon 19 en dat het andere fragment bestaat uit een neo-exon. Analyse



van de sequenties van de rearrangements doet vermoeden dat nonhomologous end joining de meest waarschijnlijke oorzaak is. Aangezien 4 van de 108 (3.7%) personen met coronale synostose en negatieve gen-specifieke testen, deleties hebben in *TCF12*, lijkt screening voor grote rearrangements in *TCF12* essentieel, wanneer gedacht wordt aan *TCF12*-gerelateerde craniosynostose.

Hoofdstuk 7 beschrijft de identificatie door middel van next generation sequencing van vijf mutaties in *ZIC1* die geassocieerd zijn met corona naad synostose en leerproblemen. Alle mutaties bevinden zich in het zeer geconserveerde C-terminus van het eiwit. Vier nonsense mutaties zijn *de novo* en 1 missense mutatie komt voor in een familie van zes aangedane personen in drie generaties. Analyse van het fenotype toont synostose van de corona naden met ernstige brachycephalie, soms is er tevens sprake van synostose van de lambdoid naden en patiënten kunnen milde tot ernstige leerproblemen hebben. Ook wordt progressieve scoliose gezien. Op de CT en MRI hersenscans wordt agenesie van het corpus callosum gezien, gedilateerde zijventrikels, een hoger en piekend tentorium, een hypoplastische pons, een cerebellum met prominente cerebellaire folia en een verwijd foramen magnum. Functionele analyse van *ZIC1* impliceert dat er geen nonsense mediated decay optreedt en dat er sprake is van een gain-of-function mechanisme. De functie van *Xenopus zic1* is bestudeerd door middel van het injecteren van verschillende getrunceerde constructen, waardoor *en-2* expressie wordt verstoord. Door middel van *in situ* hybridisatie, wordt in de supra orbitale regio overlap gezien van de gebieden waar *Zic1* en *En1* tot expressie komen. Dit suggereert een rol voor *Zic1* tijdens de vroege ontwikkeling in het supra orbitale regulatie centrum van waaruit de cellen migreren die uiteindelijk de corona naden bevolken. Deze resultaten tezamen impliceren dat de synostose van de corona naden mogelijk toe te schrijven is aan een verandering in de expressie van EN1 in het supra orbitale regulatie centrum. Bij patiënten met synostose van de corona naden en leerproblemen dient getest te worden voor mutaties in *ZIC1*.

Het laatste hoofdstuk van dit deel, **hoofdstuk 8**, beschrijft de vondst van mutaties in *TXNL4A* als een oorzaak van Burn-McKeown syndroom (BMKS) en choanen atresie. Het DNA van een patiënte met klinische kenmerken van BMKS en dat van haar ouders is geanalyseerd middels whole genome sequencing. Zodoende zijn een splice site mutatie en een promoter deletie van 34 basenparen in *TXNL4A* ontdekt. Analyse van het cDNA toont dat het allel met de splice site mutatie niet tot expressie komt en dat de expressie van het allel met de promoter deletie verminderd is. Door middel van dideoxy sequencing van een cohort van 19 patiënten met klinische kenmerken van BMKS en 17 patiënten met geïsoleerde choanen atresie zijn dezelfde splice site mutatie en promoter deletie gevonden in een patiënt met BMKS. Tevens, is een homozygote promoter deletie gevonden in een patiënt met geïsoleerde choanen atresie en een andere homozygote

promoter deletie in het DNA van een neef en een nicht met milde kenmerken van BMKS. Deze bevindingen tonen aan dat het belangrijk is om te screenen voor mutaties in *TXNL4A* in patiënten met (milde) klinische kenmerken van BMKS.

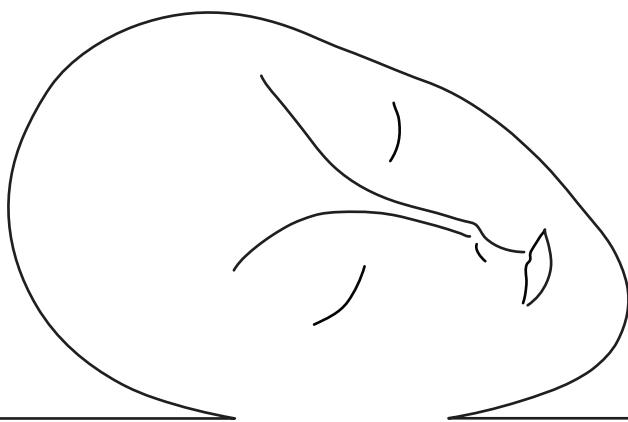
Het derde deel van dit proefschrift beschrijft het gebruik van next generation sequencing in de genetische diagnostiek van patiënten met schedel- en aangezichtsandoeningen.

In **hoofdstuk 9** wordt het gebruik van next generation sequencing beschreven (zowel exome sequencing als whole genome sequencing) bij patiënten met craniosynostose en negatieve gen-specifieke testen. In totaal is het DNA van 40 patiënten geïncubeerd en, indien beschikbaar, ook het DNA van hun ouders. Zevenendertig monsters zijn gesequenced middels exome sequencing en drie middels whole genome sequencing. De data zijn geanalyseerd voor alle mogelijke overervingspatronen en voor varianten in de 57 bekende craniosynostose genen. De gevonden varianten zijn bevestigd met dideoxy sequencing. Er zijn mutaties gevonden in 15 van de 40 index patiënten (37,5%); 13 mutaties zijn gevonden in bekende genen en ten minste twee mutaties zijn gevonden in nieuwe genen. Veel van de mutaties zijn gevonden in genen die slechts af en toe geassocieerd zijn met craniosynostose. In enkele gevallen, heeft de ontdekking van de exacte moleculaire diagnose consequenties gehad voor de genetische counseling en de behandeling. Al met al lijkt het zeker de moeite waard om next generation sequencing in te zetten. Een bijkomend voordeel van next generation sequencing is dat er ook nieuwe craniosynostose genen gevonden kunnen worden. Samenvattend kan gesteld worden dat:

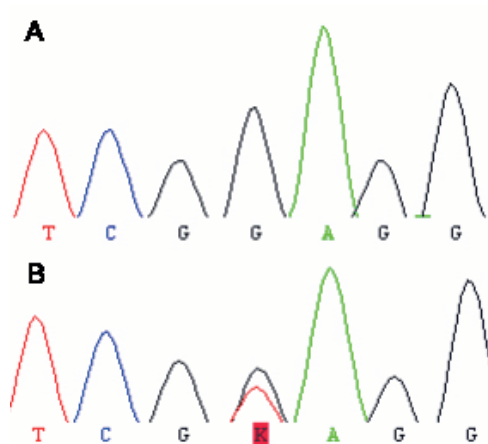
1. Er nog steeds nieuwe mutaties worden gevonden in genen die reeds geassocieerd zijn met schedel- en aangezichtsandoeningen.
2. Er door middel van next generation sequencing, steeds meer genetische oorzaken van schedel- en aangezichtsandoeningen worden gevonden.
3. En dat next generation sequencing geschikt is voor zowel genetisch onderzoek als voor de genetische diagnostiek.

Meer inzicht in de craniofaciale genetica kan leiden tot een gouden toekomst met verbeterde diagnostiek en daarmee ook verbeterde behandel mogelijkheden.



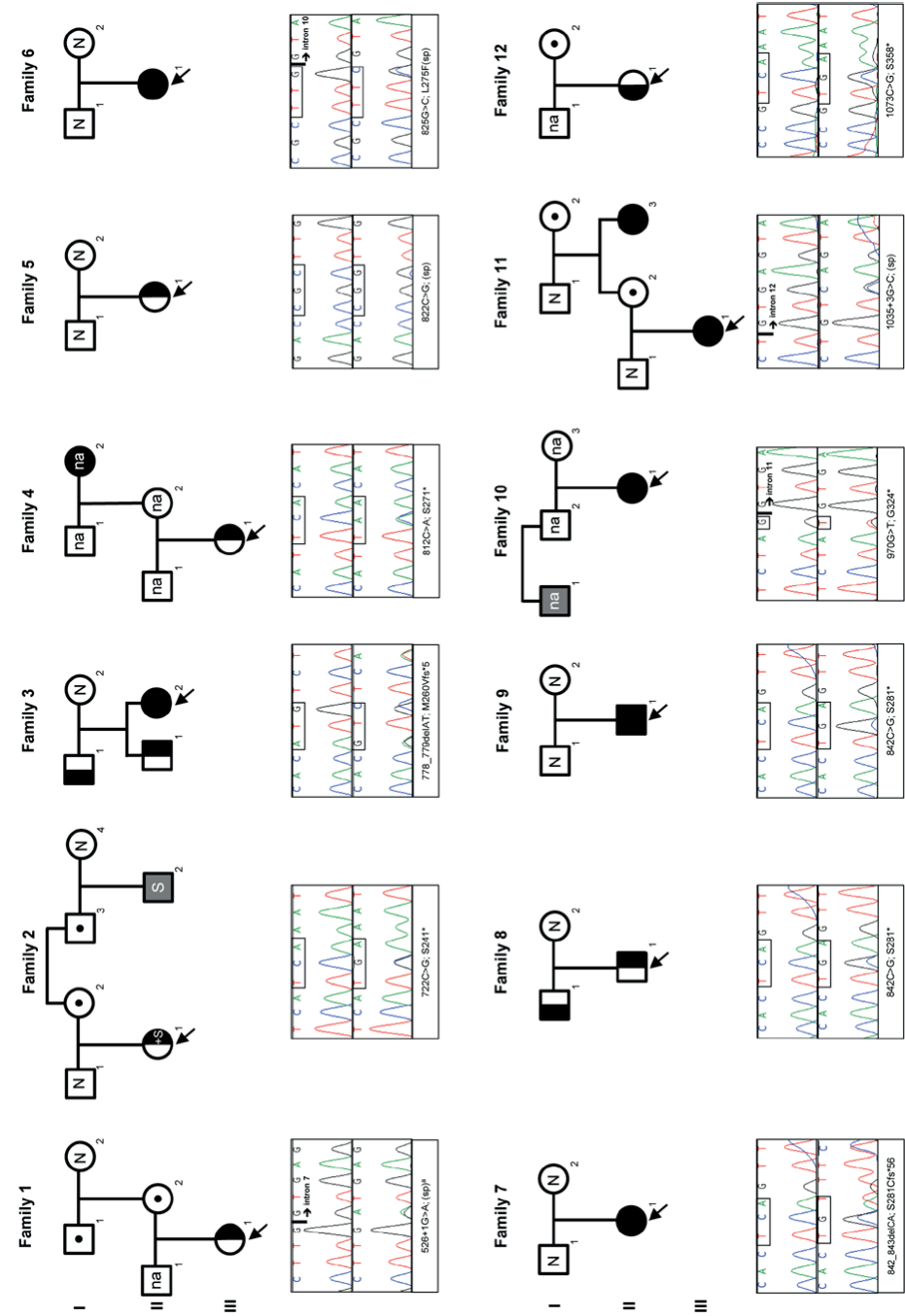


Appendices



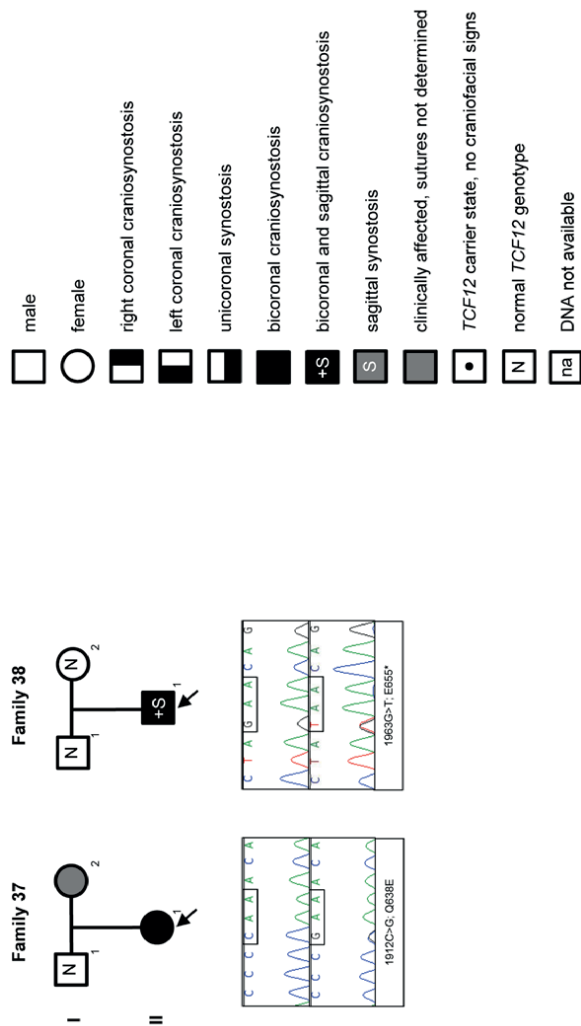
Supplementary Figure 2.1. Sequence electropherogram of Patient 1. A: normal sequence. **B:** mutated sequence.





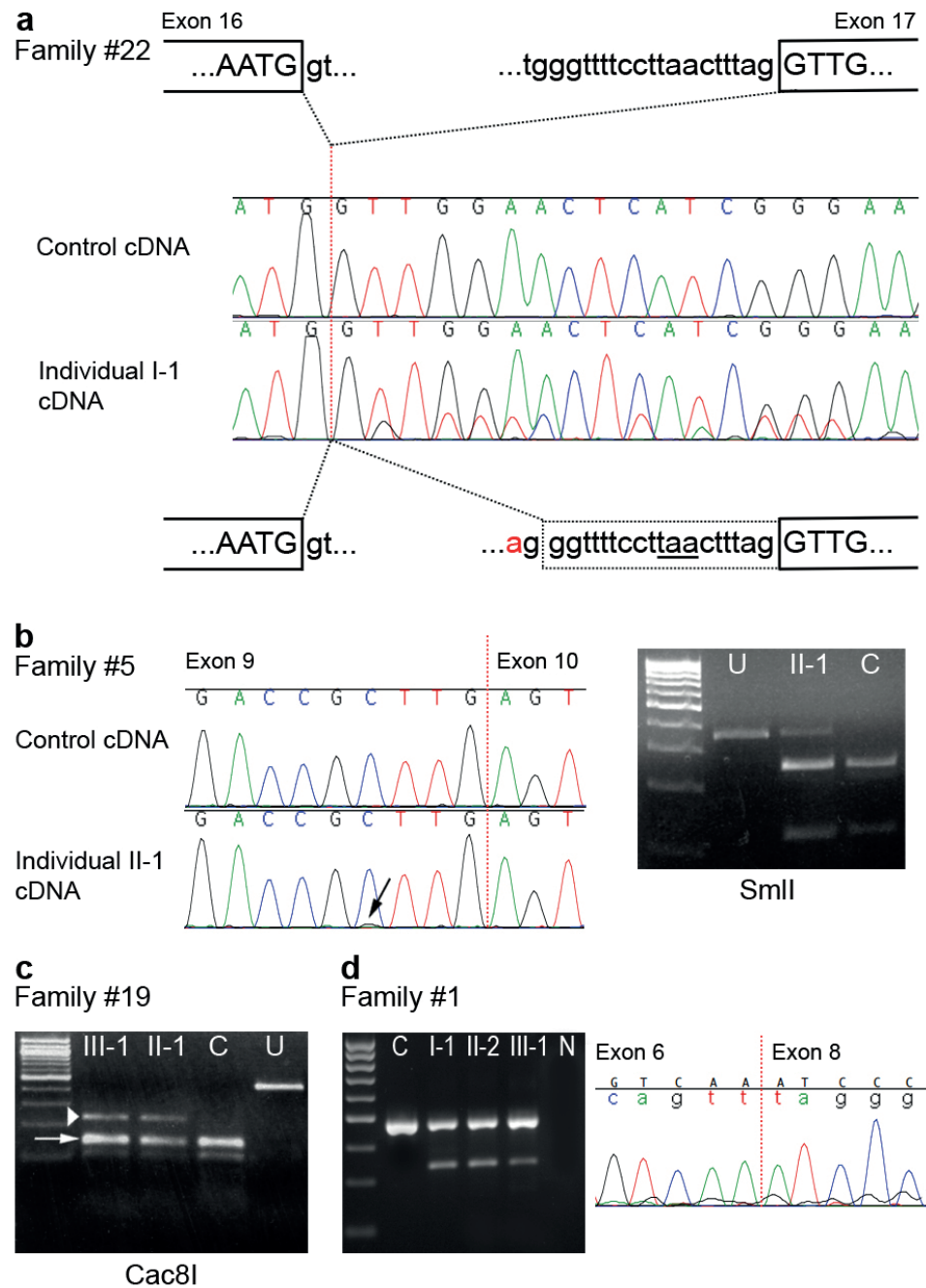






Supplementary Figure 5.1. Pedigrees and DNA sequence analysis of the 38 families in which TCF12 mutations were identified. For each family the individuals analysed in the pedigree (see key to symbols) are shown together with a representative sequence chromatogram for a normal control (above) and an affected individual (below); (rev) indicates sequence shown is from the reverse strand. For mutations within exons, the first codon (or part of codon) predicted to generate a non-synonymous substitution is enclosed within a box. Splice sites are indicated by short vertical bars.





Supplementary Figure 5.2. Selected cDNA studies on subjects heterozygous for

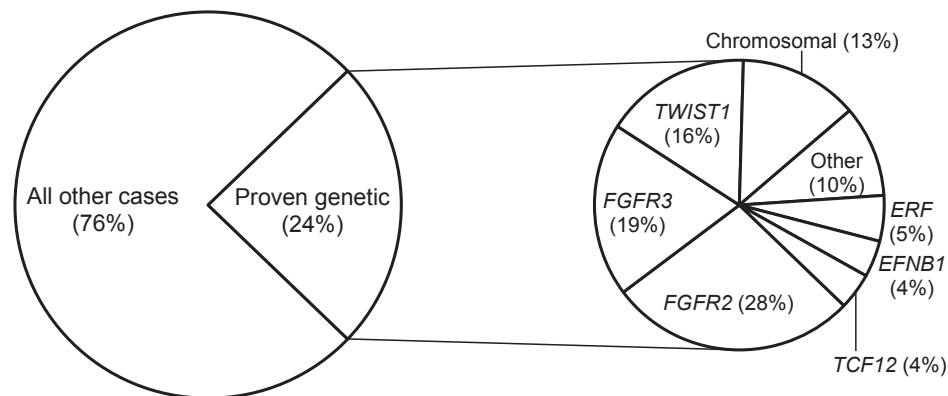
TCF12 mutations. A: family #22 (c.1468-20T>A). At the top are shown the normal splice junctions between exons 16 and 17 of *TCF12* (exon sequence is in upper case and intron sequence in lower case). The T>A point mutation (shown in red in sequence at bottom) lies within the intron, 20 nucleotides upstream of the normal acceptor splice site: this is predicted to create a cryptic acceptor with a higher score (0.99) than the normal acceptor (0.96) using the Splice Site Prediction by Neural Network program (www.fruitfly.org/seq_tools/splice.html). The use of the cryptic site was confirmed by cDNA sequencing (using primers in exons 16 and 18/19), demonstrating a low level of the neo-exon (dotted box) which contains a premature stop codon (underlined in the intron sequence).

B: family #5 (c.822C>G). This substitution creates a synonymous change and locates 4 nucleotides before the end of exon 9 (vertical red dotted line). The normal exon 9 donor site is unusually weak (score 0.09 using Splice Site Prediction by Neural Network), and the score is little changed by the substitution (score 0.06). However sequencing of cDNA generated by primers in exons 9 and 11 showed that the mutant allele is virtually absent from the normal cDNA (arrow), this was confirmed by restriction digestion using *SmlI*, which cuts only the wild type allele, showing only a small proportion of undigested product in the patient sample (U, uncut; II-1, patient; C, normal control).

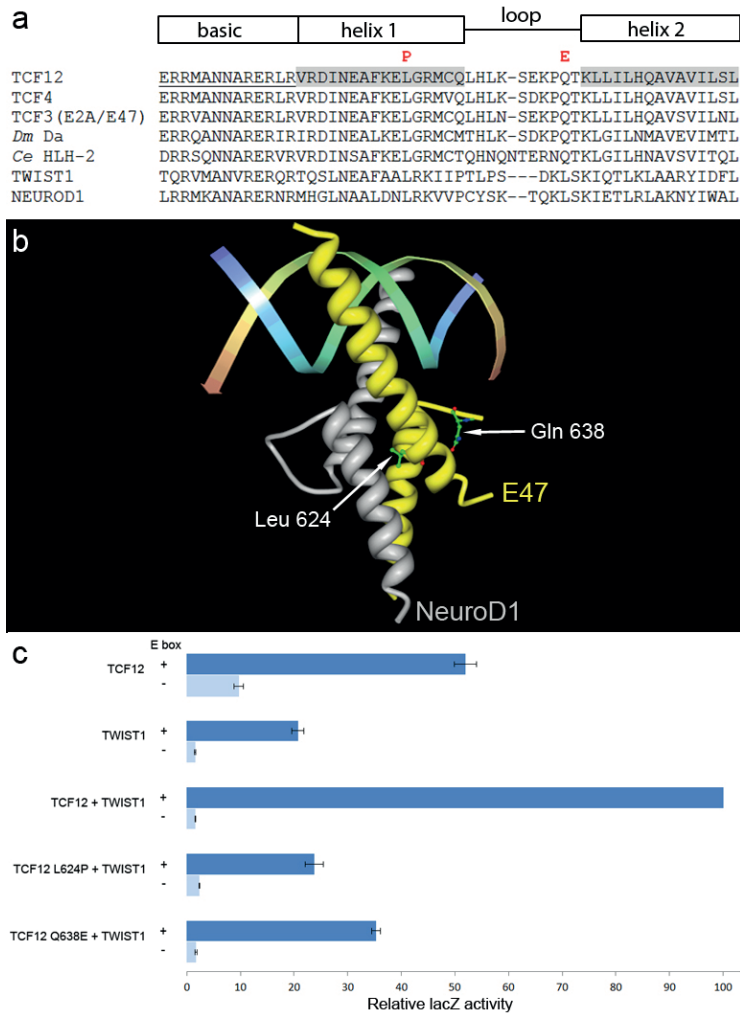
C: family #19 (c.1349delC). This mutation creates a frameshift within exon 16. The gel shows the result of digestion of the exon 13/14-18 cDNA product with restriction enzyme *Cac8I*, which cuts only the wild type allele at the site of mutation. Note the lower amount of mutant (white arrowhead) compared with wild type (white arrow) fragment, suggesting that the mutant transcript is unstable; also note the similar proportions of mutant allele in the affected child III-1 and his unaffected mother II-1. C = control, U = uncut.

D: family #1 (c.526+1G>A). This mutation disrupts the highly conserved first intronic nucleotide following exon 7, and is therefore predicted to abolish splicing at this site. This is the only mutation occurring upstream of the alternatively transcribed exon 9A, so we wished to establish its effect on splicing. When using primers located in exons 5 and 9/10 for cDNA amplification, a low level of an additional smaller fragment was present in samples from the 3 mutation carriers in this family (left panel: I-1 and II-2, blood; III-1, fibroblasts), but not in a normal fibroblast control (C); N = negative water control. DNA sequencing of this smaller fragment (right panel) demonstrated that it results from skipping of exon 7, predicted to create an out-of-frame translation product.





Supplementary Figure 5.3. Relative prevalence of mutations in *TCF12* and other genetic diagnoses in craniosynostosis. The dataset comprises all children ($n = 402$) born in the period 1998-2006, managed at a single craniofacial unit (Oxford), and requiring at least one major craniofacial procedure. Ninety-eight children had a proven genetic diagnosis, including four with *TCF12* mutations.

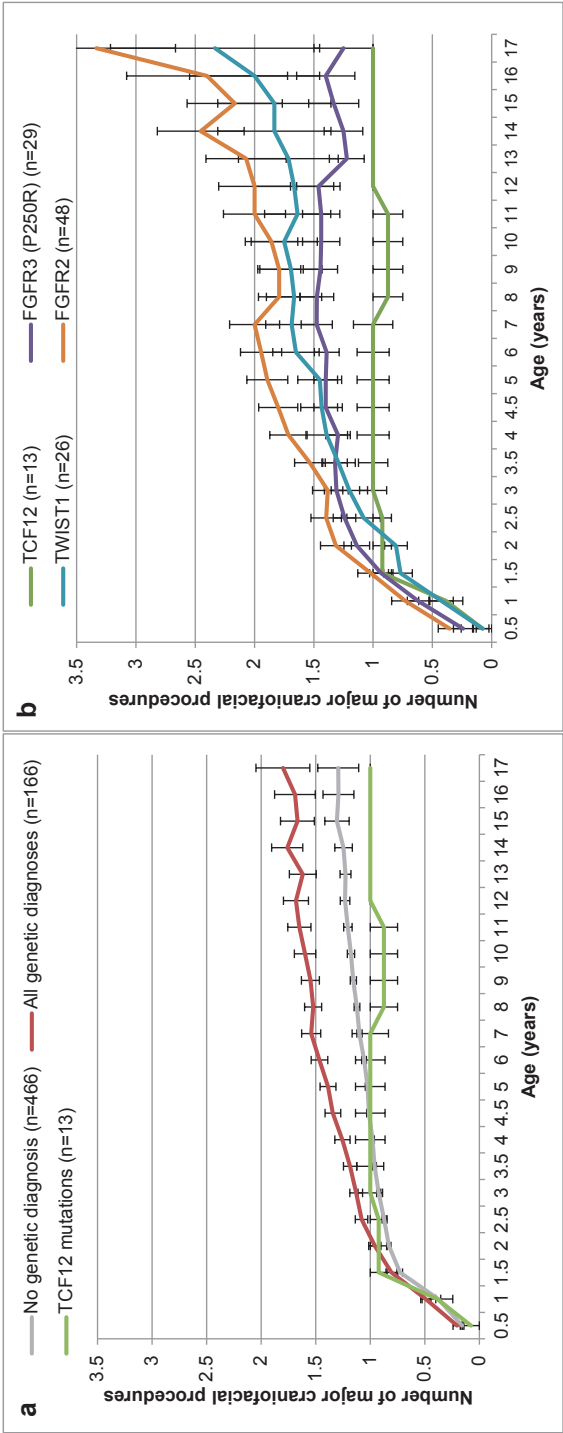


Supplementary Figure 5.4. Structural and functional analysis of missense mutations in the bHLH domain of TCF12. **A:** comparative amino acid sequence analysis of the bHLH domains of the three human class I proteins (TCF12, TCF4 and TCF3; the latter is frequently termed E2A with E12/E47 alternative spliceforms), the unique homologs in *Drosophila melanogaster* (Daughterless) and *Caenorhabditis elegans* (HLH-2), and human class II proteins TWIST1 and NEUROD1. The two missense mutations observed in TCF12 (p.Leu624Pro and p.Gln638Glu) are indicated in red. **B:** structure of a bHLH class I/II heterodimer (murine E47/NeuroD1) bound to DNA, visualized in Protein Workshop (PDB accession no. 2QL2). The side chains of the residues corresponding to p.Leu624 and p.Gln638, both of which are conserved between TCF12 and Tcf3, are highlighted. Substitutions at these buried residues are predicted to abrogate dimerization. **C:** analysis of transactivation with 1 μ g of TCF12 and/or TWIST1 wild-type or mutant proteins as shown, using reporters either including (+) or omitting (-) three E-box DNA-binding motifs. Results are shown as mean \pm SEM of 3 experiments and normalized to the output from transfecting both TCF12 and TWIST1 with the E-box reporter.



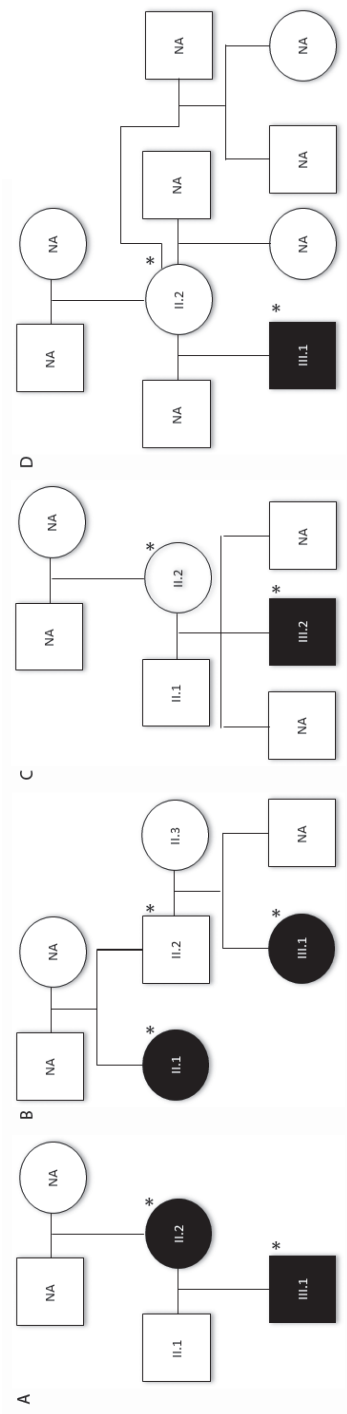


Supplementary Figure 5.5. Craniofacial appearance of individuals heterozygous for *TCF12* mutations and considered non-penetrant.
Written permission was obtained to publish the clinical photographs.

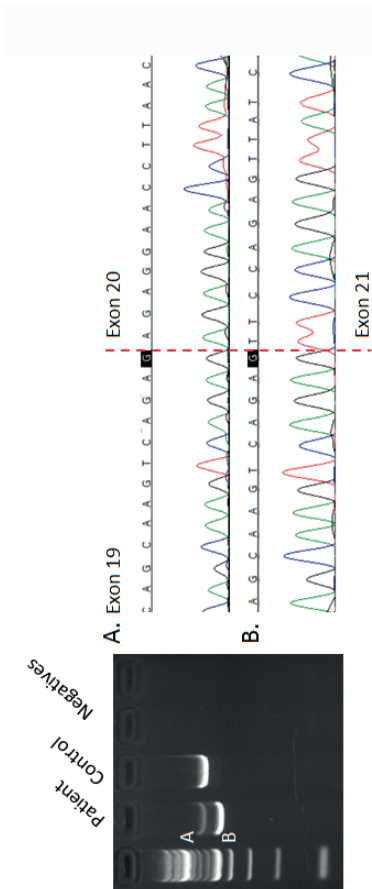


Supplementary Figure 5.6. Surgical trajectory of patients with *TCF12* mutations and other causes of craniosynostosis treated at the Oxford Craniofacial Unit over a 16-year period. The average number (\pm SEM) of craniofacial procedures was calculated for all children born between 1993 and 2008 (or, for individuals with *TCF12* mutations, all individuals born in 2008 or earlier) with a given diagnosis and reaching a specified age (calculated for each half year up to the age of 5 years, subsequently for each year). **A:** individuals with *TCF12* mutations are compared with all those with genetic diagnoses, and all those without genetic diagnoses. **B:** individuals with *TCF12* mutations are compared with those with mutations in the specified genes. Note the general lack of requirement for secondary surgery in patients with *TCF12* mutations compared with most diagnostic categories.





Supplementary Figure 6.1. Pedigrees of family 1 (A), family 2 (B) family 3 (C) and family 4 (D). Black is clinically affected, white is unaffected. Asterisks indicate carriers of rearrangements. NA= not available.



Supplementary Figure 6.2. Amplification of cDNA using primers in TCF12 exons 18 and 3' UTR; cDNA amplified from the index patient in family 3 resulted in an extra, smaller product. Sequence traces of gel-purified products from A and B are shown; product B demonstrated skipping of exon 20.

Supplementary Table 2.1 Primers and methods used for sequencing all coding exons and exon/intron junctions of *FGFR2*. Accession number reference sequence used is NM_000141.4.

Amplicon	5' → 3'		Product size (bp)
	Forward primer	Reverse primer	
Exon03B	CACTTGGGCTGGAGTGATTT	AGCCCCATTACAATGCAAG	428
Exon04	CCATTTGCAGAGCAAGAACA	GCCTGGCATCCAATTACAA	495
Exon05	CCTGGGTTGTTGACTTTGCT	CTGTGCAGCAACTGTTT	361
Exon06	TTACTCATGGAGGGGAAGCTGT	AAAAATGTAGGGCTGGGCATC	590
Exon07	TTCTTGCTCCTTCAGCTTC	TTGGGGAAATGATGCTTCTC	596
Exon08	AGGCTTTTCTGGCATGAGGT	CCTCTCTCAACTCCAACAGGA	393
Exon10	TCAGTGTGTCTCCGTGTCTC	AAAAGGGGCCATTCTGATAA	413
Exon11B	GCCTTTTGTTCTCTTGTT	GAAGTCGATGGCATCAAAGC	392
Exon12	GTTTCTGACTTCTGCCAGCC	CCTGCTGACATCATCACACC	402
Exon13	AGCGGTCCACCAGTAATTG	ACCGAAAATTCTCAACCCC	467
Exon14	TGTTTCAACTAAGTCTTTGGCAAC	GTGCTCTGGGAGCAGGATCT	296
Exon15	AAAAATGTTTGTGAATTGC	CGAGGGCTTGATCTAGCAA	368
Exon16	CCGGCCACACTGTATTCTT	TCTCAACATTGACGGCCTTT	357
Exon17	CAGCTCTTAACAGGGCATAGC	GCCACTAAGAAGGAAGAAAGG	247
Exon18	ATCCCCGTGCATCATCATT	CCAGAGAGCTTCAGCCATTC	459
Exon19	AAGTCAAAGTGCCTTTCGGA	GGGGATGTCCCTCTGTCTTT	530
Exon21A	AGCGGGTTATTTAGGTCCGT	TCCACTGCTCCAGAAACCTT	759
Methods	<p>Primers were developed for Sanger sequence analysis. PCR amplification was carried out in a total volume of 25 µl, containing 10x PCR buffer (Invitrogen, Life Technologies Ltd, Paisley, UK), 50 mM MgCl₂ (Invitrogen), 100 mM dNTP, 10 µM forward primer, 10 µM reverse primer, Platinum Taq DNA polymerase (Invitrogen), 100 ng genomic DNA. (Exon 03B 20 µM forward primer and 20 µM reverse primer.) PCR conditions were: 94°C for 2 min; followed by 30 cycles of 30 s at 94°C, 30 s at 60°C and 90 s at 72°C; followed by 10 min at 72°C, and 5 min at 20°C. PCR products were purified using Agencourt AMPure (Agencourt. Beckman Coulter Inc., Brea, CA, USA). Direct sequencing of both strands was performed using Big Dye terminator version 3.1 (Applied Biosystems, Foster City, CA, USA). Dye terminators were removed using Agencourt CleanSeQ (Agencourt) and loaded on an ABI 3130XL Genetic Analyzer (Applied Biosystems). The sequences were analysed using SeqPilot version 4.1.2 build 507 (JSI Medical Systems GmbH, Kippenheim, Germany).</p>		



Supplementary Table 2.2. Summary of the clinical features of 124 patients.

Suture	Number of patients	Other clinical signs (n)	Eyes (n)	Neurodevelopmental (n)	Family (n)	MRI (n)
S	13	Dysmaturity (1), atopic (1), dyspnoea (1), eczema (1), haemangioma (1), macrocephaly (1), occipital foramina (1), maxillary hypoplasia (1), bifid uvula (1), torticollis (1), inguinal hernia (1), hypospadias (1), undescended testes (1), and congenital hip luxation (1).	Papilledema (4), hypertelorism (1), exorbitism (1) and telecanthus (1).	PMR (1), behavioural deficits (1), concentration and attention deficit (1).	A sibling with S synostosis (2).	Hydrocephalus (1).
M	30	Bronchial hyperreactivity (1), café au lait spot (1), eczema (1), cleft lip (1), cleft palate (1), micrognathia, retrognathia (1), prominent ears (1), hearing deficit (2), hypertension (1), asystole postoperatively (1), aorta stenosis (1), septum defect (1), pyloric stenosis (1), unilateral renal agenesis (1), undescended testes (2), clinodactyly of hands (1), ulnar polydactyly of the hand (1), hip dysplasia (1), mild syndactyly of the feet (1), large halluces (1).	Papilledema (3), strabismus (2), amblyopia (1), cataract (1).	PMR (2), ADD (2), attention deficit (1), speech delay (1), speech therapy (1).	Twin brother with M suture synostosis (1), sibling with M suture synostosis (1) sibling with M ridge (1).	Closed lip schizencephaly (1), cerebellar ischemia (1), migration disorder (1), arachnoid cyst (1), periventricular nodular heterotopia (1), short callosal body (1), asymmetrical ventricles (1).
UC	28: 11 LC 17 RC 1 and PT 2 and FS	Feeding difficulties (1), visible veins on forehead (1), nasomaxillary facial cleft (1), malocclusion (1), crossbite (3), agenesis of 72 (1), radial polydactyly (1), bifid thumb (1), hip dysplasia (1), overriding digit 2 and 3, both feet (1), club foot (1), anxiety (1).	Papilledema (1), strabismus (7), nystagmus (5), amblyopia (3), enophthalmos (1), limited vision (1), relative afferent pupil defect (1).	PMR (3), Asperger (1), dyslexia (1).	Consanguineous parents (1), father with LC synostosis (1), sibling with BC synostosis (1).	Cyst near pineal gland (1).

BC	16	Small posture (1), HC<p10 (1), maxillary hypoplasia (7), bifid nose (1), retrognathia (3), drooping of the helical rim left ear (1), mild webbed neck (1), VSD (1), ASD (1), syndactyl hands (1), simian creases of the hands (1), brachydactyl (1), clinodactyl hand (1), syndactyl feet (2), OSA (1).	Papilledema (2), strabismus (1), amblyopia (1), ptosis (1), hypertelorism (1), epicanthal folds (1).	PMR (3).	2 affected children (1), sibling RC synostosis (1), aunt UC synostosis (1), cousin of father RC synostosis (1).	Ventriculomegaly (1), mild loss of white matter (1), cyst left paraventricular (1), narrow corpus callosum (1), several midline defects (1).
UL	2: both RL	Prematurity (1), dysmaturity (1), failure to thrive (1), fragmented auditory ossicles (1), VSD (1), patent ductus arteriosus (1).				
BL	2		Strabismus (1).	MR (1).		Aspecific periventricular white matter deficits (1), enlarged third and lateral ventricles (1), Chiari I malformation (1).
Pan	2	Growth retardation (1), increased intracranial pressure (1), mild sensorineural hearing loss (1), polydactyl (1), incontinence (1).	Exorbitism (1), upslanting palpebral fissures (1).	ADD (1), MR (1).		
Patent	6	Dysmaturity (1), small posture (1), macrocephaly (1), cleft palate (1), crossbite (1), missing canines and wisdom teeth (1), maxillary hypoplasia (1), torticollis (1), scoliosis (1), hypertension (1), brachydactyl (1), bilateral congenital hip dysplasia (1), hypermobility (1).	Amblyopia (1), ptosis (2), exorbitism (2), congenital glaucoma (1).	Autism (1), speech therapy (1).	Father possibly macrocephaly (1), father with a balanced translocation of chromosome 2 and 10 (1).	
S and M	1					



Supplementary Table 2.2. Summary of the clinical features of 124 patients.

Suture	Number of patients	Other clinical signs (n)	Eyes (n)	Neurodevelopmental (n)	Family (n)	MRI (n)
S and UC	4: RC 2 LC 2	Failure to thrive (1), axial mesodermal dysplasia: growth hormone deficiency, dextroposition of the heart, anal atresia, rectosigmoid fistula, bilateral inguinal hernia, Stahl's ear (1), pseudocholinesterase deficiency (1), patent ductus arteriosus (1), nephrocalcinosis (1).	Papilledema (1), strabismus (1), hypotelorism (1), exorbitism (1).	MR (1), ADD (1), autism (1), behavioural deficits (1), special education (1).		
S and BC	5: 1 Pan partial 1 BC partial	Malocclusion (2), dental crowding (1), arthrogryposis (1), brachydactyly (1).		Developmental delay (1), special education (1), learning and speech delay (1).	Affected father, aunt, and niece (1).	
S and BL	4: 1 S partial and BL 1 Pan partial	Hypotonia (1), eczema (1), asthma (1), broad digits (1), mild tibial bowing (1), mild syndactyly feet (1), OSA (1).	Papilledema (1).	Learning difficulties (1), panic attacks (1).		Chiari I malformation (2), narrow peripheral CSF cavities (1).
M and UC	4: 2 M and LC 1 M and LC and left FS 1 M and RC and right FS	Eczema (1).	Strabismus (1).			
S, M, UC	1 M partial, S and LC					
S, M, BC	1	Growth hormone deficiency (1).		Special education (1), ADD (1), autism (1).		
S, M, UL	1 S, M, LL	VSD (1), bifid thumb (1).		Mild PMR (1).		

S, BC, BL	2: 1 BC (partial), BL, S	Maxillary hypoplasia (1), conductive hearing loss (1), OSA (1).	Papilledema (1), exorbitism (1).			Hydrocephalus (1), narrow optic canals (1), corpus callosum hypoplasia (1), Chiari malformation (1).
M, BC, BL	1		Papilledema (1).	Mild PMR (1), easily distractible (1).		
BC and UL	1 BC and RL	Parietal foramina (1).	Hypoplasia of the right optic nerve (1), nystagmus (1), strabismus (1).	PMR (1), autism (1), speech therapy (1), physiotherapy (1).	Mother 3 miscarriages (1), brother died of trisomy 18 (1).	Slightly enlarged lateral ventricles (1), underdeveloped right transversal and sigmoid sinus (1), slightly underdeveloped pons (1), wide foramen magnum (1), signal void near the cervical myelum (1).

ADD = Attention Deficit Disorder, ASD = Atrial septum defect, BC = Biconal, BL = Bilateral lambdoid, CSF = Cerebrospinal fluid, FS = Frontosphenoidal, HC = Head circumference, ICP = Intracranial pressure, LC = Left coronal, LL = Left lambdoid, M = Metopic, OSA = Obstructive sleep apnoea, Pan = Pansynostosis, PMR = Psychomotor retardation, PT = Parietotemporal, RC = Right coronal, RL = Right lambdoid, S = Sagittal, UC = Uniconal, UL = Unilateral lambdoid, VP = Ventriculoperitoneal, VSD = Ventricle septum defect.



Supplementary Table 2.3. Clinical features of patients with variants identified by sequence analysis of *FGFR2* (NM_000141.4).

cDNA position	Protein position	Suture	Other clinical signs	Eyes	Neuro develop mental	Surgery (months)	Surgery (number)	FA	MRI	Clinical diagnosis
c.23T>G	p.(Ile8Ser)	M	Otitis, clinodactyly of digit 4 of both hands.		ADD, speech delay.	36	1		Slightly asymmetrical ventricles.	Complex
c.314A>G	p.(Tyr105Cys)	BC partial, S, BL	Maxillary hypoplasia, OSA, conductive hearing loss.	Papilledema preoperatively and also postoperatively, exorbitism.		66	2		Narrow optic canals.	Crouzon syndrome
c.755C>G	p.(Ser252Trp)	BC	Complex syndactyly hands and feet, maxillary hypoplasia, OSA.	Exorbitism.		9	2		Midline defects: absent left side of the septum, narrow callosal body.	Apert syndrome
c.1084+8C>T		RC				9	1		Na	Complex
c.1531G>A	p.(Ala511Thr)	BC	Maxillary hypoplasia.			11	1		Normal	Complex
c.2190C>T	p.(=)	S				4	1	Sibling S suture synostosis.	Na	Complex

ADD = Attention Deficit disorder, BC = Bicoloral, BL = Bilateral lambdoid, FA = Family anamnesis, M = Metopic, Na = Not applicable, OSA = Obstructive sleep apnoea, S = Sagittal.

Supplementary Table 5.1. Mutations of *TCF12* identified in 38 unrelated subjects with craniosynostosis^a.

Family #	Proband ID	Gender of proband	Craniosynostosis	Positive FH	Suspected SCS	Clinically non-syndromic	Exon	Mutation	Protein	<i>De novo</i> mutation	Clinically affected	Clinically unaffected
1	953	F	RC		+		7	c.526+1G>A	(sp) ^b		1	2
2	07D6887	F	RC+S	+			10	c.722C>G	p.(Ser241*)		2	2
3	06D7856	F	BC	+	+		10	c.778_779delAT	p.(Met260Valfs*5)		3	
4	3496	F	RC	+			10	c.812C>A	p.(Ser271*)		1	
5	2065	F	RC		+		10	c.822C>G	(sp) ^b	+	1	
6	98D4142	F	BC		+		10	c.825G>C	p.(Leu275Phe) (sp)	+	1	
7	838	F	BC		+		11	c.842_843delCA	p.(Ser281Cysfs*56)	+	1	
8	06D1742	M	RC	+	+		11	c.842C>G	p.(Ser281*)		2	
9	01D3258	M	BC		+		11	c.842C>G	p.(Ser281*)	+	1	
10	01D3723	F	BC	+			11	c.970G>T	p.(Gly324*) (sp)		1	
11	4438	F	BC	+	+		12	c.1035+3G>C	(sp)		2	2
12	06D4640	F	LC		+		13	c.1073C>G	p.(Ser358*)		1	1
13	07D2829	M	BC	+	+		14	c.1115-2A>G	(sp)		2	
14	09D7966	F	BC	+			14	c.1123C>T	p.(Gln375*)		2	1
15	3955	F	RC		+		14	c.1127G>A	p.(Trp376*)		1	1
16	4437	F	BC		+		16	c.1283T>G	p.(Leu428*)	+	1	
17	3956	M	BC		+		16	c.1312delC	p.(Leu438Cysfs*81)	+	1	
18	09D4333	F	RC		+		16	c.1328dupT	p.(Pro445Thrfs*11)		1	1
19	484	M	BC		+		16	c.1349delC	p.(Pro450Leufs*69)		1	1
20	4397	F	BC	+			16	c.1376T>G	p.(Leu459*)		2	1
21	5189	F	BC	+	+		16	c.1453C>T	p.(Arg485*)	+	1	
22	2636	M	BC	+			17	c.1468-20T>A	p.(Val490Glyfs*4)(sp) ^b		1	1
23	5137	M	BC		+		17	c.1491dupT	p.(Val498Cysfs*12)		1	1
24	1669	M	RC		+		17	c.1491dupT	p.(Val498Cysfs*12)		1	1
25	01D4012	F	BC		+		17	c.1514C>G	p.(Ser505*)	+	1	



Supplementary Table 5.1. (continued)

Family #	Proband ID	Gender of proband	Craniosynostosis	Positive FH	Suspected SCS	Clinically non-syndromic	Exon	Mutation	Protein	<i>De novo</i> mutation	Clinically affected	Clinically unaffected
26	4855	F	RC			+	17	c.1530dupA	p.(Val511Serfs*11)	+	1	
27	4502	F	RC	+	+		17	c.1540_1543dupTCAA	p.(Ser515Ilefs*8)		3	
28	3664	F	BC		+		17	c.1582+2T>G	(sp)		1	1
29	4618	M	RC	†		+	18	c.1628delA	p.(Lys543Argfs*20)	+	1	
30	4581	F	BC			+	18	c.1642_1645delGAAA	p.(Glu548Argfs*14)		1	1
31	00D0716	M	RC	+			18	c.1646delA	p.(Lys549Argfs*14)		3	
32	4951	F	BC			+	18	c.1691C>G	p.(Ser564*)	+	1	
33	08D7786	M	RC			+	18	c.1713delA	p.(Asp572Ilefs*19)	+	1	
34	4881	F	BC	+			19	c.1796_1799dupAGAA	p.(Arg602Glyfs*6)		3	
35	4594	M	RC	+	+		19	c.1806delG	p.(Arg602Serfs*31)	+ ^c	2	
36	1520	M	LC			+	19	c.1871T>C	p.(Leu624Pro)		1	1
37	99D0117	F	BC	+	+		19	c.1912C>G	p.(Gln638Glu)		2	
38	4379	M	BC+S	†		+	19	c.1963G>T	p.(Glu655*)	+	1	

^aAbbreviations: F = Female, M = Male, RC = Right coronal, BC = Bilateral coronal, LC = Left coronal, S = Sagittal, + = Feature present. ^bAbnormal splicing (sp) illustrated in Supplementary Figure 5.2. ^c*De novo* in grandparental generation. [†]Craniofacial signs in parent coincidental to *TCF12* mutation.

Supplementary Table 5.2. cDNA studies of subjects heterozygous for *TCF12* mutations.

Family #	Mutation	Individuals analysed (see Supplementary Figure 5.1) and disease status (RC, right coronal; BC, bilateral coronal; UA, unaffected)	Cellular source of mRNA	Reverse transcriptase-PCR result	Mutant allele under-represented compared to wild type?	Similar mutant:wt ratio in affected and unaffected individuals?	Illustrated in Supplementary Figure 5.2?
1	c.526+1G>A	I-1 (UA), II-2 (UA) III-1 (RC)	Blood fibroblasts	skipping of exon 7	yes	na ^a (different tissue sources)	panel d
5	c.822C>G	II-1 (RC)	fibroblasts	abolishes exon 10 splice donor site	yes	na (<i>de novo</i> mutation)	panel b
6	c.825G>C	II-1 (BC)	blood	retention of intron 10	yes	na (<i>de novo</i> mutation)	-
11	c.1035+3G>C	I-2 (UA), II-2 (UA), II-3 (BC)	blood	skipping of exon 12	yes	relatively less skipped product in II-3 (BC) than II-2 (UA)	-
19	c.1349delC	II-2 (UA), III-1 (BC)	blood	lower expression of mutant allele	yes	yes	panel c
22	c.1468-20T>A	I-2 (BC), II-3 (UA)	blood	use of cryptic acceptor splice site for exon 17	yes	yes	panel a
23	c.1491dupT	II-1 (UA)	blood	lower expression of mutant allele	yes	-	-
24	c.1491dupT	I-2 (UA), II-1 (RC)	blood	lower expression of mutant allele in II-1; similar expression of both alleles in I-2	yes/no	lower in affected	-
28	c.1582+2T>G	II-1 (BC)	fibroblasts	faint ~100 bp shorter fragment, consistent with skipping of exon 17	yes	-	-

^aNot applicable

Supplementary Table 5.3. Clinical features of subjects heterozygous for *TCF12* mutations.

Family	ID	Proband	Sex	Mutation (nucleotide for changes affecting splicing [sp]; otherwise protein)	Age at assessment (years)	Clinical diagnosis: SC, Saethre-Chotzen; O, other syndrome, FH, positive family history [spurious if (FH)], N, non-syndromic	Craniosynostosis diagnosed (+ or -)	Sutures fused (S, sagittal; RC, right coronal; LC, left coronal; UC, unilateral coronal; BC, bilateral coronal); ?, suspected craniosynostosis	Brain anatomy on CT/MRI scan	Normal intracranial pressure on formal measurement	Number of major craniofacial procedures	Age (years) at 1 st craniofacial procedure	Neurodevelopmental features	Developmental or language quotient	Other features
1	I-1		M	c.526+1G>A ^(sp)	63	-	-						normal	-	
1	II-2		F	c.526+1G>A ^(sp)	36	-	-					1.0	normal	108 @ 1.0 year (Griffiths)	class II malocclusion with dental crowding; additional procedure = bimaxillary osteotomy @ 17 years
1	III-1	Y	F	c.526+1G>A ^(sp)	16	N	+	RC	normal	Y	2				
2	I-2		F	p.(Ser241*)	48	FH	-						normal	-	
2	I-3		M	p.(Ser241*)	53	FH	-					0.66	normal	-	blepharoptosis requiring repair, strabismus, mild midfacial hypoplasia, class I malocclusion, camptodactyly digits 3+5, brachydactyly; additional procedure = contour correction of supraorbital rim and forehead
2	II-1	Y	F	p.(Ser241*)	22	FH	+	RC, S	na	na	2		mild LD	-	

2	II-2		M	p.(Ser241*)	27	FH	+	S	normal	na	1	1.2	mild LD	-	partial sclerosis of both coronal sutures on plain radiography, class II-1 malocclusion
3	I-1		M	p.(Met260Valfs*5)	47	FH	+	LC	na	na	0		-	-	bilateral transverse palmar creases
3	II-1		M	p.(Met260Valfs*5)	15	FH	+	RC	normal	na	1	1.0	-	-	L cleft lip, cleft palate
3	II-2	Y	F	p.(Met260Valfs*5)	12	SC, FH	+	BC	hypoplastic corpus callosum	na	1	0.5	-	-	conchal hypertrophy R ear
4	III-1	Y	F	p.(Ser271*)	7	FH	+	RC	normal	na	1	0.6	normal	-	
5	II-1	Y	F	c.822C>G ^(sp)	13	N	+	RC	normal	na	1	1.3	normal	-	bilateral parietal foramina
6	II-1	Y	F	p.(Leu275Phe) ^(sp)	13	SC	+	BC	normal	na	1	0.9	normal	-	bilateral auricular prominence with conchal hypertrophy, dental crowding
7	II-1	Y	F	p.(Ser281Cysfs*56)	19	N	+	BC	Chiari I malformation, enlarged 3rd and lateral ventricles	Y	1	11	normal	111 (WISC-III UK) @ 11.5 years	
8	I-1		M	p.(Ser281*)	37	FH	+	LC	na	na	0		normal	-	cornea abnormalities
8	II-1	Y	M	p.(Ser281*)	7	SC, FH	+	RC	small mass near pineal gland	na	1	1.0	normal	-	
9	II-1	Y	M	p.(Ser281*)	27	SC	+	BC	mild ventriculomegaly	na	2	0.4	mild LD	-	low frontal hairline, incomplete descent of testes; additional procedure to correct supraorbital retrusion
10	II-1	Y	F	p.(Gly324*) ^a	11	FH	+	BC	na	na	1	1.0	normal	-	rheumatoid arthritis
11	I-2 ^a		F	c.1035+3G>C ^(sp)	56	-	-						normal	-	
11	II-2 ^a		F	c.1035+3G>C ^(sp)	38	FH	-						normal	-	
11	II-3 ^a		F	c.1035+3G>C ^(sp)	36	SC, FH	+	BC	na	na	0		required speech therapy	-	mild brachydactyly of toes, severe early onset rheumatoid arthritis, Crohn's disease
11	III-1	Y	F	c.1035+3G>C ^(sp)	3.6	SC, FH	+	BC	normal	na	2	1.8	mild language delay	-	FOAR age 2.0 years following initial posterior release
12	I-2		F	p.(Ser358*)	29	-	-						normal	-	facial nerve paralysis
12	II-1	Y	F	p.(Ser358*)	6.8	N	+	LC	normal	na	1	0.9	normal	-	low frontal hairline, strabismus, prominent ears with conchal hypertrophy



Supplementary Table 5.3. (continued)

13	I-2	F	c.1115-2A>G ^(sp)	49	SC, FH	+	BC	na	na	0	normal	-	
13	II-1	M	c.1115-2A>G ^(sp)	17	SC, FH	+	BC	normal	na	1	0.9	normal	low frontal hairline, mild mandibular retrusion
14	I-1	M	p.(Gln375*)	36	-	-						normal	
14	II-1	F	p.(Gln375*)	5.3	FH	+	RC	thinning of optic chiasm	na	1	0.8	normal	syndactyly 2 nd +3 rd toes
14	II-2	F	p.(Gln375*)	3.5	FH	+	BC	L paraventricular cyst	na	1	0.7	mild developmental delay	mild webbed neck, syndactyly 2 nd +3 rd toes
15	I-1	M	p.(Trp376*)	46	-	-						normal	
15	II-1	F	p.(Trp376*)	7.3	N	+	RC	normal	na	1	1.1	normal	L strabismus
16	II-1	F	p.(Leu428*)	12.4	SC	+	BC	normal	na	2	1.0	normal	Myopia, small ears, low frontal hairline. Second procedure = FOAR @ 11.9 years
17	II-1	M	p.(Leu438Cysfs*81)	7.1	SC	+	BC	midline cyst at septum pellucidum, partial agenesis of corpus callosum	na	1	0.9	normal	low frontal hairline, L single palmar crease
18	I-1	M	p.(Pro445Thrfs*11)	36	-	-						normal	
18	II-1	F	p.(Pro445Thrfs*11)	4.1	N	+	RC	prominent lateral ventricles	na	1	0.9	normal	strabismus
19	II-2 ^a	F	p.(Pro450Leufs*69)	45	-	-						normal	small ears, prominent crura helices, prominent nose with deviated septum, unilateral transverse palmar crease
19	III-1 ^a	M	p.(Pro450Leufs*69)	20	N	+	BC	normal	Y	1	0.5	low average	low hairline, small cupped ears with prominent crura, hallux valgus, recurrent absence seizures until mid-teens, abnormal EEG with focal spike and slow wave discharges

20	I-2		F	p.(Leu459*)	52	-	-	BC	normal	na	1	0.7	normal	-	flat parietal region, hallux valgus
20	II-1	Y	F	p.(Leu459*)	18	FH	+	BC	normal				severe LD attributable to MPSIIIA	confounded by MPSIIIA	coincident diagnosis of Mucopolysaccharidosis type IIIA (MPSIIIA)
20	II-2		M	p.(Leu459*)	18	FH	+	BC	normal	na	1	0.6	diagnosis of infantile autism @ 2.1 years	64 @ 2.1 years (Griffiths)	exostosis on R tibia; unaffected by MPSIIIA
21	II-1	Y	F	p.(R485*)	0.9	SC, (FH)	+	BC	normal	na	1	0.7	normal	-	low frontal hairline, prominent crura, post-axial polydactyly L hand, broad thumbs, bilateral lamellar lens opacities (also present in unaffected father)
22	I-2 ^a	Y	M	c.1468-20T>A ^(sp)	54	FH	+	BC	normal	Y	0		mild LD	-	myopia, coronary heart disease, type 2 diabetes
22	II-3 ^a		F	c.1468-20T>A ^(sp)	25	-	-						normal	-	
23	II-1		M	p.(Val498Cysfs*12)	37	-	-						normal	-	
23	III-1	Y	M	p.(Val498Cysfs*12)	7.1	N	+	BC	normal	na	1	1.5	normal	86 @ 1.8 years (REEL-2)	dental crowding, bilateral transverse palmar creases, hallux valgus
24	I-2 ^a		F	p.(Val498Cysfs*12)	48	-	-						normal	-	
24	II-1 ^a	Y	M	p.(Val498Cysfs*12)	23	N	+	RC	normal	Y	2	0.4	normal	113 @ 0.5 years (Griffiths)	tall (165 cm), normal pituitary testing, R transverse palmar crease, flat thumbs, hallux valgus, vertical strabismus; additional procedure = onlay cranioplasty of forehead @18 years
25	II-1	Y	F	p.(Ser505*)	10	SC	+	BC	normal	na	1	0.8	normal	-	prominent L ear with conchal hypertrophy, L transverse palmar crease
26	II-1	Y	F	p.(Val511Serfs*11)	1.4	N	+	LC	widened surface CSF spaces	na	1	1.0	normal	102 @ 1.0 year (REEL-3)	L divergent strabismus
27	I-2		F	p.(Ser515Ilefs8*)	53	FH	+	?	-	na	0		-	-	facial asymmetry, hallux valgus, severe strabismus as child - operated



Supplementary Table 5.3. (continued)

27	II-2		F	p.(Ser515Ilefs8*)	25	SC, FH	+	RC	na	na	1	0.4	minor dyslexia / dyspraxia	-	prominent ear crura with folded pinnae, bilateral 5 th finger clinodactyly, hallux valgus, incomplete 2/3 toe syndactyly
27	III-1	Y	F	p.(Ser515Ilefs8*)	3.2	SC, FH	+	RC	normal	na	1	1.1	Delay in fine and gross motor skills, visual, hearing and language comprehension@ 3.0 years	-	low frontal hairline, beaked nose, R divergent strabismus, hallux valgus, 2 nd +4 th toes overlap 3 rd bilaterally
28	I-2		F	c.1582+2T>G ^(sp)	43	-	-						normal	-	
28	II-1	Y	F	c.1582+2T>G ^(sp)	7.6	SC	+	BC	normal with prominent extra- axial fluid spaces	na	2	0.7	normal	105 @ 2.3 years (Bay- ley cognitive scale)	prominent crura helices, additional procedure = FOAR @ 2.5 years following initial posterior calvarial release
29	II-1	Y	M	p.(Lys543Argfs*20)	3.9	N, (FH)	+	RC	normal	na	1	1.3	normal motor de- velopment immature listening, attention, eye contact, social com- munication	72 @ 3.9 years (verbal comprehension and expressive language)	(father with orbital hypertelorism and midface hypoplasia presumed affected, TCF12 mutation negative)
30	I-2 ^a		F	p.(Glu548Argfs*14)	26	-	-						normal	-	Flat parietal region, orthodontic brace, myopia
30	II-1	Y	F	p.(Glu548Argfs*14)	2.8	N	+	BC	normal	na	2	1.1	mild language delay	100 @ 1.1yr (Bayley cognitive scale); 85 @1.1 years (REEL 3)	additional procedure = FOAR aged 2.8 years following initial posterior calvarial release/distraction
31	I-1	Y	M	p.(Lys549Argfs*14)	48	FH	+	RC	na	na	0		normal	-	bilateral transverse palmar creases, brachydactyly of hands

31	II-1		M	p.(Lys549Argfs*14)	13	FH	+	S	Chiari I malformation, slightly enlarged lateral ventricles	na	1	1.0	Asperger syndrome	-	bilateral transverse palmar creases, brachydactyly of hands
31	II-2		M	p.(Lys549Argfs*14)	9	FH	+	RC	slightly enlarged lateral ventricles	na	1	0.7	autism	-	deafness, relapsing respiratory tract infections
32	II-1	Y	F	p.(Ser564*)	1.6	N	+	BC	normal	na	1	1.0	normal	-	
33	II-1	Y	M	p.(Asp572Ilefs*19)	4.8	N	+	RC	wormian bones	na	1	1.1	normal	-	
34	II-1		M	p.(Arg602Glyfs*6)	43	FH	+	RC	na	na	0		normal	-	
34	III-2	Y	F	p.(Arg602Glyfs*6)	4.2	FH	+	BC	normal	na	1	1.6	normal	-	
34	III-3		M	p.(Arg602Glyfs*6)	1.3	FH	+	BC	normal	na	1	1.1	normal	-	broad thumbs
35	II-2*		F	p.(Arg602Serfs*31)	33	SC, FH	+	RC	na	na	0		normal	-	R sided strabismus (operated as child), myopia, asthma, hypertension
35	III-1	Y	M	p.(Arg602Serfs*31)	2.7	SC, FH	+	RC	normal	na	1	1.3	normal	95 @ 1.2 years (REEL 3)	blepharoptosis, L divergent strabismus, L torticollis
36	I-1		M	p.(Leu624Pro)	56	-	-						normal	-	
36	II-1	Y	M	p.(Leu624Pro)	12.9	N	+	LC	normal	na	1	1.3	normal	-	R divergent strabismus (R eye amblyopic), asthma
37	I-2		F	p.(Gln638Glu)	44	SC	-						normal	-	bilateral blepharoptosis
37	II-1	Y	F	p.(Gln638Glu)	14.2	SC, FH	+	BC	normal	na	1	0.8	normal	-	
38	II-1	Y	M	p.(Glu655*)	3.3	N, (FH)	+	BC, S	normal	na	1	1.1	normal	107 @ 3.3 years (REEL 3)	(mother - bony exostoses around jaw, TCF12 mutation negative)

Abbreviations not defined at top: Y = Yes, F = Female, M = Male, L = Left, R = Right, + = Present, - = Absent, Na = Not available, LD = Learning disability, FOAR = Fronto-orbital advancement and remodelling.

*Serum screening of the indicated individuals showed normal indices of immune function.



Supplementary Table 5.4. Summary of clinical features of *TCF12*-associated craniosynostosis, based on assessment of 72 mutation-positive individuals (30 male, 42 female).

Clinical feature	Total positive for feature	Details and comments
Coronal craniosynostosis	50	The most common presentations were bilateral coronal synostosis ($n = 25$), right coronal synostosis ($n = 18$) and left coronal synostosis ($n = 5$). 4 individuals had sagittal synostosis, either combined with coronal synostosis or (in 2 cases) on its own. 20 adults did not have craniosynostosis; this figure indicates significant non-penetrance and is likely to represent an overall underestimate because all index cases were ascertained through craniofacial units
Strabismus	11	Strabismus always occurred in association with unilateral coronal synostosis
Class I/II dental malocclusion or dental crowding	7	Additional orthognathic surgery in 1 case
Craniofacial features suggestive of Saethre-Chotzen syndrome	19	Features commonly highlighted were minor ear anomalies ($n = 10$) (either a prominent horizontal crus helices, or deepening of the concha causing prominence of the ears), low-set frontal hairline ($n = 8$) and blepharoptosis ($n = 3$)
Limb anomalies	20	These were minor and relatively non-specific, the most commonly noted being transverse palmar creases ($n = 8$), hallux valgus ($n = 7$), syndactyly of 2 adjacent toes ($n = 3$) and brachydactyly ($n = 4$)
Abnormal brain anatomy on CT scan	12 (out of 42)	Features most commonly identified were prominent ventricles and/or cerebro-spinal fluid spaces, in two cases associated with Chiari type 1 malformation ($n = 7$); and partial or complete agenesis of the corpus callosum ($n = 2$). Miscellaneous findings were of paraventricular cyst, pineal mass, and thinning of the optic chiasm. In 30 individuals, the brain scan was reported as normal
Significant developmental delay or learning disability	10 ^a	5 adults had mild learning disability, in 1 case associated with severe autism. 2 children had mild global developmental delay, 1 had delay in verbal and social skills, 1 had Asperger syndrome, and 1 had autism. 2 further adults had speech delay or dyslexia in childhood and 2 children had mild speech delay. The majority of adults and children had normal developmental attainment

^aOne subject excluded from total because of co-existing Mucopolysaccharidosis.

Supplementary Table 5.5. Primers and amplification conditions used for genomic sequencing, MLPA, cDNA amplification and PCR mutagenesis of *TCF12*, and for detection of *Ell3-Cre* transgene.

Amplicon	Primer sequence 5'→3'		Product size (bp)	
	Forward	Reverse		
Ex2 F/R	GCGTAATCTCCCGACGACCTCTCTCTGTTTC	CTGCGTAGTCTCAGCTTGCTTCCCTCAC	293	
Ex3 F/R2	GATGGATGACTTTTGGTGACTTTTGTTTGC	CTATTTTCTACTAAATGTATCACACCAC	223	
Ex4 F/R	CTTGCTAAATGTACTCTGCTGCCGTAC	CAAAAGGTACTAGGTATTCTACTGCATTTC	300	
Ex5 F/R	TAAGTCTGTATTAAATAGGTGAGTGC	GTCCTCTGGACAAAGGGATAAAAAATG	279	
Ex6 F/R	GCAATAATAATTACCATGAATAGTCTAGC	CTTAGTTACAAATTAAACAACAGTAGTG	278	
Ex7 F/R	GGGTGGTTCTAAGTTAAGACATTGCTG	CCAGAAGTACAGATTATGGGAGG	329	
Ex8 F/R	CTGTTAATTTGAAGTCTTGATTTTTTTC	GTATGCCACTCGCATCAATCGAATGTAC	226	
Ex9 F/R	GCCCCTTACAGAATATAGAACTCATTTTAC	CTGGCTGATATACAGATGACTGCAGTAG	247	
Ex9A F/R	GTGGTTCAGTCTATTTTGCATAAGTTC	GCGAGTAATGTATACTGCTTTCTTTAAAC	288	
Ex10 F/R	GTACCCCTTGAATTTTATAAGCAACATC	CTAATCCAAAAGAAACAACAAGTGAGGAC	292	
Ex11 F/R	GACCTGTATCATAGTTGTCCATTTTATG	GGTCACTGAAAGTCCACAAACTTTTAGG	279	
Ex12 F/R	GAATAATGGCAGAGTGCTAAAATATAATAC	GATACTTATCACCTACAAAAATCTAATCACTG	220	
Ex13 F/R	CTCCATGTGAACGGATTTGTGTATGTGCTG	CACACTTCTTATAGTCAAAATCTAAATG	281	
Ex14 F/R	GTATTGAGTAITCTTTACCCCTTCTCTCAAC	CTTTATTGTTATGCCAGATTGACCAAAAAC	241	
Ex15 F/R	GCATATCAGCTATTTCTCATCTCTTTTGGAG	GTTTGATTTTAAAGATGGGAGTCTGTACAGC	260	
Ex16 F/R	CACATATCACATAGTAGGAAACGTAGCAG	GACTAATACTTAGCCAATACTTTACTGC	460	
Ex17 F/R	CAGAATAATGGCATCCAGAAAAAGTTGCTG	CCAGCTGTGAGAAAGGTGACAGTGTTCCAAATG	335	
Ex18 F/R2	GATGTGGATATATCTTTTTCAGCTCTAAATAG	GAGACAACATACACAAAAATCCTAACAC	475	
Ex19 F/R	GTGCACAATCAGCATATCTTACTTTATAG	GGAAAAACGCCCTGTATGATACAGTAGAAG	440	
Ex20 F/R	GTATGGGAATGAAGTTACACAAAAACACAG	CTGTTCAAAGATTCTAACCCAGTTTAAG	334	
Mutation confirmation				
Family #	Mutation	Primer sequence 5'→3'		Digest/dideoxy seq ^a
		Forward	Reverse	
1	c.526+1G>A	Ex7F	Ex7R	HphI
2	c.722C>G	Ex10F	Ex10R	dideoxy seq



Supplementary Table 5.5. (continued)

Mutation confirmation				
Family #	Mutation	Primer sequence 5'→3'		Digest/dideoxy seq ^a
		Forward	Reverse	
3	c.778_779delAT	Ex10F	Ex10R	dideoxy seq
4	c.812C>A	Ex10F	Ex10R	MseI
5	c.822C>G	Ex10F	Ex10R	MspI
6	c.825C>G	Ex10F	Ex10R	dideoxy seq
7	c.842_843delCA	Ex11F	Ex11R	dideoxy seq
8,9	c.842C>G	Ex11F	Ex11R	dideoxy seq
10	c.970G>T	Ex11F	Ex11R	dideoxy seq
11	c.1035+3G>C	Ex12F	Ex12R	dideoxy seq
12	c.1073T>G	Ex13F	Ex13R	dideoxy seq
13	c.1115-2A>G	Ex14F	Ex14R	dideoxy seq
14	c.1123C>T	Ex14F	Ex14R	dideoxy seq
15	c.1127C>A	Ex14F	Ex14R	HaeIII
16	c.1283T>G	Ex16F	Ex16R	TseI
17	c.1312delC	Ex16F	Ex16R	TseI
18	c.1328dupT	Ex16F	Ex16R	dideoxy seq
19	c.1349delC	Ex16F	Ex16R	TseI
20	c.1376T>G	Ex16F	Ex16R	BsaBI
21	c.1453C>T	Ex16F	Ex16R	BclI
22	c.1468-20T>A	Ex17F	Ex17R	dideoxy seq
23,24	c.1491dupT	Ex17F	Ex17R	PfFI
25	c.1514C>G	Ex17F	Ex17R	dideoxy seq
26	c.1530dupA	Ex17F	Ex17R	HpyCH4III
27	c.1540_1543dupTCAA	Ex17F	Ex17R	dideoxy seq
28	c.1582+2T>G	Ex17F	Ex17R	MaeIII
29	c.1628delA	Ex18F	Ex18R2	Hpy188III
30	c.1642_1645delGAAA	Ex18F	Ex18R2	dideoxy seq
31	c.1646delA	Ex18F	Ex18R2	dideoxy seq

32	c.1691C>G	Ex18F	Ex18R2	dideoxy seq
33	c.1713delA	Ex18F	Ex18R2	dideoxy seq
34	c.1796_1799dupAGAA	Ex19F	Ex19R	dideoxy seq
35	c.1806delG	Ex19F	Ex19R	BsrBI
36	c.1871T>C	Ex19F	Ex19R	BstNI
37	c.1912C>G	Ex19F	Ex19R	dideoxy seq
38	c.1963G>T	Ex19F	Ex19R	XbaI, dideoxy seq

Multiplex ligation-dependent probe amplification (MLPA) [®]				
Primer sequence 5' → 3'				
Exon	5' Probe	3' Probe	Product size (bp)	
2	gggttcctaaagggttggaGGACCTGCTAGAAAGTGCCGGAAGATG	AATCCCCAGCAACAGCATGGCtctagattggtctgctggcac	91	
3	gggttcctaaagggttggaGGGTATTTTGCAGATGTTTCCCCACCTGTTA	ATAGTGGGAAAAACTAGACCAACTACAC TGGGAAGctctagattggtcttgc	110	
4	gggttcctaaagggttggaCTTGGGGAACAAGTGGTCAACCAAGTCCTTCCTA	TGATTCATCTAGAGTAAAGTTTGCTGATCAACCCCTTGATTAAAGctctagattggtctgctggcac	120	
5	gggttcctaaagggttggaCAGACAGCCCTCATTACAGTGATGACCTTGAA	TGACAGTCGATTAGGAGGCCCATGAAGGctctagattggtctgctggcac	100	
6	gggttcctaaagggttggaGCAATATAATTAACATGAATAGTCTAGCAGTTTGAT	TTATATAAAGTTAATTTCTTTGTTTATAGGAAAAAATCATCAGAGAGAGGC	153	
7	gggttcctaaagggttggaCAGCTATCTTCTTCAGGAAAAACCTGGGACAGCAT	TCctagattggtctgctgctggcac	113	
10	gggttcctaaagggttggaCATCAAAATGGGATGAGCCAGCCTGGTT	TTGGTGGAAATCTGGGGACCTCCACtctagattggtctgctggcac	94	
13	gggttcctaaagggttggaCACAGGTAGGCTTCTGTTTATCTACTTCTAAGTG	ATTTC TAGTCTATTATTCTCAACAACTTTAATAAAAAATTTGTGAAAAA	150	
16	gggttcctaaagggttggaCCTTGTGCAAGCAGTCGATCAGCTTCAATGGTAA	TCATctagattggtctgctgctggcac	128	
17	gggttcctaaagggttggaCTTCAAGCACAGACCTGAACCATAAACACAAAGA	ATAGAGGTAACATAATTGTTGGTTTTCAGAAATAATGCAGACAgcttagattggtctgctggcac	125	
19	gggttcctaaagggttggaCTTTATAGGAAACCTAATAGACCTTGTGTTACTTT	ATAGAGGTAACATAATTGTTGGTTTTCAGAAATAATGCAGACAgcttagattggtctgctggcac	136	
20	gggttcctaaagggttggaGGTCATATGTAAACATCAGCCAGGTAAAGTACGGGT	ATAGAGGTAACATAATTGTTGGTTTTCAGAAATAATGCAGACAgcttagattggtctgctggcac	131	



Supplementary Table 5.5. (continued)

Primers and amplification conditions for cDNA analysis					
Mutation	Primer sequence 5'→3'		Product size (bp)	Annealing temp (°C)	Primers
	Forward	Reverse			
c.526+1G>A	AGCCCTCATACAGTGATCACTTGAATGAC	GGTCAGAAGAATTGTGGGTCCCATCTTGCAAT	475	61	Ex5F, Ex9/10R
c.822C>G	TATATGCACCATCCCCAAATTTCAGATGATTTCAAC	TGTGAGGCAGCAACGTAAGGTGAAGTCTG	355	61	Ex9F/ Ex11R
c.825G>C	TATATGCACCATCCCCAAATTTCAGATGATTTCAAC	TGTGAGGCAGCAACGTAAGGTGAAGTCTG	355	61	Ex9F/ Ex11R
c.1035+3G>C	ATGCAAGATGGGACCCCAATTCCTTGACC	GATGAAGGTGCTTGCCCTCCAGGTCT	479	61	Ex9/10F, Ex14R
c.1328dupT	AGTTGGATCACCTTCACCTCTCACAGGTAC	CAACAGTTCAGAGACTGACTTTTGAAGCCA	449	61	Ex13/14F, Ex18R
c.1349delC	AGTTGGATCACCTTCACCTCTCACAGGTAC	CAACAGTTCAGAGACTGACTTTTGAAGCCA	449	61	Ex13/14F, Ex18R
c.1468-20T>A	ACCAGTTTGCTGCTGGTGCACAGTG	CTTCATTAGTACTGCTTGTTCTGCCTCTAG	421	61	Ex16F/ Ex18/19R
c.1582+2T>G	ACCAGTTTGCTGCTGGTGCACAGTG	CTTCATTAGTACTGCTTGTTCTGCCTCTAG	421	61	Ex16F/ Ex18/19R
Primers for PCR mutagenesis of cDNA constructs					
	Forward	Reverse			
c.1871T>C	TGAAGCATTTCAAAGAGCCTGGCCGAATGTGTCAG	CTGACACATTCGGCCAGGCTCTTTGAATGCTTCA			
c.1912 C>G	GAAGAGTGAATAAACCCGAAACAAACTCCTTATTC	GAATAAGGAGTTTGTTCGGGTTTTCACACTCTTC			
Primers for detection of <i>Ella-Cre</i> transgene					
Forward		Reverse			
Cre-F	TGCTGTTTCACTGGTTATGCGG	Cre-R	TTGCCCTGTTTCACTATCCAG		

^aMutation confirmation carried out by restriction digest or direct dideoxy-sequencing as indicated.

^bCommon PCR primer annealing sequences are shown in lower case, hybridizing sequences are shown in upper case and the 3' probe sequence is 5' phosphorylated.

Supplementary Table 5.6. Antibodies used for immune function tests.

Commercial source and catalogue number			
Antibody	BD Bioscience	eBioscience	Cambridge Bioscience
CD3 APC	555335		
CD3 FITC	555332		
CD3 PE-Cy5	555334		
CD3 PE-Cy7	557851		
CD4 APC	555349		
CD4 FITC	555346		
CD4 PE-Cy5	555348		
CD19 APC-Cy7	557791		
CD14 APC	555399	17-0149-73	
CCR7 FITC	561675		
CD45RO PE-Cy5	555494		
CD62 APC	561916		
CD62L APC-Cy7			304813
CD16 PE	555407		
CD56 PE	555514		
CD56 PE-Cy7	557747		
CD25 APC-Cy7	557753		
IgD FITC	555778		
IgM PECy5	551079		
CD10 FITC	347503		
CD27 PE	555441		



Supplementary Table 6.1. Primers used for deletion PCR, breakpoint spanning PCR and dideoxy-sequencing.

Amplicon	5' → 3'		Product size (bp)
	Forward	Reverse	
Deletion family 1 F1/R1 (WT)	tgtcaaaaagcaaacaaaagtaaac	ggttttcacactgtttaccaacaa	1455
Deletion family 1 F1/R2 (M)	tgtcaaaaagcaaacaaaagtaaac	gtatactctgcccaataactgc	644
Deletion family 2 F1/R1 (WT)	caaaagtagccaaagtc aaatgg	aaacatatgaggggagatgctctg	1107
Deletion family 2 F1/R2 (M)	caaaagtagccaaagtc aaatgg	ttgaagggtgctgctccacta	556
Deletion family 3 F1/R1 (WT)	gggactacaggtgggtaccag	aagagttctaattttctaagcccctgt	1303
Deletion family 3 F1/R2 (M)	gggactacaggtgggtaccag	gctgccctgctcttgctac	646
Deletion family 3 cDNA	cttgcaagtcagtcctggaactgt	ctgtcaggtttgtgtcttcagataatctg	636 (wild-type) 482 (minus exon 20)
Duplication genomic	atcctgggcttagtgaaactaccaaccctatg	cattgccgagggtgggtgtcttccaagat	530
Duplication cDNA	cttgcaagtcagtcctggaactgt	ctgtcaggtttgtgtcttcagataatctg	636 (wild-type)
Duplication cDNA mutant specific	cagtcaccttagctagaaacagcaagtc	ctatcttctgttcagggttcaaatctcctc	231 (predicted)

Primer sequence from 5' to 3': F = Forward, M = Deleted sequence, R = Reverse, WT = Normal sequence.

Supplementary Table 7.1. Whole genome sequence analysis.

Dominant/de novo variants							gene	type	comment
chr	position	from	to						
1	3	147131157	C	A			ZIC1	stop	de novo
2	9	140777194	A	AGCGGCT			CACNA1B	splicing	maternal
3	13	21746477	C	CGTGTA			SKA3	splicing	artefact/present in multiple samples
4	1	39879157	A	C			KIAA0754	nonsynonymous	artefact/present in multiple samples
5	1	145343385	C	A			NBPF10	nonsynonymous	present in multiple samples
6	1	144823868	T	G			NBPF9	nonsynonymous	present in multiple samples
7	1	144815968	G	A			NBPF9	nonsynonymous	present in multiple samples
8	1	7890026	A	G			PER3	nonsynonymous	artefact/present in multiple samples
9	4	88537261	A	T			DSPP	nonsynonymous	maternal
10	4	85998	T	A			ZNF595	nonsynonymous	present in multiple samples
11	6	168377071	G	A			HGC6.3	nonsynonymous	paternal
12	6	168377029	G	A			HGC6.3	nonsynonymous	paternal
13	8	144940209	T	C			EPPK1	nonsynonymous	artefact
14	12	50745703	T	G			FAM186A	nonsynonymous	artefact
15	15	82637061	C	T			GOLGA6L10	nonsynonymous	artefact/present in multiple samples
16	15	20740611	C	T			GOLGA6L6	nonsynonymous	paternal
17	16	22545467	C	T			LOC100132247	nonsynonymous	artefact/present in multiple samples
18	16	88599705	G	C			ZFPM1	nonsynonymous	artefact/present in multiple samples
19	16	88599703	T	C			ZFPM1	nonsynonymous	artefact/present in multiple samples
20	17	18544392	T	C			TBC1D28	nonsynonymous	maternal
21	17	15620506	G	A			ZNF286A	nonsynonymous	maternal



Supplementary Table 7.1. (continued)

Dominant/de novo variants								
	chr	position	from	to	gene	type	comment	
	22	19	53553339	C		ERW-2	nonsynonymous	paternal
	23	19	56104423	A		FIZ1	nonsynonymous	paternal
	24	X	8434191	G		VCX3B	nonsynonymous	present in multiple samples
	25	1	144615246	A		NBPF9	frameshift insertion	artefact/present in multiple samples
	26	19	14070706	A	AGGTGGGCCACGGCGGGCAG	DCAF15	frameshift insertion/splicing	artefact/present in multiple samples
	27	Y	21154527	CTGCGTGGG		CD24	frameshift deletion	artefact/present in multiple samples
	28	1	248524966	A	AGCTCTACTTAGT	OR2T4	nonframeshift insertion	artefact/present in multiple samples
	29	4	88535832	A	ATAGCAGTGACAGCAGCAG	DSPP	nonframeshift insertion	artefact/present in multiple samples
	30	6	34857302	G	GGGCGGC	ANKS1A	nonframeshift insertion	paternal
	31	11	8414087	G	GCCAGAA	STK33	nonframeshift insertion	present in both parents
	32	12	125478381	C	CCTG	BRI3BP	nonframeshift insertion	present in multiple samples
	33	17	72889649	C	CGTAGGTTCCATGGGCTCCGTA	FAD56	nonframeshift insertion	artefact/present in multiple samples
	34	1	26608853	GCCGGACCGGACCGGGAC TGGGGCCGGA	G	UBXN11	nonframeshift deletion	paternal and other samples
	35	5	60628153	GGGCGGC	G	ZSWIM6	nonframeshift deletion	paternal
	36	6	45390486	AGGCGGCGGCGGCGTGC	A	RUNX2	nonframeshift deletion	paternal and other samples
	37	11	117789312	CGGGCTGGAGATGCCT	C	TMPPRSS13	nonframeshift deletion	paternal and other samples

38	16	29821419	TGGCGGC	T		MAZ	nonframeshift deletion	paternal
39	17	43319434	TCCG	T		FMNL1	nonframeshift deletion	present in multiple samples
Recessive variants								
1	2	99013251	G	A		CNGA3	nonsynonymous	Homozygous; p.(Val540Ile)
2	2	152376170	A	G		NEB	splicing	paternal
3	2	152530992	A	C		NEB	nonsynonymous/ splicing	maternal



Supplementary Table 7.2. Primers and amplification conditions.

Screening					
Amplicon	Primer sequence 5'→3' (M13 tags in lowercase)		Pro duct (bp)	Amplification conditions ^a	
	Forward	Reverse			
Ex1a F/R	gtaaaacgacgcccagtgccggggctgcggccgagcagcca CG	agcggaatacaatttcacacaggaATCTGCCCGTTGACCACGTT AG	555	65°C + DMSO	
Ex1b F/R	gtaaaacgacgcccaggtTTCCTCCGGGCTTCACGAGCAGGCTG C	agcggaatacaatttcacacaggaGATCCACCGAGGCTGCGT TTGTGCGACC	698	65°C + DMSO	
Ex2 F/R	gtaaaacgacgcccaggtTTTTAAGCTTGCAAAAGTGCTAATCCT G	agcggaatacaatttcacacaggaCCAAGAGAGCTCTCGCCTC AAAG	385	65°C	
Ex3 F/R	gtaaaacgacgcccagtggggtctcaagggtccaggaggaa GGG	agcggaatacaatttcacacaggaGTGTATACGTGTGTGATCAG TCTCTTAAATAGGG	404	65°C	
Primers and amplification conditions for Subject 1 cDNA ^b					
cDNA Fragment	Primer sequence 5'→3'		Product size (bp)	Amplification conditions ^a	Digest
	Forward	Reverse			
Exon 2-3	GGGAGAGCCCTTCAAGTGCAGTTTGAGGG	CGCAGGGTTCTTTCAGTAATGTTGTGTATAC	446	+ DMSO	Bfal(+)
Multiplex ligation-dependent probe amplification (MLPA) ^c					
Probe	Primer sequence 5'→3'		Product size (bp)		
	Forward	Reverse			
Exon 1	gggttccttaagggttggacATCTGCTTCTGGGAGGAGTGTCC GCGCGAGGCGCAAGCCCTTCAAAGCCAAA	TACAAACTGGTTAACCCACATCCGCGTGACACACGtctagatt ggatcttgctggcac	127		
Exon 2	gggttccttaagggttggacAGTGCAGTTCGAGGGCTGTGAC CGGGCGCTTCGCTA	ACAGCAGCGACCCGAAGAAGCACATGCCctctagattggatc ttgtgtggcac	107		
Exon 3	gggttccttaagggttggacGCCAACTGTTGTACTGAATGGCA AGAAATGTTCTAGTAAATGTATCCAA	AATGTGAATTACTTTGTACGATTACAGTCTCCACGTCGAC CTAAACCtctagattggatcttctgtggcac	139		
cDNA cloning and mutagenesis					
	Primer sequence 5'→3'				
	Forward	Reverse			
cDNA PCR ^d	CGCCTCGAGCAGCCACGATGCTCCTGG	CGATGTTTGTCTAGATTTTAAAGTACCATTCG	1380 bp		
S388*	GAATCCTCTAGCAGGGCTCG	GTGGACCTTTCATGTGTTTGC			

E402*	CTCTGGTACTAATCTCTCACGCCTCCC	CTGGCGCGCGCGGAAGGC
S436*	CGGCCACAGTTAGCTCTCTTCCAATTTTAAC	GCTGTGTGGTGGACTGCG
E299*	GCACACAGGGTAGAAGCCCTT	GTCTTTTGTGGATCTTTAAATTCTC
T414A	ATCGTGTCTCCCTCCGACAGACAACCCGACACACA	TGTGGTCGGGTTGTCTCGGAGGGGAGACACGAT
G400R	CCGGCGCCAGCTCTCGTACGAATCCTCCACG	CGTGAGGATTCTGTAGCGAGAGCTGGCGGCCGG
cDNA Ion Torrent PGM sequencing^a		
	Primer sequence 5' → 3'	
	Forward	Reverse
ZIC1 PGM f/r	CGCTCTTCCGATCTCTGcagcagcgacaagccctatctttgcaag	TGCTCTTCCGATCTGACtaaggagctgtgtcgggtgtctgtg
A-BC1Rdfw	CCATCTCATCCCTGCGTGCTCCGACTCAGacgagtgctcg CTCTTCCG ATCTCTG	CCTCTCTATGGGCAGTCGGTGATTGCTCTCCGATCTGAC P1-Rdrev

^aDNA was obtained from whole blood samples by phenol-chloroform extraction and was amplified in a total volume of 20 µl containing 15 mM TrisHCl (pH 8.0), 50 mM KCl, 2.5 mM MgCl₂, 100 µM each dNTP, 0.4 µM primers, and 0.5 units of FastStart Taq (Roche) with or without 10% DMSO. Cycling conditions consisted of an 8 min denaturation step at 94°C, followed by 35 cycles of 94°C for 30 s, 65°C for 30 s and 72°C for 30 s, with a final extension at 72°C for 10 min. ^bMutation confirmation was carried out by PCR using the above conditions and indicated primers, followed by restriction digest of 8 µl of PCR product. ^cMultiplex-ligation-dependent probe amplification was performed using synthetic oligonucleotide probes designed to ZIC1 according to protocols available from MRC-Holland: <http://www.mrc-holland.com/pages/indexpag.html>. Fragments were analysed by capillary electrophoresis using an ABI 3130 containing POP-7 polymer. Peaks were visualized using Gene Mapper v3.7 (Applied Biosystems). Common PCR primer annealing sequences are shown in lower case, hybridizing sequences are shown in upper case and the 3' probe sequence is 5' phosphorylated. ^dcDNA amplification was performed using pCR4-Topo-ZIC1 (ThermoFisher) as template and PCR conditions as described above except that the high fidelity FastStart Taq (Roche) was used. Bold letters within the primer sequences are the mutated bases. The amplification product was cloned into pcDNA3 using XhoI and XbaI (sites are in italics in the primer sequences). ^eAmplification to generate templates for PGM sequencing was performed on fibroblast cDNA (see Methods) using primers PGM F and PGM R (ZIC1 specific sequences are shown in lower case) and the conditions as above except that the cycle number was 30. The product was diluted 1 in 100 and a second amplification carried out to add the Ion Torrent PGM adapters P1 and A with conditions as above except that high fidelity FastStart Taq (Roche) was used and cycle number was reduced to 8. Lowercase bases in the A-BC1-Rdfw primer correspond to barcode sequence.



Supplementary Table 8.1. Primers used for PCR and dideoxy-sequence analysis. Primer sequence from 5' to 3'.

Primers used for PCR and Sanger sequence analysis					5' → 3'		Product size (bp)
	Amplicon	Forward	Reverse				
DNA analysis	Promoter2 F/R	gcctgatgtgacattcctc	ctgacggcatgtgctatag				457
	Promoter1 F/R	ctccgacagctgctatgacg	gaggatggcctgtgtccac				400
	Exon1 F/R	gggccggggagtgag	ggaggaatgcctgaacg				377
	Exon2 F/R	gccctgatccacacaattc	ctgtacaaccaactctctcaaaa				318
	Exon3 F/R	gcttgtcacagtgggaaaaat	gccttgagcttctctgtat				366
cDNA analysis	F1/R3	gatctacgtgcatgaagatggacg	agtagtctctgggggacacca				307
	F2/F3	aattttgcagttatttcttgtggatattacag	agtagtctctgggggacacca				250
	F2/ln2R1	cttgtggatatcacagaagtgcctgacttc	ctaagcgtacacctatatacaaccacc				999
	F2/ln2R2	cttgtggatatcacagaagtgcctgacttc	caaaaacaacacactcgggatatattagc				1902
	F2/ln2R3	cttgtggatatcacagaagtgcctgacttc	gatgcaggagaatacacaggaagcagc				3679
	F2/R5	cttgtggatatcacagaagtgcctgacttc	aggctcacaggataaacaaccttctttta				535
	F2/R8	cttgtggatatcacagaagtgcctgacttc	cagctgtgtgctactacgaaaagg				847
	F2/R9	cttgtggatatcacagaagtgcctgacttc	ctaactatatgaactgaaggccatggc				1160
	F4/R5	cacctctgagatggaattgataacatgg	aggctcacaggataaacaccttctgttta				178
	F4/R8	cacctctgagatggaattgataacatgg	cagctgtgtgctactacgaaaagg				490
Digest PGM	F4/R9	cacctctgagatggaattgataacatgg	ctaactatatgaactgaaggccatggc				803
	F10/R11	cagagatgtgtgctctcacagctttgcagacg9999	ccaacacagctgtgtgtactactacgaaaagg				249
	F12/R13	cgcctctccgatctctgctgttttgcatactgggtgtgttt	tgctcttccgatctgacgtatccacacacgaagggaactgaa				225
	F14/R15	ccatctatccctgctgtgtctccgactcagagcactgtagcgtctcttccgatctctg	ccctctatctgggcagctggtgattgtcttctccgatctgac				225

Supplementary Table 9.1. Extended phenotypic information for samples processed for ES and whole genome sequencing.

Family #	Sample	Sex	Sample ID	Referring Clinic	Seq method	Library kit	Syndromic	Suture involvement	Additional clinical manifestations	Family history	Population (if non-European)	Mutation Positive			Inheritance/allelic state
Clinical genetic cases															
1	Proband	M	5490	BCH	Exome	TruSeq	Y	P	Learning disability, prominent eyes, hypertelorism, ?submucous cleft, mild syndactyly fingers, limited pronation both arms, broad great toes, perimembranous ventricular septal defect, coarctation of aorta, choanal atresia, bilateral inguinal hernia, hearing loss (bone anchored hearing aids)	Mother with similar facial features, atrial septal defect, mild learning disability, no craniosynostosis	-	-	-	-	-
	Proband	F	5383						Exorbitism, abnormal posture R arm, long, slender fingers, evolving pansynostosis and recurrent synostosis post-surgery		-	-	-	-	-
	Unaffected mother	F	5406	BCH	Exome	TruSeq	Y	S, BC							
2	Unaffected father	M	5407												
	Proband	F	4964	GOS	Exome	TruSeq	Y	BC	Short stature, thin eyebrows, anteriorly placed anus					p.[Asn76His]; [Arg157Cys]	Compound heterozygous
4	Proband	M	5627	GOS	Exome	TruSeq	Y	P	Exorbitism, intellectual disability, atopy (eczema, asthma, dietary allergies), ?Crouzon syndrome	Parents 1 st cousins	South Asian		c.[226A>C]; [469C>T]	p.[Arg296Trp]; [Arg296Trp]	Homozygous
5	Proband	M	5630						Exorbitism, gum hypertrophy, disrupted dental eruption, hairy external auditory meatus						
	Unaffected mother	F	5631	GOS	Exome	TruSeq	Y	S, BC							
	Unaffected father	M	5632												
6	Proband	F	5626	GOS	Exome	TruSeq	Y	S, BL	Upslanting palpebral fissures, mild exorbitism, hypertelorism, mild ptosis, mild 5 th finger clinodactyly, anterior anus, dilated cardiomyopathy						
7	Proband	F	5169	Liv	Exome	TruSeq	Y	P	Mid-face hypoplasia, obstructive sleep apnoea, corneal ulceration, progressive scoliosis, multiple severe respiratory tract infections with bronchiectasis, mild-moderate cognitive impairment		South Asian				



Appendices

8	Proband	F	5333				TruSeq	Y	S, LC, LL	None	Affected father and sister also analysed						
	Affected father	M	5335	BCH	Exome		ss v5	Y	S	Head shape compatible with sagittal synostosis, no imaging confirmation							-
	Affected sibling	F	6931					Y	BC	Ollier disease, scoliosis, nonprogressive muscular dystrophy (myopathic pseudo dystrophic changes on muscle biopsy)							-
9	Proband	M	5520							Crouzonoid facies, mild developmental delay, delayed dental eruption, small pointed teeth, class III malocclusion, patent ductus arteriosus, atrial septal defect, umbilical hernia	Parents 1 st cousins	South Asian	IL11RA	c.[98dupC]; [98dupC]	p.[Gly34fs*]; [Gly34fs*]	Homozygous	
	Unaffected mother	F	5518	BCH	Exome		ss v5	Y	S, BC			c.98dupC	p.(Gly34fs*)	Heterozygous			
	Unaffected father	M	5519									c.98dupC	p.(Gly34fs*)	Heterozygous			
10	Proband	M	6306					Y	BC	Mild learning difficulties, slightly short, broad thumbs, 5 th finger clinodactyly, thick hair, squint and hydrocele requiring surgery at 7yrs of age	Affected mother also analysed	MSX2		c.443C>T	p.(Pro148Leu)	Heterozygous	
	Affected mother	F	5326	BCH	Exome		ss v5	Y	BC	Short 5 th fingers, thick hair			c.443C>T	p.(Pro148Leu)	Heterozygous		
11	Proband	M	5219	GOS	Exome		ss v5	Y	S, M	Exorbitism, hypoplastic midface, downslanting palpebral fissures, blue sclerae, micrognathia, prominent nasal bridge, ligamentous laxity, recurrent inguinal hernia, tall stature, lens subluxation and mild aortic dilatation aged 8 years			FBW1	c.8226+5G>A	(splice site)	De novo	
	Unaffected mother	F	6772							Brachycephaly, slightly deviated septum, mild exorbitism, slightly deviated halluces		South Asian			-	-	
12	Unaffected father	M	6380														
	Proband	M	6796							High anterior hairline, hypertelorism, divergent squint, mild exorbitism, left upper eyelid retention cyst, wide eyebrows					-	-	
13	Unaffected father	M	5891	GOS	Exome		ss v5	N	P								
	Unaffected mother	F	5892														
14	Proband	M	6589	Liv	Exome		ss v5	Y	M	Flat mid-face, downslanting palpebral fissures, low set ears, facial asymmetry, retracted pre-maxilla, right choanal stenosis, micrognathia, peg-like teeth with conical incisors, absent lateral incisors, pectus excavatum, scoliosis, long palms, slight digital shortening, mild 4/5 syndactyly of toes, Chiari malformation, moderate - severe learning difficulties	Parents 1 st cousins	Middle East	HUWE1	c.328C>T	p.(Arg110Trp)	De novo	
15	Proband	M	6463	GOS	Exome		ss v5	N	BC	Beta-Thalassaemia	Parents 1 st cousins	South Asian			-	-	-

16	Proband	M	6966	GOS	Exome	ss v5	Y	S, BL	Microcephaly, asymmetric ventriculomegaly, possible abnormalities on MRI brain scan involving the corpus callosum, posterior fossa and frontal and perisylvian cortex		ZIC1	c.1101C>A	p.(Cys367*)	Heterozygous; absent in mother, father not available	
17	Proband	M	6223	Liv	Exome	ss v5	N	P	None			-	-	-	
	Unaffected mother	F	6803												
	Unaffected father	M	6804												
18	Proband	M	5856	Liv	Exome	ss v5	Y	M	Hypertelorism, wide anterior fontanelle, upper eyelid colobomata, deficient bony orbits with pseudoproptosis, small low-set dysplastic cupped ears, 2,3,4 syndactyly of fingers, bilateral talipes, bilateral undescended testes, imperforate anus, hypertrichosis, mild-moderate learning disability		TWIST1	c.350A>T	p.(Glu117Val)	De novo	
	Unaffected mother	M	5854												
	Unaffected father	F	5855												
19	Proband	M	5629	GOS	Exome	ss v5	Y	LC	Cleft soft palate, severe micrognathia, hypoplastic tongue with ankyloglossia, double outlet right ventricle (Fallots type), pulmonary artery stenosis, gastro-oesophageal reflux, small right pelvic kidney, partial 3/4 cutaneous syndactyly left hand and foot		-	-	-	-	
	Unaffected father	M	5673												
	Unaffected mother	F	5674												
20	Proband	F	5285	BCH	Exome	ss v5	N	BC	None		South Asian	-	-	-	
21	Proband	F	6701	GOS	Whole Genome	Complete Genomics	Y	P	Exorbitism, clover leaf skull			KRAS	c.40G>A	p.(Val141Ile)	De novo
	Unaffected mother	F	6254												
	Unaffected father	M	6256												
22	Proband	M	6246	BCH	Whole Genome	Complete Genomics	Y	S, BC	Mild facial dysmorphism, mild bilateral ptosis, prominent eyes, small nose, short fingers, bilateral palmar creases, recurrent raised intracranial pressure requiring repeat surgery, seizures pre-op and 9 months of age. Father has minor digit anomalies.		-	-	-	-	-
	Unaffected mother	F	5301												
	Unaffected father	M	5302												
23	Proband	F	5561	Ox	Exome	ss v4	Y	BC	Bilateral superior vena cava, dilated cardiomyopathy, rudimentary right thumb, left hip dislocation, duplex kidney, anterior anus, bilateral inguinal hernia, growth deficiency			-	-	-	-



294

294

31	Proband	F	5944	Ox	Exome	Nimble Gen SeqCap EZ Exome v2.0	Y	S, LC	Left hemifacial hypertrophy, high anterior hairline, frontal bossing, low set ears, single palmar creases, mild bilateral cutaneous syndactyly, 4/5 clinobrachydactyly of fingers, small toes, hypotonic with moderate speech and cognitive delay			-	-	-	-	-
32	Proband	F	6136	BCH	Exome	Nimble Gen SeqCap EZ Exome v2.0	N	BC	3,4,5 clinodactyly of toes (medially deviated), mild hypertelorism, mother clinically normal			-	-	-	-	-
33	Proband	M	5322	Ox	Exome	Nimble Gen SeqCap EZ Exome v2.0	N	S, BL	None	African		-	-	-	-	-
34*	Proband	M	6569	Liv	Exome	Nimble Gen SeqCap EZ Exome v2.0	Y	P	Low anterior hairline, synophrys, small mouth, visual loss secondary to raised intracranial pressure, shunted, empty sella, moderate developmental delay and learning disability, attention deficit disorder, behavioural problems			-	-	-	-	-
35	Proband	F	6568	GOS	Exome	Nimble Gen SeqCap EZ Exome v2.0	N	BC	None			-	-	-	-	-
36	Proband	M	4332	Ox	Exome	Nimble Gen SeqCap EZ Exome v2.0	Y	S, M	Trigonocephaly associated with hypertelorism, small ventricular septal defect, mild expressive language deficit			-	-	-	-	-
37	Proband	F	4473	Ox	Exome	Nimble Gen SeqCap EZ Exome v2.0	Y	LC	Facial asymmetry, progressive onset of aggressive outbursts, ritualised behaviours and language delay, hyperphagic obesity, streak ovaries			NTRK2	c.1330G>T	p.(Gly444*)	Heterozygous; absent in mother, father not available	-
38	Proband	F	6721	BCH	Exome	Nimble Gen SeqCap EZ Exome v2.0	Y	BC	Developmental delay, congenital hip dislocation (treated with Spica), positional talipes, congenital dislocation left knee resolved spontaneously, midface hypoplasia, downslanting palpebral fissures, bilateral sensorineural hearing loss, seizures, both parents have learning disability and father has epilepsy			-	-	-	-	-



Appendices

39	Proband	F	6722	Ox	Exome	Nimble Gen SeqCap EZ Exome v2.0	N	LC	None								
40	Proband	M	6368	Ox	Exome	Nimble Gen SeqCap EZ Exome v2.0	Y	S	None	Male sibling and maternal uncle also reported to have sagittal synostosis							

S = Sagittal, LC = Left coronal, RC = Right coronal, BC = Biconal, M = Metopic, LL = Left lambdoid, RL = Right lambdoid, BL = Bilambdoid, P = Pansynostosis.

*Also prioritised by clinical geneticist

[‡]Based on additional clinical features or positive family history

[†]Likely novel disease gene, still undergoing validation

[†]BCH, Birmingham Children's Hospital; GOS, Great Ormond Street Hospital; Liv, Alder Hey Children's Hospital; Ox, John Radcliffe Hospital.

[‡]Parental DNA unavailable.

Supplementary Table 9.2. Primer sequences and conditions used for confirmation of variants^A.

Gene	Forward primer sequence	Reverse primer sequence	Product size (bp)	T _m (°C)	DMSO	Digest
CDC45	TAGTGATGAAGAAAGGGGCTCTCTCG	CTGTCCAGTCCACAGGGTAGTCAG	314	63	N	-
	ACCAGTGTTGTTAACTCTGGTGCCTCAC	CTTGCCCTGGCAGGCTTCAGGATGAC	436	63	N	-
IL11RA	*(4) GTAGATGGTGGCTGGGAAGGCC	GCTAAGACAGGCTGTAGGCAACAAG	369	60	N	Aval @ 37°C
MSX2	*(9) CAGGCTTTAGCTCCCATCTCAGG	GGGACATGAGGACTAGGCAGAGTC	557	61	N	-
	TTGCTAATCCGCTCTCTCTCTCTG	AAACAAGCATCCATCATGGAG	496	58	N	-
FBN1	ACTCTTTTAGGCCCAAGACTAG	AGCTCAGAACCCCTTAACCCAC	812	58	N	SmlI @ 55°C
HUWE1	CACCAGAACTCTTGTAACACC	CAGAGGAAATGAGCAAGTATGTG	483	58	N	-
	GATGCTGGACAGACAGTGGA	ACAGGGTACACAGGCTTTAACC	183	60	N	HpaII @ 37°C
ZIC1	TTTAAAGCTTGCAAGTGCTAATCCTG	CCAAGAGAGCTCTGCCTCAAAAG	344	65	N	-
TWIST1	CGGCAAGAAGTCTGCGGCTG	CCTGGCCGGCTGCGCTCTGCCACCTGAGAG	490	63	Y	HaeII @ 37°C
KRAS ^B	GACTGAATATAACTTGTGTAGTTGG	TTGGATCATATTGCTCCACAA	101	55	N	-
AHDC1	CCGGAAGAATGGGACTCTG	CCGGTGAAGAGGTTTTTGCC	282	58	N	-
EFNB1	(A) TTGTCCGCTTCCCTGGTTCT	TGCACCACTTAGAAGCTCCCACT	443	63	N	-
	(B) CCCCCAACCTTGAGGCTGACCATC	GAGTTAAGCCAGGAGAGAGCCAGAGG	367	63	N	-
STAT3	ACAGGGTTCAGGGTCTC	CCTCCTGGGAATGTCAGG	286	63	N	-
NTRK2	AGATGGATGGAGAGAGAGCTG	TGGAAAGTGGGTAGTGCTG	598	64	N	-

^APCR amplifications were performed in a 20 µl reaction containing 20 ng DNA, 15–50 mM TrisHCl, 10–50 mM KCl, 0–55 mM (NH₄)₂SO₄, 2–2.5 mM MgCl₂, 100 µM each dNTP, 0.4–0.5 µM primers and 0.75 units of FastStartTM Taq DNA polymerase (Roche) with the addition of 10% DMSO (Sigma), where indicated. Cycling conditions consisted of an 8 min denaturation step at 95°C, followed by 35 cycles of 95°C for 30 s, annealing at 58–63°C for 30–60 s and extension at 72°C for 30 s–1 min, with a final extension at 72°C for 10 min. PCR reactions performed by the clinical lab for confirmation of variants (i.e. *EFNB1*) were amplified in a 20 µl reaction using KAPA2G Fast HS ready mix (KAPA Biosystems) with 10 mM MgCl₂, 10 µM each primer and 150–200 ng DNA. Cycling conditions consisted of a 3 min denaturation step at 95°C, followed by 35 cycles of 95°C for 10 s, 63°C for 10 s and 72°C for 1 s, with a final extension at 72°C for 10 min. Restriction digests were carried out in a total volume of 20 µl, containing 5 µl PCR product, 10 U of enzyme (NEB), 1x buffer solution and 1x bovine serum albumin (BSA) if necessary. Incubation was carried out at the specified temperature for 1 h–overnight.

^BMutation was confirmed diagnostically using pyrosequencing technology, on a PyroMark Q96 system with biotinylation of the reverse primer and the following pyrosequencing primer: 5'-CTGTGGTAGTTGGAG-3'.

*Family ID, refer to Supplementary Table 9.1



- 1 Hennekam, R. C. *et al.* Elements of morphology: general terms for congenital anomalies. *Am J Med Genet A* **161A**, 2726-2733 (2013).
- 2 Lajeunie, E., Le Merrer, M., Bonaiti-Pellie, C., Marchac, D. & Renier, D. Genetic study of nonsyndromic coronal craniosynostosis. *Am J Med Genet* **55**, 500-504 (1995).
- 3 Boulet, S. L., Rasmussen, S. A. & Honein, M. A. A population-based study of craniosynostosis in metropolitan Atlanta, 1989-2003. *Am J Med Genet A* **146A**, 984-991 (2008).
- 4 Miller, K. A. *et al.* Diagnostic value of exome and whole genome sequencing in craniosynostosis. *J Med Genet* (2016).
- 5 Cornelissen, M. *et al.* Increase of prevalence of craniosynostosis. *J Craniomaxillofac Surg* **44**, 1273-1279 (2016).
- 6 Utria, A. F. *et al.* The importance of timing in optimizing cranial vault remodelling in syndromic craniosynostosis. *Plast Reconstr Surg* **135**, 1077-1084 (2015).
- 7 Gorlin, R. J. C., M. M.; Levin, L.S. *Syndromes of the head and neck*. (Oxford University Press, 1990).
- 8 Stricker, M. *Craniofacial malformations*. (Churchill Livingstone, 1990).
- 9 Tessier, P. Anatomical classification facial, cranio-facial and latero-facial clefts. *J Maxillofac Surg* **4**, 69-92 (1976).
- 10 van der Meulen, J. C., Mazzola, R., Vermey-Keers, C., Stricker, M. & Raphael, B. A morphogenetic classification of craniofacial malformations. *Plast Reconstr Surg* **71**, 560-572 (1983).
- 11 Wicczorek, D. Human facial dysostoses. *Clin Genet* **83**, 499-510 (2013).
- 12 Halonen, K., Hukki, J., Arte, S. & Hurmerinta, K. Craniofacial structures and dental development in three patients with Nager syndrome. *J Craniofac Surg* **17**, 1180-1187 (2006).
- 13 Twigg, S. R. & Wilkie, A. O. New insights into craniofacial malformations. *Hum Mol Genet* **24**, R50-59 (2015).
- 14 Ten Donkelaar, H. J. L., A. H. M.; Vermeij-Keers, Ch.; Van den Broek, P.; Zaal, M. J. W.; Keyser, A.; Thijssen, H. O. M. . *Klinische anatomie en embryologie*. Tweede druk edn, Vol. Deel II (Elsevier Gezondheidszorg, 2001).
- 15 Richtsmeier, J. T. & Flaherty, K. Hand in glove: brain and skull in development and dysmorphogenesis. *Acta Neuropathol* **125**, 469-489 (2013).
- 16 Opperman, L. A. Cranial sutures as intramembranous bone growth sites. *Dev Dyn* **219**, 472-485 (2000).
- 17 Carlson, B. M. *Human embryology and developmental biology, third edition*. (Mosby, Inc., 2004).
- 18 Reece, J. B. U., L. A.; Cain, M. L.; Wasserman, S. A.; Minorsky, P. V.; Jackson, R. B. . *Campbell biology*. (Pearson Education, Inc., 2011).
- 19 Szabo-Rogers, H. L., Smithers, L. E., Yakob, W. & Liu, K. J. New directions in craniofacial morphogenesis. *Dev Biol* **341**, 84-94 (2010).
- 20 Tapadia, M. D., Cordero, D. R. & Helms, J. A. It's all in your head: new insights into craniofacial development and deformation. *J Anat* **207**, 461-477 (2005).
- 21 Scheurer, L. B., SM. *Developmental Juvenile Osteology*. (Academic Press, 2000).
- 22 Kronenberg, H. M. Developmental regulation of the growth plate. *Nature* **423**, 332-336 (2003).
- 23 Long, F. Building strong bones: molecular regulation of the osteoblast lineage. *Nat Rev Mol Cell Biol* **13**, 27-38 (2012).
- 24 Ting, M. C. *et al.* EphA4 as an effector of Twist1 in the guidance of osteogenic precursor cells during calvarial bone growth and in craniosynostosis. *Development* **136**, 855-864 (2009).
- 25 Beederman, M., Farina, E. M. & Reid, R. R. Molecular basis of cranial suture biology and disease: Osteoblastic and osteoclastic perspectives. *Genes Dis* **1**, 120-125 (2014).
- 26 Moss, M. L. The pathogenesis of premature cranial synostosis in man. *Acta Anat (Basel)* **37**, 351-370 (1959).



Appendices

- 27 Moss, M. L. & Young, R. W. A functional approach to craniology. *Am J Phys Anthropol* **18**, 281-292 (1960).
- 28 Moss-Salentijn, L. Melvin L. Moss and the functional matrix. *J Dent Res* **76**, 1814-1817 (1997).
- 29 Jiang, X., Iseki, S., Maxson, R. E., Sucov, H. M. & Morriss-Kay, G. M. Tissue origins and interactions in the mammalian skull vault. *Dev Biol* **241**, 106-116 (2002).
- 30 Yoshida, T., Vivatbutsiri, P., Morriss-Kay, G., Saga, Y. & Iseki, S. Cell lineage in mammalian craniofacial mesenchyme. *Mech Dev* **125**, 797-808 (2008).
- 31 Grenier, J., Teillet, M. A., Grifone, R., Kelly, R. G. & Duprez, D. Relationship between neural crest cells and cranial mesoderm during head muscle development. *PLoS One* **4**, e4381 (2009).
- 32 Kuratani, S. Developmental studies of the lamprey and hierarchical evolutionary steps towards the acquisition of the jaw. *J Anat* **207**, 489-499 (2005).
- 33 Meulemans, D. & Bronner-Fraser, M. Amphioxus and lamprey AP-2 genes: implications for neural crest evolution and migration patterns. *Development* **129**, 4953-4962 (2002).
- 34 Noden, D. M. Patterns and organization of craniofacial skeletogenic and myogenic mesenchyme: a perspective. *Prog Clin Biol Res* **101**, 167-203 (1982).
- 35 Schilling, T. F. & Kimmel, C. B. Segment and cell type lineage restrictions during pharyngeal arch development in the zebrafish embryo. *Development* **120**, 483-494 (1994).
- 36 Lana-Elola, E., Rice, R., Grigoriadis, A. E. & Rice, D. P. Cell fate specification during calvarial bone and suture development. *Dev Biol* **311**, 335-346 (2007).
- 37 Deckelbaum, R. A. *et al.* Regulation of cranial morphogenesis and cell fate at the neural crest-mesoderm boundary by engrailed 1. *Development* **139**, 1346-1358 (2012).
- 38 Couly, G. F., Coltey, P. M. & Le Douarin, N. M. The triple origin of skull in higher vertebrates: a study in quail-chick chimeras. *Development* **117**, 409-429 (1993).
- 39 Le Douarin, N. M., Ziller, C. & Couly, G. F. Patterning of neural crest derivatives in the avian embryo: in vivo and in vitro studies. *Dev Biol* **159**, 24-49 (1993).
- 40 McBratney-Owen, B., Iseki, S., Bamforth, S. D., Olsen, B. R. & Morriss-Kay, G. M. Development and tissue origins of the mammalian cranial base. *Dev Biol* **322**, 121-132 (2008).
- 41 Bancroft, C., Bowler, T., Bloom, B. & Clelland, C. T. Long-term storage of information in DNA. *Science* **293**, 1763-1765 (2001).
- 42 Bonnet, J. *et al.* Chain and conformation stability of solid-state DNA: implications for room temperature storage. *Nucleic Acids Res* **38**, 1531-1546 (2010).
- 43 Paabo, S. *et al.* Genetic analyses from ancient DNA. *Annu Rev Genet* **38**, 645-679 (2004).
- 44 Church, G. M., Gao, Y. & Kosuri, S. Next-generation digital information storage in DNA. *Science* **337**, 1628 (2012).
- 45 Alberts, B. B., D.; Hopkin, K.; Johnson, A.; Lewis, J.; Raff, M.; Roberts, K.; Walter, P. *Essential cell biology, second edition.* (Garland Science, 2004).
- 46 Strachan, T. R., A. P. *Human Molecular Genetics* 3. 241-242 (Garland Science, 2004).
- 47 Consortium, E. P. *et al.* Identification and analysis of functional elements in 1% of the human genome by the ENCODE pilot project. *Nature* **447**, 799-816 (2007).
- 48 Consortium, E. P. An integrated encyclopedia of DNA elements in the human genome. *Nature* **489**, 57-74 (2012).
- 49 Breathnach, R., Benoist, C., O'Hare, K., Gannon, F. & Chambon, P. Ovalbumin gene: evidence for a leader sequence in mRNA and DNA sequences at the exon-intron boundaries. *Proc Natl Acad Sci U S A* **75**, 4853-4857 (1978).
- 50 Breathnach, R. & Chambon, P. Organization and expression of eucaryotic split genes coding for proteins. *Annu Rev Biochem* **50**, 349-383 (1981).
- 51 Kapustin, Y. *et al.* Cryptic splice sites and split genes. *Nucleic Acids Res* **39**, 5837-5844 (2011).

- 52 Visscher, P. M., Hill, W. G. & Wray, N. R. Heritability in the genomics era--concepts and misconceptions. *Nat Rev Genet* **9**, 255-266 (2008).
- 53 Gilissen, C. *Disease gene identification through next generation sequencing* PhD thesis, Radboud University Nijmegen Medical Centre, (2012).
- 54 Genomes Project, C. *et al.* A map of human genome variation from population-scale sequencing. *Nature* **467**, 1061-1073 (2010).
- 55 Frazer, K. A., Murray, S. S., Schork, N. J. & Topol, E. J. Human genetic variation and its contribution to complex traits. *Nat Rev Genet* **10**, 241-251 (2009).
- 56 Bhangale, T. R., Rieder, M. J., Livingston, R. J. & Nickerson, D. A. Comprehensive identification and characterization of diallelic insertion-deletion polymorphisms in 330 human candidate genes. *Hum Mol Genet* **14**, 59-69 (2005).
- 57 Haraksingh, R. R. & Snyder, M. P. Impacts of variation in the human genome on gene regulation. *J Mol Biol* **425**, 3970-3977 (2013).
- 58 Fenwick, A. L. *et al.* Apparently synonymous substitutions in FGFR2 affect splicing and result in mild Crouzon syndrome. *BMC Med Genet* **15**, 95 (2014).
- 59 Sharma, V. P. *et al.* Mutations in TCF12, encoding a basic helix-loop-helix partner of TWIST1, are a frequent cause of coronal craniosynostosis. *Nat Genet* **45**, 304-307 (2013).
- 60 Nieminen, P. *et al.* Inactivation of IL11 signalling causes craniosynostosis, delayed tooth eruption, and supernumerary teeth. *Am J Hum Genet* **89**, 67-81 (2011).
- 61 Wieczorek, D. *et al.* Compound heterozygosity of low-frequency promoter deletions and rare loss-of-function mutations in TXNL4A causes Burn-McKeown syndrome. *Am J Hum Genet* **95**, 698-707 (2014).
- 62 Twigg, S. R. *et al.* Mutations in multidomain protein MEGF8 identify a Carpenter syndrome subtype associated with defective lateralization. *Am J Hum Genet* **91**, 897-905 (2012).
- 63 Twigg, S. R. *et al.* Mutations of ephrin-B1 (EFNB1), a marker of tissue boundary formation, cause craniofrontonasal syndrome. *Proc Natl Acad Sci U S A* **101**, 8652-8657 (2004).
- 64 Williams, C. A. *et al.* Maternal origin of 15q11-13 deletions in Angelman syndrome suggests a role for genomic imprinting. *Am J Med Genet* **35**, 350-353 (1990).
- 65 Twigg, S. R. *et al.* Gain-of-Function Mutations in ZIC1 Are Associated with Coronal Craniosynostosis and Learning Disability. *Am J Hum Genet* **97**, 378-388 (2015).
- 66 Conrad, D. F. *et al.* Variation in genome-wide mutation rates within and between human families. *Nat Genet* **43**, 712-714 (2011).
- 67 Kong, A. *et al.* Rate of de novo mutations and the importance of father's age to disease risk. *Nature* **488**, 471-475 (2012).
- 68 Michaelson, J. J. *et al.* Whole-genome sequencing in autism identifies hot spots for de novo germline mutation. *Cell* **151**, 1431-1442 (2012).
- 69 Nachman, M. W. & Crowell, S. L. Estimate of the mutation rate per nucleotide in humans. *Genetics* **156**, 297-304 (2000).
- 70 Genome of the Netherlands, C. Whole-genome sequence variation, population structure and demographic history of the Dutch population. *Nat Genet* **46**, 818-825 (2014).
- 71 Roach, J. C. *et al.* Analysis of genetic inheritance in a family quartet by whole-genome sequencing. *Science* **328**, 636-639 (2010).
- 72 Veltman, J. A. & Brunner, H. G. De novo mutations in human genetic disease. *Nat Rev Genet* **13**, 565-575 (2012).
- 73 Lynch, M. Rate, molecular spectrum, and consequences of human mutation. *Proc Natl Acad Sci U S A* **107**, 961-968 (2010).
- 74 Itsara, A. *et al.* De novo rates and selection of large copy number variation. *Genome Res* **20**, 1469-1481 (2010).



Appendices

- 75 Hodgkinson, A. & Eyre-Walker, A. Variation in the mutation rate across mammalian genomes. *Nat Rev Genet* **12**, 756-766 (2011).
- 76 Francioli, L. C. *et al.* A framework for the detection of de novo mutations in family-based sequencing data. *Eur J Hum Genet* **25**, 227-233 (2017).
- 77 Chen, J. M., Ferec, C. & Cooper, D. N. Revealing the human mutome. *Clin Genet* **78**, 310-320 (2010).
- 78 *Molecular diagnostics, techniques and applications.* (IVA GROEP bv, 2009).
- 79 Sanger, F., Nicklen, S. & Coulson, A. R. DNA sequencing with chain-terminating inhibitors. *Proc Natl Acad Sci U S A* **74**, 5463-5467 (1977).
- 80 Maxam, A. M. & Gilbert, W. A new method for sequencing DNA. *Proc Natl Acad Sci U S A* **74**, 560-564 (1977).
- 81 Venter, J. C. *et al.* The sequence of the human genome. *Science* **291**, 1304-1351 (2001).
- 82 Lander, E. S. *et al.* Initial sequencing and analysis of the human genome. *Nature* **409**, 860-921 (2001).
- 83 Smith, L. M. *et al.* Fluorescence detection in automated DNA sequence analysis. *Nature* **321**, 674-679 (1986).
- 84 Prober, J. M. *et al.* A system for rapid DNA sequencing with fluorescent chain-terminating dideoxynucleotides. *Science* **238**, 336-341 (1987).
- 85 Murray, V. Improved double-stranded DNA sequencing using the linear polymerase chain reaction. *Nucleic Acids Res* **17**, 8889 (1989).
- 86 Swerdlow, H., Wu, S. L., Harke, H. & Dovichi, N. J. Capillary gel electrophoresis for DNA sequencing. Laser-induced fluorescence detection with the sheath flow cuvette. *J Chromatogr* **516**, 61-67 (1990).
- 87 Cohen, A. S., Najarian, D. R. & Karger, B. L. Separation and analysis of DNA sequence reaction products by capillary gel electrophoresis. *J Chromatogr* **516**, 49-60 (1990).
- 88 Heiger, D. N., Cohen, A. S. & Karger, B. L. Separation of DNA restriction fragments by high performance capillary electrophoresis with low and zero crosslinked polyacrylamide using continuous and pulsed electric fields. *J Chromatogr* **516**, 33-48 (1990).
- 89 Van Prooijen-Knegt, A. C. *et al.* In situ hybridisation of DNA sequences in human metaphase chromosomes visualized by an indirect fluorescent immunocytochemical procedure. *Exp Cell Res* **141**, 397-407 (1982).
- 90 Chang, T. W. Binding of cells to matrixes of distinct antibodies coated on solid surface. *J Immunol Methods* **65**, 217-223 (1983).
- 91 Solinas-Toldo, S. *et al.* Matrix-based comparative genomic hybridisation: biochips to screen for genomic imbalances. *Genes Chromosomes Cancer* **20**, 399-407 (1997).
- 92 Pinkel, D. *et al.* High resolution analysis of DNA copy number variation using comparative genomic hybridisation to microarrays. *Nat Genet* **20**, 207-211 (1998).
- 93 Lucito, R. *et al.* Representational oligonucleotide microarray analysis: a high-resolution method to detect genome copy number variation. *Genome Res* **13**, 2291-2305 (2003).
- 94 Cooper, G. M., Zerr, T., Kidd, J. M., Eichler, E. E. & Nickerson, D. A. Systematic assessment of copy number variant detection via genome-wide SNP genotyping. *Nat Genet* **40**, 1199-1203 (2008).
- 95 Redon, R. *et al.* Global variation in copy number in the human genome. *Nature* **444**, 444-454 (2006).
- 96 Jeuken, J., Cornelissen, S., Boots-Sprenger, S., Gijzen, S. & Wesseling, P. Multiplex ligation-dependent probe amplification: a diagnostic tool for simultaneous identification of different genetic markers in glial tumors. *J Mol Diagn* **8**, 433-443 (2006).
- 97 Alvizi, L. *et al.* Differential methylation is associated with non-syndromic cleft lip and palate and contributes to penetrance effects. *Sci Rep* **7**, 2441 (2017).
- 98 Schouten, J. P. *et al.* Relative quantification of 40 nucleic acid sequences by multiplex ligation-dependent probe amplification. *Nucleic Acids Res* **30**, e57 (2002).
- 99 Margulies, M. *et al.* Genome sequencing in microfabricated high-density picolitre reactors. *Nature* **437**, 376-380 (2005).

- 100 Dressman, D., Yan, H., Traverso, G., Kinzler, K. W. & Vogelstein, B. Transforming single DNA molecules into fluorescent magnetic particles for detection and enumeration of genetic variations. *Proc Natl Acad Sci U S A* **100**, 8817-8822 (2003).
- 101 Bentley, D. R. *et al.* Accurate whole human genome sequencing using reversible terminator chemistry. *Nature* **456**, 53-59 (2008).
- 102 Fedurco, M., Romieu, A., Williams, S., Lawrence, I. & Turcatti, G. BTA, a novel reagent for DNA attachment on glass and efficient generation of solid-phase amplified DNA colonies. *Nucleic Acids Res* **34**, e22 (2006).
- 103 Shendure, J. *et al.* Accurate multiplex polony sequencing of an evolved bacterial genome. *Science* **309**, 1728-1732 (2005).
- 104 Drmanac, R. *et al.* Human genome sequencing using unchained base reads on self-assembling DNA nanoarrays. *Science* **327**, 78-81 (2010).
- 105 Blanco, L. *et al.* Highly efficient DNA synthesis by the phage phi 29 DNA polymerase. Symmetrical mode of DNA replication. *J Biol Chem* **264**, 8935-8940 (1989).
- 106 Drmanac, R. *et al.* DNA sequence determination by hybridisation: a strategy for efficient large-scale sequencing. *Science* **260**, 1649-1652 (1993).
- 107 Pihlak, A. *et al.* Rapid genome sequencing with short universal tiling probes. *Nat Biotechnol* **26**, 676-684 (2008).
- 108 Carnevali, P. *et al.* Computational techniques for human genome resequencing using mated gapped reads. *J Comput Biol* **19**, 279-292 (2012).
- 109 Davydov, E. V. *et al.* Identifying a high fraction of the human genome to be under selective constraint using GERP++. *PLoS Comput Biol* **6**, e1001025 (2010).
- 110 Erikson, G. A. *et al.* Whole-Genome Sequencing of a Healthy Aging Cohort. *Cell* **165**, 1002-1011 (2016).
- 111 Lek, M. *et al.* Analysis of protein-coding genetic variation in 60,706 humans. *Nature* **536**, 285-291 (2016).
- 112 Exome Variant Server, N. G. E. S. P. E., Seattle, WA. <<http://evs.gs.washington.edu/EVS/>> (
- 113 Genomes Project, C. *et al.* A global reference for human genetic variation. *Nature* **526**, 68-74 (2015).
- 114 Kumar, P., Henikoff, S. & Ng, P. C. Predicting the effects of coding non-synonymous variants on protein function using the SIFT algorithm. *Nat Protoc* **4**, 1073-1081 (2009).
- 115 Adzhubei, I. A. *et al.* A method and server for predicting damaging missense mutations. *Nat Methods* **7**, 248-249 (2010).
- 116 Chun, S. & Fay, J. C. Identification of deleterious mutations within three human genomes. *Genome Res* **19**, 1553-1561 (2009).
- 117 Schwarz, J. M., Rodelsperger, C., Schuelke, M. & Seelow, D. MutationTaster evaluates disease-causing potential of sequence alterations. *Nat Methods* **7**, 575-576 (2010).
- 118 Shihab, H. A. *et al.* Predicting the functional, molecular, and phenotypic consequences of amino acid substitutions using hidden Markov models. *Hum Mutat* **34**, 57-65 (2013).
- 119 Dong, C. *et al.* Comparison and integration of deleteriousness prediction methods for nonsynonymous SNVs in whole exome sequencing studies. *Hum Mol Genet* **24**, 2125-2137 (2015).
- 120 Carter, H., Douville, C., Stenson, P. D., Cooper, D. N. & Karchin, R. Identifying Mendelian disease genes with the variant effect scoring tool. *BMC Genomics* **14 Suppl 3**, S3 (2013).
- 121 Kircher, M. *et al.* A general framework for estimating the relative pathogenicity of human genetic variants. *Nat Genet* **46**, 310-315 (2014).
- 122 King, M. C. & Wilson, A. C. Evolution at two levels in humans and chimpanzees. *Science* **188**, 107-116 (1975).
- 123 Fujiyama, A. *et al.* Construction and analysis of a human-chimpanzee comparative clone map. *Science* **295**, 131-134 (2002).
- 124 Pollard, K. S., Hubisz, M. J., Rosenbloom, K. R. & Siepel, A. Detection of nonneutral substitution rates on mammalian phylogenies. *Genome Res* **20**, 110-121 (2010).



Appendices

- 125 Johnson, D. & Wilkie, A. O. Craniosynostosis. *Eur J Hum Genet* **19**, 369-376 (2011).
- 126 Greenwood, J., Flodman, P., Osann, K., Boyadjiev, S. A. & Kimonis, V. Familial incidence and associated symptoms in a population of individuals with nonsyndromic craniosynostosis. *Genet Med* **16**, 302-310 (2014).
- 127 Twigg, S. R. & Wilkie, A. O. A Genetic-Pathophysiological Framework for Craniosynostosis. *Am J Hum Genet* **97**, 359-377 (2015).
- 128 Wilkie, A. O. *et al.* Prevalence and complications of single-gene and chromosomal disorders in craniosynostosis. *Pediatrics* **126**, e391-400 (2010).
- 129 Cohen, M. M. M., R.E. *Craniosynostosis: diagnosis, evaluation, and management.* (Oxford University Press, 2000).
- 130 Jabs, E. W. *et al.* A mutation in the homeodomain of the human MSX2 gene in a family affected with autosomal dominant craniosynostosis. *Cell* **75**, 443-450 (1993).
- 131 Wilkie, A. O. *et al.* Apert syndrome results from localized mutations of FGFR2 and is allelic with Crouzon syndrome. *Nat Genet* **9**, 165-172 (1995).
- 132 Oldridge, M. *et al.* De novo alu-element insertions in FGFR2 identify a distinct pathological basis for Apert syndrome. *Am J Hum Genet* **64**, 446-461 (1999).
- 133 Reardon, W. *et al.* Mutations in the fibroblast growth factor receptor 2 gene cause Crouzon syndrome. *Nat Genet* **8**, 98-103 (1994).
- 134 Jabs, E. W. *et al.* Jackson-Weiss and Crouzon syndromes are allelic with mutations in fibroblast growth factor receptor 2. *Nat Genet* **8**, 275-279 (1994).
- 135 Moloney, D. M. *et al.* Prevalence of Pro250Arg mutation of fibroblast growth factor receptor 3 in coronal craniosynostosis. *Lancet* **349**, 1059-1062 (1997).
- 136 Bellus, G. A. *et al.* Identical mutations in three different fibroblast growth factor receptor genes in autosomal dominant craniosynostosis syndromes. *Nat Genet* **14**, 174-176 (1996).
- 137 Muenke, M. *et al.* A unique point mutation in the fibroblast growth factor receptor 3 gene (FGFR3) defines a new craniosynostosis syndrome. *Am J Hum Genet* **60**, 555-564 (1997).
- 138 Howard, T. D. *et al.* Mutations in TWIST, a basic helix-loop-helix transcription factor, in Saethre-Chotzen syndrome. *Nat Genet* **15**, 36-41 (1997).
- 139 el Ghouzzi, V. *et al.* Mutations of the TWIST gene in the Saethre-Chotzen syndrome. *Nat Genet* **15**, 42-46 (1997).
- 140 Twigg, S. R. *et al.* Reduced dosage of ERF causes complex craniosynostosis in humans and mice and links ERK1/2 signalling to regulation of osteogenesis. *Nat Genet* **45**, 308-313 (2013).
- 141 Wieland, I. *et al.* Mutations of the ephrin-B1 gene cause craniofrontonasal syndrome. *Am J Hum Genet* **74**, 1209-1215 (2004).
- 142 Kim, S. *et al.* Localized TWIST1 and TWIST2 basic domain substitutions cause four distinct human diseases that can be modeled in *Caenorhabditis elegans*. *Hum Mol Genet* **26**, 2118-2132 (2017).
- 143 Gilissen, C. *et al.* Genome sequencing identifies major causes of severe intellectual disability. *Nature* **511**, 344-347 (2014).
- 144 Twigg, S. R. *et al.* Reduced dosage of ERF causes complex craniosynostosis in humans and mice and links ERK1/2 signalling to regulation of osteogenesis. *Nat Genet* (2013).
- 145 Deciphering Developmental Disorders, S. Large-scale discovery of novel genetic causes of developmental disorders. *Nature* **519**, 223-228 (2015).
- 146 Goos, J. A. *et al.* Identification of Intragenic Exon Deletions and Duplication of TCF12 by Whole Genome or Targeted Sequencing as a Cause of TCF12-Related Craniosynostosis. *Hum Mutat* **37**, 732-736 (2016).
- 147 Plon, S. E. *et al.* Sequence variant classification and reporting: recommendations for improving the interpretation of cancer susceptibility genetic test results. *Hum Mutat* **29**, 1282-1291 (2008).

- 148 den Dunnen, J. T. & Antonarakis, S. E. Mutation nomenclature extensions and suggestions to describe complex mutations: a discussion. *Hum Mutat* **15**, 7-12 (2000).
- 149 Rutland, P. *et al.* Identical mutations in the FGFR2 gene cause both Pfeiffer and Crouzon syndrome phenotypes. *Nat Genet* **9**, 173-176 (1995).
- 150 Przylepa, K. A. *et al.* Fibroblast growth factor receptor 2 mutations in Beare-Stevenson cutis gyrata syndrome. *Nat Genet* **13**, 492-494 (1996).
- 151 Park, W. J. *et al.* Novel FGFR2 mutations in Crouzon and Jackson-Weiss syndromes show allelic heterogeneity and phenotypic variability. *Hum Mol Genet* **4**, 1229-1233 (1995).
- 152 Chun, K., Siegel-Bartelt, J., Chitayat, D., Phillips, J. & Ray, P. N. FGFR2 mutation associated with clinical manifestations consistent with Antley-Bixler syndrome. *Am J Med Genet* **77**, 219-224 (1998).
- 153 Stubbs, A. *et al.* Huvarome: a web server resource of whole genome next-generation sequencing allelic frequencies to aid in pathological candidate gene selection. *J Clin Bioinforma* **2**, 19 (2012).
- 154 Genomes Project, C. *et al.* An integrated map of genetic variation from 1,092 human genomes. *Nature* **491**, 56-65 (2012).
- 155 Forbes, S. A. *et al.* The Catalogue of Somatic Mutations in Cancer (COSMIC). *Curr Protoc Hum Genet* **Chapter 10**, Unit 10 11 (2008).
- 156 Forbes, S. A. *et al.* COSMIC: mining complete cancer genomes in the Catalogue of Somatic Mutations in Cancer. *Nucleic Acids Res* **39**, D945-950 (2011).
- 157 Ng, P. C. & Henikoff, S. Predicting deleterious amino acid substitutions. *Genome Res* **11**, 863-874 (2001).
- 158 Tavtigian, S. V. *et al.* Comprehensive statistical study of 452 BRCA1 missense substitutions with classification of eight recurrent substitutions as neutral. *J Med Genet* **43**, 295-305 (2006).
- 159 Suh, Y. J. *et al.* A novel FGFR2 mutation in tyrosine kinase II domain, L617F, in Crouzon syndrome. *J Cell Biochem* **115**, 102-110 (2014).
- 160 Johnson, D. E. & Williams, L. T. Structural and functional diversity in the FGF receptor multigene family. *Adv Cancer Res* **60**, 1-41 (1993).
- 161 Jaye, M., Schlessinger, J. & Dionne, C. A. Fibroblast growth factor receptor tyrosine kinases: molecular analysis and signal transduction. *Biochim Biophys Acta* **1135**, 185-199 (1992).
- 162 Kan, S. H. *et al.* Genomic screening of fibroblast growth-factor receptor 2 reveals a wide spectrum of mutations in patients with syndromic craniosynostosis. *Am J Hum Genet* **70**, 472-486 (2002).
- 163 Lajeunie, E. *et al.* Mutation screening in patients with syndromic craniosynostoses indicates that a limited number of recurrent FGFR2 mutations accounts for severe forms of Pfeiffer syndrome. *Eur J Hum Genet* **14**, 289-298 (2006).
- 164 Roscioli, T. *et al.* Genotype and clinical care correlations in craniosynostosis: findings from a cohort of 630 Australian and New Zealand patients. *Am J Med Genet C Semin Med Genet* **163C**, 259-270 (2013).
- 165 Muenke, M. W., A. O. M. *Craniosynostosis syndromes*. 8th edn edn, 6117-6146 (Mc-Graw-Hill, 2001).
- 166 Pulleyn, L. J. *et al.* Spectrum of craniosynostosis phenotypes associated with novel mutations at the fibroblast growth factor receptor 2 locus. *Eur J Hum Genet* **4**, 283-291 (1996).
- 167 Lajeunie, E. *et al.* FGFR2 mutations in Pfeiffer syndrome. *Nat Genet* **9**, 108 (1995).
- 168 Schell, U. *et al.* Mutations in FGFR1 and FGFR2 cause familial and sporadic Pfeiffer syndrome. *Hum Mol Genet* **4**, 323-328 (1995).
- 169 Merrill, A. E. *et al.* Bent bone dysplasia-FGFR2 type, a distinct skeletal disorder, has deficient canonical FGF signalling. *Am J Hum Genet* **90**, 550-557 (2012).
- 170 Agochukwu, N. B., Solomon, B. D. & Muenke, M. Impact of genetics on the diagnosis and clinical management of syndromic craniosynostoses. *Childs Nerv Syst* **28**, 1447-1463 (2012).
- 171 Mohammadi, M., Olsen, S. K. & Ibrahimi, O. A. Structural basis for fibroblast growth factor receptor activation. *Cytokine Growth Factor Rev* **16**, 107-137 (2005).



- 172 Eswarakumar, V. P., Lax, I. & Schlessinger, J. Cellular signalling by fibroblast growth factor receptors. *Cytokine Growth Factor Rev* **16**, 139-149 (2005).
- 173 Kan, R. *et al.* Expression analysis of an FGFR2 IIIc 5' splice site mutation (1084+3A->G). *J Med Genet* **41**, e108 (2004).
- 174 Podkrajsek, K. T. *et al.* Detection of a complete autoimmune regulator gene deletion and two additional novel mutations in a cohort of patients with atypical phenotypic variants of autoimmune polyglandular syndrome type 1. *Eur J Endocrinol* **159**, 633-639 (2008).
- 175 Everett, E. T., Britto, D. A., Ward, R. E. & Hartsfield, J. K., Jr. A novel FGFR2 gene mutation in Crouzon syndrome associated with apparent nonpenetrance. *Cleft Palate Craniofac J* **36**, 533-541 (1999).
- 176 Plotnikov, A. N., Hubbard, S. R., Schlessinger, J. & Mohammadi, M. Crystal structures of two FGF-FGFR complexes reveal the determinants of ligand-receptor specificity. *Cell* **101**, 413-424 (2000).
- 177 Robertson, S. C. *et al.* Activating mutations in the extracellular domain of the fibroblast growth factor receptor 2 function by disruption of the disulfide bond in the third immunoglobulin-like domain. *Proc Natl Acad Sci U S A* **95**, 4567-4572 (1998).
- 178 Johnson, D., Wall, S. A., Mann, S. & Wilkie, A. O. A novel mutation, Ala315Ser, in FGFR2: a gene-environment interaction leading to craniosynostosis? *Eur J Hum Genet* **8**, 571-577 (2000).
- 179 Li, X., Park, W. J., Pyeritz, R. E. & Jabs, E. W. Effect on splicing of a silent FGFR2 mutation in Crouzon syndrome. *Nat Genet* **9**, 232-233 (1995).
- 180 Del Gatto, F. & Breathnach, R. A Crouzon syndrome synonymous mutation activates a 5' splice site within the IIIc exon of the FGFR2 gene. *Genomics* **27**, 558-559 (1995).
- 181 Cornejo-Roldan, L. R., Roessler, E. & Muenke, M. Analysis of the mutational spectrum of the FGFR2 gene in Pfeiffer syndrome. *Hum Genet* **104**, 425-431 (1999).
- 182 Kress, W., Collmann, H., Busse, M., Halliger-Keller, B. & Mueller, C. R. Clustering of FGFR2 gene mutations inpatients with Pfeiffer and Crouzon syndromes (FGFR2-associated craniosynostoses). *Cytogenet Cell Genet* **91**, 134-137 (2000).
- 183 Cohen, M. M., Jr. Craniofrontonasal dysplasia. *Birth Defects Orig Artic Ser* **15**, 85-89 (1979).
- 184 Reynolds, J. F., Haas, R. J., Edgerton, M. T. & Kelly, T. E. Craniofrontonasal dysplasia in a three-generation kindred. *J Craniofac Genet Dev Biol* **2**, 233-238 (1982).
- 185 Grutzner, E. & Gorlin, R. J. Craniofrontonasal dysplasia: phenotypic expression in females and males and genetic considerations. *Oral Surg Oral Med Oral Pathol* **65**, 436-444 (1988).
- 186 Kere, J., Ritvanen, A., Marttinen, E. & Kaitila, I. Craniofrontonasal dysostosis: variable expression in a three-generation family. *Clin Genet* **38**, 441-446 (1990).
- 187 Suzuki, H., Nara, T., Minato, S. & Kamiishi, H. Experience of surgical treatment for craniofrontonasal dysplasia. *Tohoku J Exp Med* **164**, 251-257 (1991).
- 188 Kapusta, L., Brunner, H. G. & Hamel, B. C. Craniofrontonasal dysplasia. *Eur J Pediatr* **151**, 837-841 (1992).
- 189 Natarajan, U., Baraitser, M., Nicolaiades, K. & Gosden, C. Craniofrontonasal dysplasia in two male sibs. *Clin Dysmorphol* **2**, 360-364 (1993).
- 190 Saavedra, D., Richieri-Costa, A., Guion-Almeida, M. L. & Cohen, M. M., Jr. Craniofrontonasal syndrome: study of 41 patients. *Am J Med Genet* **61**, 147-151 (1996).
- 191 Orr, D. J., Slaney, S., Ashworth, G. J. & Poole, M. D. Craniofrontonasal dysplasia. *Br J Plast Surg* **50**, 153-161 (1997).
- 192 Wieacker, P. & Wieland, I. Clinical and genetic aspects of craniofrontonasal syndrome: towards resolving a genetic paradox. *Mol Genet Metab* **86**, 110-116 (2005).
- 193 Kawamoto, H. K. *et al.* Craniofrontonasal dysplasia: a surgical treatment algorithm. *Plast Reconstr Surg* **120**, 1943-1956 (2007).
- 194 Young, I. D. Craniofrontonasal dysplasia. *J Med Genet* **24**, 193-196 (1987).

- 195 Moffat, S. M., Posnick, J. C., Pron, G. E. & Armstrong, D. C. Frontonasal and craniofrontonasal dysplasia: preoperative quantitative description of the cranio-orbito-zygomatic region based on computed and conventional tomography. *Cleft Palate Craniofac J* **31**, 97-105 (1994).
- 196 Mahore, A., Shah, A., Nadkarni, T. & Goel, A. Craniofrontonasal dysplasia associated with Chiari malformation. *J Neurosurg Pediatr* **5**, 375-379 (2010).
- 197 Hurst, J. & Baraitser, M. Craniofrontonasal dysplasia. *J Med Genet* **25**, 133-134 (1988).
- 198 Wieland, I. *et al.* Mapping of a further locus for X-linked craniofrontonasal syndrome. *Cytogenet Genome Res* **99**, 285-288 (2002).
- 199 Compagni, A., Logan, M., Klein, R. & Adams, R. H. Control of skeletal patterning by ephrinB1-EphB interactions. *Dev Cell* **5**, 217-230 (2003).
- 200 Shotelersuk, V., Siriwan, P. & Ausavarat, S. A novel mutation in EFNB1, probably with a dominant negative effect, underlying craniofrontonasal syndrome. *Cleft Palate Craniofac J* **43**, 152-154 (2006).
- 201 Wieland, I. *et al.* Twenty-six novel EFNB1 mutations in familial and sporadic craniofrontonasal syndrome (CFNS). *Hum Mutat* **26**, 113-118 (2005).
- 202 Vasudevan, P. C. *et al.* Expanding the phenotype of craniofrontonasal syndrome: two unrelated boys with EFNB1 mutations and congenital diaphragmatic hernia. *Eur J Hum Genet* **14**, 884-887 (2006).
- 203 Twigg, S. R. *et al.* The origin of EFNB1 mutations in craniofrontonasal syndrome: frequent somatic mosaicism and explanation of the paucity of carrier males. *Am J Hum Genet* **78**, 999-1010 (2006).
- 204 Davy, A., Bush, J. O. & Soriano, P. Inhibition of gap junction communication at ectopic Eph/ephrin boundaries underlies craniofrontonasal syndrome. *PLoS Biol* **4**, e315 (2006).
- 205 Wallis, D. *et al.* Additional EFNB1 mutations in craniofrontonasal syndrome. *Am J Med Genet A* **146A**, 2008-2012 (2008).
- 206 Wieland, I. *et al.* Dissecting the molecular mechanisms in craniofrontonasal syndrome: differential mRNA expression of mutant EFNB1 and the cellular mosaic. *Eur J Hum Genet* **16**, 184-191 (2008).
- 207 Hogue, J. *et al.* A novel EFNB1 mutation (c.712delG) in a family with craniofrontonasal syndrome and diaphragmatic hernia. *Am J Med Genet A* **152A**, 2574-2577 (2010).
- 208 Makarov, R. *et al.* The impact of CFNS-causing EFNB1 mutations on ephrin-B1 function. *BMC Med Genet* **11**, 98 (2010).
- 209 Apostolopoulou, D. *et al.* A novel de novo mutation within EFNB1 gene in a young girl with Craniofrontonasal syndrome. *Cleft Palate Craniofac J* (2011).
- 210 Zafeiriou, D. I., Pavlidou, E. L. & Vargiami, E. Diverse clinical and genetic aspects of craniofrontonasal syndrome. *Pediatr Neurol* **44**, 83-87 (2011).
- 211 Klein, R. Eph/ephrin signalling in morphogenesis, neural development and plasticity. *Curr Opin Cell Biol* **16**, 580-589 (2004).
- 212 Kwee, M. L. & Lindhout, D. Frontonasal dysplasia, coronal craniosynostosis, pre- and postaxial polydactyly and split nails: a new autosomal dominant mutant with reduced penetrance and variable expression? *Clin Genet* **24**, 200-205 (1983).
- 213 Twigg, S. R. *et al.* Cellular interference in craniofrontonasal syndrome: males mosaic for mutations in the X-linked EFNB1 gene are more severely affected than true hemizygotes. *Hum Mol Genet* **22**, 1654-1662 (2013).
- 214 Farkas, L. & Munro, I. *Anthropometric Facial Proportions in Medicine*. 1 edn, 181, 208, 223, 285, 290, 298, 312, 313 (Charles C Thomas, 1987).
- 215 Reardon, W., Temple, I. K., Jones, B. & Baraitser, M. Frontonasal dysplasia or craniofrontonasal dysplasia and the Poland anomaly? *Clin Genet* **38**, 233-236 (1990).
- 216 Jabs, E. W. *TWIST and the Saethre-Chotzen syndrome*. 2nd edn, 474-481 (Oxford University Press, 2008).
- 217 Ng, S. B. *et al.* Exome sequencing identifies the cause of a mendelian disorder. *Nat Genet* **42**, 30-35 (2010).



Appendices

- 218 Hu, J. S., Olson, E. N. & Kingston, R. E. HEB, a helix-loop-helix protein related to E2A and ITF2 that can modulate the DNA-binding ability of myogenic regulatory factors. *Mol Cell Biol* **12**, 1031-1042 (1992).
- 219 Nielsen, A. L., Pallisgaard, N., Pedersen, F. S. & Jorgensen, P. Murine helix-loop-helix transcriptional activator proteins binding to the E-box motif of the Akv murine leukemia virus enhancer identified by cDNA cloning. *Mol Cell Biol* **12**, 3449-3459 (1992).
- 220 Gan, T. I. *et al.* Genomic organization of human TCF12 gene and spliced mRNA variants producing isoforms of transcription factor HTF4. *Cytogenet Genome Res* **98**, 245-248 (2002).
- 221 Hiraki, Y. *et al.* Craniosynostosis in a patient with a de novo 15q15-q22 deletion. *Am J Med Genet A* **146A**, 1462-1465 (2008).
- 222 Wang, D. *et al.* The basic helix-loop-helix transcription factor HEBAlt is expressed in pro-T cells and enhances the generation of T cell precursors. *J Immunol* **177**, 109-119 (2006).
- 223 Whalen, S. *et al.* Novel comprehensive diagnostic strategy in Pitt-Hopkins syndrome: clinical score and further delineation of the TCF4 mutational spectrum. *Hum Mutat* **33**, 64-72 (2012).
- 224 Laursen, K. B., Mielke, E., Iannaccone, P. & Fuchtbauer, E. M. Mechanism of transcriptional activation by the proto-oncogene Twist1. *J Biol Chem* **282**, 34623-34633 (2007).
- 225 Aronheim, A., Shiran, R., Rosen, A. & Walker, M. D. The E2A gene product contains two separable and functionally distinct transcription activation domains. *Proc Natl Acad Sci U S A* **90**, 8063-8067 (1993).
- 226 Markus, M., Du, Z. & Benezra, R. Enhancer-specific modulation of E protein activity. *J Biol Chem* **277**, 6469-6477 (2002).
- 227 Wojciechowski, J., Lai, A., Kondo, M. & Zhuang, Y. E2A and HEB are required to block thymocyte proliferation prior to pre-TCR expression. *J Immunol* **178**, 5717-5726 (2007).
- 228 Connerney, J. *et al.* Twist1 dimer selection regulates cranial suture patterning and fusion. *Dev Dyn* **235**, 1345-1357 (2006).
- 229 Lakso, M. *et al.* Efficient in vivo manipulation of mouse genomic sequences at the zygote stage. *Proc Natl Acad Sci U S A* **93**, 5860-5865 (1996).
- 230 Chen, Z. F. & Behringer, R. R. twist is required in head mesenchyme for cranial neural tube morphogenesis. *Genes Dev* **9**, 686-699 (1995).
- 231 Chai, Y. & Maxson, R. E., Jr. Recent advances in craniofacial morphogenesis. *Dev Dyn* **235**, 2353-2375 (2006).
- 232 Merrill, A. E. *et al.* Cell mixing at a neural crest-mesoderm boundary and deficient ephrin-Eph signalling in the pathogenesis of craniosynostosis. *Hum Mol Genet* **15**, 1319-1328 (2006).
- 233 Bialek, P. *et al.* A twist code determines the onset of osteoblast differentiation. *Dev Cell* **6**, 423-435 (2004).
- 234 Hayashi, M. *et al.* Comparative roles of Twist-1 and Id1 in transcriptional regulation by BMP signalling. *J Cell Sci* **120**, 1350-1357 (2007).
- 235 Longo, A., Guanga, G. P. & Rose, R. B. Crystal structure of E47-NeuroD1/beta2 bHLH domain-DNA complex: heterodimer selectivity and DNA recognition. *Biochemistry* **47**, 218-229 (2008).
- 236 di Rocco, F. *et al.* Clinical spectrum and outcomes in families with coronal synostosis and TCF12 mutations. *Eur J Hum Genet* **22**, 1413-1416 (2014).
- 237 Paumard-Hernandez, B. *et al.* Expanding the mutation spectrum in 182 Spanish probands with craniosynostosis: identification and characterization of novel TCF12 variants. *Eur J Hum Genet* **23**, 907-914 (2015).
- 238 Fukushima, Y., Wakui, K., Nishida, T. & Nishimoto, H. Craniosynostosis in an infant with an interstitial deletion of 15q [46,XY,del(15)(q15q22.1)]. *Am J Med Genet* **36**, 209-213 (1990).
- 239 Shur, N., Cowan, J. & Wheeler, P. G. Craniosynostosis and congenital heart anomalies associated with a maternal deletion of 15q15-22.1. *Am J Med Genet A* **120A**, 542-546 (2003).
- 240 Le Tanno, P. *et al.* Maternal complex chromosomal rearrangement leads to TCF12 microdeletion in a patient presenting with coronal craniosynostosis and intellectual disability. *Am J Med Genet A* **164A**, 1530-1536 (2014).

- 241 Piard, J. *et al.* TCF12 microdeletion in a 72-year-old woman with intellectual disability. *Am J Med Genet A* **167A**, 1897-1901 (2015).
- 242 Ye, K., Schulz, M. H., Long, Q., Apweiler, R. & Ning, Z. Pindel: a pattern growth approach to detect break points of large deletions and medium sized insertions from paired-end short reads. *Bioinformatics* **25**, 2865-2871 (2009).
- 243 Chen, J. M., Cooper, D. N., Ferec, C., Kehrer-Sawatzki, H. & Patrinos, G. P. Genomic rearrangements in inherited disease and cancer. *Semin Cancer Biol* **20**, 222-233 (2010).
- 244 Gu, W., Zhang, F. & Lupski, J. R. Mechanisms for human genomic rearrangements. *Pathogenetics* **1**, 4 (2008).
- 245 Stankiewicz, P. *et al.* Genome architecture catalyzes nonrecurrent chromosomal rearrangements. *Am J Hum Genet* **72**, 1101-1116 (2003).
- 246 Zhang, Y. *et al.* HTF4: a new human helix-loop-helix protein. *Nucleic Acids Res* **19**, 4555 (1991).
- 247 Hajihosseini, M. K. *et al.* Evidence that Fgf10 contributes to the skeletal and visceral defects of an Apert syndrome mouse model. *Dev Dyn* **238**, 376-385 (2009).
- 248 Holmes, G. *et al.* Early onset of craniosynostosis in an Apert mouse model reveals critical features of this pathology. *Dev Biol* **328**, 273-284 (2009).
- 249 Deckelbaum, R. A., Majithia, A., Booker, T., Henderson, J. E. & Loomis, C. A. The homeoprotein engrailed 1 has pleiotropic functions in calvarial intramembranous bone formation and remodelling. *Development* **133**, 63-74 (2006).
- 250 Ali, R. G., Bellchambers, H. M. & Arkell, R. M. Zinc fingers of the cerebellum (Zic): transcription factors and co-factors. *Int J Biochem Cell Biol* **44**, 2065-2068 (2012).
- 251 Benedyk, M. J., Mullen, J. R. & DiNardo, S. odd-paired: a zinc finger pair-rule protein required for the timely activation of engrailed and wingless in Drosophila embryos. *Genes Dev* **8**, 105-117 (1994).
- 252 Aruga, J. *et al.* A wide-range phylogenetic analysis of Zic proteins: implications for correlations between protein structure conservation and body plan complexity. *Genomics* **87**, 783-792 (2006).
- 253 Merzdorf, C. S. Emerging roles for zic genes in early development. *Dev Dyn* **236**, 922-940 (2007).
- 254 Grinberg, I. *et al.* Heterozygous deletion of the linked genes ZIC1 and ZIC4 is involved in Dandy-Walker malformation. *Nat Genet* **36**, 1053-1055 (2004).
- 255 Aruga, J. *et al.* Mouse Zic1 is involved in cerebellar development. *J Neurosci* **18**, 284-293 (1998).
- 256 Blank, M. C. *et al.* Multiple developmental programs are altered by loss of Zic1 and Zic4 to cause Dandy-Walker malformation cerebellar pathogenesis. *Development* **138**, 1207-1216 (2011).
- 257 Eley, K. A. *et al.* Raised intracranial pressure is frequent in untreated nonsyndromic unicoronal synostosis and does not correlate with severity of phenotypic features. *Plast Reconstr Surg* **130**, 690e-697e (2012).
- 258 Taylor, J. C. *et al.* Factors influencing success of clinical genome sequencing across a broad spectrum of disorders. *Nat Genet* **47**, 717-726 (2015).
- 259 Rimmer, A. *et al.* Integrating mapping-, assembly- and haplotype-based approaches for calling variants in clinical sequencing applications. *Nat Genet* **46**, 912-918 (2014).
- 260 Lunter, G. & Goodson, M. Stampy: a statistical algorithm for sensitive and fast mapping of Illumina sequence reads. *Genome Res* **21**, 936-939 (2011).
- 261 Merzdorf, C. S. & Sive, H. L. The zic1 gene is an activator of Wnt signalling. *Int J Dev Biol* **50**, 611-617 (2006).
- 262 Sive, H. L., Hattori, K. & Weintraub, H. Progressive determination during formation of the anteroposterior axis in *Xenopus laevis*. *Cell* **58**, 171-180 (1989).
- 263 Nieuwkoop, P. D. F., J. *Normal table of Xenopus laevis* (Daudin). (North-Holland Publishing Co, 1967).
- 264 Kolm, P. J. & Sive, H. L. Regulation of the *Xenopus* labial homeodomain genes, HoxA1 and HoxD1: activation by retinoids and peptide growth factors. *Dev Biol* **167**, 34-49 (1995).



- 265 Harland, R. M. In situ hybridisation: an improved whole-mount method for *Xenopus* embryos. *Methods Cell Biol* **36**, 685-695 (1991).
- 266 Brivanlou, A. H. & Harland, R. M. Expression of an engrailed-related protein is induced in the anterior neural ectoderm of early *Xenopus* embryos. *Development* **106**, 611-617 (1989).
- 267 Wilkinson, D. G. *In situ Hybridisation: A practical Approach*. (Oxford University Press, 1998).
- 268 Gaston-Massuet, C., Henderson, D. J., Greene, N. D. & Copp, A. J. Zic4, a zinc-finger transcription factor, is expressed in the developing mouse nervous system. *Dev Dyn* **233**, 1110-1115 (2005).
- 269 Wurst, W., Auerbach, A. B. & Joyner, A. L. Multiple developmental defects in Engrailed-1 mutant mice: an early mid-hindbrain deletion and patterning defects in forelimbs and sternum. *Development* **120**, 2065-2075 (1994).
- 270 Ferraris, A. *et al.* Dandy-Walker malformation and Wisconsin syndrome: novel cases add further insight into the genotype-phenotype correlations of 3q23q25 deletions. *Orphanet J Rare Dis* **8**, 75 (2013).
- 271 Khajavi, M., Inoue, K. & Lupski, J. R. Nonsense-mediated mRNA decay modulates clinical outcome of genetic disease. *Eur J Hum Genet* **14**, 1074-1081 (2006).
- 272 Kuo, J. S. *et al.* Opl: a zinc finger protein that regulates neural determination and patterning in *Xenopus*. *Development* **125**, 2867-2882 (1998).
- 273 Li, S., Shin, Y., Cho, K. W. & Merzdorf, C. S. The Xfeb gene is directly upregulated by Zic1 during early neural development. *Dev Dyn* **235**, 2817-2827 (2006).
- 274 Milet, C., Maczkowiak, F., Roche, D. D. & Monsoro-Burq, A. H. Pax3 and Zic1 drive induction and differentiation of multipotent, migratory, and functional neural crest in *Xenopus* embryos. *Proc Natl Acad Sci U S A* **110**, 5528-5533 (2013).
- 275 Nagai, T. *et al.* The expression of the mouse Zic1, Zic2, and Zic3 gene suggests an essential role for Zic genes in body pattern formation. *Dev Biol* **182**, 299-313 (1997).
- 276 Brown, S. A. *et al.* Holoprosencephaly due to mutations in ZIC2, a homologue of *Drosophila* odd-paired. *Nat Genet* **20**, 180-183 (1998).
- 277 Gebbia, M. *et al.* X-linked situs abnormalities result from mutations in ZIC3. *Nat Genet* **17**, 305-308 (1997).
- 278 Aruga, J. *et al.* Zic1 regulates the patterning of vertebral arches in cooperation with Gli3. *Mech Dev* **89**, 141-150 (1999).
- 279 Braddock, S. R., Jones, K. L., Superneau, D. W. & Jones, M. C. Sagittal craniosynostosis, Dandy-Walker malformation, and hydrocephalus: a unique multiple malformation syndrome. *Am J Med Genet* **47**, 640-643; discussion 644 (1993).
- 280 DiNardo, S. & O'Farrell, P. H. Establishment and refinement of segmental pattern in the *Drosophila* embryo: spatial control of engrailed expression by pair-rule genes. *Genes Dev* **1**, 1212-1225 (1987).
- 281 Plouhinec, J. L. *et al.* Pax3 and Zic1 trigger the early neural crest gene regulatory network by the direct activation of multiple key neural crest specifiers. *Dev Biol* **386**, 461-472 (2014).
- 282 Chen, H. *et al.* Multiple calvarial defects in *Imx1b* mutant mice. *Dev Genet* **22**, 314-320 (1998).
- 283 Dreyer, S. D. *et al.* Mutations in *LMX1B* cause abnormal skeletal patterning and renal dysplasia in nail patella syndrome. *Nat Genet* **19**, 47-50 (1998).
- 284 Brown, L., Paraso, M., Arkell, R. & Brown, S. In vitro analysis of partial loss-of-function ZIC2 mutations in holoprosencephaly: alanine tract expansion modulates DNA binding and transactivation. *Hum Mol Genet* **14**, 411-420 (2005).
- 285 Cowan, J., Tariq, M. & Ware, S. M. Genetic and functional analyses of ZIC3 variants in congenital heart disease. *Hum Mutat* **35**, 66-75 (2014).
- 286 Burn, J., McKeown, C., Wagget, J., Bray, R. & Goodship, J. New dysmorphic syndrome with choanal atresia in siblings. *Clin Dysmorphol* **1**, 137-144 (1992).
- 287 Wieczorek, D., Teber, O. A., Lohmann, D. & Gillissen-Kaesbach, G. Two brothers with Burn-McKeown syndrome. *Clin Dysmorphol* **12**, 171-174 (2003).

- 288 Liu, S., Rauhut, R., Vornlocher, H. P. & Luhrmann, R. The network of protein-protein interactions within the human U4/U6.U5 tri-snRNP. *RNA* **12**, 1418-1430 (2006).
- 289 Lehalle, D. *et al.* A review of craniofacial disorders caused by spliceosomal defects. *Clin Genet* **88**, 405-415 (2015).
- 290 Wang, K., Li, M. & Hakonarson, H. ANNOVAR: functional annotation of genetic variants from high-throughput sequencing data. *Nucleic Acids Res* **38**, e164 (2010).
- 291 Flicek, P. *et al.* Ensembl 2014. *Nucleic Acids Res* **42**, D749-755 (2014).
- 292 Ramos-Arroyo, M. A. *et al.* Familial choanal atresia with maxillary hypoplasia, prognathism, and hypodontia. *Am J Med Genet* **95**, 237-240 (2000).
- 293 Nieminen, P., Arte, S., Pirinen, S., Peltonen, L. & Thesleff, I. Gene defect in hypodontia: exclusion of MSX1 and MSX2 as candidate genes. *Hum Genet* **96**, 305-308 (1995).
- 294 Pauws, E. *et al.* Tbx22null mice have a submucous cleft palate due to reduced palatal bone formation and also display ankyloglossia and choanal atresia phenotypes. *Hum Mol Genet* **18**, 4171-4179 (2009).
- 295 Morriss-Kay, G. M. & Wilkie, A. O. Growth of the normal skull vault and its alteration in craniosynostosis: insights from human genetics and experimental studies. *J Anat* **207**, 637-653 (2005).
- 296 Twigg, S. R. *et al.* A Recurrent Mosaic Mutation in SMO, Encoding the Hedgehog Signal Transducer Smoothened, Is the Major Cause of Curry-Jones Syndrome. *Am J Hum Genet* **98**, 1256-1265 (2016).
- 297 Fennell, N. *et al.* Association of mutations in FLNA with craniosynostosis. *Eur J Hum Genet* **23**, 1684-1688 (2015).
- 298 Langmead, B. & Salzberg, S. L. Fast gapped-read alignment with Bowtie 2. *Nat Methods* **9**, 357-359 (2012).
- 299 Li, H. *et al.* The Sequence Alignment/Map format and SAMtools. *Bioinformatics* **25**, 2078-2079 (2009).
- 300 Fu, W. *et al.* Analysis of 6,515 exomes reveals the recent origin of most human protein-coding variants. *Nature* **493**, 216-220 (2013).
- 301 Yeo, G. & Burge, C. B. Maximum entropy modeling of short sequence motifs with applications to RNA splicing signals. *J Comput Biol* **11**, 377-394 (2004).
- 302 Landrum, M. J. *et al.* ClinVar: public archive of relationships among sequence variation and human phenotype. *Nucleic Acids Res* **42**, D980-985 (2014).
- 303 Stein, L. D. *et al.* The generic genome browser: a building block for a model organism system database. *Genome Res* **12**, 1599-1610 (2002).
- 304 Fenwick, A. L. *et al.* Mutations in CDC45, Encoding an Essential Component of the Pre-initiation Complex, Cause Meier-Gorlin Syndrome and Craniosynostosis. *Am J Hum Genet* **99**, 125-138 (2016).
- 305 Florisson, J. M. *et al.* Boston type craniosynostosis: report of a second mutation in MSX2. *Am J Med Genet A* **161A**, 2626-2633 (2013).
- 306 Janssen, A. *et al.* Second family with the Boston-type craniosynostosis syndrome: novel mutation and expansion of the clinical spectrum. *Am J Med Genet A* **161A**, 2352-2357 (2013).
- 307 Kempers, M. S., Spruijt, L., Marcelis, C., Loeys, B. in *The Fourth Cardiff Cardiovascular Genetics Symposium "Current Trends in Diagnosis and Therapies"* (Cardiff, UK, 2013 Nov 21-22).
- 308 Schubbert, S. *et al.* Germline KRAS mutations cause Noonan syndrome. *Nat Genet* **38**, 331-336 (2006).
- 309 Xia, F. *et al.* De novo truncating mutations in AHDC1 in individuals with syndromic expressive language delay, hypotonia, and sleep apnea. *Am J Hum Genet* **94**, 784-789 (2014).
- 310 Woellner, C. *et al.* Mutations in STAT3 and diagnostic guidelines for hyper-IgE syndrome. *J Allergy Clin Immunol* **125**, 424-432 e428 (2010).
- 311 Schepers, D. *et al.* The SMAD-binding domain of SKI: a hotspot for de novo mutations causing Shprintzen-Goldberg syndrome. *Eur J Hum Genet* **23**, 224-228 (2015).
- 312 Jacquinet, A. *et al.* Neonatal progeroid variant of Marfan syndrome with congenital lipodystrophy results from mutations at the 3' end of FBN1 gene. *Eur J Med Genet* **57**, 230-234 (2014).



Appendices

- 313 Kosaki, K. *et al.* Molecular pathology of Shprintzen-Goldberg syndrome. *Am J Med Genet A* **140**, 104-108; author reply 109-110 (2006).
- 314 Sood, S., Eldadah, Z. A., Krause, W. L., McIntosh, I. & Dietz, H. C. Mutation in fibrillin-1 and the Marfanoid-craniosynostosis (Shprintzen-Goldberg) syndrome. *Nat Genet* **12**, 209-211 (1996).
- 315 Addissie, Y. A. *et al.* Craniosynostosis and Noonan syndrome with KRAS mutations: Expanding the phenotype with a case report and review of the literature. *Am J Med Genet A* **167A**, 2657-2663 (2015).
- 316 Ozyilmaz, B., Gezdirici, A., Ozen, M. & Kalenderer, O. Report of a family with craniofrontonasal syndrome. *Clin Dysmorphol* **24**, 79-83 (2015).
- 317 Yeo, G. S. *et al.* A de novo mutation affecting human TrkB associated with severe obesity and developmental delay. *Nat Neurosci* **7**, 1187-1189 (2004).
- 318 Gray, J. *et al.* Functional characterization of human NTRK2 mutations identified in patients with severe early-onset obesity. *Int J Obes (Lond)* **31**, 359-364 (2007).
- 319 Wallis, Y. P., S.; McNulty, C.; Bodmer, D.; Sistermans, E.; Robertson, K.; Moore, D.; Abbs, S.; Deans, Z.; Devereau, A. (ed Association for Clinical Genetic Science) (2013).
- 320 Brasil, A. S. *et al.* KRAS gene mutations in Noonan syndrome familial cases cluster in the vicinity of the switch II region of the G-domain: report of another family with metopic craniosynostosis. *Am J Med Genet A* **158A**, 1178-1184 (2012).
- 321 Kratz, C. P. *et al.* Craniosynostosis in patients with Noonan syndrome caused by germline KRAS mutations. *Am J Med Genet A* **149A**, 1036-1040 (2009).
- 322 Kokkoris, P. & Pi-Sunyer, F. X. Obesity and endocrine disease. *Endocrinol Metab Clin North Am* **32**, 895-914 (2003).
- 323 Richards, S. *et al.* Standards and guidelines for the interpretation of sequence variants: a joint consensus recommendation of the American College of Medical Genetics and Genomics and the Association for Molecular Pathology. *Genet Med* **17**, 405-424 (2015).
- 324 Gahr, M., Muller, W., Allgeier, B. & Speer, C. P. A boy with recurrent infections, impaired PMN-chemotaxis, increased IgE concentrations and cranial synostosis—a variant of the hyper-IgE syndrome? *Helv Paediatr Acta* **42**, 185-190 (1987).
- 325 Hoger, P. H., Boltshauser, E. & Hitzig, W. H. Craniosynostosis in hyper-IgE-syndrome. *Eur J Pediatr* **144**, 414-417 (1985).
- 326 Smithwick, E. M. *et al.* Cranial synostosis in Job's syndrome. *Lancet* **1**, 826 (1978).
- 327 Michalec, D. in *Encyclopedia of Child Behavior and Development* (ed Naglieri JA Goldstein S, editors) 215 (Springer US, 2011).
- 328 Zimmerman, I. L. P., R.E.; Steiner, V.G. *PLS-5UK: Preschool Language Scale Fifth Edition.* (2014).
- 329 Goos, J. A. *et al.* A novel mutation in FGFR2. *Am J Med Genet A* **167A**, 123-127 (2015).
- 330 Goos, J. A. C. *et al.* Identification of causative variants in TXNL4A in Burn-McKeown syndrome and isolated choanal atresia. *Eur J Hum Genet* **25**, 1126-1133 (2017).
- 331 Rieber, N. *et al.* Coverage bias and sensitivity of variant calling for four whole-genome sequencing technologies. *PLoS One* **8**, e66621 (2013).
- 332 Lam, H. Y. *et al.* Performance comparison of whole-genome sequencing platforms. *Nat Biotechnol* **30**, 78-82 (2012).
- 333 O'Rawe, J. *et al.* Low concordance of multiple variant-calling pipelines: practical implications for exome and genome sequencing. *Genome Med* **5**, 28 (2013).
- 334 Kohane, I. S., Masys, D. R. & Altman, R. B. The incidentalome: a threat to genomic medicine. *JAMA* **296**, 212-215 (2006).
- 335 Dorschner, M. O. *et al.* Actionable, pathogenic incidental findings in 1,000 participants' exomes. *Am J Hum Genet* **93**, 631-640 (2013).

- 336 Green, R. C. *et al.* ACMG recommendations for reporting of incidental findings in clinical exome and genome sequencing. *Genet Med* **15**, 565-574 (2013).
- 337 Joly, Y., Ngueng Feze, I. & Simard, J. Genetic discrimination and life insurance: a systematic review of the evidence. *BMC Med* **11**, 25 (2013).
- 338 in *Journal of the State* 636-642 (1997).
- 339 Christiaans, I. *et al.* Obtaining insurance after DNA diagnostics: a survey among hypertrophic cardiomyopathy mutation carriers. *Eur J Hum Genet* **18**, 251-253 (2010).
- 340 Marang-van de Mheen, P. J., van Maarle, M. C. & Stouthard, M. E. Getting insurance after genetic screening on familial hypercholesterolaemia; the need to educate both insurers and the public to increase adherence to national guidelines in The Netherlands. *J Epidemiol Community Health* **56**, 145-147 (2002).
- 341 Timberlake, A. T. *et al.* Two locus inheritance of non-syndromic midline craniosynostosis via rare SMAD6 and common BMP2 alleles. *Elife* **5** (2016).
- 342 Wu, E., Vargevik, K. & Slavotinek, A. M. Subtypes of frontonasal dysplasia are useful in determining clinical prognosis. *Am J Med Genet A* **143A**, 3069-3078 (2007).
- 343 Fogelgren, B. *et al.* Misexpression of Six2 is associated with heritable frontonasal dysplasia and renal hypoplasia in 3H1 Br mice. *Dev Dyn* **237**, 1767-1779 (2008).
- 344 Hufnagel, R. B. *et al.* A new frontonasal dysplasia syndrome associated with deletion of the SIX2 gene. *Am J Med Genet A* **170A**, 487-491 (2016).
- 345 Terrazas, K., Dixon, J., Trainor, P. A. & Dixon, M. J. Rare syndromes of the head and face: mandibulofacial and acrofacial dysostoses. *Wiley Interdiscip Rev Dev Biol* **6** (2017).
- 346 Lelieveld, S. H., Spielmann, M., Mundlos, S., Veltman, J. A. & Gilissen, C. Comparison of Exome and Genome Sequencing Technologies for the Complete Capture of Protein-Coding Regions. *Hum Mutat* **36**, 815-822 (2015).
- 347 Strom, S. P. *et al.* Assessing the necessity of confirmatory testing for exome-sequencing results in a clinical molecular diagnostic laboratory. *Genet Med* **16**, 510-515 (2014).
- 348 Meienberg, J., Bruggmann, R., Oexle, K. & Matyas, G. Clinical sequencing: is WGS the better WES? *Hum Genet* **135**, 359-362 (2016).
- 349 Sun, Y. *et al.* Next-generation diagnostics: gene panel, exome, or whole genome? *Hum Mutat* **36**, 648-655 (2015).
- 350 de Ligt, J. *et al.* Diagnostic exome sequencing in persons with severe intellectual disability. *N Engl J Med* **367**, 1921-1929 (2012).
- 351 Tetreault, M., Bareke, E., Nadaf, J., Alirezaie, N. & Majewski, J. Whole-exome sequencing as a diagnostic tool: current challenges and future opportunities. *Expert Rev Mol Diagn* **15**, 749-760 (2015).
- 352 Belkadi, A. *et al.* Whole-genome sequencing is more powerful than whole-exome sequencing for detecting exome variants. *Proc Natl Acad Sci U S A* **112**, 5473-5478 (2015).
- 353 Dewey, F. E. *et al.* Clinical interpretation and implications of whole-genome sequencing. *JAMA* **311**, 1035-1045 (2014).
- 354 Clark, M. J. *et al.* Performance comparison of exome DNA sequencing technologies. *Nat Biotechnol* **29**, 908-914 (2011).
- 355 Chinen, Y. *et al.* Opitz trigonocephaly C syndrome in a boy with a de novo balanced reciprocal translocation t(3;18)(q13.13;q12.1). *Am J Med Genet A* **140**, 1655-1657 (2006).
- 356 Kaname, T. *et al.* Mutations in CD96, a member of the immunoglobulin superfamily, cause a form of the C (Opitz trigonocephaly) syndrome. *Am J Hum Genet* **81**, 835-841 (2007).
- 357 Loucks, C. M. *et al.* Matching two independent cohorts validates DPH1 as a gene responsible for autosomal recessive intellectual disability with short stature, craniofacial, and ectodermal anomalies. *Hum Mutat* **36**, 1015-1019 (2015).



Appendices

- 358 Boissel, S. *et al.* Loss-of-function mutation in the dioxygenase-encoding FTO gene causes severe growth retardation and multiple malformations. *Am J Hum Genet* **85**, 106-111 (2009).
- 359 Tabler, J. M., Rice, C. P., Liu, K. J. & Wallingford, J. B. A novel ciliopathic skull defect arising from excess neural crest. *Dev Biol* **417**, 4-10 (2016).
- 360 Au, P. Y. B. *et al.* GeneMatcher aids in the identification of a new malformation syndrome with intellectual disability, unique facial dysmorphisms, and skeletal and connective tissue abnormalities caused by de novo variants in HNRNPK. *Hum Mutat* **36**, 1009-1014 (2015).
- 361 Pena-Padilla, C. *et al.* Compound heterozygous mutations in the IFT140 gene cause Opitz trigonocephaly C syndrome in a patient with typical features of a ciliopathy. *Clin Genet* **91**, 640-646 (2017).
- 362 Perrault, I. *et al.* Mainzer-Saldino syndrome is a ciliopathy caused by IFT140 mutations. *Am J Hum Genet* **90**, 864-870 (2012).
- 363 Cunningham, M. L. *et al.* IGF1R variants associated with isolated single suture craniosynostosis. *Am J Med Genet A* **155A**, 91-97 (2011).
- 364 Munye, M. M. *et al.* COLEC10 is mutated in 3MC patients and regulates early craniofacial development. *PLoS Genet* **13**, e1006679 (2017).
- 365 Urquhart, J. *et al.* Exploring the genetic basis of 3MC syndrome: Findings in 12 further families. *Am J Med Genet A* **170A**, 1216-1224 (2016).
- 366 Nyboe, D., Kreiborg, S., Kirchhoff, M. & Hove, H. B. Familial craniosynostosis associated with a microdeletion involving the NFIA gene. *Clin Dysmorphol* **24**, 109-112 (2015).
- 367 Rao, A. *et al.* An intragenic deletion of the NFIA gene in a patient with a hypoplastic corpus callosum, craniofacial abnormalities and urinary tract defects. *Eur J Med Genet* **57**, 65-70 (2014).
- 368 Rivera-Pedroza, C. I. *et al.* Chromosome 1p31.1p31.3 Deletion in a Patient with Craniosynostosis, Central Nervous System and Renal Malformation: Case Report and Review of the Literature. *Mol Syndromol* **8**, 30-35 (2017).
- 369 Rauch, F. *et al.* Cole-Carpenter syndrome is caused by a heterozygous missense mutation in P4HB. *Am J Hum Genet* **96**, 425-431 (2015).
- 370 Faden, M. *et al.* Identification of a Recognizable Progressive Skeletal Dysplasia Caused by RSPRY1 Mutations. *Am J Hum Genet* **97**, 608-615 (2015).
- 371 Gonorazky, H. D. *et al.* Congenital myopathy with "corona" fibres, selective muscle atrophy, and craniosynostosis associated with novel recessive mutations in SCN4A. *Neuromuscul Disord* **27**, 574-580 (2017).
- 372 Tagariello, A. *et al.* Balanced translocation in a patient with craniosynostosis disrupts the SOX6 gene and an evolutionarily conserved non-transcribed region. *J Med Genet* **43**, 534-540 (2006).
- 373 Hiraki, Y. *et al.* Aortic aneurysm and craniosynostosis in a family with Cantu syndrome. *Am J Med Genet A* **164A**, 231-236 (2014).
- 374 Searle, C. *et al.* Craniosynostosis: a previously unreported association with CHST3-related skeletal dysplasia (autosomal recessive Larsen syndrome). *Clin Dysmorphol* **23**, 12-15 (2014).
- 375 Balasubramanian, M. *et al.* CRTAP mutation in a patient with Cole-Carpenter syndrome. *Am J Med Genet A* **167A**, 587-591 (2015).
- 376 Dimitri, P. *et al.* Expanding the Clinical Spectrum Associated With GLIS3 Mutations. *J Clin Endocrinol Metab* **100**, E1362-1369 (2015).
- 377 Arts, H. H. *et al.* C14ORF179 encoding IFT43 is mutated in Sensenbrenner syndrome. *J Med Genet* **48**, 390-395 (2011).
- 378 Zollino, M. *et al.* Intragenic KANSL1 mutations and chromosome 17q21.31 deletions: broadening the clinical spectrum and genotype-phenotype correlations in a large cohort of patients. *J Med Genet* **52**, 804-814 (2015).

- 379 Yamamoto, T., Shimojima, K., Ondo, Y., Shimakawa, S. & Okamoto, N. MED13L haploinsufficiency syndrome: A de novo frameshift and recurrent intragenic deletions due to parental mosaicism. *Am J Med Genet A* **173**, 1264-1269 (2017).
- 380 Mahmoud Adel, A. H., Abdullah, A. A. & Eissa, F. Infantile osteopetrosis, craniosynostosis, and Chiari malformation type I with novel OSTEM1 mutation. *J Pediatr Neurosci* **8**, 34-37 (2013).
- 381 Bertola, D. *et al.* The recurrent PPP1CB mutation p.Pro49Arg in an additional Noonan-like syndrome individual: Broadening the clinical phenotype. *Am J Med Genet A* **173**, 824-828 (2017).
- 382 Choucair, N. *et al.* Evidence that homozygous PTPRD gene microdeletion causes trigonocephaly, hearing loss, and intellectual disability. *Mol Cytogenet* **8**, 39 (2015).
- 383 Garbes, L. *et al.* Mutations in SEC24D, encoding a component of the COPII machinery, cause a syndromic form of osteogenesis imperfecta. *Am J Hum Genet* **96**, 432-439 (2015).
- 384 Takenouchi, T. *et al.* Severe craniosynostosis with Noonan syndrome phenotype associated with SHOC2 mutation: clinical evidence of crosslink between FGFR and RAS signalling pathways. *Am J Med Genet A* **164A**, 2869-2872 (2014).
- 385 Bredrup, C. *et al.* Ciliopathies with skeletal anomalies and renal insufficiency due to mutations in the IFT-A gene WDR19. *Am J Hum Genet* **89**, 634-643 (2011).
- 386 Uz, E. *et al.* Disruption of ALX1 causes extreme microphthalmia and severe facial clefting: expanding the spectrum of autosomal-recessive ALX-related frontonasal dysplasia. *Am J Hum Genet* **86**, 789-796 (2010).
- 387 Twigg, S. R. *et al.* Frontorhiny, a distinctive presentation of frontonasal dysplasia caused by recessive mutations in the ALX3 homeobox gene. *Am J Hum Genet* **84**, 698-705 (2009).
- 388 Kayserili, H. *et al.* ALX4 dysfunction disrupts craniofacial and epidermal development. *Hum Mol Genet* **18**, 4357-4366 (2009).
- 389 Kayserili, H., Altunoglu, U., Ozgur, H., Basaran, S. & Uygur, Z. O. Mild nasal malformations and parietal foramina caused by homozygous ALX4 mutations. *Am J Med Genet A* **158A**, 236-244 (2012).
- 390 Kariminejad, A. *et al.* Skull defects, alopecia, hypertelorism, and notched alae nasi caused by homozygous ALX4 gene mutation. *Am J Med Genet A* **164A**, 1322-1327 (2014).
- 391 Wuyts, W. *et al.* The ALX4 homeobox gene is mutated in patients with ossification defects of the skull (foramina parietalia permagna, OMIM 168500). *J Med Genet* **37**, 916-920 (2000).
- 392 Sheen, V. L. *et al.* Mutations in ARFGEF2 implicate vesicle trafficking in neural progenitor proliferation and migration in the human cerebral cortex. *Nat Genet* **36**, 69-76 (2004).
- 393 Robertson, S. P. *et al.* Localized mutations in the gene encoding the cytoskeletal protein filamin A cause diverse malformations in humans. *Nat Genet* **33**, 487-491 (2003).
- 394 Slavotinek, A. M. *et al.* Manitoba-oculo-tricho-anal (MOTA) syndrome is caused by mutations in FREM1. *J Med Genet* **48**, 375-382 (2011).
- 395 Mears, A. J. *et al.* Mutations of the forkhead/winged-helix gene, FKHL7, in patients with Axenfeld-Rieger anomaly. *Am J Hum Genet* **63**, 1316-1328 (1998).
- 396 Roessler, E. *et al.* Loss-of-function mutations in the human GLI2 gene are associated with pituitary anomalies and holoprosencephaly-like features. *Proc Natl Acad Sci U S A* **100**, 13424-13429 (2003).
- 397 Rosenthal, A., Jouet, M. & Kenwrick, S. Aberrant splicing of neural cell adhesion molecule L1 mRNA in a family with X-linked hydrocephalus. *Nat Genet* **2**, 107-112 (1992).
- 398 Semina, E. V. *et al.* Cloning and characterization of a novel bicoid-related homeobox transcription factor gene, RIEG, involved in Rieger syndrome. *Nat Genet* **14**, 392-399 (1996).
- 399 Roessler, E. *et al.* Mutations in the human Sonic Hedgehog gene cause holoprosencephaly. *Nat Genet* **14**, 357-360 (1996).
- 400 Wallis, D. E. *et al.* Mutations in the homeodomain of the human SIX3 gene cause holoprosencephaly. *Nat Genet* **22**, 196-198 (1999).
- 401 van de Laar, I. M. *et al.* Mutations in SMAD3 cause a syndromic form of aortic aneurysms and dissections with early-onset osteoarthritis. *Nat Genet* **43**, 121-126 (2011).



Appendices

- 402 de la Cruz, J. M. *et al.* A loss-of-function mutation in the CFC domain of TDGF1 is associated with human forebrain defects. *Hum Genet* **110**, 422-428 (2002).
- 403 Gripp, K. W. *et al.* Mutations in TGIF cause holoprosencephaly and link NODAL signalling to human neural axis determination. *Nat Genet* **25**, 205-208 (2000).
- 404 Loeys, B. L. *et al.* A syndrome of altered cardiovascular, craniofacial, neurocognitive and skeletal development caused by mutations in TGFBR1 or TGFBR2. *Nat Genet* **37**, 275-281 (2005).
- 405 Mizuguchi, T. *et al.* Heterozygous TGFBR2 mutations in Marfan syndrome. *Nat Genet* **36**, 855-860 (2004).
- 406 Marchegiani, S. *et al.* Recurrent Mutations in the Basic Domain of TWIST2 Cause Ablepharon Macrostomia and Barber-Say Syndromes. *Am J Hum Genet* **97**, 99-110 (2015).
- 407 Tükel, T. *et al.* Homozygous nonsense mutations in TWIST2 cause Setleis syndrome. *Am J Hum Genet* **87**, 289-296 (2010).
- 408 Smith, J. D. *et al.* Exome sequencing identifies a recurrent de novo ZSWIM6 mutation associated with acromelic frontonasal dysostosis. *Am J Hum Genet* **95**, 235-240 (2014).
- 409 Riviere, J. B. *et al.* De novo mutations in the actin genes ACTB and ACTG1 cause Baraitser-Winter syndrome. *Nat Genet* **44**, 440-444, S441-442 (2012).
- 410 Zeevaert, R. *et al.* Cerebrocostomandibular-like syndrome and a mutation in the conserved oligomeric Golgi complex, subunit 1. *Hum Mol Genet* **18**, 517-524 (2009).
- 411 Gordon, C. T. *et al.* Mutations in endothelin 1 cause recessive auriculocondylar syndrome and dominant isolated question-mark ears. *Am J Hum Genet* **93**, 1118-1125 (2013).
- 412 Gordon, C. T. *et al.* Mutations in the endothelin receptor type A cause mandibulofacial dysostosis with alopecia. *Am J Hum Genet* **96**, 519-531 (2015).
- 413 Lines, M. A. *et al.* Haploinsufficiency of a spliceosomal GTPase encoded by EFTUD2 causes mandibulofacial dysostosis with microcephaly. *Am J Hum Genet* **90**, 369-377 (2012).
- 414 Favaro, F. P. *et al.* A noncoding expansion in EIF4A3 causes Richieri-Costa-Pereira syndrome, a craniofacial disorder associated with limb defects. *Am J Hum Genet* **94**, 120-128 (2014).
- 415 Ruiz-Perez, V. L. *et al.* Mutations in a new gene in Ellis-van Creveld syndrome and Weyers acrodermal dysostosis. *Nat Genet* **24**, 283-286 (2000).
- 416 Galdzicka, M. *et al.* A new gene, EVC2, is mutated in Ellis-van Creveld syndrome. *Mol Genet Metab* **77**, 291-295 (2002).
- 417 Valencia, M. *et al.* Widening the mutation spectrum of EVC and EVC2: ectopic expression of Weyer variants in NIH 3T3 fibroblasts disrupts Hedgehog signalling. *Hum Mutat* **30**, 1667-1675 (2009).
- 418 Rieder, M. J. *et al.* A human homeotic transformation resulting from mutations in PLCB4 and GNAI3 causes auriculocondylar syndrome. *Am J Hum Genet* **90**, 907-914 (2012).
- 419 Fernet, M. *et al.* Identification and functional consequences of a novel MRE11 mutation affecting 10 Saudi Arabian patients with the ataxia telangiectasia-like disorder. *Hum Mol Genet* **14**, 307-318 (2005).
- 420 Matsuura, S. *et al.* Genetic mapping using microcell-mediated chromosome transfer suggests a locus for Nijmegen breakage syndrome at chromosome 8q21-24. *Am J Hum Genet* **60**, 1487-1494 (1997).
- 421 Weaver, K. N. *et al.* Acrofacial Dysostosis, Cincinnati Type, a Mandibulofacial Dysostosis Syndrome with Limb Anomalies, Is Caused by POLR1A Dysfunction. *Am J Hum Genet* **96**, 765-774 (2015).
- 422 Dauwerse, J. G. *et al.* Mutations in genes encoding subunits of RNA polymerases I and III cause Treacher Collins syndrome. *Nat Genet* **43**, 20-22 (2011).
- 423 Sergi, C. & Kamnasaran, D. PRRX1 is mutated in a fetus with agnathia-otocephaly. *Clin Genet* **79**, 293-295 (2011).
- 424 Celik, T. *et al.* PRRX1 is mutated in an otocephalic newborn infant conceived by consanguineous parents. *Clin Genet* **81**, 294-297 (2012).
- 425 Kalscheuer, V. M. *et al.* Mutations in the polyglutamine binding protein 1 gene cause X-linked mental retardation. *Nat Genet* **35**, 313-315 (2003).

- 426 Gazda, H. T. *et al.* Ribosomal protein L5 and L11 mutations are associated with cleft palate and abnormal thumbs in Diamond-Blackfan anemia patients. *Am J Hum Genet* **83**, 769-780 (2008).
- 427 Doherty, L. *et al.* Ribosomal protein genes RPS10 and RPS26 are commonly mutated in Diamond-Blackfan anemia. *Am J Hum Genet* **86**, 222-228 (2010).
- 428 Gripp, K. W. *et al.* Diamond-Blackfan anemia with mandibulofacial dystostosis is heterogeneous, including the novel DBA genes TSR2 and RPS28. *Am J Med Genet A* **164A**, 2240-2249 (2014).
- 429 Kohlhase, J., Wischermann, A., Reichenbach, H., Froster, U. & Engel, W. Mutations in the SALL1 putative transcription factor gene cause Townes-Brocks syndrome. *Nat Genet* **18**, 81-83 (1998).
- 430 Bernier, F. P. *et al.* Haploinsufficiency of SF3B4, a component of the pre-mRNA spliceosomal complex, causes Nager syndrome. *Am J Hum Genet* **90**, 925-933 (2012).
- 431 Lynch, D. C. *et al.* Disrupted auto-regulation of the spliceosomal gene SNRPB causes cerebro-costomandibular syndrome. *Nat Commun* **5**, 4483 (2014).
- 432 Milunsky, J. M. *et al.* TFAP2A mutations result in branchio-oculo-facial syndrome. *Am J Hum Genet* **82**, 1171-1177 (2008).
- 433 Wakamatsu, N. *et al.* Mutations in SIP1, encoding Smad interacting protein-1, cause a form of Hirschsprung disease. *Nat Genet* **27**, 369-370 (2001).
- 434 Faita, F., Vecoli, C., Foffa, I. & Andreassi, M. G. Next generation sequencing in cardiovascular diseases. *World J Cardiol* **4**, 288-295 (2012).
- 435 Swen, J. J. *et al.* Pharmacogenetics: from bench to byte--an update of guidelines. *Clin Pharmacol Ther* **89**, 662-673 (2011).
- 436 Bell, C. J. *et al.* Carrier testing for severe childhood recessive diseases by next-generation sequencing. *Sci Transl Med* **3**, 65ra64 (2011).
- 437 Shukla, V., Coumoul, X., Wang, R. H., Kim, H. S. & Deng, C. X. RNA interference and inhibition of MEK-ERK signalling prevent abnormal skeletal phenotypes in a mouse model of craniosynostosis. *Nat Genet* **39**, 1145-1150 (2007).
- 438 Wang, Y. *et al.* p38 Inhibition ameliorates skin and skull abnormalities in Fgfr2 Beare-Stevenson mice. *J Clin Invest* **122**, 2153-2164 (2012).
- 439 Jones, N. C. *et al.* Prevention of the neurocristopathy Treacher Collins syndrome through inhibition of p53 function. *Nat Med* **14**, 125-133 (2008).
- 440 Komarov, P. G. *et al.* A chemical inhibitor of p53 that protects mice from the side effects of cancer therapy. *Science* **285**, 1733-1737 (1999).
- 441 Sakai, D., Dixon, J., Achilleos, A., Dixon, M. & Trainor, P. A. Prevention of Treacher Collins syndrome craniofacial anomalies in mouse models via maternal antioxidant supplementation. *Nat Commun* **7**, 10328 (2016).
- 442 Jinek, M. *et al.* A programmable dual-RNA-guided DNA endonuclease in adaptive bacterial immunity. *Science* **337**, 816-821 (2012).
- 443 Rahman, Z. H. *In the light of what we know.* (Farrar, Straus and Giroux, 2014).



A *de novo* mutation in *BCL11B* leads to loss of interaction with the NuRD and PRC2 transcriptional complexes and is associated with craniosynostosis

Jacqueline A.C. Goos, Walter K. Vogel, Christopher J. Millard, Wisam H. Selman, Eduardo Calpena, Nils Koelling, Evan L. Carpenter, Sigrid M.A. Swagemakers, Elahe Esfandiari, Peter J. van der Spek, Theresa M. Filtz, John W.R. Schwabe, Irene M.J. Mathijssen, Andrew O.M. Wilkie, Stephen R.F. Twigg, Mark Leid
Submitted to Human Mutation October 2017

Dental arch morphology in Saethre-Chotzen syndrome, Muenke and *TCF12*-related craniosynostosis

Robert M. Choi, Lea Kragt, **Jacqueline A.C. Goos**, Irene M.J. Mathijssen, Eppo B. Wolvius, Edwin M. Ongkosuwito
Submitted to Journal of Dental Research September 2017

Identification of mutations in *TXNL4A* in Burn-McKeown syndrome and isolated choanal atresia

Jacqueline A.C. Goos, Sigrid M.A. Swagemakers, Stephen R.F. Twigg, Marieke F. van Dooren, A. Jeannette M. Hoogeboom, Christian Beetz, Sven Günther, Frank J. Magielsen, Charlotte W. Ockeloen, Maria Ramos-Arroyo, Rolph Pfundt, Helger G. Yntema, Peter J. van der Spek, Philip Stanier, Dagmar Wiczorek, Andrew O.M. Wilkie, Ans M.W. van den Ouweland, Irene M.J. Mathijssen, Jane Hurst
European Journal of Human Genetics July 2017

Diagnostic value of exome and whole genome sequencing in craniosynostosis

Kerry A. Miller, Stephen R.F. Twigg, Simon J. McGowan, Julie M. Phipps, Aimée L Fenwick, David Johnson, Steven A. Wall, Peter Noons, Katie E.M. Rees, Elizabeth A. Tidey, Judith Craft, John Taylor, Jenny C. Taylor, **Jacqueline A.C. Goos**, Sigrid M.A. Swagemakers, Irene M.J. Mathijssen, Helen Lord, Tracy Lester, Noina Abid, Deirdre Cilliers, Jane A. Hurst, Jenny E.V. Morton, Elizabeth Sweeney, Astrid Weber, Louise C. Wilson, Andrew O.M. Wilkie
Journal of Medical Genetics November 2016

Identification of intragenic exon deletions and duplication of *TCF12* by whole genome or targeted sequencing as a cause of *TCF12*-related craniosynostosis

Jacqueline A.C. Goos, Aimée L. Fenwick, Sigrid M.A. Swagemakers, Simon J. McGowan, Samantha J.L. Knight, Stephen R.F. Twigg, A. Jeannette M. Hoogeboom, Marieke F. van Dooren, Frank J. Magielsen, Steven A. Wall, Irene M.J. Mathijssen, Andrew O.M. Wilkie, Peter J. van der Spek, Ans M.W. van den Ouweland
Human Mutation June 2016



Gain-of-function mutations in *ZIC1* are associated with coronal craniosynostosis and learning disability

Stephen R.F. Twigg, Jennifer Forecki, **Jacqueline A.C. Goos**, Ivy C. Richardson, A. Jeannette M. Hoozeboom, Ans M.W. van den Ouweland, Sigrid M.A. Swagemakers, Maarten H. Lequin, Daniel van Antwerp, Simon J. McGowan, Isabelle Westbury, Kerry A. Miller, Steven A. Wall, WGS500 Consortium, Peter J. van der Spek, Irene M.J. Mathijssen, Erwin Pauws, Christa S. Merzdorf, Andrew O.M. Wilkie
American Journal of Human Genetics September 2015

A novel mutation in *FGFR2*

Jacqueline A.C. Goos, Ans M.W. van den Ouweland, Sigrid M.A. Swagemakers, Annemiek J.M.H. Verkerk, A. Jeannette M. Hoozeboom, Marie-Lise van Veelen, Irene M.J. Mathijssen, Peter J. van der Spek
American Journal of Medical Genetics part A November 2014

Apparently synonymous substitutions in *FGFR2* affect splicing and result in mild Crouzon syndrome

Aimée L. Fenwick, **Jacqueline A.C. Goos**, Julia Rankin, Helen Lord, Tracy Lester, A. Jeannette M. Hoozeboom, Ans M.W. van den Ouweland, Steven A. Wall, Irene M.J. Mathijssen, Andrew O.M. Wilkie
BMC Medical Genetics August 2014

Phenotypes of craniofrontonasal syndrome in patients with a pathogenic mutation in *EFNB1*

Marijke E.P. van den Elzen, Stephen R.F. Twigg, **Jacqueline A.C. Goos**, A. Jeannette M.H. Hoozeboom, Ans M.W. van den Ouweland, Andrew O.M. Wilkie, Irene M.J. Mathijssen
European Journal of Human Genetics November 2013

Mutations in *TCF12*, encoding a basic helix-loop-helix partner of *TWIST1*, are a frequent cause of coronal craniosynostosis

Vikram P. Sharma, Aimée L. Fenwick, Mia S. Brockop, Simon J. McGowan, **Jacqueline A.C. Goos**, A. Jeannette M. Hoozeboom, Angela F. Brady, Nu Owase Jeelani, Sally Ann Lynch, John B. Mulliken, Dylan J. Murray, Julie M. Phipps, Elizabeth Sweeney, Susan E. Tomkins, Louise C. Wilson, Sophia Bennett, Richard J. Cornall, John Broxholme, Alexander Kanapin, 500 Whole-Genome Sequences (WGS500) Consortium, David Johnson, Steven A. Wall, Peter J. van der Spek, Irene M.J. Mathijssen, Robert E. Maxson, Stephen R.F. Twigg, Andrew O.M. Wilkie
Nature Genetics January 2013

Distribution of glycine/GABA neurons in the ventromedial medulla with descending spinal projections and evidence for an ascending Glycine/GABA projection

Mehdi Hossaini, **Jacqueline A.C. Goos**, Somesh K. Kohli, Jan C. Holstege
PLoS one April 2012

Assessment of volumetric changes with a best fit method in 3D stereophotograms

Edwin M. Ongkosuwito, **Jacqueline A.C. Goos**, Evert Wattel, Karel G.H. van der Wal, Léon N.A. van Adrichem, Johan W. van Neck
The cleft palate-craniofacial Journal July 2012



- N. Abid:** Department of Paediatric Endocrinology, The Royal Belfast Hospital for Sick Children, Belfast, UK
- C. Allan:** The Wellcome Trust Centre for Human Genetics, Oxford, UK
- D. van Antwerp:** Department of Cell Biology and Neuroscience, Montana State University, Bozeman, Montana, USA
- M. Attar:** The Wellcome Trust Centre for Human Genetics, Oxford, UK
- C. Beetz:** Department of Clinical Chemistry and Laboratory Medicine, Jena University Hospital, Jena, Germany
- J. Bell:** Office of the Regius Professor of Medicine, Oxford, UK
- S. Bennett:** Medical Research Council (MRC) Human Immunology Unit, Weatherall Institute of Molecular Medicine, University of Oxford, Oxford, UK
- D. Bentley:** Illumina Cambridge Ltd., Essex, UK
- A.F. Brady:** Kennedy Galton Centre, North West London Hospitals NHS Trust, London, UK
- M.S. Brockop:** 1. Department of Biochemistry and Molecular Biology, University of Southern California/Norris Cancer Centre, Los Angeles, California, USA; 2. Université Paris-Sud, Orsay, France
- J. Broxholme:** The Wellcome Trust Centre for Human Genetics, University of Oxford, Oxford, UK
- D. Buck:** The Wellcome Trust Centre for Human Genetics, Oxford, UK
- E. Calpena:** Clinical Genetics Group, MRC Weatherall Institute of Molecular Medicine, University of Oxford, John Radcliffe Hospital, Oxford, UK
- E.L. Carpenter:** Department of Pharmaceutical Sciences, College of Pharmacy, Oregon State University, Corvallis, Oregon, USA
- J.B. Cazier:** The Wellcome Trust Centre for Human Genetics, Oxford, UK
- T.M. Choi:** 1. Department of Oral Maxillofacial Surgery, Special Dental Care and Orthodontics, Dutch Craniofacial Centre, Erasmus MC, University Medical Centre Rotterdam, Rotterdam, The Netherlands; 2. Department of Orthodontics, Academic Centre of Dentistry, Amsterdam, The Netherlands
- D. Cilliers:** 1. Department of Clinical Genetics, Oxford University Hospitals NHS Foundation Trust, Oxford, UK; 2. Craniofacial Unit, Oxford University Hospitals NHS Foundation Trust, Oxford, UK
- R. Copley:** The Wellcome Trust Centre for Human Genetics, Oxford, UK
- R.J. Cornall:** Medical Research Council (MRC) Human Immunology Unit, Weatherall Institute of Molecular Medicine, University of Oxford, Oxford, UK
- J. Craft:** Oxford Medical Genetics Laboratories, Oxford University Hospitals NHS Foundation Trust, Oxford, UK
- P. Donnelly:** The Wellcome Trust Centre for Human Genetics, Oxford, UK



M.F. van Dooren: Department of Clinical Genetics, Erasmus MC, University Medical Centre Rotterdam, Rotterdam, The Netherlands

M.E.P. van den Elzen: Department of Plastic and Reconstructive Surgery, Erasmus MC, University Medical Centre Rotterdam, Rotterdam, The Netherlands

E. Esfandiari: Department of Pharmaceutical Sciences, College of Pharmacy, Oregon State University, Corvallis, Oregon, USA

A.L. Fenwick: Clinical Genetics Group, Weatherall Institute of Molecular Medicine, University of Oxford, Oxford, UK

S. Fiddy: The Wellcome Trust Centre for Human Genetics, Oxford, UK

T.M. Filtz: Department of Pharmaceutical Sciences, College of Pharmacy, Oregon State University, Corvallis, Oregon, USA

J. Forecki: Department of Cell Biology and Neuroscience, Montana State University, Bozeman, Montana, USA

A. Green: The Wellcome Trust Centre for Human Genetics, Oxford, UK

L. Gregory: The Wellcome Trust Centre for Human Genetics, Oxford, UK

R. Grocock: Illumina Cambridge Ltd., Essex, UK

S. Günther: Department of Clinical Chemistry and Laboratory Medicine, Jena University Hospital, Jena, Germany

E. Hatton: The Wellcome Trust Centre for Human Genetics, Oxford, UK

C. Holmes: The Wellcome Trust Centre for Human Genetics, Oxford, UK

A.J.M. Hoogeboom: Department of Clinical Genetics, Erasmus MC, University Medical Centre Rotterdam, Rotterdam, The Netherlands

L. Hughes: The Wellcome Trust Centre for Human Genetics, Oxford, UK

P. Humburg: The Wellcome Trust Centre for Human Genetics, Oxford, UK

S. Humphray: Illumina Cambridge Ltd., Essex, UK

J.A. Hurst: North East Thames Regional Genetics Service, Great Ormond Street Hospital for Children NHS Foundation Trust, London, UK

N.O. Jeelani: Department of Neurosurgery, Great Ormond Street Hospital for Children NHS Trust, London, UK

D. Johnson: Craniofacial Unit, Oxford University Hospitals NHS Foundation Trust, Oxford, UK

A. Kanapin: The Wellcome Trust Centre for Human Genetics, University of Oxford, Oxford, UK

Z. Kingsbury: Illumina Cambridge Ltd., Essex, UK

J. Knight: The Wellcome Trust Centre for Human Genetics, Oxford, UK

S.J.L. Knight: NIHR Biomedical Research Centre, The Wellcome Trust Centre for Human Genetics, University of Oxford, Oxford, UK

N. Koelling: Clinical Genetics Group, MRC Weatherall Institute of Molecular Medicine, University of Oxford, John Radcliffe Hospital, Oxford, UK

L. Kragt: Department of Oral Maxillofacial Surgery, Special Dental Care and Orthodontics, Dutch Craniofacial Centre, Erasmus MC, University Medical Centre Rotterdam, Rotterdam, The Netherlands

S. Lambie: The Wellcome Trust Centre for Human Genetics, Oxford, UK

M. Leid: 1. Department of Pharmaceutical Sciences, College of Pharmacy, Oregon State University, Corvallis, Oregon, USA; 2. Department of Integrative Biosciences, Oregon Health & Science University, Portland, Oregon, USA

T. Lester: Oxford Medical Genetics Laboratories, Oxford University Hospitals NHS Foundation Trust, Oxford, UK

M.H. Lequin: Department of Paediatric Radiology, Erasmus MC, University Medical Centre Rotterdam, Rotterdam, The Netherlands

S. Lise: The Wellcome Trust Centre for Human Genetics, Oxford, UK

L. Lonie: The Wellcome Trust Centre for Human Genetics, Oxford, UK

H. Lord: Oxford Medical Genetics Laboratories, Oxford University Hospitals NHS Foundation Trust, Oxford, UK

G. Lunter: The Wellcome Trust Centre for Human Genetics, Oxford, UK

S.A. Lynch: National Centre for Medical Genetics, Our Lady's Children's Hospital, Dublin, Ireland

F.M. Magielsen: Department of Clinical Genetics, Erasmus MC, University Medical Centre Rotterdam, Rotterdam, The Netherlands

H. Martin: The Wellcome Trust Centre for Human Genetics, Oxford, UK

I.M.J. Mathijssen: Department of Plastic and Reconstructive Surgery and Hand Surgery, Erasmus MC, University Medical Centre Rotterdam, Rotterdam, The Netherlands

R.E. Maxson: Department of Biochemistry and Molecular Biology, University of Southern California/Norris Cancer Centre, Los Angeles, California, USA

D. McCarthy: The Wellcome Trust Centre for Human Genetics, Oxford, UK

S.J. McGowan: Computational Biology Research Group, Weatherall Institute of Molecular Medicine, University of Oxford, Oxford, UK

G. McVean: The Wellcome Trust Centre for Human Genetics, Oxford, UK

C.S. Merzdorf: Department of Cell Biology and Neuroscience, Montana State University, Bozeman, Montana, USA

C.J. Millard: Henry Wellcome Laboratories of Structural Biology, Department of Molecular and Cell Biology, University of Leicester, Leicester, UK

K.A. Miller: Clinical Genetics Group, Weatherall Institute of Molecular Medicine, University of Oxford, Oxford, UK

J. Morton: Clinical Genetics Unit, Birmingham Women's Hospital NHS Foundation Trust,



Birmingham, UK

J.B. Mulliken: Department of Plastic and Oral Surgery, Children's Hospital, Boston, Massachusetts, USA

D.J. Murray: National Paediatric Craniofacial Centre, Children's University Hospital, Dublin, Ireland

L. Murray: Illumina Cambridge Ltd., Essex, UK

P. Noons: Department of Craniofacial Surgery, Birmingham Children's Hospital NHS Foundation Trust, Birmingham, UK

C.W. Ockelo: Department of Human Genetics, Radboud University Medical Centre, Nijmegen, The Netherlands

A.M.W van den Ouweland: Department of Clinical Genetics, Erasmus MC, University Medical Centre Rotterdam, Rotterdam, The Netherlands

A. Pagnamenta: The Wellcome Trust Centre for Human Genetics, Oxford, UK

E. Pauws: Developmental Biology and Cancer Programme, UCL Institute of Child Health, London, UK

R. Pfundt: Department of Human Genetics, Radboud University Medical Centre, Nijmegen, The Netherlands

J.M. Phipps: 1. Clinical Genetics Group, Weatherall Institute of Molecular Medicine, University of Oxford, Oxford, UK; 2. Department of Clinical Genetics, Oxford University Hospitals NHS Foundation Trust, Oxford, UK

P. Piazza: The Wellcome Trust Centre for Human Genetics, Oxford, UK

G. Polanco: The Wellcome Trust Centre for Human Genetics, Oxford, UK

M.A. Ramos-Arroyo: Department of Medical Genetics, Complejo Hospitalario de Navarra, IdiSNA, Navarra Institute for Health Research, Pamplona, Navarra, Spain

J. Rankin: Clinical Genetics Department, Royal Devon and Exeter NHS Foundation Trust, Exeter, UK

P. Ratcliffe: The Wellcome Trust Centre for Human Genetics, Oxford, UK

K.E.M. Rees: North East Thames Regional Genetics Service, Great Ormond Street Hospital for Children NHS Foundation Trust, London, UK

I.C. Richardson: Developmental Biology and Cancer Programme, UCL Institute of Child Health, London, UK

A. Rimmer: The Wellcome Trust Centre for Human Genetics, Oxford, UK

N. Sahgal: The Wellcome Trust Centre for Human Genetics, Oxford, UK

J.W.R. Schwabe: Henry Wellcome Laboratories of Structural Biology, Department of Molecular and Cell Biology, University of Leicester, Leicester, UK

W.H. Selman: 1. Department of Pharmaceutical Sciences, College of Pharmacy, Oregon State University, Corvallis, Oregon, USA; 2. College of Veterinary Medicine, University of Al-Qadisiyah, Al Diwaniyah, Iraq

V.P. Sharma: 1. Clinical Genetics Group, Weatherall Institute of Molecular Medicine, University of Oxford, Oxford, UK; 2. Craniofacial Unit, Oxford University Hospitals National Health Service (NHS) Trust, Oxford, UK

P.J. van der Spek: Department of Bioinformatics, Erasmus MC, University Medical Centre Rotterdam, Rotterdam, The Netherlands

P. Stanier: Genetics and Genomic Medicine, UCL Institute of Child Health, London, UK

S.M.A. Swagemakers: Department of Bioinformatics, Erasmus MC, University Medical Centre Rotterdam, Rotterdam, The Netherlands

E. Sweeney: Department of Clinical Genetics, Liverpool Women's NHS Foundation Trust, Liverpool, UK

J. Taylor: Oxford Medical Genetics Laboratories, Oxford University Hospitals NHS Foundation Trust, Oxford, UK

J.C. Taylor: 1. Oxford Biomedical Research Centre, National Institute for Health Research, Oxford, UK; 2. The Wellcome Trust Centre for Human Genetics, University of Oxford, Oxford, UK

E.A. Tidey: North East Thames Regional Genetics Service, Great Ormond Street Hospital for Children NHS Foundation Trust, London, UK

S.E. Tomkins: Clinical Genetics Department, Musgrove Park Hospital, Taunton, UK

I. Tomlinson: 1. The Wellcome Trust Centre for Human Genetics, Oxford, UK; 2. NIHR Oxford Biomedical Research Centre, Oxford, UK

A. Trebes: The Wellcome Trust Centre for Human Genetics, Oxford, UK

S.R.F. Twigg: Clinical Genetics Group, Weatherall Institute of Molecular Medicine, University of Oxford, Oxford, UK

M.L. van Veelen: Department of Neurosurgery, Erasmus MC, University Medical Centre Rotterdam, Rotterdam, the Netherlands

A.J. Verkerk: 1. Department of Bioinformatics, Erasmus MC, University Medical Centre Rotterdam, Rotterdam, The Netherlands; 2. Department of Internal Medicine, Erasmus MC, University Medical Centre Rotterdam, Rotterdam, The Netherlands

W.K. Vogel: Department of Pharmaceutical Sciences, College of Pharmacy, Oregon State University, Corvallis, Oregon, USA

S.A. Wall: Craniofacial Unit, Oxford University Hospitals NHS Foundation Trust, Oxford, UK

A. Weber: Department of Clinical Genetics, Liverpool Women's NHS Foundation Trust, Liverpool, UK

I. Westbury: Clinical Genetics Group, Weatherall Institute of Molecular Medicine, University of Oxford, John Radcliffe Hospital, Oxford, UK

WGS500 Consortium:

Steering Committee: Peter Donnelly (Chair), John Bell, David Bentley, Gil McVean,



Peter Ratcliffe, Jenny Taylor, Andrew Wilkie

Operations Committee: Peter Donnelly (Chair), John Broxholme, David Buck, Jean-Baptiste Cazier, Richard Cornall, Lorna Gregory, Julian Knight, Gerton Lunter, Gil McVean, Jenny Taylor, Ian Tomlinson, Andrew Wilkie

Sequencing & Experimental Follow up: David Buck (Lead), Christopher Allan, Moustafa Attar, Angie Green, Lorna Gregory, Sean Humphray, Zoya Kingsbury, Sarah Lambie, Lorne Lonie, Alistair Pagnamenta, Paolo Piazza, Guadelupe Polanco, Amy Trebes

Data Analysis: Gil McVean (Lead), Peter Donnelly, Jean-Baptiste Cazier, John Broxholme, Richard Copley, Simon Fiddy, Russell Grocock, Edouard Hatton, Chris Holmes, Linda Hughes, Peter Humburg, Alexander Kanapin, Stefano Lise, Gerton Lunter, Hilary Martin, Lisa Murray, Davis McCarthy, Andy Rimmer, Natasha Sahgal, Ben Wright, Chris Yau

D. Wiczorek: Institute of Human Genetics, Heinrich-Heine-University, Medical Faculty, Düsseldorf, Germany

A.O.M. Wilkie: 1. Clinical Genetics Group, Weatherall Institute of Molecular Medicine, University of Oxford, Oxford, UK; 2. Department of Clinical Genetics, Oxford University Hospitals NHS Foundation Trust, Oxford, UK; 3. Craniofacial Unit, Oxford University Hospitals NHS Foundation Trust, Oxford, UK

L.C. Wilson: North East Thames Regional Genetics Service, Great Ormond Street Hospital for Children NHS Foundation Trust, London, UK

E.B. Wolvius: Department of Oral Maxillofacial Surgery, Special Dental Care and Orthodontics, Dutch Craniofacial Centre, Erasmus MC, University Medical Centre, Rotterdam, The Netherlands

B. Wright: The Wellcome Trust Centre for Human Genetics, Oxford, UK

C. Yau: Imperial College London, London, UK

H. Yntema: Department of Human Genetics, Radboud University Medical Centre, Nijmegen, The Netherlands

Name PhD student: Jacqueline A.C. Goos
 Erasmus MC Department: Plastic and Reconstructive Surgery and Hand Surgery
 PhD period: 2011-2016
 Promotors: Prof.dr. I.M.J. Mathijssen and Prof.dr. P.J. van der Spek
 Copromotor: Dr. A.M.W. van den Ouweland

1. PhD training

General courses	Year	ECTS
Clinical Business Administration, TIAS Utrecht	2016-2017	5
Masterclass Medical Business	2016	0.2
The workshop on Photoshop and Illustrator CS6 for PhD-students and other researchers	2013	0.3
Systematic Literature search in other databases	2013	0.3
Systematic Literature search in PubMed	2013	0.3
EndNote Course	2013	0.2
Research Integrity	2013	2
BROK course ('Basiscursus Regelgeving Klinisch Onderzoek')	2012	1
Statistics: Biostatistics for Clinicians	2012	1
Biomedical English Writing and Communication	2012	3

Specific courses	Year	ECTS
ATLS	2017	1
Weekly microsurgery training (432 hours)	2011-2016	15
ALS course week	2016	1
Basic Wound Care	2016	0.2
SEH Course Week	2016	1
Training how to deal with aggressive patients	2016	0.3
Communication Concerning Organ Donation	2016	0.2
Capita Selecta Pain	2014	0.3
Complete Genomics Course	2013	0.3
MGC Next Generation Sequencing data analysis (7 th ed.)	2013	1.4
The Course on Molecular Diagnostics VIII	2013	1
Capita selecta Clinical Genetics	2013	0.3
SNP course IX	2012	2
SNP course VIII	2011	2
PGM experience tour (Life technologies)	2012	0.3
The Basic Human Genetics Course: Genetics for Dummies	2011	0.7
Basic Data Analysis on gene expression arrays	2011	0.7
Complete Genomics course	2011	0.3



Appendices

Presentations, posters and abstracts	Year	ECTS
Overview genetic research 2016-2017 Four centre meeting 2017 Presentation	2017	0.3
Genetic research in craniofacial malformations Aangeboren Anatomische Afwijkingen Presentation Invited speaker	2016	0.3
Identification of intragenic exon deletions of <i>TCF12</i> by whole genome sequencing ESCFS 2016 Abstract and presentation	2016	1
Overview genetic research 2015-2016 Four centre meeting 2016 Presentation	2016	0.3
Identification of intragenic exon deletions of <i>TCF12</i> by whole genome sequencing ESHG 2016 Abstract and poster	2016	1
Whole genome sequencing; een krachtige aanvulling op de huidige diagnostiek van craniofaciale afwijkingen NVPC 2016 Abstract and presentation	2016	0.3
Two unsolved cases after whole genome sequencing EuroDysmoClub and Course 2015 Presentation	2015	1
Sequencing the Whole Genome; a revolution for craniofacial genetics? ISCFS meeting 2015 Abstract and presentation	2015	1
Overview genetic research 2014-2015 Four centre meeting 2015 Presentation	2015	0.3
Een afspraak bij de klinisch geneticus; waarom? Genetische achtergronden van schedel- en aangezichtsafwijkingen presentation NVSCA Presentation Invited speaker	2014	0.3
<i>IL11RA</i> related craniosynostosis: A clinical and molecular review of 7 new cases Manchester dysmorphology meeting Abstract and poster	2014	0.2

Presentations, posters and abstracts	Year	ECTS
Overview genetic research 2013-2014 Four centre meeting 2014 Presentation	2014	0.3
Single-gene testing and Next Generation Sequencing in a Dutch cohort of syndromic craniosynostosis patients ESHG Abstract and poster	2014	1
Mutations in <i>IL11RA</i> ; a genetic cause of scaphocephaly ESPN Abstract	2014	0.2
Mutations in <i>TCF12</i> are a frequent cause of coronal craniosynostosis ISCF meeting 2013 Abstract and presentation	2013	1
Mutaties in <i>TCF12</i> zijn een frequente oorzaak van coronale synostose NVPC Abstract and presentation Awarded as best presentation	2013	0.3
Overview genetic research 2012-2013 Four centre meeting 2013 Presentation	2013	0.3
De genetische achtergrond van craniofaciale afwijkingen Symposiareeks van de kinderchirurgische groep in het kader van het 150-jarig bestaan van het Sophia 2013 Presentation Invited speaker	2013	0.3
De Centrale Genetische Database als Bibliotheek voor de Zorg ICT Delta Pitch	2012	0.3
Implementation of Next Generation Sequencing (NGS) in Dutch Health Care: Discovery of a Novel Causal Variant for Craniosynostosis AGBT Abstract and poster	2012	1
Een nieuw recessief craniofaciaal syndroom NVSCA Abstract and presentation	2011	0.3



Appendices

Visited seminars, workshops and conferences*	Year	ECTS
Four centre meeting 2017	2017	
NVSCA autumn meeting	2016	0.2
NVPC autumn meeting 2016	2016	0.2
ESCFS 2016	2016	
Four centre meeting 2016	2016	
ESHG 2016	2016	
NVPC spring meeting 2016	2016	
Gordon Research Conference, craniofacial morphogenesis and tissue regeneration	2016	1
16th Hand Therapy and Surgery Symposium "Anatomy of the Hand-Back to basic"	2015	0.2
EuroDysmoClub and Course	2015	
NVSCA autumn meeting Mienskip	2015	0.2
KNAW "Genetic screening: Who, why and when?"	2015	0.2
NVPC autumn meeting	2015	0.2
ISCFS meeting	2015	
Presymposium "Cerebral Palsy Course" and "10th World Symposium of Congenital Malformations of the Hand and Upper Limb"	2015	1
Four centre meeting	2015	
Kortjakje	2015	0.2
NVSCA autumn meeting	2014	
ESCFS	2014	0.5
Four centre meeting	2014	
ESHG	2014	
Kortjakje	2014	0.2
Verwijzersavond schisis en schedel- en aangezichtsafwijkingen	2014	0.2
22nd Esser Course: What's New in Breast Reconstruction: Live surgery and Lectures	2014	0.3
21st Esser Course: Wide awake: A live surgery event	2013	0.3
Kortjakje	2013	0.2
NVPC autumn meeting	2013	0.2
ISCFS meeting	2013	
Four centre meeting	2013	
19th Esser Course: To the base of the thumb, the CMC joint	2013	0.3
NVPC spring meeting	2013	
Symposiareeks kinderchirurgische groep Sophia 150 jaar	2013	
Visualization symposium and opening collaboration (SARA and ESCIENCE centre)	2012	0.2
NVPC spring meeting	2012	0.2
18th Esser Course: Bend... or Break	2012	0.3
ICT Delta (pitch)	2012	
AGBT	2012	
NVPC autumn meeting	2011	0.2
NVSCA	2011	

2. Teaching activities

Lecturing	Year	ECTS
Anatomy of the upper extremities	2012-2015	0.5
Microsurgery	2012-2015	3.5
Dysmorphology	2012-2014	1
Tendon repair	2013	0.1
Macroscopic suture techniques	2012	0.1

Supervision of students	Year	ECTS
Supervision master thesis M. van Pelt	2015	3
Supervision (tutor) of freshmen Medical School	2014	1
Supervision minor students	2013	1

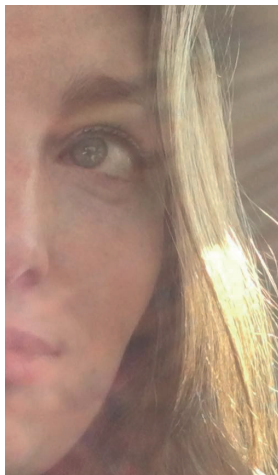
3. Organizing activities

Conferences and meetings	Year	ECTS
Autumn meeting NVSCA	2014	2
Esser Course "To the base of the thumb"	2012-2013	2

Administrative activities	Year	ECTS
General board member Promeras (PhD association Erasmus University Medical Centre)	2011-2014	2
Author of the booklet "Starting your PhD at Erasmus MC"		2
General board member PNN (Dutch PhD association)	2012-2014	2
General board member EPAR (PhD association Erasmus University)	2011-2013	1

* In case the seminar, workshop or conference was visited without presenting a paper, ECTS are given in this table





Jacqueline Antonia Christiana was born in Rotterdam on the 1st of May 1986. She attended grammar school at the Erasmiaans Gymnasium in Rotterdam. Besides the regular classes, she attended History, French, Economy, Greek and Latin. Via a selection procedure (decentrale selectie) she was admitted to Medicine at the Erasmus University in Rotterdam. During her fourth year of Medicine she was selected to participate in the extracurricular Neuroscience research master at the Erasmus Medical Centre. She received her MSc degree in Neuroscience in 2009 and graduated from Medicine in 2011. Immediately after completing her Medicine degree, she started the PhD trajectory that has led to the thesis in front of you.



Mijn dank gaat uit naar alle patiënten en familieleden van patiënten die hebben geholpen bij dit onderzoek. Zonder hen hadden we niet tot zoveel nieuwe inzichten kunnen komen!

Daarnaast wil ik mijn lieve moeder en lieve broer bedanken voor hun onvoorwaardelijke steun.

Uiteraard wil ik ook alle anderen bedanken die op welke manier dan ook hebben bijgedragen aan dit onderzoek.

De mensen die je in je leven ontmoet zijn een soort vragen die je helpen erachter te komen wie je bent, hoe je in elkaar zit en wat je wilt (uit: "In het licht van wat wij weten").⁴⁴³

Hartelijk dank!

